HEAT TRANSFER EFFECTS DURING COLD DENSE GAS DISPERSION

FINAL REPORT

(AUGUST 1982 - SEPTEMBER 1983)

Gas Research Institute
8600 West Bryn Mawr Avenue
Chicago, Illinois 60631

GRI-83/0082

HEAT TRANSFER EFFECTS DURING COLD DENSE GAS DISPERSION

by

G. Andreiev[1]
D. E. Neff[2]
R. N. Meroney[3]

Fluid Mechanics and Wind Engineering Program
Civil Engineering Department
Colorado State University
Fort Collins, Colorado

for

Gas Research Institute
Contract No. 5014-352-0203
GRI Project Manager
Steve J. Wiersma
Environment and Safety Research Department

[1] Graduate Student, Colorado State University
[2] Research Associate, Colorado State University
[3] Professor, Colorado State University

November 1983

50272-101

REPORT DOCUMENTATION PAGE	1. REPORT NO. GRI-83/0022	2.	3. Recipient's Accession No.

4. Title and Subtitle
HEAT TRANSFER EFFECTS DURING COLD DENSE GAS DISPERSION

5. Report Date
November 1983

6.

7. Author(s)
G. Andreiev, D. E. Neff, R. N. Meroney

8. Performing Organization Rept. No.
CER 83-84/GA-DEN/RNM-3

9. Performing Organization Name and Address
Civil Engineering Department
Colorado State University
Fort Collins, CO 80523

10. Project/Task/Work Unit No.

11. Contract(C) or Grant(G) No.
(C)GRI No. 5014-352-0203
(G)

12. Sponsoring Organization Name and Address
Environmental & Safety Research Department
Gas Research Institute
8600 West Bryn Mawr Avenue
Chicago, Illinois 60631

13. Type of Report & Period Covered
Final Report
Aug. 1982-Sept. 1983

14.

15. Supplementary Notes

16. Abstract (Limit: 200 words)

Wind tunnel concentration data were obtained for continuous area releases of isothermal, cold N_2, cold CO_2 and cold CH_4 clouds. Wind tunnel results were compared to field test results and to a computer model simulation. Heat transfer and humidity effects on model concentration distributions were significant for methane plumes when surface Richardson numbers, Ri_*, were large (i.e. low wind speed and high boiloff rates conditions). At field scales heat transfer and humidity still play a role in the dispersion of methane spill cases, but plume dilution and lift off are not as exaggerated as for the model cases.

17. Document Analysis a. Descriptors

Liquified Natural Gas, wind tunnel, vapor cloud dispersion, dispersion of heavy plumes

b. Identifiers/Open-Ended Terms

c. COSATI Field/Group

18. Availability Statement	19. Security Class (This Report)	21. No. of Pages
Distribution Unlimited	Unclassified	239
	20. Security Class (This Page) Unclassified	22. Price

(See ANSI-Z39.18) See Instructions on Reverse

OPTIONAL FORM 272 (4-77)
(Formerly NTIS-35)
Department of Commerce

GRI DISCLAIMER

LEGAL NOTICE This report was prepared by Colorado State University as account of work sponsored by the Gas Research Institute (GRI). Neither GRI, members of GRI, not any person acting on behalf of either:

a. Makes any warranty of representation, expressed or implied with respect to the accuracy, completeness, or usefulness of the information contained in this report, or that the use of any information, apparatus, method or process disclosed in this report may not infringe privately owned rights; or

b. Assumes any liability with respect to the use of, or for damages resulting from the use of, any information, apparatus, method, or process disclosed in this report.

RESEARCH SUMMARY

Title	Heat Transfer Effects During Cold Dense Gas Dispersion
Contractor	Civil Engineering Department Colorado State University Fort Collins, CO 80523
Principal Investigators	G. Andreiev, D. E. Neff, and R. N. Meroney
Report Period	August 1982 - July 1983 Final Report
Objective	To determine through utilization of wind tunnel experiments, the mechanisms of heattransfer during cold dense gas dispersion and the effect that heat transfer has on subsequent cloud dilution.
Technical Perspective	A Liquefied Natural Gas (LNG) spill will result in a cold LNG vapor plume exhibiting negative buoyancy. The presence of atmospheric shear flows causes entrainment of warm, humid air thereby resulting in latent and sensible heat transfer across plume boundaries. There is a need to determine how heat transfer affects cold cloud dilution as compared to entrained air mixing of an isothermal cloud.
Results	A large data base detailing heavy gas plume temperatures and concentrations was obtained. Releases included isothermal, cold N_2, cold CO_2 and cold CH_4 clouds. Wind tunnel results were compared to field test results and with a numerical model simulation. Heat transfer and humidity effects on model concentration distributions are significant for methane plumes when buoyancy length ratio, ℓ_b/L or surface Richardson number, Ri_* are large (i.e. low wind speed and high boiloff rate conditions). Isothermal and heavier molecular weight cold simulants always produced a more conservative concentration distribution than the buoyant methane plumes. At field scales heat transfer and humidity still play a role in the dispersion of methane or propane spill cases examined, but plume dilution and lift off are not as exaggerated as for the model cases.

Technical Approach

Wind tunnel tests were performed at model scale to determine heat transfer effects on an LNG plume. A LNG plume is heavier than air at boiloff conditions and is expected to remain negatively bouyant for most conditions until it is adequately dispersed. The negatively buoyant plume can be simulated in the wind tunnel by an isothermal heavy gas or cooled lighter gases such that the specific gravity of the source gas is equal to that of LNG vapor at boiloff. The measured results were scaled to account for differences in moles of cold methane gas versus the source moles of alternative model source gas. Heavy gases were introduced into the wind tunnel via a constant area source mounted flush with the wind tunnel floor. Mean gas concentrations and mean temperatures were evaluated at various locations both downwind and upwind of the source. Concentration samples were analyzed using a gas chromatograph. Temperatures were evaluated throughout the plume with a thermocouple multiplexer system. From the concentration and temperature profiles for each run, the plume structure was determined.

Project Implications

This task in the wind-tunnel test program has shown that in most cases of interest, LNG vapor cloud dispersion can be well chracterized by isothermal heavy gas dispersion throughout its flammable cloud existence. No further research is planned on ambient heat transfer effects during LNG vapor cloud dispersion. The reslts of this research will be used in the development of guidelines for fluid modeling of LNG dispersion and will help define the capabilities and limitations of wind-tunnel modeling of heavy gas dispersion.

GRI Project Manager
Steve J. Wiersma
Environment and Safety Research

TABLE OF CONTENTS

LIST OF TABLES

LIST OF FIGURES

LIST OF SYMBOLS

Dimension are given in terms of mass (m), length (L), time(t), moles (n), and temperature (T).

Symbol	Definition	
A	Area	$[L^2]$
@	at	-
B	Plume width	[L]
C_f	Surface friction coefficient	-
C_p	Specific heat capacity at constant pressure	$[L^2t^{-2}T^{-1}]$
C_p^*	Molar specific heat capacity at constant pressure	$[L^2mt^{-2}T^{-1}n^{-1}]$
D	Crosswind plume width at source	[L]
E	Entrainment velocity ratio W_e/W_* or Total Enthalpy	- $[mLt^{-2}]$
f()	Function of ()	-
g	Gravitational acceleration	$[Lt^{-2}]$
g'	$(= g(\rho_o-\rho_a)/\rho_a)$ gravitational parameter	$[Lt^{-2}]$
H	Gas layer depth	[L]
k	von Karman constant	-
K	Dimensionless concentration coefficient or diffusivity	-
ℓ_b	Buoyancy length scale	[L]
L	Length	[L]
L_{mo}	Monin-Obukhov stability length	[L]
M,MW	Molecular weight	$[mn^{-1}]$
n	Mole or frequency	$[n],[t^{-1}]$
p	Velocity power law exponent	-
P	Pressure	$[mL^{-1}t^{-2}]$

q	Turbulent kinetic energy	$[mL^2t^{-2}]$
Q	Volumetric rate of gas flow	$[L^3t^{-1}]$
R	Universal gas constant	$[nm^{-1}L^2t^{-1}T^{-1}]$
$S_u(n)$	Spectral power density	$[L^2t^{-1}]$
T	Temperature	$[T]$
t	Time	$[t]$
t_R	Time duration of source release	$[t]$
T^*	Dimensionless temperature $((T_a-T)/T_a-T_o))$	-
u_*	Friction velocity	$[Lt^{-1}]$
U,u	Mean velocity	$[Lt^{-1}]$
u_x	Local plume velocity	$[Lt^{-1}]$
v_e	Horizontal entrainment velocity into plume	$[Lt^{-1}]$
v_*	Weighted sum of mechanical and thermal entrainment velocities	$[Lt^{-1}]$
W,w	Plume vertical velocity	$[Lt^{-1}]$
w_e	Vertical entrainment velocity into plume	$[Lt^{-1}]$
w_*	Thermal convective velocity scale	$[Lt^{-1}]$
x	General downwind coordinate	$[L]$
y	General lateral coordinate	$[L]$
z	General vertical coordinate	$[L]$
$z_{1/2}$	Plumes vertical half width	$[L]$
z_o	Surface roughness parameter	$[L]$
α	Constant or thermal diffusivity	-
β	Coefficient of thermal expansion	$[T^{-1}]$
δ	Boundary layer thickness	$[L]$
$\Delta\theta$	Temperature difference across some reference layer	$[T]$

η	General vertical position	[L]
λ	Thermal conductivity	$[mLT^{-1}t^{-3}]$
Λ	Longitudinal integral scale of turbulence	[L]
μ	Dynamic Viscosity	$[mL^{-1}t^{-1}]$
ν	Kinematic viscosity	$[L^2t^{-1}]$
ξ	General lateral position or constant	[L]
ρ	Density	$[mL^{-3}]$
σ	Standard deviation or plume surface area	[L], $[L^2]$
ϕ	Relative humidity	-
$\phi()$	Function of ()	-
χ	Mole fraction of gas component	-
ω	Specific humidity	-
Ω	Angular velocity of earth = 0.726×10^{-4} (radians/sec)	$[t^{-1}]$

Subscripts

a	Ambient conditions
dpt	Dewpoint
L	On centerline
H	Evaluated at height H
LNG	Liquefied Natural Gas
m	Model
o	Initial conditions
p	Prototype
R, ref, r	Reference conditions
w	Wall

Superscripts

()	Mean of a quantity

$()'$	Fluctuating part of a quantity
$(\dot{})$	Quantity per unit time
$()$	Quantity per unit area
$()^*$	Non-dimensionalized quantity

Dimensionless Parameters

Ec	Eckert number
f	Dimensionless plume parameter
F	Momentum flux ratio
ϕ_ε	Dimensionless dissipation rate for turbulent energy
Fr	Densimetric Froude number
Fr	Flux Froude number
Fr_s	Densimetric Froude number relative to inertia of the plume
K	Dimensionless concentration
K_e	Dimensionless eddy diffusivity
M	Mass flux ratio
Ma	Mach number
Nu	Nusselt number
Pr	Prandtl number
Ra	Rayleigh number
Re	Reynolds number
Ri	Bulk Richardson number
Ro	Rossby number
SG	Specific gravity
St	Stanton number
V	Volume flux ratio

1.0 INTRODUCTION

Storage and transport of flammable hydrocarbon fuels with subambient boiling points have potential hazards associated with inadvertant releases into the atmosphere. Fuels in this category include liquefied natural gas (LNG), ethane, propane, and butane (LPG). At ambient temperature, these liquids rapidly boil and form cold gas clouds that will usually remain negatively buoyant at least until the cloud is diluted to its lower flammability limit (LFL).

Previous analysis of laboratory experiments modeling dense gas plumes have not extensively discussed thermal effects on plume mixing behavior, so a series of experiments was performed to study the effect of heat transfer on cold dense cloud dispersion. The experiments were sponsored by the Gas Research Institute (GRI) and were performed in the Environmental Wind Tunnel facility of the Fluid Dynamics and Diffusion Laboratory at Colorado State University.

This report is structured as follows: Section 1 contains a brief discussion of dense gas kinematics along with a survey of the status of stratified dispersion results. Section 2 is a theoretical discussion of cold plume dispersion modeling at the wind tunnel scale. Section 3 describes modeling, data acquisition and analysis techniques. Section 4 outlines the test program undertaken. Section 5 is a discussion of the test results and Section 6 presents conclusions obtained from analysis of the test results.

1.1 Dense Gas Kinematics

Low boiling point liquefied gases demonstrate extreme volatility upon exposure to the ambient atmosphere. Primary concern has been given to clouds in which density effects are important, i.e. clouds which

to clouds in which density effects are important, i.e. clouds which exhibit a high initial layer Richardson number (Ri_o). The Richardson number relates the stabilizing effect of the cloud density to the kinetic energy of the ambient turbulence and is defined as $Ri_o = \frac{g'V^{1/3}}{u_*^2}$ where $g' = |\bar{g}| \frac{\rho_g - \rho_a}{\rho_a}$ (the buoyancy of the plume), V is the initial plume volume, and u_* is the square root of the kinematic surface shear due to the atmospheric boundary layer (more commonly referred to as the atmospheric friction velocity). Puttock, Blackmore and Colenbrander (1981) use $Ri_o > 10$ as the criterion for density effects to be important. For continuous spills, $V^{1/3} = \frac{Q}{UD}$ where Q is the source volume flow rate, U is the ambient mean velocity and D is the crosswind extent of the plume at the source.

Dense gas clouds are classified as either instantaneous or continuous releases. Puttock et al. (1982) suggest that for finite volume releases when $\frac{t_R U^2}{\sqrt{\frac{g'V}{\pi}}} < 10$ the cloud can be considered as instantaneously formed where t_R is the time taken for the release to occur. If this parameter is greater then 10, the cloud is classified as a continuous or finite time release. Note the anamoly, however, that any release in calm conditions is considered instantaneous even when boiloff rates and initial cloud potential energies are low.

Continuous source-like hazards may arise in situations such as pipeline ruptures without valve closedowns, or releases of very large quantities of cryogenic liquid gas onto land or water in the presence of low to moderate wind speeds. Puttock et al. (1982) describe a number of field tests which modeled continuous spills.

Extensive laboratory tests of instantaneous releases have been reported by Meroney and Lohmeyer (1982, 1983a, 1983b). Their lab results are compared against numerical box model data and available instantaneous field experiments. Neff and Meroney (1982) reported on an extensive set of isothermal wind tunnel experiments in which continuous heavy gas releases were studied. Meroney et al. (1977) and Neff et al. (1976) performed scaled continuous cold gas releases in the presence of dikes and tanks which tended to produce active wakes thereby reducing the influence of surface heating and humidity. The experiments reported herein were designed to evaluate thermal effects on continuous dense cloud dispersion.

Initially, continuous cold plumes exhibit density effects as evidenced by rapid horizontal spreading caused by the excess hydrostatic head of the cloud. The result is a low wide plume, the effect being more pronounced at low wind speeds. In instances of moderate wind speed, the plume will even extend upwind, although the gas will eventually lose its initial momentum and be rolled back over or around the source. A consequence of the velocity reversal of gas upwind from the source is the generation of a horseshoe shaped vortex which bounds the parabolic gas cloud.

The gravity spreading initially evident in the cloud converts potential energy into kinetic energy part of which is in turn transmitted to the surrounding ambient fluid where it is dissipated by turbulence. The energy transfer occurs at the head of the spreading cloud and in its wake. The cloud will reach a point where the gravitational spreading velocity is small compared to the mean ambient wind velocity. Presumably, significant amounts of air will be entrained due to mixing

and the cloud will be advected downwind at ambient air speeds. Hence the cloud takes on a parabolic shape with plume depth being symmetric about the center line.

Surface heating of the plume and entrainment of water vapor with the air reduces the plume's negative buoyancy. The result is to decrease the instantaneous Richardson number thereby enhancing both dispersion by atmospheric turbulence and the subsequent downwind advection of the plume. As the buoyancy becomes positive and less stably stratified the plume may actually lift off of the ground surface. Meroney (1980) found that lift off will not occur immediately upon attaining positive buoyancy unless a lift off parameter, $L_p = \frac{g'H}{u_*^2}$, is sufficiently large. For large spills of LNG under moderate conditions it is not likely that lift off will occur before the lower flammability limit, LFL, is attained.

It should be noted that for small field spills or laboratory scale spills, surface heating effects will be exaggerated. When a large Rayleigh number condition exists (i.e. large temperature differences or large depth spill), it is hypothesized that heat transfer will go as $h_s \frac{L^3}{U}$, where L is the characteristic length scale of the plume, U is the characteristic velocity scale, and h_s, the convective heat transfer coefficient, is not a strong function of the length scale. The thermal capacity of a gas cloud will vary as $\rho C_p L^3$. The ratio of surface heat transport to thermal capacitance, then, will go as $\frac{h_s}{\rho C_p} \frac{1}{U}$. Since wind speed is normally scaled by a Froude number $\frac{U^2}{g'L}$, smaller model scale plumes will see a temperature increase (or density decrease) which

does not scale to the field equivalent. Cold model plumes will entrain air faster and lift off before the comparable field situation.

1.2 Status of Cold Cloud Dispersion Research

Classically fluid mixing or entrainment has been characterized by an entrainment velocity at the edge of a mixed layer or as a flux of mass down a species gradient due to a local diffusivity. Entrainment velocities are usually made proportional to some average velocity scale such as friction velocity, u_*, or plume rise velocity, w. They are subsequently modified by functions dependent on some local stability parameter to account for supression or acceleration of mixing due to gravity effects.

Local diffusivity methods solve for vertical distributions of velocity, mass, or temperature. These local diffusivities are often related to other flow characteristics such as local turbulence and length scales, which can also be modified by empirical expressions relating to cloud stratification.

Mixing is both a local and a globally governed phenomenon. In recent atmospheric problems a weighted mix of locally determined diffusivity together with a gross parameter diffusivity has been used successfully (McNider and Pielke 1981).

Since both models are required to compliment box and depth integrated approaches as well as for the solution of modified sets of primitive equations of motion a review of the alternative mixing expressions is given in Section 1.2.1. The rather limited laboratory data by means of which coefficients in the models are specified are considered in Section 1.2.2.

1.2.1 Alternative Mixing Expression:

Mixing theories may be classified as either entrainment models for mixing velocity or local diffusivity models. The former are used with box models or depth averaged slab models, while the latter are necessary for closure of the primitive equations of turbulent motion.

Entrainment Models:

Entrainment models presume that ambient air is mixed across a cloud surface at a rate characterized by an entrainment velocity, w_e (i.e. volume entrained/unit area/time). Extensive studies of free jets and plumes suggest that w_e is proportional to an along-jet velocity or a plume rise velocity (Csanady, 1973). Studies of the growth of turbulent boundary layers suggest w_e is proportional to the turbulent vertical velocity correlation, $\sqrt{\overline{w'^2}}$. But in neutral boundary layers $\sqrt{\overline{w'^2}}$ is related to $\sqrt{\overline{u'w'}}$ or friction velocity, u_* (Reynolds, 1968).

For an isothermal heavy gas cloud it is reasonable to expect entrainment rate to be initially proportional to spread velocity, u_g, and asymptotically constrained by the magnitude of friction velocity, u_*, (Jensen, 1981; Jensen and Mikkelsen, 1982; Meroney and Lohmeyer 1982, 1983). Between these two limits the mixing velocity will depend on a weighted sum of the two velocity scales modified by any tendency of buoyancy effects to suppress turbulence; i.e.

$$w_e = c_z u_g + \alpha_4 v_* f(Ri) \quad . \tag{1-1}$$

where u_g usually approaches zero as time or distance increases, and, f(Ri), a function of a Richardson number, Ri, adjusts for stabilizing influence of the vertical density gradient. f(Ri) may take many forms

ranging from 1/Ri to $1/(C_1 + C_2\ Ri)^d$, where C_1, C_2 are of order one and d ranges from 1/2 to 1. The coefficients are specified from laboratory experiments on stratified mixing layers (see Section 1.2.2) or from a regression against heavy gas cloud field and laboratory experiments. v_* is a weighted sum of vertical velocities due to mechanical shear, u_*, and vertical velocities due to thermal effects, w_*.

Eidsvik (1980) proposed an empirical expression for w_e which approaches the approximately correct value for diffusion of a passive scalar as the density difference vanishes. He used a Zeman-Tennekes type of entrainment expression, where

$$w_e = \frac{\alpha_4\ v_*}{\frac{\alpha_4}{\alpha_6} + Ri_*} \qquad (1\text{-}2)$$

and $$Ri_* = \frac{g'H}{v_*^2} \ ,$$

$$\alpha_i = \text{constants}$$

$$v_*^2 = (\alpha_2 w_*)^2 + (\alpha_3 u_*)^2 \ ,$$

$$u_* = (C_f/2)^{1/2}\ \bar{u}_{ref} \ ,$$

$$w_* = \left[\overline{(T'w')}_o \frac{gH}{T} \right]^{1/3} \ , \text{ and}$$

$$\bar{u}^2_{ref} = (\tfrac{2}{3}\ \bar{u}_g)^2 + (\bar{u}_a)^2 \ .$$

Note as $Ri_* \rightarrow 0$ and $(\overline{T'w'})_o \rightarrow 0$ then

$$w_e \rightarrow \alpha_6 \alpha_3 u_* .$$

Eidsvik assumed that since initially there is an imposed gravity flow sensible heat transfer from the surface, $\overline{T'w'}$, may be approximated by forced convection heat transfer, i.e. $(\overline{T'w'})_o = \frac{C_f}{2} \bar{u}_{ref}(T - \bar{T})$ or $St = \frac{C_f}{2}$. This choice may be adequate for some spill scenarios; however, it is likely that for large field spills or small cold laboratory releases the heat flux is dominated by free or mixed convection. Constants were initially specified from stratified shear layer data of Kato and Phillips (1969), and the growth of a neutral turbulent boundary layer (Tennekes and Lumley, 1972), but final values were adjusted to the average behavior of some of the Porton instantaneous spill data (Picknett, 1978). Recent arguments by Jensen, 1981, and Jensen and Mikkelson, 1982, also support the format for w_e proposed by Eidsvik.

Fay and Ranck (1983) proposed an empirical entrainment model, which they felt has the correct asymptotic variation and is simple. Since they were primarily interested in long time or asymptotic behavior, they proposed

$$w_e = u_* f(Ri_*) \qquad (1\text{-}3)$$

where

$$f = \left[C_1^{-2} + (C_2/Ri_*)^{-2} \right]^{-1/2}$$

in which C_1 and C_2 are constants of order unity. Note for $Ri_* >> 1$ that $w_e \propto \frac{C_2 u_*}{Ri_*}$, but if $Ri_* \rightarrow 0$ that $u_e \propto C_1 u_*$. They specified the constants C_1 and C_2 through a regression over a large set of field and laboratory releases of heavy gases. Unfortunately, it is likely that most of the data examined did not represent instantaneous or near-instantaneous release conditions required by the basic box model they used. It also seems likely that the initial source conditions were more important then expected.

Ermak et al. (1982) modified an earlier depth integrated model proposed by Zeman (1982). In this case the entrainment is specified in terms of vertical and horizontal entrainment velocities. The vertical entrainment is taken to be a density weighted combination of an ambient air entrainment rate and a stably stratified dense layer entrainment rate based on Kato and Phillip's (1969) experiments and is:

$$w_e = \frac{\pi^{1/2}\, k u_* (\rho_s - \rho)}{\phi(Ri_a)(\rho_s - \rho_a)} + \frac{2.5\, u_{g*}}{Ri_{g*}} \qquad (1\text{-}4)$$

where $u_{g*} = \sqrt{\frac{C_f}{2}}\, u_x$

u_x = Local cloud velocity

$$\phi(Ri_a) = \begin{cases} (1 - 16Ri_a)^{-1/4} & , Ri_a \leq 0, \\ 1 + 5Ri_a & , Ri_a > 0 \end{cases}$$

$Ri_{g*} = g'H/u_{g*}^2$

Ri_a = Ambient Richardson number, and

$\frac{C_f}{2}$ = Surface friction coefficient .

Ermak et al. (1982) note that the second term is much less than the first except when $\rho \sim \rho_s$ or $H \sim 0$. The horizontal entrainment rate they proposed is $v_e = (1.8)^2(H/B)w_e$. The expression empirically adjusts for the assumption that when the cloud is very flat horizontal entrainment will do little to dilute the cloud. The Ermak et al. (1982) model assumes only the ambient stratification influences entrainment, not the stratification of the cloud itself. This model also does not consider any entrainment enhancement due to surface heat transfer effects.

In the earlier version suggested by Zeman (1982) it was proposed based on superposition of mechanical and buoyancy-generated vertical scales and energy arguments, that

$$w_e = \frac{\left[K_e - \frac{u_*}{\delta\bar{U}}\right]u_*}{(1 + 2Ri_o)} + \frac{\frac{\alpha w_*^3}{\delta\bar{U}^2}}{(1 + 2Ri_o)} \qquad (1\text{-}5)$$

where $$K_e = \begin{cases} \dfrac{0.56(1 - 2Ri_o)}{1 + 5H/L_{mo}} & \text{if } \dfrac{H}{L} \geq 0, \\ 0.56\left(1 - 2Ri_o\right)\left(1 - \dfrac{H}{L}\right)^{+1/3} & \text{if } \dfrac{H}{L} < 0, \end{cases}$$

= Dimensionless eddy diffusivity,

$\delta\bar{U} = \bar{u}_a - \bar{u}_x$

= Relative velocity between ambient air and cloud,

$$Ri_o = \frac{\frac{1}{2}g'H}{\delta\bar{U}^2} = \frac{1}{2}\frac{C_f}{2} Ri_*$$

= Outer layer (bulk) Richardson number,

L_{mo} = Monin-Obukhov stability length for ambient air, and

$$w_* = \left[\frac{g}{T} (\overline{T'w'})_o H \right]^{1/3}.$$

= Convective velocity scale.

For an isothermal gravity current in a neutrally stratified shear layer when $\delta\bar{U} \sim \bar{u}_a$ and $Ri_o \rightarrow 0$

$$w_e = \left[0.56 - \sqrt{\frac{C_f}{2}} \right] |u_*| \simeq 0.28|u_*|, \tag{1-6}$$

which agrees with flat plate boundary layer experience. Alternatively when $\delta\bar{U} = -\bar{u}_x$ and $Ri_o > 0$ then

$$w_e = |u_*| \frac{[0.56(1 - 2Ri_o) + u_*/\bar{u}_x]}{(1 + 2Ri_o)}, \tag{1-7}$$

A critical Richardson number, Ri_{oc}, occurs when $Ri_{oc} = 0.5$ (i.e. $w_e \sim 0$ for $Ri_o > Ri_{oc}$). In the absence of a mean flow ($\bar{u}_a = \bar{u}_g = 0$) the model reduces to a single convective entrainment formula

$$w_e = \alpha\, w_*^3/\delta U^2/(1 + 2Ri_o) \approx \alpha\, w_*^3/g'H \approx \alpha\, w_*/Ri_* \tag{1-8}$$

Zeman assumed that the surface heat flux to a cold gas cloud is governed by a mixed forced and free convection modes represented by

$$h_s = \frac{\rho C_p \overline{T'w'}}{(T_w - \bar{T})} = \frac{\rho C_p T w_*^3}{gH(T_w - \bar{T})} \qquad (1\text{-}9)$$

$$= \rho c_p |u_*| \sqrt{\frac{C_f}{2}} + 0.21 \frac{\lambda}{H}[R_a]^{1/3}$$

where $Ra = g(T_w - \bar{T})H^3/(T \nu \alpha)$

= Rayleigh number, and

$$\frac{C_f}{2} = \left(\frac{u_*}{u_{ref}}\right)^2$$

= Surface friction coefficient.

Figure 1-1a displays the variation of w_e/u_* versus Ri_* predicted by the various models when isothermal heavy gas clouds disperse in a neutrally stratified environment and the gravity head is small (i.e. $u_g \rightarrow 0$). Figure 1-1b displays the variation of w_e/w_* versus Ri_* predicted by the relevent entrainment models when there is no mean motion (i.e. $\bar{u}_a = u_g \simeq 0$) and mixing results from surface generated convective motions. Other than the agreement that w_e/u_* should decrease monatonically with an increase in Ri_*, there is neither concensus concerning asymptotic behavior of the curve as $Ri_* \rightarrow 0$, nor is there agreement concerning the functional dependence on Ri_*.

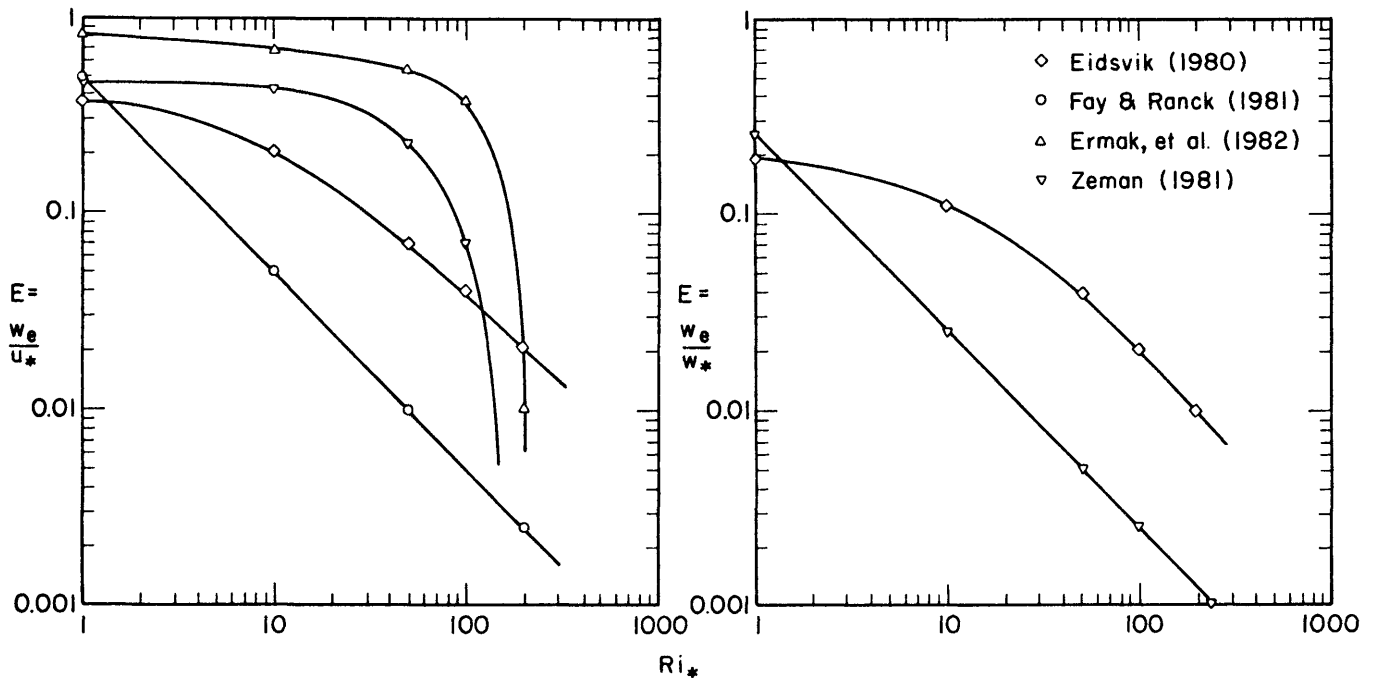

Figure 1-1a. Proposed Models for Mechanical Mixing Influence on Entrainment Across Stably Stratified Fluid Layers

Figure 1-1b. Proposed Models for Convective Mixing Influence on Entrainment Across Stably Stratified Fluid Layers

Diffusivity Models:

Diffusivity models postulate that the flux of some scalar $\bar{\xi}$ is related to gradients of mean values of the scaler $\bar{\xi}$, i.e.

$$\overline{w'\xi'} = -K_{\xi} \frac{d\bar{\xi}}{dx_i}. \qquad (1\text{-}10)$$

Most models which utilize a diffusivity approach assume that the transport of the scalar of interest is similar to transport of momentum flux, $\overline{u'w'}$; thus, one can utilize the large literature available concerning momentum transport rates. Expressions used for heavy gas dispersion include algebraic equations for $K_{\xi} = f(z, u_*, Ri_*, z_o, \text{etc.})$ or are calculated from additional transport equations for turbulent kinetic energy, q, or length scale, ℓ, where one assumes $K_{\xi} = \alpha q^{1/2} \ell$.

Algebraic equations for diffusivity have been used by Colenbrander (1980) in his vertically integrated slab model. The transport equation approach has been used by England et al. (1978).

Colenbrander (1980) constructed a depth averaged model for dense gas dispersion based on a similarity solution of two dimensional diffusion equations for plume vertical and lateral standard deviations. He presumed the vertical diffusivity varied as

$$K_z = \frac{k u_* z}{\phi(Ri_*)} \qquad \text{and} \qquad (1\text{-}11)$$

the lateral diffusivity varied as

$$K_y = K_o u W^{\gamma}$$

where k = von Karman constant

$\phi(Ri_*)$ = Stratification function determined from the empirical data of Kantha et al. (1977) and McQuaid (1976)

$$= 0.74 + 0.25\ Ri_*^{0.7} + 1.2 \times 10^{-7} Ri_*^3,$$

$$Ri_* = g'H/u_*^2,$$

W = characteristic plume width of concentration profile, and

K_o and γ = constants determined from the crosswind behavior of the dispersion coefficient σ_y during ground level passive gas dispersion experiments (Turner, 1969)

Although this model does not account for source spread at the origin, Colenbrander provides an ad hoc method based on maximum permissible vertical vapor flux to specify an initial source length and width. The model has been adapted to include adiabatic entrainment of moist ambient air, but it does not correct for surface heat transfer.

Chan (1983) also used an algebraic diffusivity model in a finite element model developed for simulation of heavy gas dispersion. The vertical diffusion coefficient was given as

$$K = \frac{k\ [(u_* z)^2 + (w_* \ell)^2]^{1/2}}{\phi(Ri_*)} \qquad (1\text{-}12)$$

where k is the von Karman's coefficient, u_* and w_* are the familiar friction and convective velocities respectively, ℓ is a cloud height

function weighted by the total cloud height, and $\phi(Ri_*)$ is a stability factor. Ri_* is a Richardson number weighted between the ambient stratification conditions and the state of the heavy cloud itself, i.e.

$$Ri_* = u_*^2 \frac{Ri_a}{(u_*^2 + w_*^2)} + \alpha_2 \frac{(\rho - \rho_a)}{\rho} \frac{g\ell}{u_*^2 + w_*^2} \qquad (1\text{-}13)$$

and $Ri_a = z/L_{mo}$, L_{mo} being the Monin-Obukhov length scale, * corresponding to the stability class of the ambient atmosphere. Note the similarity in defining parameters in the entrainment and diffusivity expressions despite the wide variability in the functions themselves.

Mixing Due to Thermally Driven Motions:

As a cold dense gas advects over a warmer underlying surface there is an opportunity for unstable buoyancy effects to cause a large increase in cloud temperature, cloud turbulence, and subsequent entrainment over the top of the cloud. The extensive evidence for fluid motions and mixing caused by convection from heated surface has been reviewed by Turner (1973). At the large Rayleigh numbers ($Ra > 10^5$) frequently associated with geophysical scales he suggests

$$Nu = C\ Ra^{1/3} \qquad (1\text{-}14)$$

where Nu = Nusselt number $= \frac{h_s H}{\lambda}$

Ra = Rayleigh number $= \frac{g\ \Delta T\ H^3}{T\ \alpha\ \nu}$,

---

* L_{mo} is a length scale uniquely defined from the parameters of buayoncy, g/T, friction velocity, u_*, and heat flux, $\overline{w'T'}$

$$= - \frac{u_*^3 T}{kg\overline{w'T'}}.$$

and C = 0.069 when ΔT is the temperature difference between the surface and the environment or C = 0.193 when ΔT is one half the temperature difference. (A value of 0.21 is sometimes used in atmospheric calculations.) λ is the thermal conductivity.

When convective motions produced by surface heating cause an unstable region to penetrate into an adjacent stable layer the term "penetrative" convection is used. Deardorff, Willis and Lilly (1969) set up a nearly linear stable temperature gradient in a tank of water, increased the temperature of the bottom to a new fixed value so that convection began, and measured vertical profiles of the horizontally averaged temperature with time. A convective turbulence velocity, w_*, can be defined which characterizes the turbulent motions,

$$w_* = [+ \frac{g}{T} (\overline{T'w'})_o H]^{1/3}, \qquad (1\text{-}15)$$

and $$E = \frac{w_e}{w_*} = f(Ri_*),$$

where now $Ri_* = \frac{g'H}{w_*^2}$. Analytical manipulations by Tennekes and Driedonks (1980) with the assumption that the initial temperature gradients are linear and that mixed region temperature regions are uniform suggest

$$\frac{w_e}{w_*} = \frac{0.5}{Ri_*}. \qquad (1\text{-}16)$$

The experimental results of Deardorff et al. (1969) indicated that the constant of proportionally falls between 0.3 to 1.5. (See Figure 1-2.)

Mixing Due to Simultaneous Mechanical and Thermally Driven Motions:

Gravity driven cold vapor clouds mix due to turbulence generated both by mechanical shear stresses and thermal convection. The cloud initially spreads like a wall jet beneath an overlaying boundary layer; thus the cloud sees disturbing forces from both above and below. Since no laboratory measurements have previously combined these modes of mixing for stratified layers it is common to assume superposition of effects in semi-emperical solution techniques (i.e. Eidsvik, 1980; Zeman 1982; Ermak et al. 1982).

1.2.2 Laboratory Data on Turbulent Entrainment Across a Stable Density Interface

Although there are many experiments which involve the mixing of a dense fluid with a surrounding medium, relatively few have been designed to specifically illuminate the mixing rates as a function of specified buoyancy and mixing scales. The exceptions are a set of liquid experiments involving the mixing of fresh and salt water performed by Lofquist (1960), Kato and Phillips (1969), Kantha, Phillips, and Azad (1977), and Deardorff, Willis, and Lilly (1969). The data from these experiments are frequently referenced to specify constants in entrainment models like those discussed in Section 1.2.1.

Mixing Due to Mechanically Driven Motions:

Lofquist (1960) made observations on a density current system in which salt water flowed turbulently under a pool of fresh water. The density and rate of flow of the salt water were varied, resulting in varying degrees of agitation of the interface. During the Lofquist

experiments density was specified by conducting measurements on drawn samples, and velocities were measured with a cylindrical drag balance or timed dye and pellet particles. Interface slope and variation with time of the depth of fresh and salt water were followed with dye tracers. Surface stresses were not measured directly, but they were calculated from the velocity profiles and a solution of the equations of motion. Entrainment was found to be a function of Reynolds number and a densimetric Froude number (reciprocal Richardson number). At sufficiently large flow rates (large Reynolds number) the interface surface was agitated and subsequent mixing variations appeared to depend only upon the densimetric Froude number, $Fr = u^2/(g(\Delta\rho/\rho_s)H$.

Lofquist found that $w_e/u = f(Fr)$. If one assumes $u_*^2/u_R^2 \rightarrow 0.0025$ at sufficiently high Reynolds numbers, then one concludes that $w_e/u_* = \alpha_4/Ri_*$ and $\alpha_4 \simeq 2.4$ are not inconsistent with the data scatter. Germeles and Drake (1975) extrapolated the Lofquist data to field scale LNG spill conditions and concluded $w_e/u \simeq 0.1$. Since the data set comprises a rather limited range of either Ri_* or $\Delta\rho/\rho_s$ it is likely any expressions for w_e contain large errors.

Kato and Phillips (1969) and Kantha et al. (1977) performed measurements on the penetration of a turbulent layer into a stratified fluid using an annular race-track-shaped flume, where the flow was driven by dragging a plastic screen over the top of the liquid layer at a constant rate. Kato and Phillips studied the mixing of a linearly stratified fluid with time, whereas Kantha et al. began with a stable two-layer stratified fluid. Measurements included surface shear, velocity, interface variation with time, and density variations.

Kato and Phillips concluded that mechanical mixing results in entrainment velocities which vary with Richardson number as,

$$\frac{w_e}{u_*} = \frac{2.5}{Ri_*} \quad . \tag{1-17}$$

Kantha et al. studied a wider range of Ri_* and avoided radiation of internal gravity waves by use of a homogenous lower layer. They found the entrainment rate had no simple power-law dependance on Ri_* over the whole range studied (see Figure 1.2). The slope of measurements is like Ri_*^{-1} over the range $90 < Ri_* < 400$. In addition the later measurements produced entrainment rates about twice as large as the Kato and Phillips data. The reduced entrainment rate in the Kato and Phillips experiments was attributed to energy lost to internal waves.

Mixing Due to Thermally Driven Motions

Deardorff et al. (1969) performed laboratory experiments of non-steady penetraive convection in water to simulate the lifting of an atmospheric inversion above heated ground. A cylindrical tank with an inside diameter of 54.8 cm and a height of 35.5 cm was filled with distilled water. Its side walls were insulated. A metal tray containing a circulating water both maintained the upper surface of the distilled water at a constant temperature. The lower boundary of the container was an aluminum disk in thermal contact with copper heating coils beneath.

Initially a continuous, approximately linear, temperature increase with height was maintained by setting the upper and lower surface temperatures constant over a period of 6 hours. Thermal convection were initiated by replacing the lower boundary cooling water with warm water.

During the unsteady re-establishment of new temperature profiles resistance thermoeters and thermocouples were traversed vertically through the water. Vertical profiles of horizontally averaged temperatures and heat flux were determined. This data permitted the calculation of layer entrainment velocities which are plotted on Figure 1-2. Note that the Richardson number range is limited to values near $Ri_* = 100$ and that the entrainment ratio, E, varies by a factor of five.

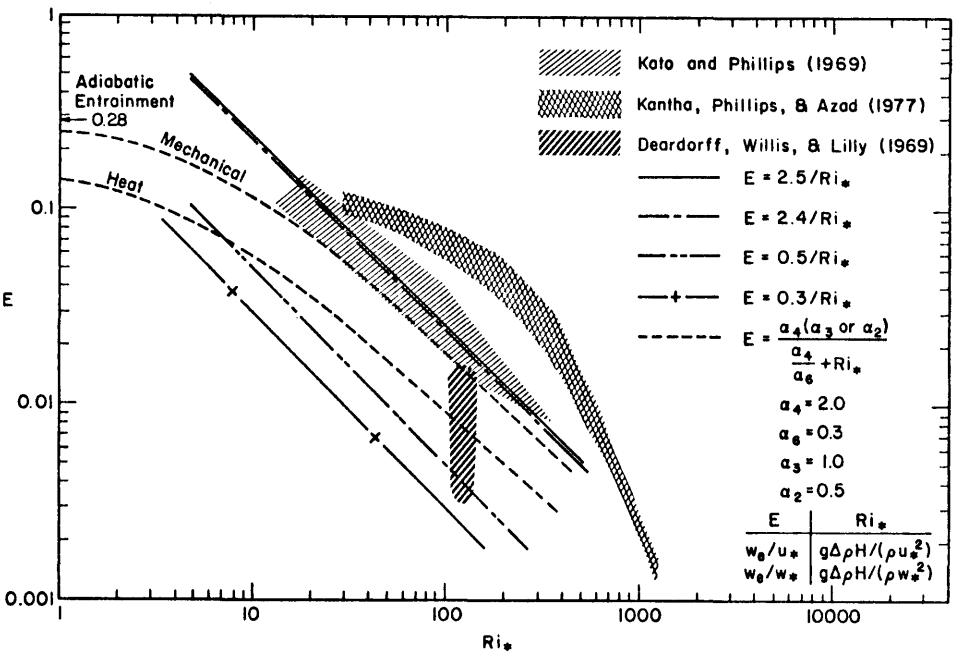

Figure 1-2. Laboratory Data on Turbulent Entrainment Across Stably Stratified Fluid Layers

2.0 PHYSICAL MODELING OF COLD DENSE CLOUD MOTION

To obtain a model for a heavy gas plume dispersion problem one must combine pertinent physical variables and parameters into a logical expression. This task is achieved for analytic or numerical models by formulating the conservation equations for mass, momentum, and energy. These equations together with site and source conditions and constitutive relations describe the actual physical interrelationship between the various independent (space and time) and dependent (velocity, temperature, pressure, density, concentration, etc.) variables.

These generalized conservation statements are too complex to be solved by present analytical or numerical techniques. It is also impossible to create a physical model at a reduced geometric scale for which exact similarity exists for all the dependent variables over all the scales of motion present in the atmospnere. Thus, one must resort to various degrees of approximation to obtain a solution. At present purely analytical or numerical solutions of plume dispersion are unavailable because of the classical problem of turbulent closure. Alternative techniques rely heavily upon empirical input from observed or physically modeled data. The empirical-analytical-numerical solutions have been combined into several different predictive approaches (reviewed in Section 1.2.1). The estimates of dispersion by these approaches are often crude; hence, they should only be used when the approach and site terrain are uniform and without obstacles. Boundary-layer wind tunnels are capable of accurately modeling plume processes in the atmosphere under certain restrictions. These restrictions are discussed in the next few sections.

2.1 Simulation of the Atmospheric Surface Layer

The atmospheric boundary layer is that portion of the atmosphere extending from ground level to a height of approximately 1000 meters within which the major exchanges of mass, momentum, and heat occur. This region of the atmosphere is described mathematically by statements of conservation of mass, momentum, and energy (Cermak, 1975). The mathematical requirements for rigid laboratory-atmospheric-flow similarity may be obtained by fractional analysis of these governing equations (Kline, 1965). This methodology is accomplished by scaling the pertinent dependent and independent variables and then casting the equations into dimensionless form by dividing by one of the coefficients (the inertial terms in this case). Performing these operations on such dimensional equations yields dimensionless parameters commonly known as:

Reynolds number	$Re = (UL/\nu)_r$	$= \frac{\text{Inertial Force}}{\text{Viscous Force}}$
Bulk Richardson number	$Ri = [Lg(\Delta T/T)/U^2]_r$	$= \frac{\text{Gravitational Force}}{\text{Inertial Force}}$
Rossby number	$Ro = (U/L\Omega)_r$	$= \frac{\text{Inertial Force}}{\text{Coriolis Force}}$
Prandtl number	$Pr = [\nu/(\lambda/\rho C_p)]_r$	$= \frac{\text{Viscous Diffusivity}}{\text{Thermal Diffusivity}}$
Eckert number	$Ec = [U^2/C_p(\Delta T)]_r$	

For exact similarity between different flows which are described by the same set of equations, each of these dimensionless parameters must be equal for both flow systems. In addition to this requirement, there

must be similarity between the surface-boundary conditions and the approach flow wind field.

Surface-boundary condition similarity requires equivalence of the following features:

a. Surface-roughness distributions,

b. Topographic relief, and

c. Surface-temperature distribution.

If all the foregoing requirements are met simultaneously, all atmospheric scales of motion ranging from micro to mesoscale could be simulated within the same flow field. However, all of the requirements cannot be satisfied simultaneously by existing laboratory facilities; thus, a partial or approximate simulation must be used. This limitation requires that atmospheric simulation for heavy gas dispersion must be designed to simulate most accurately those scales of motion which are of greatest significance for transport and dispersion of dense gas clouds.

2.1.1 Partial Simulation of the Atmospheric Boundary Layer

For the case of the interactions between a heavy plume released at ground level and the atmospheric boundary layer several of the aforementioned parameters are unnecessarily restrictive and may be relaxed without causing a significant effect on the resultant concentration field. The Rossby number magnitude controls the extent to which the mean wind direction changes with height. The effect of coriolis-force-driven lateral wind shear on plume dispersion is only significant when the plume height is of the same order of magnitude as the boundary layer height. Ground level dense plume heights are usually two orders of magnitude smaller than the atmospheric boundary layer height. The Eckert

number (in air Ec = 0.4 Ma^2 ($T_r/\Delta T_r$), where Ma is the Mach number) is the ratio of energy dissipation to the convection of energy. In both the atmosphere and the laboratory flow the wind velocities and temperature differences are such that the Eckert number is very small; hence, it is neglected. Prandtl number equality guarantees equivalent rates of momentum and heat transport. Since air is the working fluid in both the atmosphere and the laboratory Prandtl number equality is always maintained.

The approach flow Richardson number (Ri) and Reynolds number (Re) determine the kinematic and dynamic structure of turbulent flow within a boundary layer. This influence is apparent in the variations that occur in the spectral distribution of turbulent kinetic energies with changing Ri (Figure 2-1) and changing Re (Figure 2-2).

Richardson numbers characteristic of non-neutrally stable conditions can be obtained in wind tunnel facilities that control air and floor temperatures. Figure 2-1 displays the influence of stratification on the turbulent structure in the atmospheric boundary layer. Unstable conditions cause the energy of large scale fluctuations to increase and stable conditions cause the energy of large scale fluctuations to decrease.

Re equality implies $u_m = (L_p/L_m)u_p$. Re equality at a significantly reduced length scale would cause the models flow velocity to be above sonic; hence, its equality must be distorted. Figure 2-2 shows that a reduced Re changes only the higher frequency portion of an Eulerian type description of the spectral energy distribution.

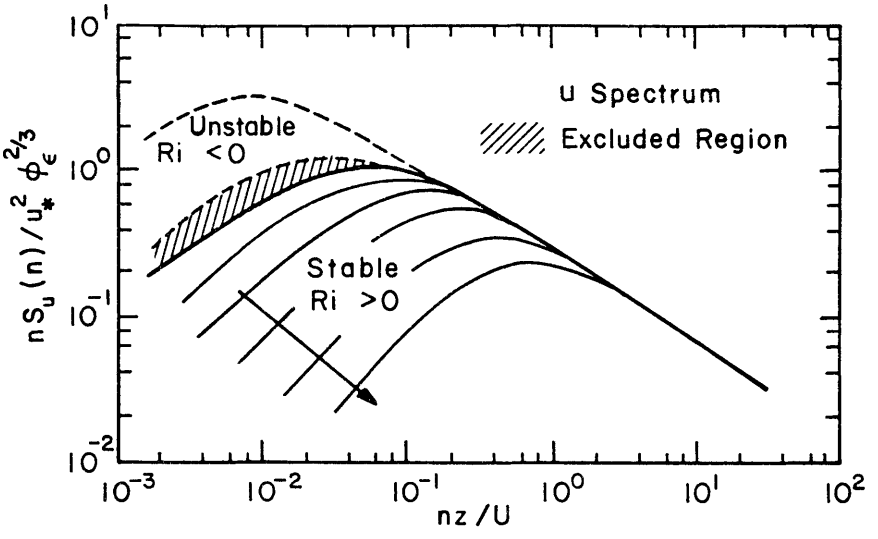

Figure 2-1. Variation of Turbulent Velocity Power Spectrum with Richardson Number

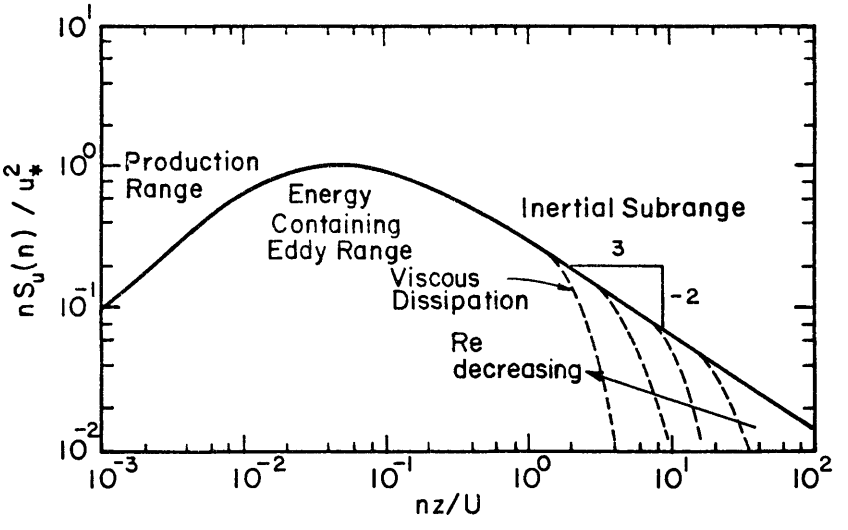

Figure 2-2. Variation of Turbulent Velocity Power Spectrum with Reynolds Number

Unfortunately there is no precise definition as to which portion of an Eulerian Spectrum is dominant in dispersing ground level dense plumes.

Most investigators use a minimum Reynolds number requirement based on roughwalled pipe measurements, i.e. $Re = u_* z_o/\nu > 2.5$, where u_*, the friction velocity, and z_o, the roughness length, are derived from a log-linear fit to a measured mean velocity profile. The value 2.5 is an empirically determined constant. At Re below 2.5 it is observed that the mean velocity profiles in turbulent pipe flow lose similarity in shape and deviate from the universal curve of a rough wall turbulent boundary layer. For Re above 2.5 it is observed that the surface drag coefficient (and thus the normalized mean velocity profile) is invariant with respect to increasing Re. For Re between 0.11 and 2.5 the velocity profiles are characteristic of smooth wall turbulent boundary layers, and for values below 0.11 the growth of a laminar sublayer on the wall is observed to increase with decreasing Re.

Extrapolation of results from pipe flow measurements to flat plate boundary layers may cause a shift in the magnitude of the minimum Re requirement, but it is generally felt that this shift is small. Precise similarity in the universal form of mean wind shear may be necessary for invariance with respect to the surface drag coefficient, but this does not necessitate that precise similarity must exist for the invariance of dispersion. It is the distribution of turbulent velocities which has the greatest effect on dispersion. It is the mean wind shear, however, which generates the turbulent velocities. It is possible that the specification of a miniumum Re of 2.5 is overly conservative. The

criteria, Re > 2.5, for example, is not applicable for flow over complex terrain or building clusters.

To define the lower limit of Re for which turbulent dispersion is invariant in a particular model setting, the investigator should perform several passive plume releases at decreasing wind speeds (decreasing Re). The source strength corrected concentration fields (see Section 2.3) of the Re invariant plumes will all display a similar structure. The minimum acceptable Re is the lower limit of this class of similar plumes. At Re below this value the proper portion of the spectral energy distribution is not simulated.

Halitsky (1969) reported such tests performed for dispersion in the vicinity of a cube placed in a near uniform flow field. He found that for Re invariance of the concentration distributions over the cube surface and downwind the Re magnitude (based on H, the height of the cube and u_H, the velocity at H) must exceed 11,000.

The presence of a heavy gas plume could significantly change the Re range over which dispersion invariance exists. Velocities within a heavy plume released at ground level have been observed to be significantly less than those in the approach flow. The laminarization of the velocity field within the dense plume under these situations is highly possible; hence, the effect of Re magnitude on plume similarity can only be evaluated by direct comparison to field results.

2.2 Simulation of Heavy Cloud Motion

In addition to modeling the turbulent structure of the atmosphere in the vicinity of a test site it is necessary to properly scale the plume source conditions. One approach would be to follow the

methodology used in Section 2.1, i.e., writing the conservation statements for the combined flow system followed by fractional analysis to find the governing parameters. An alternative approach, the one which will be used here, is that of similitude. The method of similitude obtains scaling parameters by reasoning that the mass ratios, force ratios, energy ratios, and property ratios should be equal for both model and prototype. When one considers the dynamics of gaseous plume behavior the following nondimensional parameters of importance are identified *

$$\text{Mass Flux Ratio (M)} = \frac{\text{mass flow of plume}}{\text{effective mass flow of air}} = \frac{\rho_g W_g A_g}{\rho_a U_a A_a} = \left[\frac{\rho_s Q}{\rho_a U_a L^2}\right]_{\text{source}}$$

$$\text{Momentum Flux Ratio (F)} = \frac{\text{inertia of plume}}{\text{effective inertia of air}} = \frac{\rho_g W_g^2 A_g}{\rho_a U_a^2 A_a} = \left[\frac{\rho_s Q^2}{\rho_a U_a^2 L^4}\right]_{\text{source}}$$

$$\text{Densimetric Froude No. relative to the inertia of air (Fr)} = \frac{\text{effective inertia of air}}{\text{buoyancy of plume}} = \frac{\rho_a U_a^2 A_a}{g(\rho_g - \rho_a)V_g} = \left[\frac{U_a^2}{g\left(\frac{\rho_s - \rho_a}{\rho_a}\right)L}\right]_{\text{source}}$$

$$\text{Densimetric Froude No. relative to inertia of the plume (Fr}_s\text{)} = \frac{\text{inertia of plume}}{\text{buoyancy of plume}} = \frac{\rho_g W_g^2 A_g}{g(\rho_g - \rho_a)V_g} = \left[\frac{Q^2}{g\left(\frac{\rho_s - \rho_a}{\rho_s}\right)L^5}\right]_{\text{source}}$$

$$\text{Flux Froude No. (Fr)} = \frac{\text{momentum flux of air}}{\text{buoyancy momentum flux of plume}} = \frac{\rho_a U_a^2 A_a}{Qg(\rho_g - \rho_a)(L/U_a)} = \left[\frac{U_a^3 L}{Qg\left(\frac{\rho_s - \rho_a}{\rho_a}\right)}\right]_{\text{source}}$$

$$\text{Volume Flux Ratio (V)} = \frac{\text{volume flow of plume}}{\text{effective volume flow of air}} = \frac{W_g A_g}{U_a A_a} = \left[\frac{Q}{U_a L^2}\right]_{\text{source}}$$

---

* The scaling of plume Reynolds number is also a significant parameter. Its effects are invariant over a large range. This makes it possible to accurately model its influence by maintaining model tests above a minimum plume Reynolds number requirement. For the spread of a dense plume in a calm environment Simpson and Britter (1979) demonstrate that to obtain invariance for the entrainment rate and gravity head shape the Reynolds number, $Re = UH/\nu$ must exceed 500, where U is the head velocity and H is the height of the intrusion just behind the gravity head.

It is necessary to maintain equality of the plumes specific gravity, ρ/ρ_a, over the plumes entire lifetime to obtain simultaneous simulation of all of these parameters. Unfortunately a requirement for equality of the plume gas specific gravity leads to several complications in practice. These are:

1) Equality of the source gas specific gravity between a model and its atmospheric equivalent leads to a wind speed scaling of $u_m = (Lm/L_p)^{1/2} u_p$. For a significant range of atmospheric wind speeds this relationship leads to wind tunnel speeds at which there is a possible loss of the Reynolds number invariance in the approach flow.

2) A thermal plume in the atmosphere is frequently simulated in the laboratory by an isothermal plume formed from a gas of appropriate molecular weight. Under certain situations this practice will lead to a variation of the equality of plume density as the plume mixes with air.

3) When a thermal plume in the atmosphere is modeled by a thermal laboratory plume non-adiabatic heat transfer mechanisms are not modeled properly. Thus a variation of the equality of plume density occurs as the plume moves downwind.

It is important to examine each modeling situation and decide if an approximation to complete plume behavior may be employed without a significant loss in the similarity of the modeled plume structure. Section 2.2.1 discusses several different approximation methodologies which help formulate a physical model, and it addresses the errors incurred by such approximations.

2.2.1 Scaling of Isothermal Heavy Clouds

The range of applicability of a physical models predictive capabilities for full scale behavior depends upon the parameter combinations (wind speed, flow rate, density, etc.) which yield similar plume behavior. Given a set of parameter combinations, measurements on a sin-

gle plume will yield the behavior of all plumes in this category. Section 2.2.1.1 describes research of the similarity between plumes of different initial source specific gravities. Section 2.2.1.2 discusses the similarity between plumes of equal Flux Froude Numbers but different volume flux ratios. Section 2.2.1.3 discusses the similarity between plumes exposed to wind fields of slightly different characteristic length scales.

2.2.1.1 The Relaxation of Source Density Equality

The relaxation of source density equality during the modeling of plume dispersion has been proposed to avoid low wind speeds that are operationally difficult to maintain in most wind-tunnel facilities. Low wind speeds also introduce questions concerning the Reynolds number invariance of the approach flow. All enhanced scaling schemes which use the relaxation of source density equality increase the velocities used in the model. The relaxation of source density equality prohibits simultaneous equality of the remaining plume parameters. One must now choose which of these parameters are dominant for the plume being studied.

During the ground level release of a dense plume in which the release momentum is small it has been consistently argued that the dominate parameters are the Densimetric Froude No. with respect to the air (Fr) and the Volume Flux ratio (V). Since plume momentum is negligible and equality of the Flux Froude No. (Fr) is guaranteed with Fr and V equality the only neglected parameter of significance is the Mass Flux Ratio (M). Hall (1979) found good agreement between two tests in which the source gas specific gravities were 2.37 and 4.74. Recent tests con-

ducted by TNO (1980), however, found significant differences between plumes which had source specific gravities of 1.38 and 4.18. Tests conducted at Colorado State University (CSU) by Neff and Meroney (1982) demonstrate that the relaxation of source specific gravity will lead to significant errors when the source specific gravity is below a value of 2.0. All of the CSU tests were for continuous releases in which there were no topographic or building wake effects.

2.2.1.2 Relaxation of Volume Flux Equality

In this technique it is assumed the the Flux Froude Number (Fr) is the only dominant parameter, but the Volume Flux Ratio must not be grossly distorted.* Figures 2-3 and 2-4 demonstrate the potential for using this technique to enhance model scale wind speeds for the specific case of liquefied natural gas (LNG) spills.

Figure 2-3 converts the variables associated with a field reference plume (u_p, Q_p, SG_p) to those used in a physical model as constrained by the equality of the Densimetric Froude No., Fr and the Volume Flux Ratio, V (and thus equality of Fr). The intersection of the dark line with the dashed line representative of wind-tunnel to field length scale ratio yields the unique point for rigid similarity. If distortion in source density is allowed the simulation variables may be any point along a dashed line characteristic of the chosen length scale.

Figure 2-4 describes an alternative enhanced situation where only equality of the Flux Froude No. (Fr) is specified. Instead of a unique

---

* Whenever the Volume Flux Ratio is distorted between model and field plumes, then the model concentraton field must be scaled to that which would be seen in the field (Section 2.3).

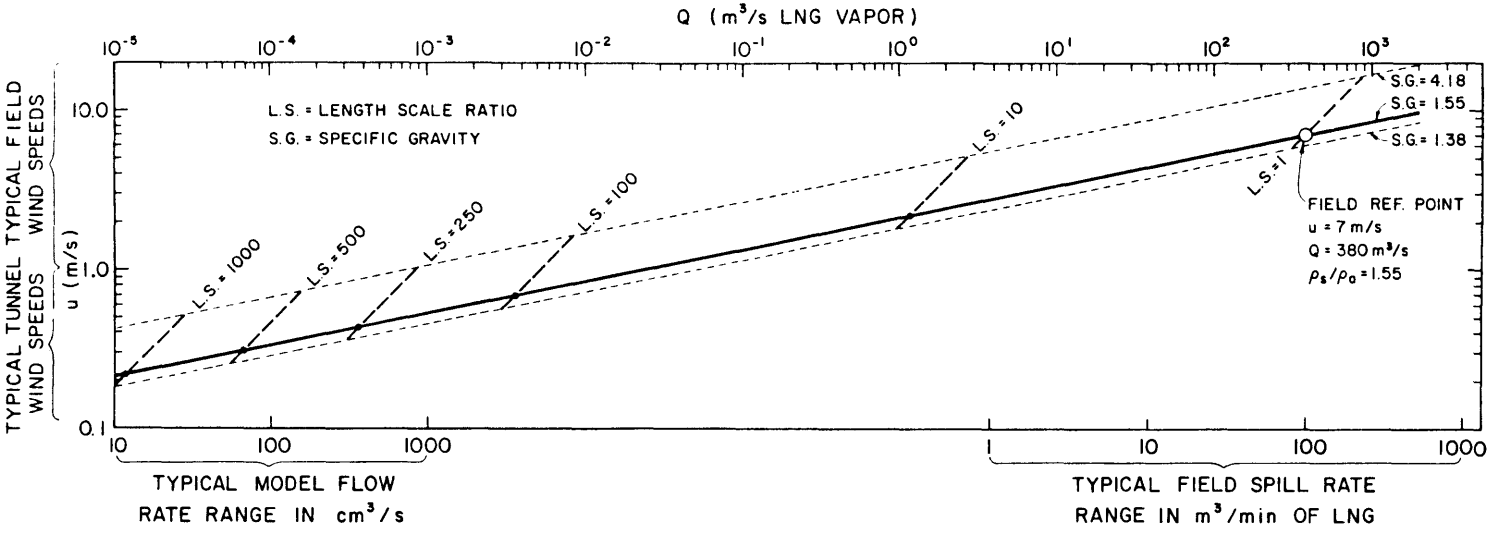

Figure 2-3. Field to Model Conversion Diagram for Densimetric Froude Number and Volume Flux Ratio Equality

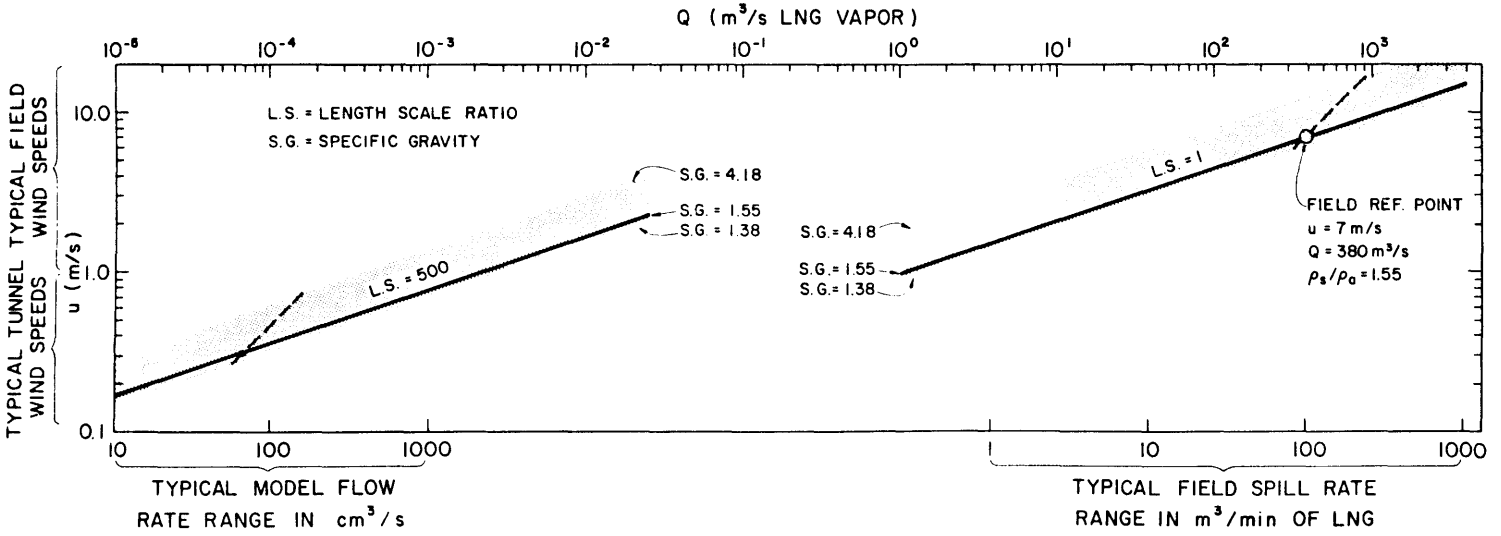

Figure 2-4. Field to Model Conversion Diagram for Flux Froude Number Equality

similarity point at a given length scale there is now a locus of points expressed by Q is proportional to u^3. If a distortion of plume source density is permissible then there is a broad band over which similar wind tunnel conditions may be chosen.

Neff and Meroney (1982) describe the results from a dense plume test series during which only a Fr criteria was used. It was found that the plumes were similar within experimental error for volume ratio distortions up to 1.5. All of the plumes studied were negatively-buoyant, ground-level releases with no topographic or building wake effects.

2.2.1.3 Velocity Field Length Scale Distortion

The choice of a length scale which is characteristic of a model boundary layer is a subject of some debate. Several different length scaling criteria have been cited. Some of these proposed scaling lengths are the roughness length, z_o, the boundary layer thickness, δ, the longitudinal integral scale of turbulence, Λ, and the peak wave number of the energy spectra of turbulent velocity fluctuations, k_p. Each of these scaling lengths has large variations associated with its calculation. For example, the parameter z_o can vary over a factor of two in describing the same velocity profile. This wide latitude in geometric scale partially explains why model length scale ratios for similar atmospheric situations often vary by a factor of ten in the literature. Some variation in model length scale ratio is permissible because many plume dispersion problems will be dominated by only a small portion of the scales of motion presented in a turbulent flow.

In light of the above arguments one way to enhance a model's wind speed would be to model the flow at a larger length scale. This type of

model enhancement is particularly viable if the plume being modeled only occupies a small portion of the boundary layer. Figure 2-5 displays the distortion in the mean shear flow for a length scale exaggeration of two. The deviation is quite small when on considers errors of this magnitude could be made in the estimation of the velocity profile in either boundary layer.

Neff and Meroney (1982) utilize this technique to compare different plumes released into the same velocity field. The results indicate that the technique works quite well for the case of near-field dispersion of ground based heavy plumes in the absence of topographic or wake effects. This same technique can be used to extend the measured results from a single plume released into the atmosphere to predict the behavior of many other atmospheric plumes over a limited scale distortion range.

2.2.2 Scaling of Cold Heavy Clouds

All of the scaling considerations mentioned in Section 2.2.1 for isothermal heavy clouds are equally applicable to the scaling of cold heavy clouds. But in the case of thermal plumes additional considerations must be made to insure that the model plumes specific gravity history is similar to that of its full scale counterpart. These additional considerations are:

1. Thermal expansion or contraction of the plume due to differences in the molar specific heat capacity of the plume source gas and air (i.e. $C^*_{p_a} \neq C^*_{p_g}$).
2. Release of latent heat during the entrainment of humid air, and
3. Heat transfer by conduction, convection or radiation across plume boundaries.

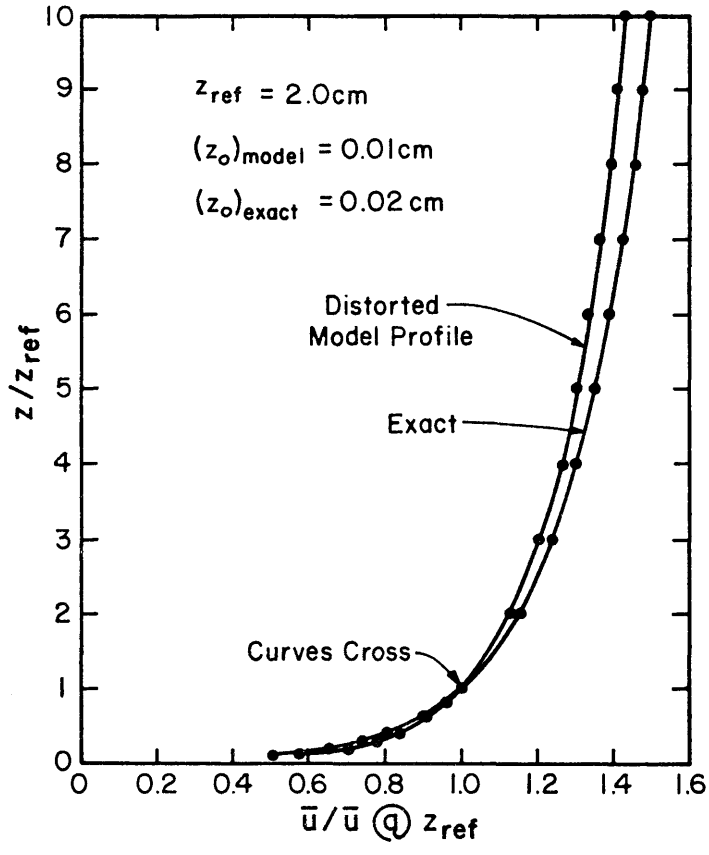

Figure 2-5. Mean Wind Shear Variation for a Two-fold Model Length Scale Distortion

The effect of molar specific heat capacity differences between the air and the plume is portrayed by considering the adiabatic mixing of two volumes of gas, one being the source gas, $\forall_s$, the other being ambient air, $\forall_a$. Consideration of the conservation of mass and energy for this system yields (Skinner and Ludwig, 1978)*:

$$\frac{\rho_g}{\rho_a} = \frac{\frac{\rho_s}{\rho_a}\forall_s + \forall_a}{\left(\frac{T_a}{T_s}\forall_s + \forall_a\right)\left(\frac{(C_p^*)_s}{C_p^*)_a}\forall_s + \forall_a\right)\left(\frac{(C_p^*)_s}{C_p^*)_a}\frac{T_a}{T_s}\forall_s + \forall_a\right)^{-1}} \qquad (2\text{-}1)$$

If the temperature of the air, T_a, equals the temperature of the source gas, T_s, or if the molar specific heat capacity, C_p^*, is equal for both source gas and air when the equation reduces to:

$$\frac{\rho_g}{\rho_a} = \frac{\frac{\rho_s}{\rho_a}\forall_s + \forall_a}{\forall_s + \forall_a} \qquad (2\text{-}2)$$

Thus for two prototype cases: 1) an isothermal plume and 2) a thermal plume which is mostly composed of air; it does not matter how one models the density ratio, thermally or isothermally as long as the initial density ratio value is equal for both model and prototype. For the case of a thermal plume whose molar specific heat capacity is different from air, such as an LNG vapor plume, the modeling of the density history variation within the plume can only be approximate. Figure 2-6 displays the variation in the density history behavior for the isothermal

---

* The pertinent assumption in this derivation is that the gases are ideal and properties are constant.

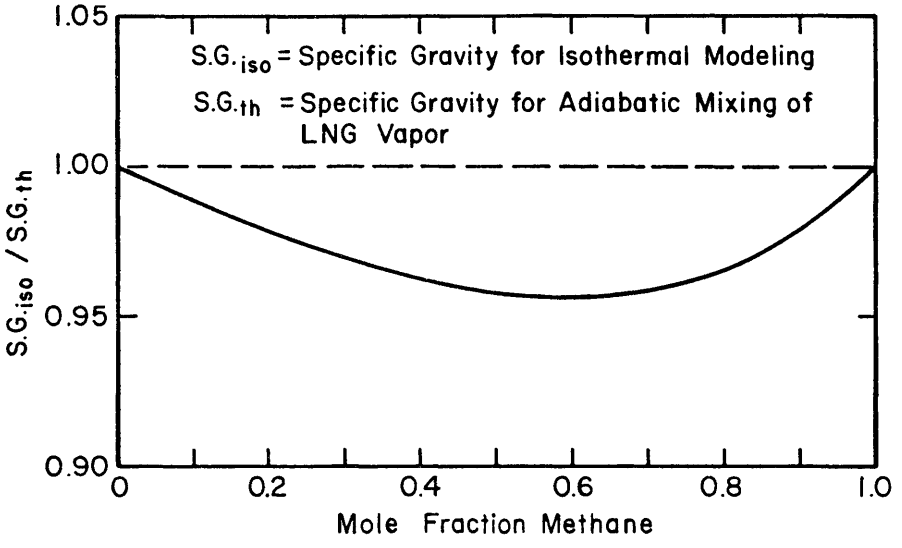

Figure 2-6. Specific Gravity Deviation in an Isothermal Model of LNG Vapor Dispersion

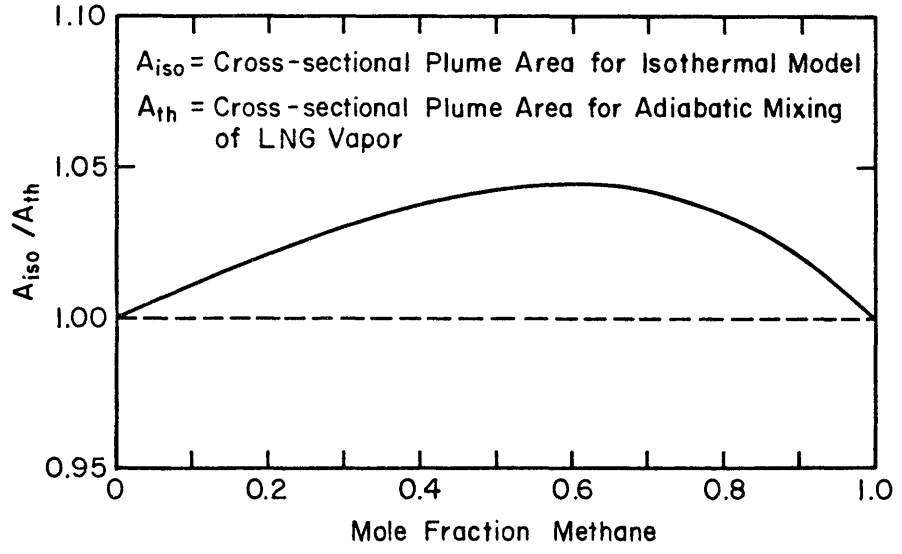

Figure 2-7. Plume Cross-sectional Area Deviation in an Isothermal Model of LNG Vapor Dispersion

simulation of a LNG vapor plume. Figure 2-7 displays the variation in the plume cross sectional area as the plume mixes with air for this same situation. Consideration of these two figures suggests that, although an isothermal simulation of an adiabatic LNG vapor cloud as it entrains dry air is not exact, it is a good approximation to actual behavior.

The release of latent heat through the entrainment of humid air can have a very significant effect on the density history of a thermal plume. Figure 2-8 displays the variation of plume density versus mole fraction of cold methane vapors when adiabatically mixed with atmospheres of different humidities. During an isothermal physical simulation of humid air/cold gas mixing large deviations in plume similarity would occur.

Heat transfer across the boundaries of an LNG vapor plume will be primarily governed by the modes of free, forced, or mixed convection. To assist in an improved understanding of the modeling of heat convection into an LNG vapor plume consider a simple energy balance between the cloud (g) and the ground (w):

$$\rho\, C_p \frac{d\, T_g}{dt} = h_s\, A(T_w - T_g).$$

Using the ideal gas law and non-dimensionalizing the equation by the reference scales ρ_a, L, $\Delta\theta$ and T = L/U yields,

$$\frac{d(S.G.)}{dt^*} = \left[\frac{-h_s\, \Delta\theta\, R/(MW)}{\rho_a\, C_p\, U}\right] S.G.\frac{A^*}{V^*}\, \Delta T^*.$$

This equation shows that in order to have the same specific gravity history between model and prototype plumes the quantity $\left[\frac{h_s\, \Delta\theta\, R/(MW)}{\rho_a\, C_p\, U}\right]$ must be equal. Since R/(MW), ρ and C_p are equal for model and prototype

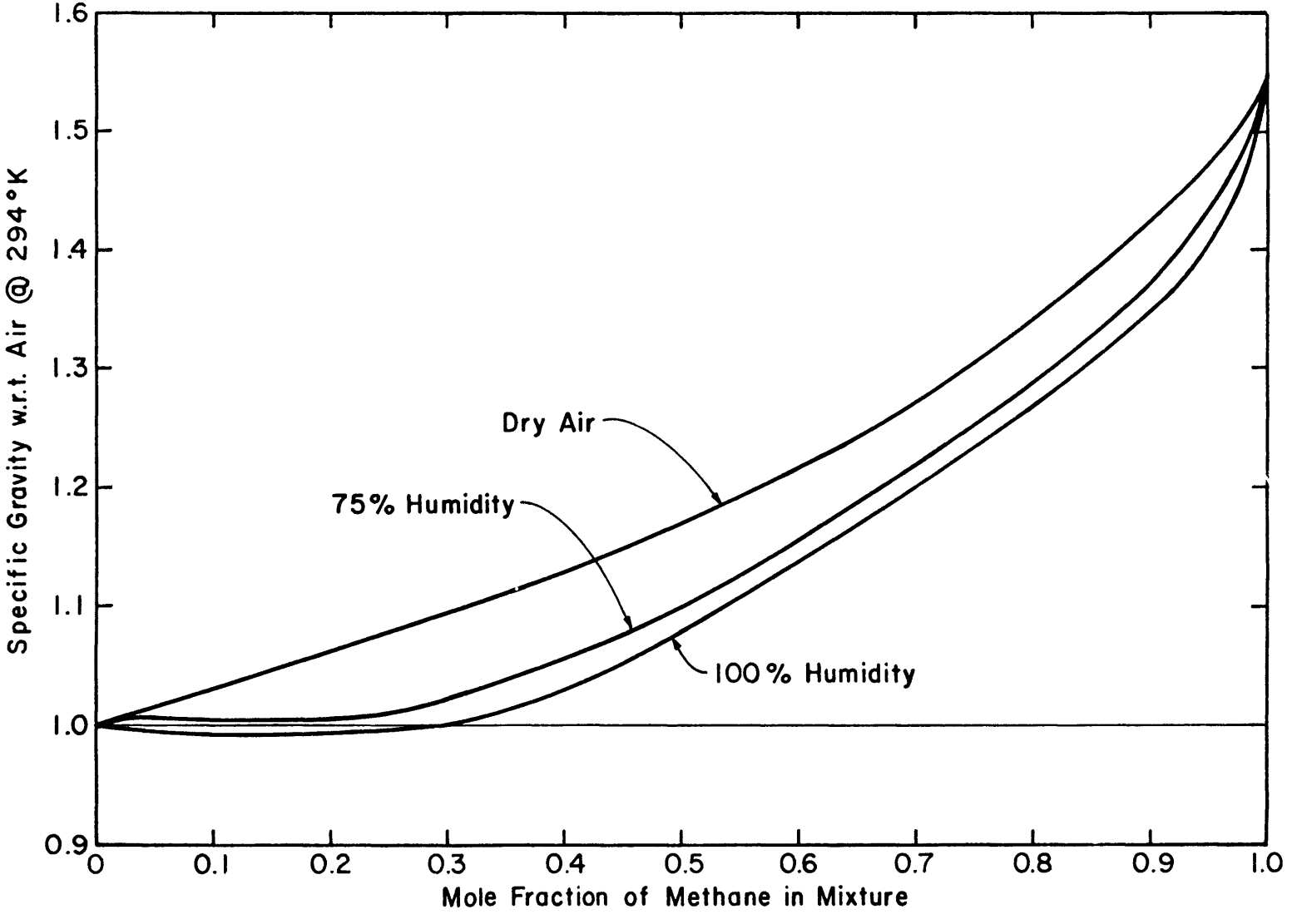

Figure 2-8. Specific Gravity of LNG Vapor-Humid Atmosphere Mixtures

this is equivalent to stating

$$\Delta\theta_m = \left(\frac{(h_s)_p}{(h_s)_m}\right)\left(\frac{U_m}{U_p}\right)\Delta\theta_p \qquad (2\text{-}3)$$

For the forced convection of turbulent flow over a flat plate a common empirical correlation is that the Stanton Number, $St = C_f/2$. From this relationship it is seen (with the assumptions that $\nu_m = \nu_p$, $Pr_m = Pr_p$, and $\lambda_m = \lambda_p$) that $(h_s)_p/(h_s)_m = (C_{f_p}/C_{f_m})(U_p/U_m)$. Due to the Reynolds No. independence of full rough turbulent flow $C_{f_m} = C_{f_p}$. Incorporation of this expression for $(h_s)_p/(h_s)_m$ into Equation (2-3) above shows that forced convection will be properly modeled when $\Delta\theta_m = \Delta\theta_p$.

For free convection from a horizontal plate a common empirical correlation is that the Nusselt number, $Nu = Gr^{1/3}$ where $Gr = \beta\Delta TL^3/\nu^2$ is the Grashof number. From this relationship it is seen (with the assumptions that $\beta = 1/T$ from ideal gas law, $\nu_m = \nu_p$ and $\lambda_m = \lambda_p$) that $\frac{(h_s)_p}{(h_s)_m} = \left(\frac{\Delta\theta_p}{\Delta\theta_m}\right)^{1/3}\left(\frac{(T)_m}{(T)_p}\right)^{1/3}$ Incorporation of this expression for $(h_s)_p/(h_s)_m$ into Equation (2-3) above along with the Froude no. modeling requirements of $U_m/U_p = (L_m/L_p)^{1/2}$ yields, $\Delta\theta_m = [(T)_m/(T)_p]^{1/4}(L_m/L_p)^{3/8}\,\Delta\theta_p$ When the requirements for proper modeling of forced convection) of $\Delta\theta_m = \Delta\theta_p$ is stipulated then the model clouds temperature is given by $(T)_m = (L_p/L_m)^{1.5}\,(T)_p$, an unrealistic requirement for the length scale ratios of practical interest. Consideration of the case where one models forced convection properly, i.e. $\Delta\theta_m = \Delta\theta_p$, and one forces $(T)_m = (T)_p$ this equation demonstrates that the heat transfer by free convection will be too large in the model plume.

2.3 Concentration Scaling Theory

Most plume studies measure the concentration magnitudes at distances far downwind from the source. In the limit as concentrations approached zero, the conventional concentration scaling laws for steady state plumes were developed. The form of this expression is:

$$K(x) = \chi U_H L^2 (\frac{T_a}{T_s}) Q,$$

where T_a and T_s are the temperatures of the ambient air and the source gas respectively. Q in this expression is the total source gas flow rate evaluated at source conditions. When modeling the plume at a reduced scale the function K(x) is determined by experimental measurements usually in an isothermal setting where $T_a = T_s$. Provided that the proper similarity requirements were satisfied then the function K(x) will be equal for field and model plumes. The effects caused by volume flux ratio distortion and source gas temperature differences between model and prototype are accounted for by the expression. This technique is completely satisfactory in the limit as concentration approaches zero. In the case of modeling plume concentration in the near field, such as is the case with flammable plumes, this relationship is not satisfactory. The problems lie in the asymptotic behavior as the concentration, χ, approaches one. $K(0) = U_H L^2 / (\frac{T_a}{T_s}) Q$ indicates that K is not a function of the downwind position, x, alone. It is a function of both x and $U_H L^2 / (\frac{T_a}{T_s}) Q$. To alleviate these problems the following generalized concentration scaling methodology was formulated.

Figure 2-9 will aid in understanding the derivation of this generalized concentration scaling methodology. Continuity of total molar flow rate of source gas at the source (section A-A) and at some downwind cross-sectional area (section B-B) requires that

$$\dot{n}_s = \int_{B-B} \dot{n}''_s \, dB \ .$$

where $\dot{n}_s$ is the total molar flow rate of source gas and $\dot{n}''_s$ is the molar flux of source gas through some differential area dB. Definition of concentration χ requires that

$$\chi = \frac{\dot{n}''_s}{\dot{n}''_s + \dot{n}''_a} \ .$$

Rewriting this expression as $\dot{n}''_s = (\frac{\chi}{1-\chi})\dot{n}''_a$ and substituting it into the expression for $\dot{n}_s$ yields

$$\dot{n}_s = \int_{B-B} (\frac{\chi}{1-\chi})\dot{n}''_a \, dB \ .$$

The mean value theorem of integral calculus allows one to rewrite the equation as

$$\dot{n}_s = \frac{\chi(\xi,\eta)}{1 - \chi(\xi,\eta)} \int_{B-B} \dot{n}''_a \, dB \ ,$$

where $\chi(\xi,\eta)$ is the value of χ at some point, (ξ,η) on the surface B-B. The total molar flow rate of air across the entire plume boundary up to section B-B (surface σ) and the molar flow rate of air through section B-B are equal; hence,

$$\dot{n}_s = \frac{\chi(\xi,\eta)}{1-\chi(\xi,\eta)} \int_{\sigma} \dot{n}''_a \, d\sigma \ .$$

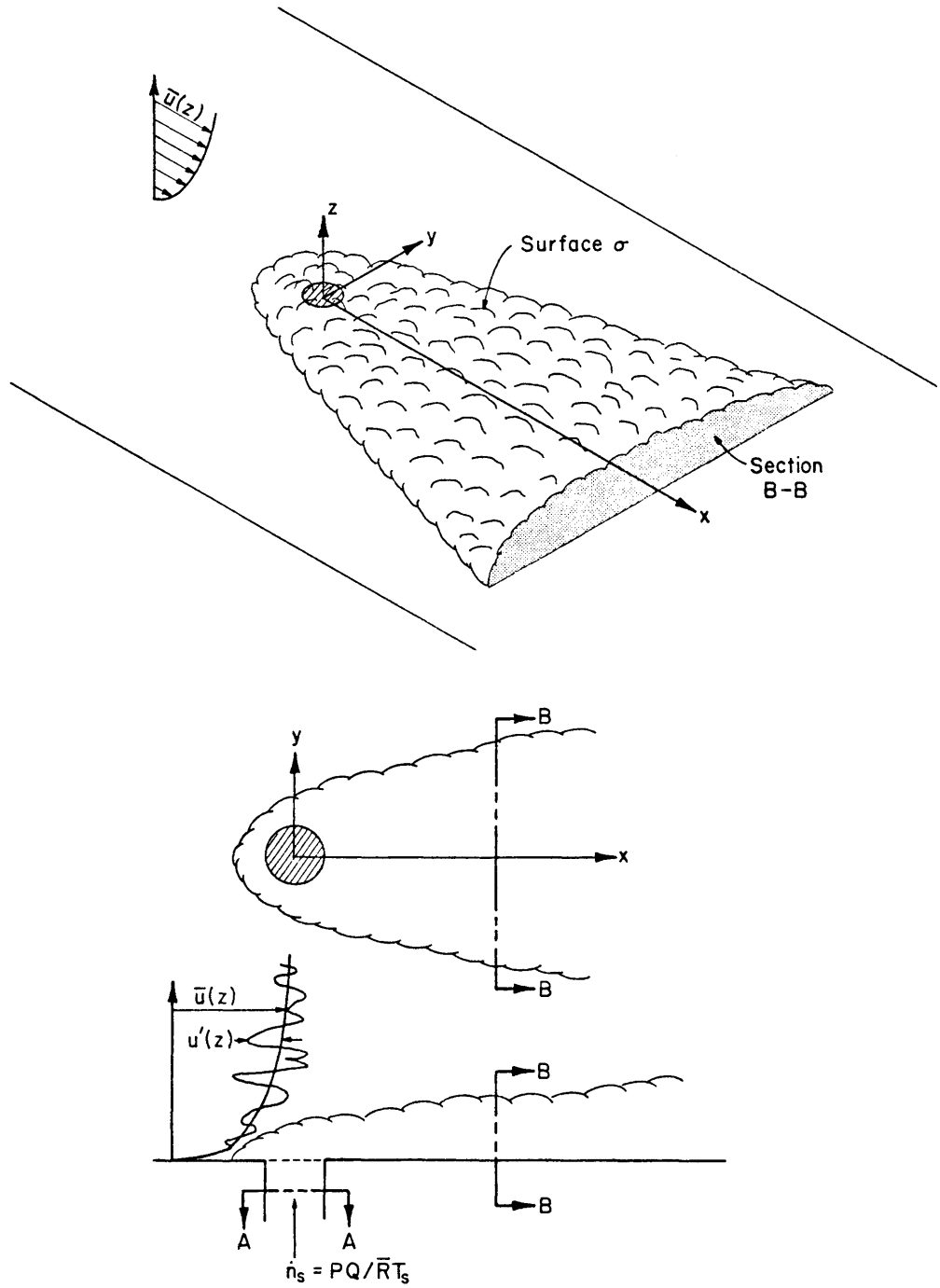

Figure 2-9 Notation Definition Diagram for Concentration Scaling Theory Derivation

Let $\dot{n}_s = \frac{PQ}{\bar{R}T_s}$ and $\dot{n}''_a = \frac{Pw_e}{\bar{R}T_a}$ where u_e is the entrainment velocity of air across the boundary σ. Dividing the entire equation by $\frac{\chi}{1-\chi}$, where χ is evaluated at the point of interest on the surface B-B, say χ_t and rearranging the equation cancelling constant quantities such as P and $\bar{R}$ yields

$$\left(\frac{T_s}{T_a}\right)\left(\frac{\chi_{\ell}}{1-\chi_{\ell}}\right)\frac{\int_{\sigma} w_e \, d\sigma}{Q} = \frac{\chi_{\ell}/(1-\chi_{\ell})}{\chi(\xi,\eta)/(1-\chi(\xi,\eta)} \quad .$$

The expression on the right side of this equation is a function of the χ profile at the surface B-B; thus, it is a function of downwind position position, x, only. Provided that two plumes satisfy the proper similarity requirements when $\frac{(w_e)_m}{(w_e)_p} = \frac{(u_H)_m}{(u_H)_p}$ or ($w_e \alpha u_H$), $\sigma_m/\sigma_p = L_m^2/L_p^2$ (or $\sigma \alpha L^2$), and the concentration profiles will have the same form. Utilizing these factors, the final form of a concentration scaling law that relates the concentration distributions in plumes that are physically similar is

$$\left(\frac{T_s}{T_a}\right)\left(\frac{\chi}{1-\chi}\right)\left(\frac{u_H L^2}{Q}\right) = K(x) \quad .$$

Some observations on the utility of this expression are summarized below.

- As concentration, χ approaches zero this expression becomes the first part of this section.
- Note that the quantity $u_H L^2/Q$ is the inverse of the Volume Flux Ratio; thus this expression corrects the entire concentration field for distortions in the similarity of this parameter as specified in some of the enhanced simulation techniques described in Section 2.2.1.

- The quantity T_s/T_a corrects for the fact that concentrations measured at spacially similar points will be different for a thermal plume than for an isothermal plume.

- The function K(x) can be viewed quite simply in the following format

$$K(x) = \frac{\dot{n}_a/\dot{n}_s}{\dot{n}''_a/\dot{n}''_s} .$$

Thus it is the ratio of the quantity $\dot{n}_a/\dot{n}_s$ evaluated for the entire plume to that same quantity evaluated at a single point within the plume.

- Given the equality of $K(x)_m = K(x)_p$ then a convenient formula for the conversion from a modeled concentration to a prototype concentration is given by

$$\chi_p = \frac{\chi_m}{\chi_m + (1-\chi_m)[(\frac{T_a}{T_s})V]_m / [(\frac{T_a}{T_s})V]_p} \quad , \text{ where } V = \frac{Q}{u_H L^2}$$

For reciprocal conversion from prototype to model simple exchange the m's and p's.

- If the indeterminant behavior of this formulation of $K(x)_{\chi}$ as $\chi \rightarrow 1$ is bothersome note that by the transformation $K'(x)=\frac{K(x)}{K(x)+1}$ this problem is allevated.

$$K'(x) = \frac{\chi}{\chi + (1-\chi)[(\frac{T_a}{T_s})Q/u_H L^2]}$$

This new function K'(x) has the convenient property that as $\chi \rightarrow 0$, $K'(x) \rightarrow 0$ and as $\chi \rightarrow 1$, $K'(x) \rightarrow 1$.

It is reemphasized that K(x) is only a universal function for plumes that are similar in both entrainment physics and normalized concentration variation in downwind plume cross-sections. All passive plumes in the absence of wake effects and significant initial momentum meet these conditions; hence, K(x) should be a universal function for

passive plume dispersion. Measurements on plumes of this type have universally confirmed such correlations. As the source and near field factors such as initial momentum, building wakes, and buoyancy effects become more dominant than the background flow in determining the entrainment physics and plume profiles, the universal character of K(x) is lost. For the specific case of downwind dispersion from negatively buoyant sources it is easily envisioned that, unless the buoyancy and inertial effects are properly matched, the resultant plume profiles will be drastically different.

3.0 DATA ACQUISITION AND ANALYSIS

Laboratory measurement techniques are discussed in this section, along with conversion methods which provide a basis for interpretation of model data in terms of field equivalent quantities. Some of the methods used are conventional and need little elaboration.

3.1 Wind-tunnel Facilities

The Environmental Wind Tunnel (EWT) shown in Figure 3-1 was used for all tests performed. This wind tunnel, specially designed to study atmospheric flow phenomena, incorporates special features such as an adjustable ceiling, rotating turntables, transparent boundary walls, and a long test section to permit reproduction of micrometeorological behavior at larger scales. Mean wind speeds of 0.10 to 12 m/s can be obtained in the EWT. A boundary layer depth of 1 m thickness at 6 m downstream of the test entrance can be obtained with the use of vortex generators and a trip at the test section entrance and surface roughness on the floor. The flexible test section roof on the EWT is adjustable in height to permit the longitudinal pressure gradient to be set to zero. The vortex generators and trip at the tunnel entrance were followed by 9.2 m. of smooth floor.

3.2 Model

A constant area continuous release model was constructed as shown in Figure 3-2a and was mounted flush with the floor of the EWT, where the boundary layer was fully developed. Two kinds of isothermal gases and three cooled gases were used in the series of experiments described herein. A heat exchanger, shown in Figure 3-2b, was used to carefully establish the proper thermal conditions of the source gas.

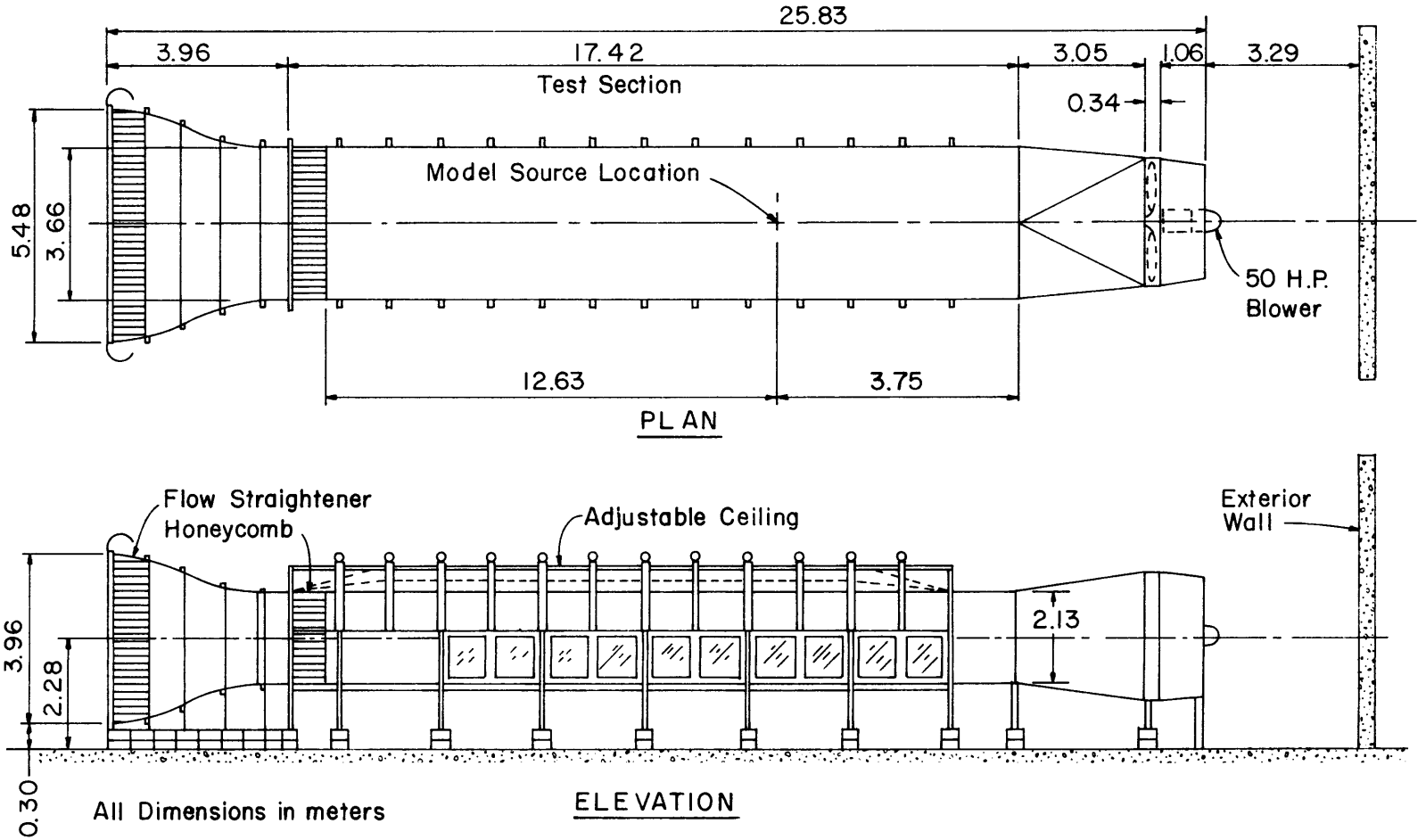

Figure 3-1. Environmental Wind Tunnel

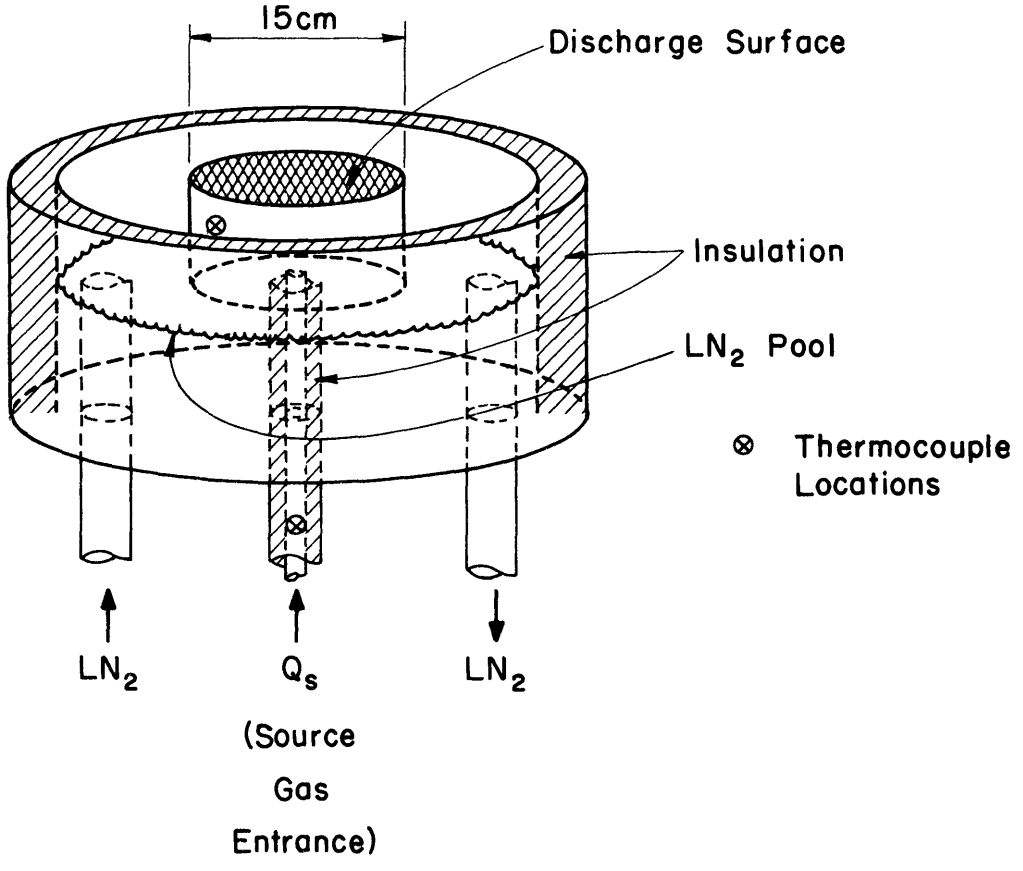

Figure 3-2a. Source Plenum Construction Details

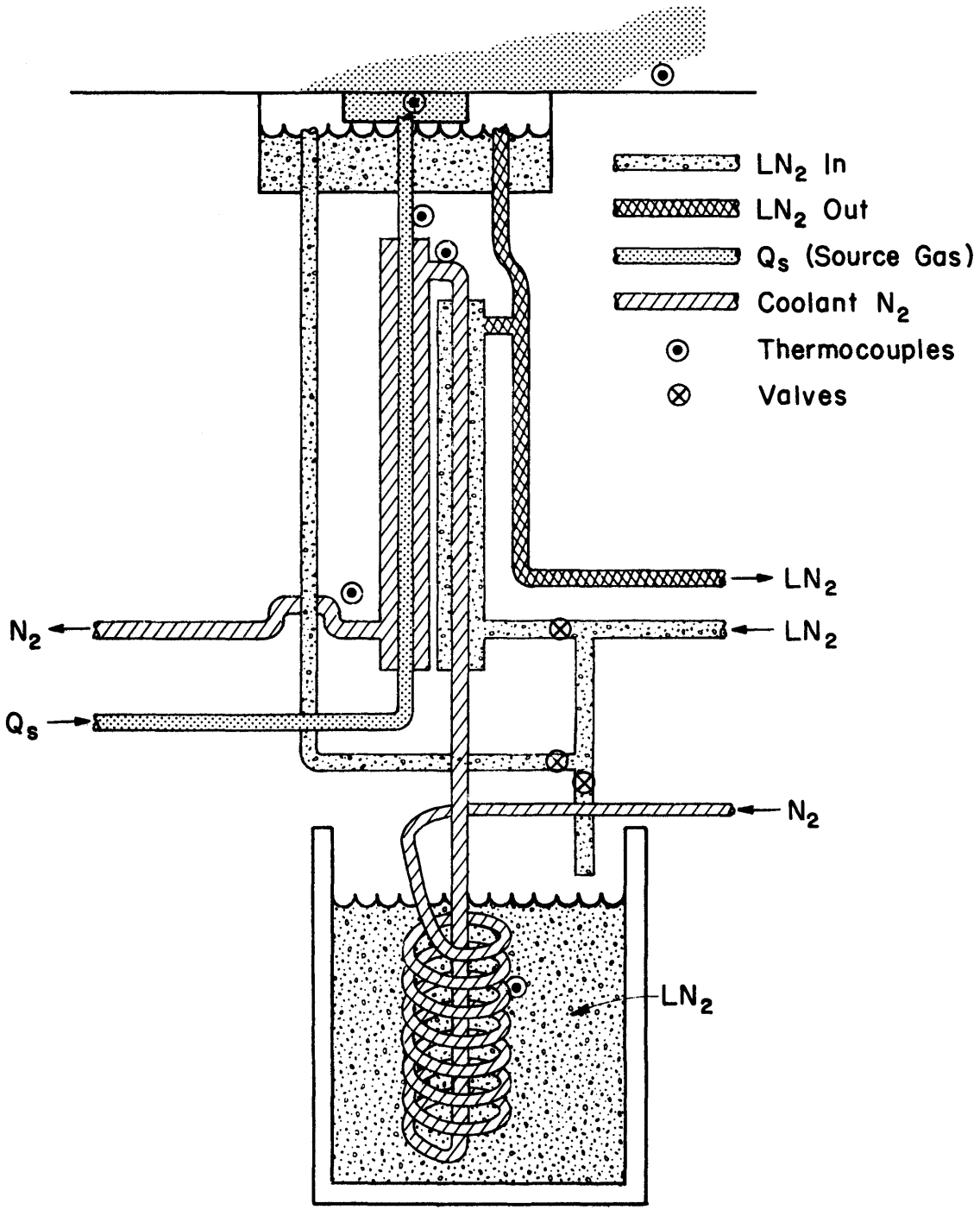

Figure 3-2b Schematic Diagram Cryogenic Heat Exchanger to Cool Source Gases and Plenum

The heat exchanger used nitrogen as the cold fluid both in gaseous and in liquid form. The source plenum contained a cavity in which a pool of liquid nitrogen was maintained, so that when the cooled source gas was released into the source plenum, little if any heating would result until the gas became exposed to the ambient atmosphere. The source gas was cooled in a gas to gas counter flow heat exchanger, the cold gas being very carefully monitored. In order to specify the source gas temperature to within $\pm$ 3 K, the heat transfer across the counter flow section, and consequently, the cold fluid inlet temperature had to be readily adjustable. This was accomplished by establishing a two stage cooling process for the coolant nitrogen. Bottled nitrogen was initially precooled by passing it through a copper coil submerged in liquid nitrogen. The cooled nitrogen was then further cooled in a parallel flow heat exchanger with the temperature decrease being controlled by the flow rate of the colder liquid nitrogen on the shell side. The temperature drop from the tube outlet of the parallel flow exchanger to the shell inlet of the counter flow exchanger was minimized to about 2-3 K by reducing the connecting pipe length to ~4 cm. Heat loss was further reduced by wrapping the counter flow and parallel flow exchangers together and covering the assembly with ~3 cm of fiberglass insulation. The cooled source gas was conveyed through copper tubing from the counter flow exchanger to the source plenum. Since the tubing was at or perhaps slightly cooler than desired outlet temperatures as it passed through the source nitrogen pool, the tubing was insulated to prevent undesirable condensation (see Figure 3-2a).

All the gases released contained a known percentage of a hydrocarbon tracer to allow concentrations to be determined using a gas chromatograph.

3.3 Flow Visualization Techniques

Smoke was used to define isothermal plume behavior. The smoke was produced by passing the LNG vapor simulant through an oil smoke generator (fog/smoke machine manufactured by Roscolab, Ltd.).

The cold gas runs could not be observed using the smoke generator or $TiCl_4$ because the smoke particles tended to freeze in the plenum rendering them useless. Plume boundaries could be observed, though, as a result of background humidity condensation within the plume. Plume appearance was recorded onto video cassettes.

3.4 Wind Profile and Turbulence Measurements

The velocity profile, reference wind speed conditions, and turbulence were measured with a Thermo-Systems Inc. (TSI) 1050 anemometer and a TSI model 1212 hot-film probe. Since the voltage response of these anemometers is nonlinear with respect to velocity, a multipoint calibration of system response versus velocity was utilized for data reduction. A velocity standard described in Neff and Meroney (1982) was used to calibrate the hot film anemometer.

During calibration of the single film anemometer, the anemometer voltage response values over the velocity range of interest were fit to an expression similar to that of King's law (Sandborn, 1972) but with a variable exponent. The accuracy of this technique is approximately $\pm$ 2 percent of the actual longitudinal velocity.

The velocity sensors were mounted on a vertical traverse and positioned over the measurement location on the model. The anemometer responses were fed to a Preston analog-to-digital converter and then directly to a HP-1000 minicomputer for immediate interpretation. The HP-1000 computer also controlled probe position.

3.5 Concentration Measurements

The experimental measurement of concentration was performed using gas-chromatograph and sampling systems (Figure 3-3) designed by Fluid Dynamics and Diffusion Laboratory staff. A grid map showing locations where concentration measurements were made is shown in Figure 3-4.

3.5.1 Gas Chromatograph

The (Hewlett-Packard Model 5710A) gas chromatograph with Flame Ionization Detector (FID) operates on the principle that the electrical conductivity of a gas is directly proportional to the concentration of charge particles within the gas. The ions in this case are formed by effluent gas being mixed in the FID with hydrogen and then burned in air. The ions and electrons formed enter an electrode gap and decrease the gap resistance. The resulting voltage drop is amplified by an electrometer and fed to the HP 3390A integrator. When no effluent gas is flowing, a carrier gas (nitrogen) flows through the FID. Due to certain impurities in the carrier, some ions and electrons are formed creating a background voltage or zero shift. When the effluent gas enters the FID, the voltage increase above this zero shift is proportional to the degree of ionization or correspondingly the amount of tracer gas present. Since the chromatograph used in this study features a temperature control on the flame and electrometer, there is very low drift of the zero

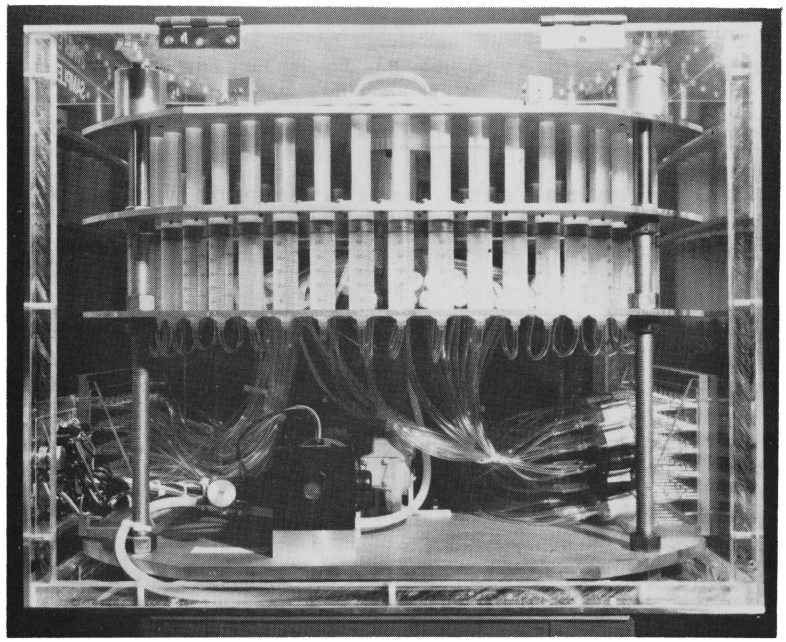

(a)

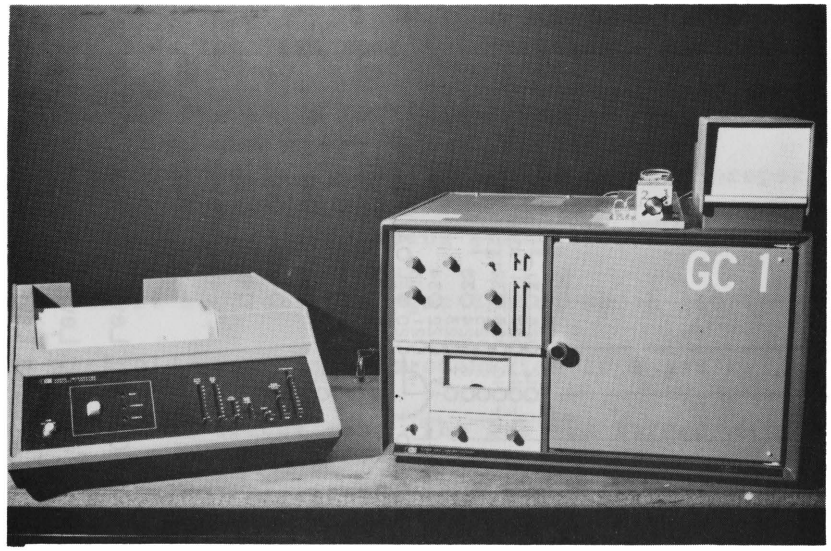

(b)

Figure 3-3 Photographs of (a) the Gas Sampling System, and (b) the HP Integrator and Gas Chromotograph

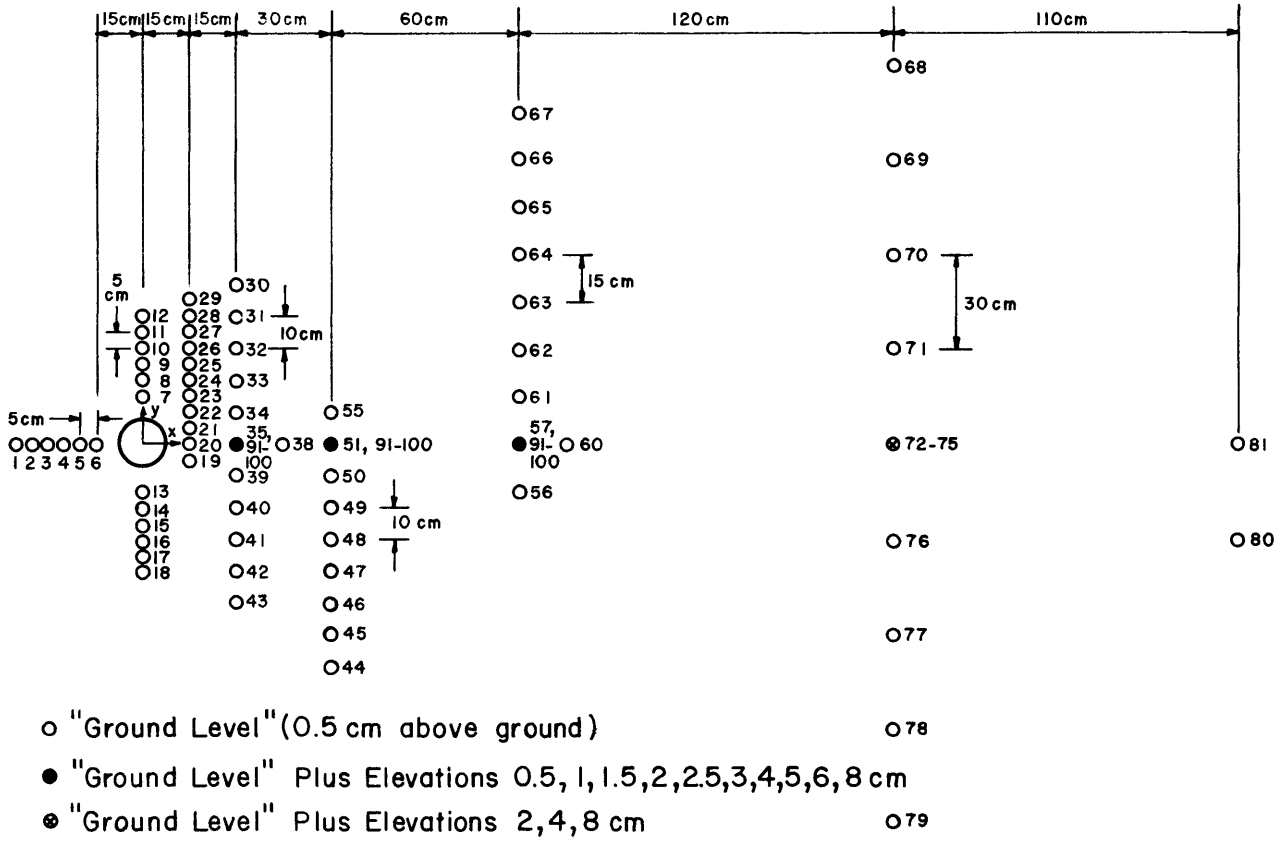

Figure 3-4. Concentration Sample Location Map

shift. In case of any zero drift, the 3390A, which integrates the effluent peak, also subtracts out the zero drift.

The lower limit of measurement is imposed by the instrument sensitivity and the background concentration of tracer within the air in the wind tunnel. Background concentrations were measured and subtracted from all data quoted herein.

3.5.2 Concentration Sampling System

The CSU tracer gas sampling system consists of a series of fifty 30 cc syringes mounted between two circular aluminum plates. A variable-speed motor raises a third plate, which in turn raises all 50 syringe plungers simultaneously. A set of check valves and tubing are connected such that airflow from each tunnel sampling point passes over the top of each designated syringe. When the syringe plunger is raised, a sample from the tunnel is drawn into the syringe container. The sampling procedure consists of flushing (taking and expending a sample) the syringe three times after which the test sample is retained. The draw rate is variable and generally set to be approximately 6 cc/min.

The sampler was periodically calibrated to insure proper function of each of the check valve and tubing assemblies. The sampler intake was connected to short sections of Tygon tubing which led to a sampling manifold. The manifold, in turn, was connected to a gas cylinder having a known concentration of tracer gas. The gas was turned on and a valve on the manifold opened to release the pressure produced in the manifold. The manifold was allowed to flush for about 1 min. Normal sampling procedures were carried out to insure exactly the same procedure as when taking a sample from the tunnel. Each sample was then analyzed for tracer gas concentration. Any sample having an error of greater than 2

percent indicated a failure in the check valve assembly and the check valve was replaced or the bad syringe was not used for sampling from the tunnel.

3.5.3 Test Procedure

The test procedure consisted of: 1) setting the proper tunnel wind speed, 2) releasing a metered mixture of source gas from the release area source, 3) withdrawing samples of air from the tunnel at the locations designated, and 4) analyzing the samples with a Flame Ionization Gas Chromatograph (FIGC). The samples were drawn into each syringe over a 300 s (approximate) time period and subsequently analyzed by injection into the FIGC.

The procedure used for analyzing air samples from the tunnel is as follows: 1) a 2 cc sample volume which was drawn from the wind tunnel and collected in a syringe is introduced into the Flame Ionization Detector (FID), 2) the output from the electrometer (in microvolts) is sent to the Hewlett-Packard 3390 or 3390A Integrator, 3) the output signal is analyzed by the integrator to obtain the proportional amount of hydrocarbons present in the sample, 4) the record is integrated, and the ethane concentration is determined by multiplying the integrated signal (μv-s) by calibration factor (ppm/μv-s), 5) a summary of the integrator analysis (gas retention time and integrated area (μv-s)) is printed out on the terminal at the wind tunnel, along with pertinent run parameters, and 8) the computer program converts the raw data into mean concentration. The calibration factor was obtained by introducing a known quantity, χ_s, of tracer into the FIGC and recording the integrated value, I, in μv-s.

Calibrations were obtained at the beginning and end of each measurement period.

3.6 Temperature Measurements

During the cold gas runs (22-45) thermocouples were fixed at various locations throughout the plume flow field. A thermocouple multiplexer (model Digitrend 22 manufactured by Doric) was used to obtain temperatures from the thermocouples at 60 second intervals during each run.

In addition a fast response (.001 in. diameter) thermocouple was placed at a fixed location for each run. This thermocouple was continuously monitored and its output was connected to a strip chart recorder. All thermocouples used were copper/constantan manufactured by Omega Engineering, Inc. Figure 3-5 is a grid map detailing thermocouple locations.

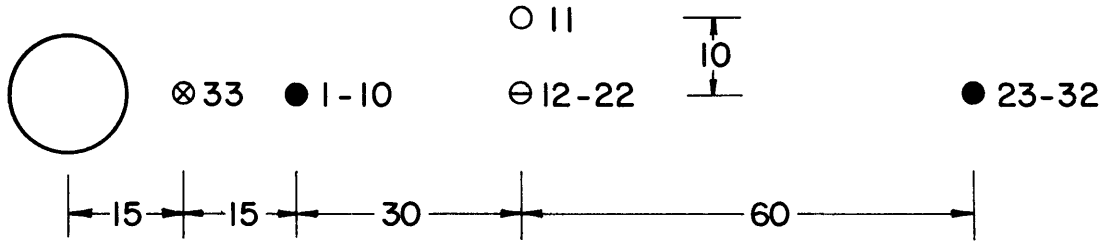

⊗ High Sensitivity Continuous Response Thermocouple

○ Ground Level

⊖ Ground Level - 0.5, 1, 1.5, 2, 2.5, 3, 4, 5, 6, 8 Elevations

● 0.5, 1, 2, 2.5, 3, 4, 5, 6, 8 Elevations

All Dimensions in centimeters.

Figure 3-5. Thermocouple Location Map

4.0 TEST PROGRAM AND DATA

The cold dense plume measurement program was designed to provide a basis for the analysis of heat transfer effects on plume dispersion, the evaluation of plume scaling laws, and to assist in the development of and verification of numerical models. All tests were performed in the wind tunnel described in Section 3.1. The plumes were released through the source and heat exchanger system described in Section 3.2 with zero initial longitudinal momentum and minimal source generated dilution.

Experiments were performed in two sequences. Runs 1 through 12 were performed together to determine the reaction of plume behavior to a range of initial conditions. Sample tubes for vertical and surface concentration samples were arranged above the floor and may have produced wakes which caused additional dilution. No experimental replication occurred during Runs 1 - 12 and although thermal control was adequate some temperature drift occurred during individual experiments.

The second test series emphasized situations where thermal effects were most pronounced. Surface sampling tubes were mounted flush with the surface and connected to the sampler via a hollow chamber beneath the wind-tunnel floor. Several improvements were incorporated into the heat exchanger to provide for better source gas temperature control during operation.

The floor in the vicinity of the plumes was always flat and smooth with no obstacles to cause wake effects. To obtain a series of vertical profiles, experiments were replicated up to five times and only data at or upwind of any concentration rake should be considered accurate. The replications also provided redundant data that defined concentration

variability, i.e. the data scatter for individual locations. The scatter was found to be very small, usually less than 10%.

Source gas mixtures were prepared to provide gases which were all initially heavy; but they were either isothermal, or cold with $C^*_{p_o}/C^*_{p_a} = 1.0$, or cold with $C^*_{p_o}/C^*_{p_a} > 1.0$. Thus one could evaluate whether dilution resulted from adiabatic entrainment, heat transfer effects, or unbalanced thermal contraction. Table 4-1 summarizes mixture and thermal conditions desired during the experiments. Since wind tunnel velocity and heat exchanger temperatures sometimes drifted from the ideal set points, the actual conditions examined are noted in Table 4-2.

It is hypothesized that gravity effects should be a function of a bouyancy length scale (or Richardson number) that characterizes the plume. Two buoyancy conditions were selected for examination, $\ell_b = 1$ and $\ell_b = 5$. Under the first condition (Runs 4-6 and 10-12) background turbulence was expected to dominate entrainment very quickly, but under the latter condition (Runs 1-3 and 7-9) gravity spreading and suppression of vertical mixing was expected to persist. Two combinations of initial molecular weight and initial temperature were arranged for each bouyancy length scale. If equality of Richardson number alone is adequate for proper plume scaling, then in the absence of heat transfer effects Runs 1-3 and 7-9 or Runs 4-6 and 10-12 should give identical concentration isopleths in space. If thermal expansion effects are minimal then Runs 1-3, 4-6, 7-9, or 10-12 should each produce coincident dimensionless K isopleths.

Table 4-1

Heat Transfer Tests Series

Design Conditions

Run	Source Gas Mixture	SG	ℓ_b (cm)	$C^*_{p_o}/C^*_{p_a}$	MW	Source T_o (°K)	Flow Rate Q (ccs)	Wind Velocity u_R (cm/s)
1, 13-17	94.1% CO_2 5.9% CH_4	1.46	5.0	1	42.3	amb	130	22.7
2, 22-26	99.5% N_2 0.5% CH_4	1.46	5.0	1	28	195	130	22.7
3, 35-41	100% CH_4	1.46	5.0	1.22	16	111	130	22.7
4	94.1% CO_2 5.9% CH_4	1.46	1.0	1	42.3	amb	130	38.8
5	99.5% N_2 0.5% CH_4	1.46	1.0	1	28	195	130	38.8
6, 42	100% CH_4	1.46	1.0	1.22	16	111	130	38.8
7, 18-21	68% CO_2 31% CCl_2F_2 1% C_2H_6	2.35	5.0	1	68	amb	223	38.8
8, 23-26	99.5% N_2 0.5% CH_4	2.35	5.0	1	28	121	223	38.8
9, 31-34	99.5% CO_2 0.5% CH_4	2.35	5.0	1.30	44	195	223	38.8
10	68% CO_2 31% CCl_2F_2 1% C_2H_6	2.35	1.0	1	68	amb	223	66.6
11	99.5% N_2 0.5% CH_4	2.35	1.0	1	28	121	223	66.6
12	99.5% CO_2 0.5% CH_4	2.35	1.0	1.30	44	195	223	66.6
43-44	100% CH_4	1.46	9.0	1.22	16	111	195	20.0

u_R @ 2 cm height

$\frac{u_*}{u_R} = 0.075$

$z_o = 0.0001$ m

ϕ Specific Humidity $\simeq$ 35%

TABLE 4-2

TEST CONDITIONS THERMAL EFFECTS EXPERIMENTS

Run No.	SG	ℓ_b (cm)	$C^*_{p_o}/C^*_{p_a}$	MW	T_o (K)	Q (ccs)	u_R (cm/s)	u_* (cm/s)	T_a (K)	L^Δ (cm)	T (sec)	U (cm/s)	$(Ri_*)_o$	Re	Gr
1	1.46	5.0	1	42.3	294	130	22.7	1.70	294.0	0.2	0.021	9.5	31.4	18.7	0
2	1.46	5.0	1	28.0	195	130	22.7	1.70	294.0	0.2	0.021	9.5	31.4	18.7	118
3	1.28	3.1	1.22	16.0	128	130	22.7	1.70	294.0	0.2	0.027	7.4	19.1	9.9	198
4	1.46	1.0	1	42.3	294	130	38.8	2.90	294.0	0.2	0.021	9.5	10.8	12.7	0
5	1.46	1.0	1	28.0	195	130	38.8	2.90	294.0	0.2	0.021	9.5	10.8	12.7	118
6	1.33	0.7	1.22	16.0	123	130	38.8	2.90	294.0	0.2	0.025	8.0	7.7	10.8	241
7	2.35	5.1	1	68.0	293	223	38.8	2.90	294.0	0.2	0.012	16.6	31.6	21.8	0
8	2.41	5.3	1	28.0	118	223	38.8	2.90	294.0	0.2	0.012	16.6	33.1	22.2	210
9	2.20	4.5	1.30	44.0	203	223	38.8	2.90	294.0	0.2	0.013	15.4	28.1	20.5	109
10	2.35	1.0	1	68.0	294	223	66.6	5.00	294.0	0.2	0.012	16.6	10.6	21.8	0
11	2.41	1.1	1	28.0	118	223	66.6	5.00	294.0	0.2	0.012	16.6	11.1	22.2	210
12	2.18	0.9	1.30	44.0	205	223	66.6	5.00	294.0	0.2	0.013	15.4	9.3	20.3	109
13	1.46	5.0	1	42.3	296	130	22.7	1.70	296.0	0.2	0.021	9.5	31.4	12.7	0
14	1.46	4.0	1	42.3	298	130	24.4	1.85	298.0	0.2	0.021	9.5	31.4	18.7	0
15	1.46	4.0	1	42.3	298	130	24.4	1.85	298.0	0.2	0.021	9.5	31.4	18.7	0
16	1.46	4.0	1	42.3	298	130	24.4	1.85	298.0	0.2	0.021	9.5	31.4	18.7	0
17	1.46	4.0	1	42.5	298	130	24.4	1.85	298.0	0.2	0.021	9.5	31.4	18.7	0
18	2.36	4.0	1	68.0	298	223	42.3	3.20	298.0	0.2	0.012	16.6	26.2	21.8	0
19	2.36	4.0	1	68.0	298	223	42.3	3.20	298.0	0.2	0.012	16.6	26.2	21.8	0
20	2.36	4.0	1	68.0	298	223	42.3	3.20	298.0	0.2	0.012	16.6	26.2	21.8	0
21	2.36	4.0	1	68.0	298	223	42.3	3.20	298.0	0.2	0.012	16.6	26.2	21.8	0
22	1.46	4.0	1	28.0	195	130	24.7	1.85	294.0	0.2	0.021	9.5	31.4	18.7	118
23	1.46	4.0	1	28.0	195	130	24.7	1.85	294.0	0.2	0.021	9.5	31.4	18.7	118
24	1.46	4.0	1	28.0	195	130	24.7	1.85	294.0	0.2	0.021	9.5	31.4	18.7	118
25	1.46	4.0	1	28.0	195	130	24.7	1.85	295.4	0.2	0.021	9.5	31.4	18.7	118
26	1.46	4.0	1	28.0	195	130	24.7	1.85	295.7	0.2	0.021	9.5	31.4	18.7	118
27	2.37	4.0	1	28.0	121	223	42.3	3.20	295.4	0.2	0.012	16.6	26.4	21.9	207
28	2.37	4.0	1	28.0	121	223	42.3	3.20	295.4	0.2	0.012	16.6	26.4	21.9	207
29	2.37	4.0	1	28.0	121	223	42.3	3.20	295.4	0.2	0.012	16.6	26.4	21.9	207
30	2.37	4.0	1	28.0	121	223	42.3	3.20	294.0	0.2	0.012	16.6	26.4	21.9	207
31	2.30	3.9	1.30	44.0	195	223	42.3	3.20	294.0	0.2	0.012	16.6	25.0	21.3	118
32	2.30	3.9	1.30	44.0	195	223	42.3	3.20	294.0	0.2	0.012	16.6	25.0	21.3	118
33	2.30	3.9	1.30	44.0	195	223	42.3	3.20	294.0	0.2	0.012	16.6	25.0	21.3	118

u_R @ 2 cm height

$\frac{u_*}{u_R}$ = 0.075, z_o = 0.0001 m, ϕ Specific Humidity = 35% (T_{dpt} = 284°K)

TABLE 4-2

Continued

Run No.	SG	ℓ_b (cm)	$C^*_{p_o}/C^*_{p_a}$	MW	T_o (K)	Q (ccs)	u_R (cm/s)	u_* (cm/s)	T_a (K)	L^Δ (cm)	T (sec)	U (cm/s)	$(Ri_*)_o$	Re	Gr
34	2.30	3.9	1.30	44.0	195	223	42.3	3.20	294	0.2	0.012	16.6	25.0	21.3	118
35	1.34	2.9	1.22	16.0	121	130	24.7	1.85	292	0.2	0.024	8.3	19.6	10.9	209
36	1.34	2.9	1.22	16.0	121	130	24.7	1.85	292	0.2	0.024	8.3	19.6	10.9	209
37	1.34	2.9	1.22	16.0	121	130	24.7	1.85	292	0.2	0.024	8.3	19.6	10.9	209
38	1.34	2.9	1.22	16.0	121	130	24.7	1.85	292	0.2	0.024	8.3	19.6	10.9	209
39	1.34	2.9	1.22	16.0	121	130	24.7	1.85	292	0.2	0.024	8.3	19.6	10.9	209
40	1.34	2.9	1.22	16.0	121	130	24.7	1.85	292	0.2	0.024	8.3	19.6	10.9	209
41	1.34	2.9	1.22	16.0	121	130	24.7	1.85	292	0.2	0.024	8.3	19.6	10.9	209
42	1.34	0.8	1.22	16.0	121	130	38.3	2.87	293	0.2	0.024	8.3	8.1	10.9	206
43	1.34	9.2	1.22	16.0	121	195	19.3	1.45	293	0.2	0.024	8.3	31.9	10.9	206
44	1.34	9.2	1.22	16.0	121	195	19.3	1.45	293	0.2	0.024	8.3	31.9	10.9	206

$L = H_o$

$T = (H_o/g_o')^{1/2}$

$U = (H_o g_o')^{1/2}$

$(Ri_*)_o = g_o' H_o / u_*^2$

$Re = (g_o' H_o^3)^{1/2}/\nu$

$Gr = g H_o^3 \Theta/\nu^2$

$\Theta = 1 - T_o/T_a$

$L_o = 18.2(\ell_b/f^{0.8})$

$f = Q^{1/2} g_o'/u_R^{5/2}$

$\ell_b = g_o' Q/u_R^3$

$H_o = Q/L_o/[u_*/k\ \ell n(H_o/z_o) + \alpha_1(g_o' H_o)^{1/2}]$

(Note L_o and H_o are solved for iteratively)

$^\Delta$ Since H_o is not very well defined we will use H_o = 0.002 m for all cases here.

$\nu = 1.5 \times 10^{-5}\ m^2/s$

The zero position of the coordinate system is located over the center of the sources apparatus 12.63 m from the wind tunnel entrance vortex generators. The positive x coordinate will be downwind, and the positive z coordinate is upward. The right hand coordinate rule applies.

Section 4.1 reviews the approach-wind flow conditions for all tests, Section 4.2 discusses the visual appearance of the plumes, Section 4.3 reports the results of the concentration measurements, and Section 4.4 reports temperature measurements. In all, 44 separate tests were performed for 14 different initial conditions.

4.1 Velocity and Turbulence Results

Wind tunnel entrance and floor geometries were identical to conditions examined by Neff and Meroney (1982). Their conclusions concerning similarity of the tunnel boundary layer to the atmospheric boundary remain relevant. The boundary layer thickness in all cases extended above 40 cm. The wind tunnel ceiling was set to produce a zero pressure gradient along the tunnel centerline.

4.1.1 Mean Velocity Profiles

Velocity and turbulence profiles have been measured upwind and downwind of the source location in the wind tunnel. Representative measurements over the source location are provided in Figure 4-1. The mean wind speed profile is commonly described by a logarithmic relationship $u(z)/u_* = 2.5\ \ell n(z/z_o)$, where u_* is the friction velocity at the wall and z_o is the roughness length. A logarithmic relationship fits all profiles well between heights of 1 to 40 cm. Over a wide range of

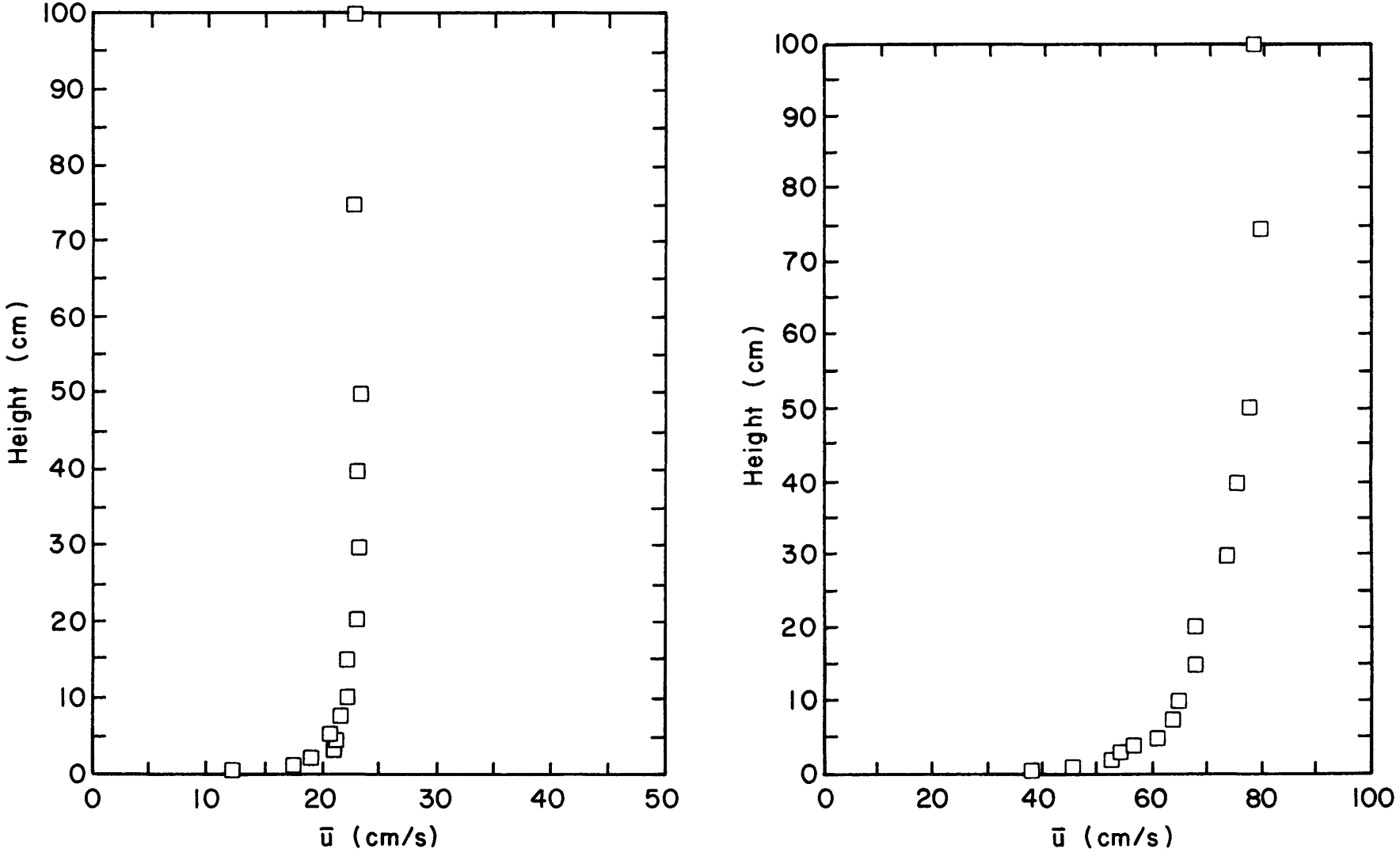

Figure 4-1. Velocity Profiles over Source Location

velocities (u_{ref} = 0.20 to 1.0 m/sec) the surface friction coefficient $\frac{C_f}{2} = \left(\frac{u_*}{u_{ref}}\right)^2$ was effectively 0.075 and the surface roughness, z_o, was 0.0001 m.

A value of the power law index, p, can also be defined if the assumption is made that $u(z)/u_{ref} = (z/z_{ref})^p$. Values of p range from .22 to .18 for wind speeds ranging from 19 to 67 cm/sec. Power law profiles were not found to fit measurements when $z/\delta < 0.1$. Most of the cloud dispersion occurs below 1 to 3 cm; hence a power law profile relationship is not representative of the advective wind field. Logarithmic-law formulas will be somewhat better, but they may over estimate wind speeds at 0.5 cm by as much as 50%. Formulas which include laminar sublayer corrections may be more suitable to describe model profiles.

4.1.2 Turbulence Intensity Profiles

The turbulent intensity of a turbulent velocity is defined as the r.m.s. of the velocity fluctuations divided by the local mean velocity. Figure 4-2 shows a typical variation of the turbulent intensity of the longitudinal velocity component. Magnitudes fall off at upper levels faster then equivalent atmospheric profiles. Nonetheless at z = 1 to 5 cm, turbulent intensity levels are comparable to empirical expressions proposed for field measurements for scale ratios between 1:1000 to 1:2000.

Turbulence spectra and integral scales of the model boundary layer were not measured during this test series. Nonetheless, as noted earlier, the boundary conditions are equivalent to those examined extensively by Neff and Meroney (1982). Their data supports the conclusion

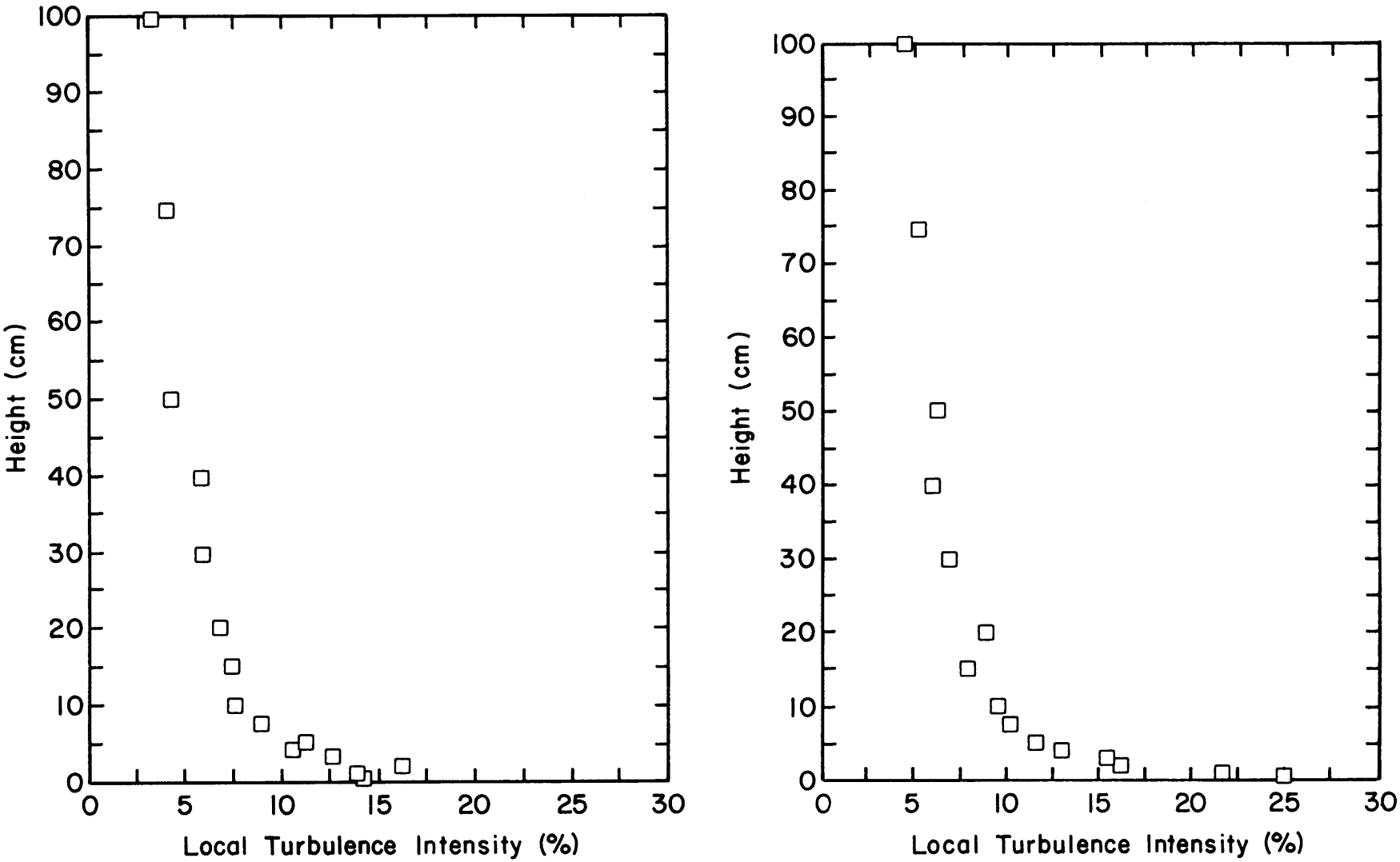

Figure 4-2. Turbulence Intensity Profiles over Source Location

that the wind tunnel boundary has an effective scale ratio near 1:1000. Integral scales estimated from the spectral measurements of Neff and Meroney suggested equivalent field values ranging from 100 to 150 m at a height of 10 meters for scale ratios near 1:1000.

Although the apparent scale ratio for the wind tunnel to atmosphere boundary layer comparisons at low velocities is near 1:1000, this need not constrain model scales for smaller scale ratio heavy plume experiments. Apparently the dense gas plume is not sensitive to a mismatch between cloud size and the boundary layer integral scales. Earlier measurements under similar tunnel conditions performed by Neff and Meroney (1981) revealed that 1:85 scale simulations of the 40 m^3 LNG spill tests at China Lake, California, reproduced field results quite well.

4.2 Visual Appearance of the Clouds

For the $\ell_b \sim 5$ cases the plume gases moved upwind against the wind field several centimeters until they were turned back and around the main body of the plume. These gases produced a horseshoe vortex which bent downwind around the source. For the $\ell_b \sim 1.0$ situation upwind motion was minimal, but lateral spreading still occurred.

As the plumes moved downwind, their lateral extent increased so that a roughly parabolic shape took form with the open end pointing downwind. A small secondary flow crosswind tended to slightly deflect the plumes subjected to lower wind speeds in the positive y direction.

Isothermal, cold nitrogen, and cold carbon dioxide plumes always remained negatively bouyant; thus the maximum visual extent of the plume rarely exceeded z = 3 cm at x = 3m. The stable stratification in the plumes suppressed vertical mixing, so vertical mixing followed the character of a Pasquill-Gifford G category plume rather than the C

conditions associated with the neutral background flow.

The cold methane plumes became positively buoyant after contact with the warm wooden wind tunnel floor had increased plume temperatures. Thus for the $\ell_b \sim 5$ case the plume height grew rapidly within 20 cm of the source. Growth rates appeared to approach Pasquill-Gifford category A rates (unstable atmosphere), and the cloud was 20 cm deep by x = 3 m. In addition the buoyant plume lofted above the floor. The vertical rise of the cloud resulted in a narrow plume width and a very dilute wispy plume at x = 2.5 m. For the $\ell_b \sim 1$ methane plume the higher wind speed suppressed lofting; nonetheless, vertical plume growth exceeded the heavier isothermal and cold nitrogen counterpart plumes.

4.3 Concentration Test Results

Heat transfer effects may be observed in the relative mixing rates of the various plumes, the resultant variation in centerline concentration decay with distance, ground level plume isopleths, and vertical concentration profiles. Concentration data is tabulated in terms of model values, equivalent methane values, and K (dimensionless concentration) values in the tables contained in Appendix D.

Figures 4-3 through 4-9 show surface centerline cloud dilution, plotted versus downwind distance, x, in terms of the methane equivalent values of all data. The methane equivalent values must be used to avoid making conclusions based on the different source molar flux rates associated with different initial temperature conditions.

On Figures 4-3, 4-5, 4-7, and 4-8 where $\ell_b \sim 5$, the isothermal Runs 1, 14-17, and 18-21 are essentially coincident. This suggests that for cases where source vertical momentum is small, bouyancy scale equality or Richardson number equality is sufficient for source specific

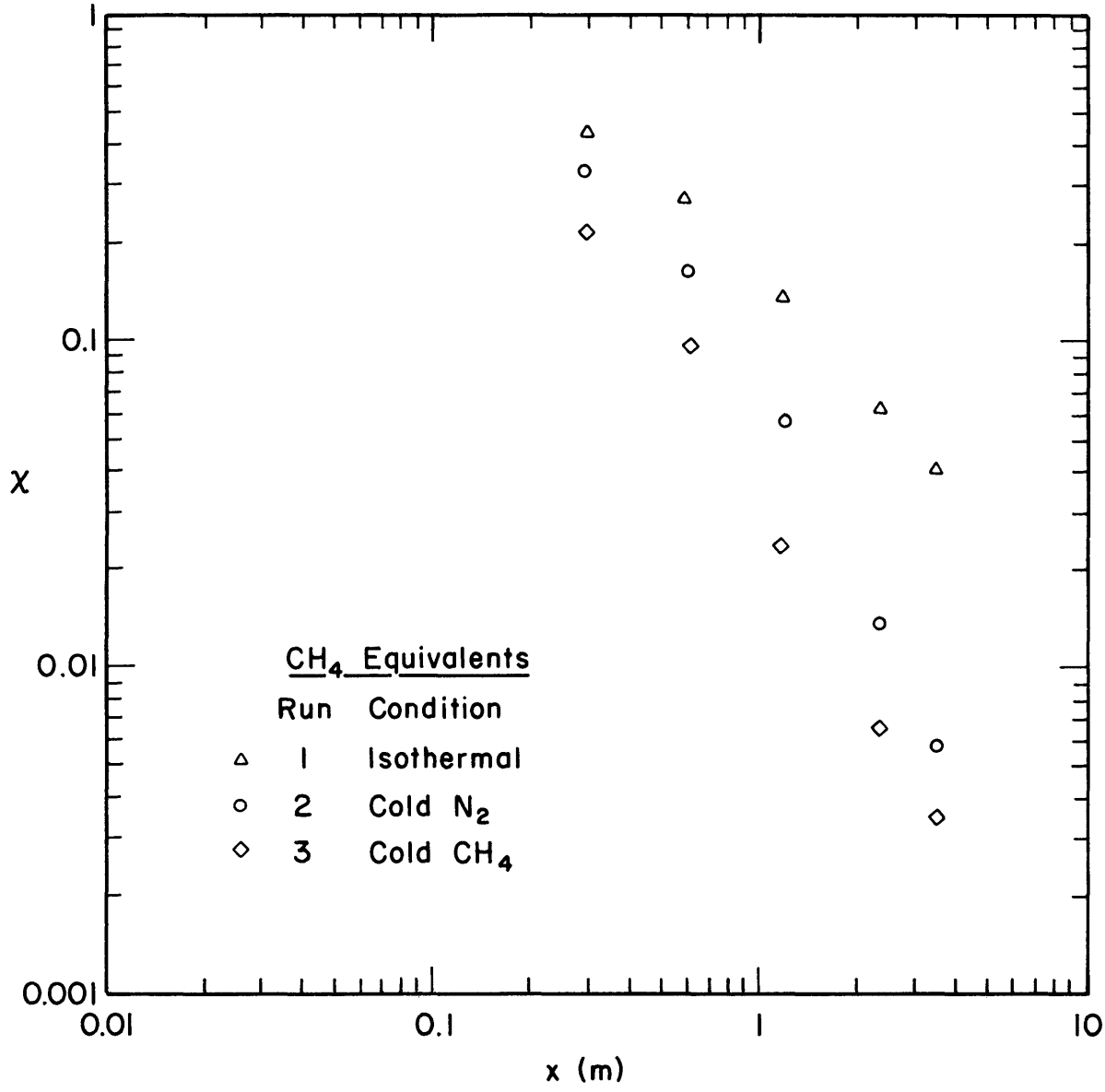

Figure 4-3. Surface Centerline Concentration Variation with Distance, $\ell_b \sim 4.0$, Q = 130 ccs, $u_* = 1.7$ cm/s

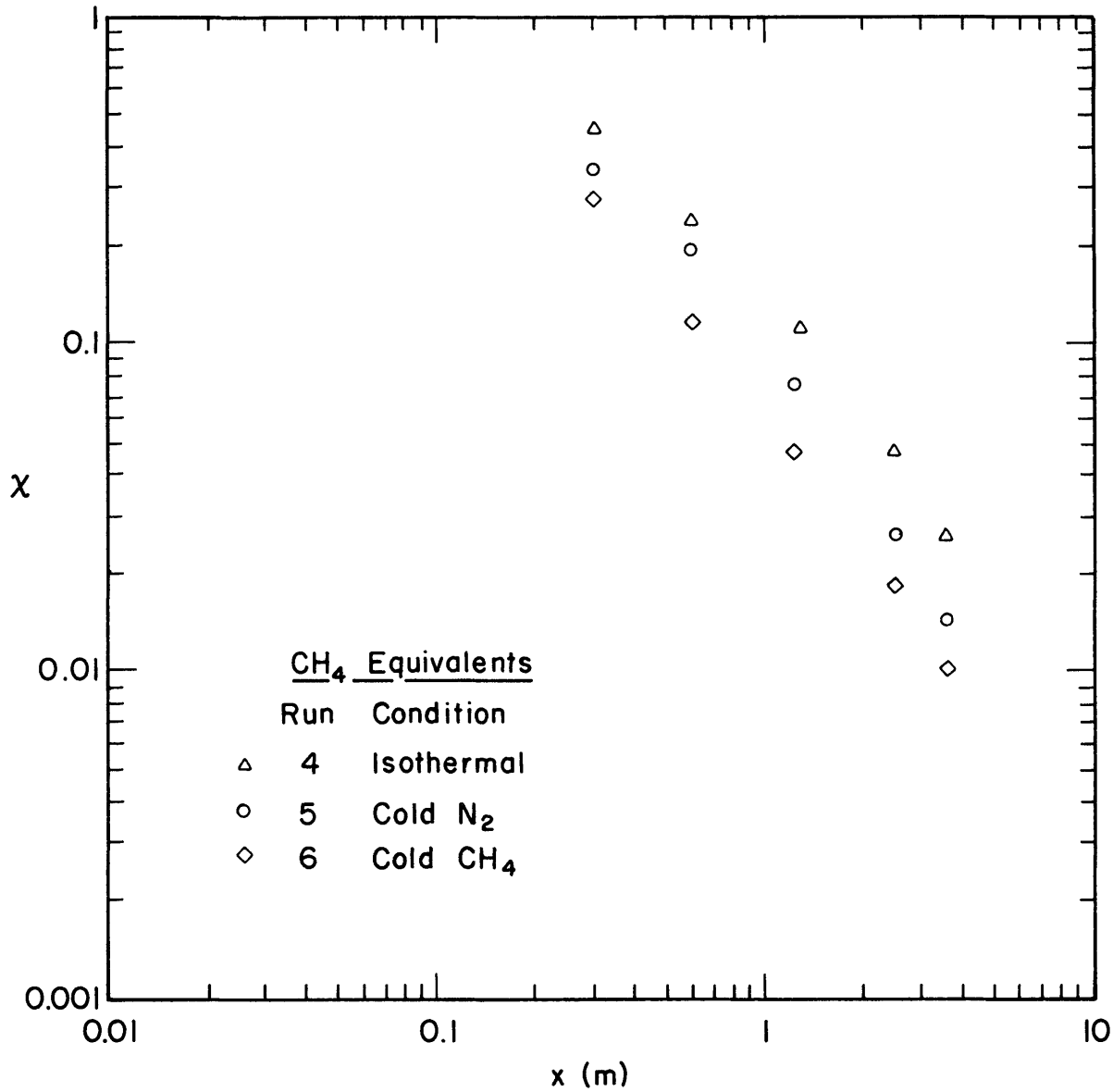

Figure 4-4. Surface Centerline Concentration Variation with Distance, $\ell_b \sim 1.0$, Q = 130 ccs, $u_* = 2.9$ cm/s

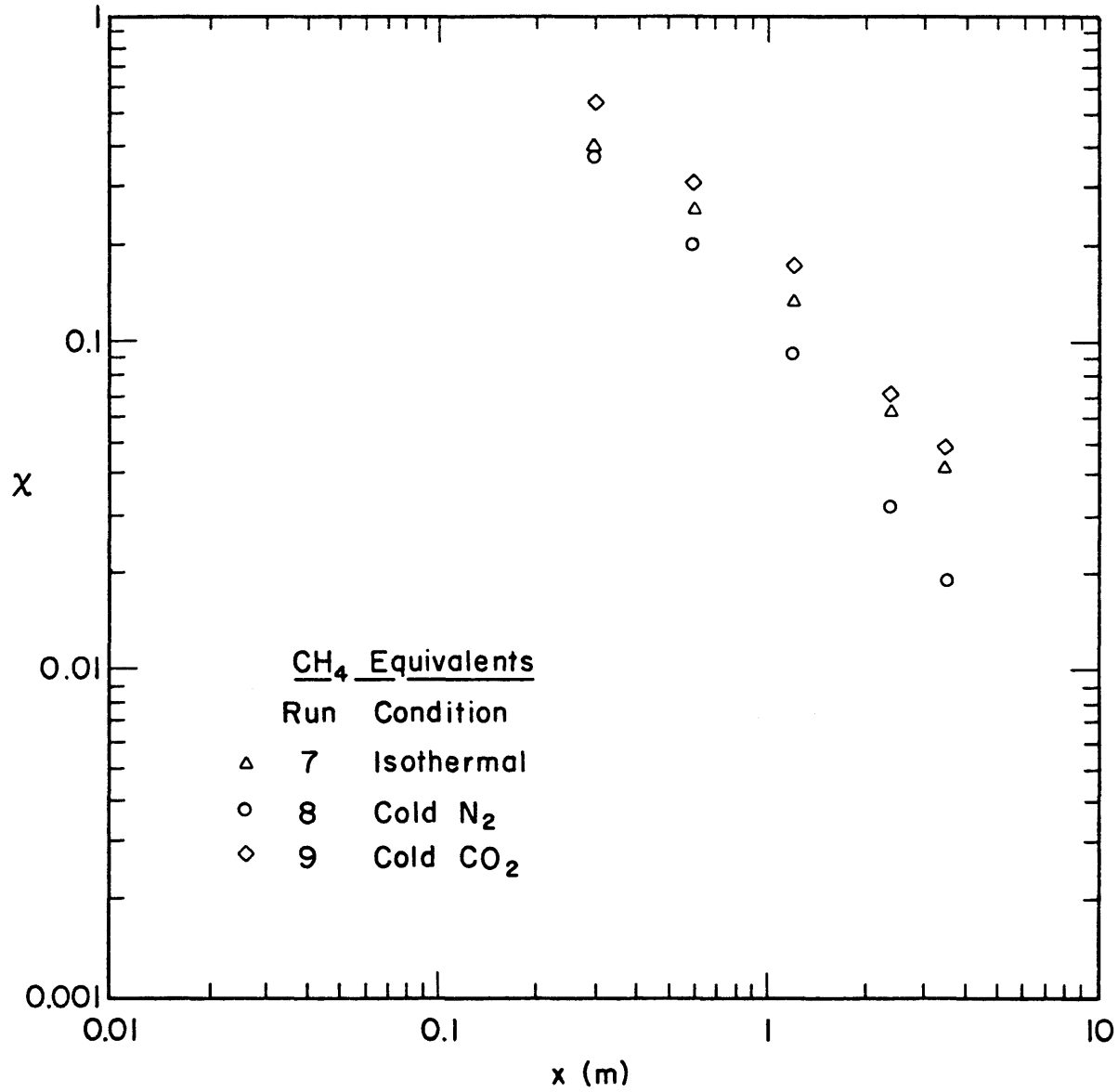

Figure 4-5. Surface Centerline Concentration Variation with Distance, $\ell_b \sim 4.0$, Q = 223 ccs, $u_* = 2.9$ cm/s

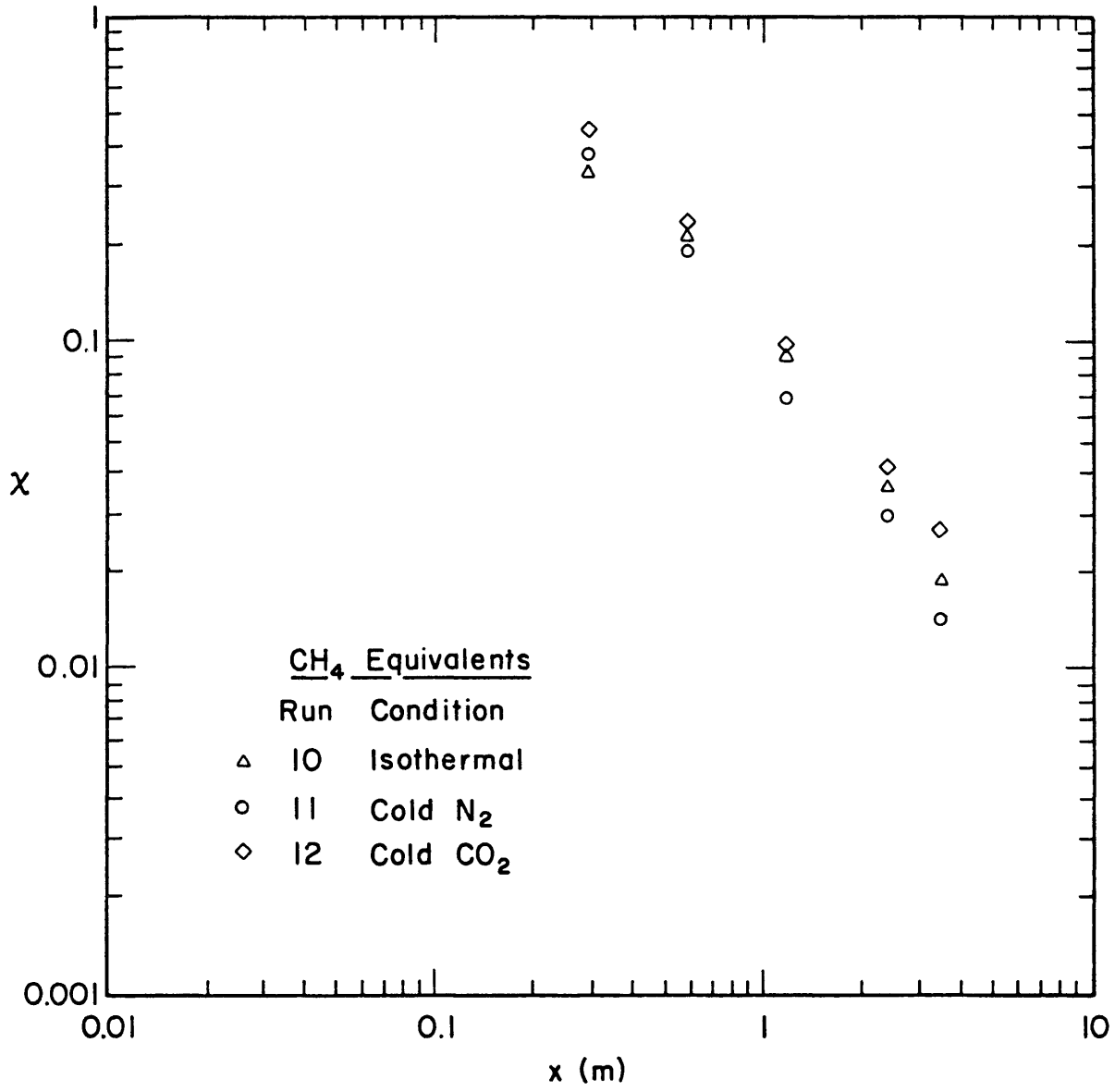

Figure 4-6. Surface Centerline Concentration Variation with Distance, $\ell_b \sim 4.0$, Q = 223 ccs, $u_* = 5$ cm/s

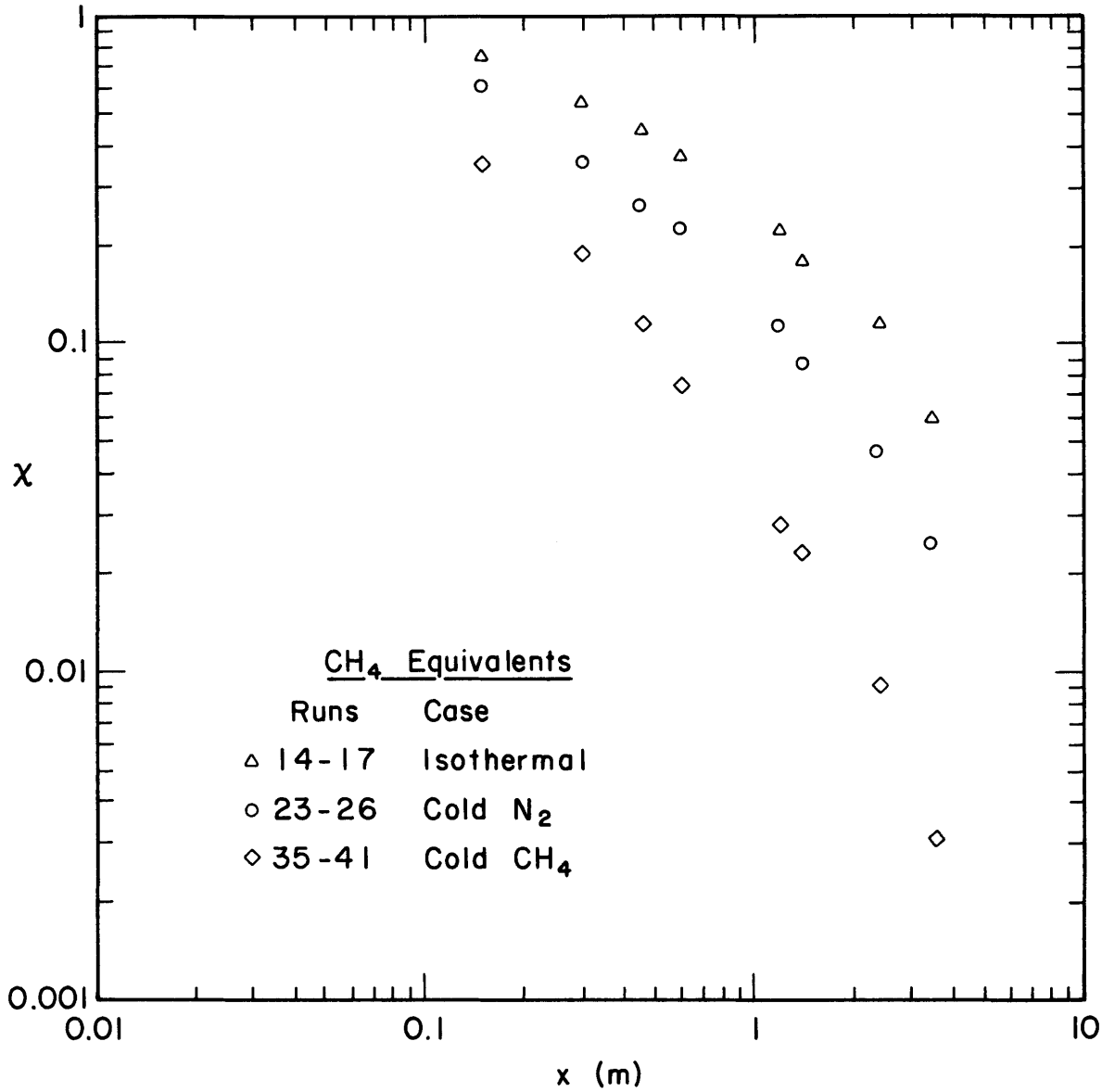

Figure 4-7. Surface Centerline Concentration Variation with Distance, $\ell_b \sim 4.0$, Q = 130 ccs, $u_* = 1.85$ cm/s

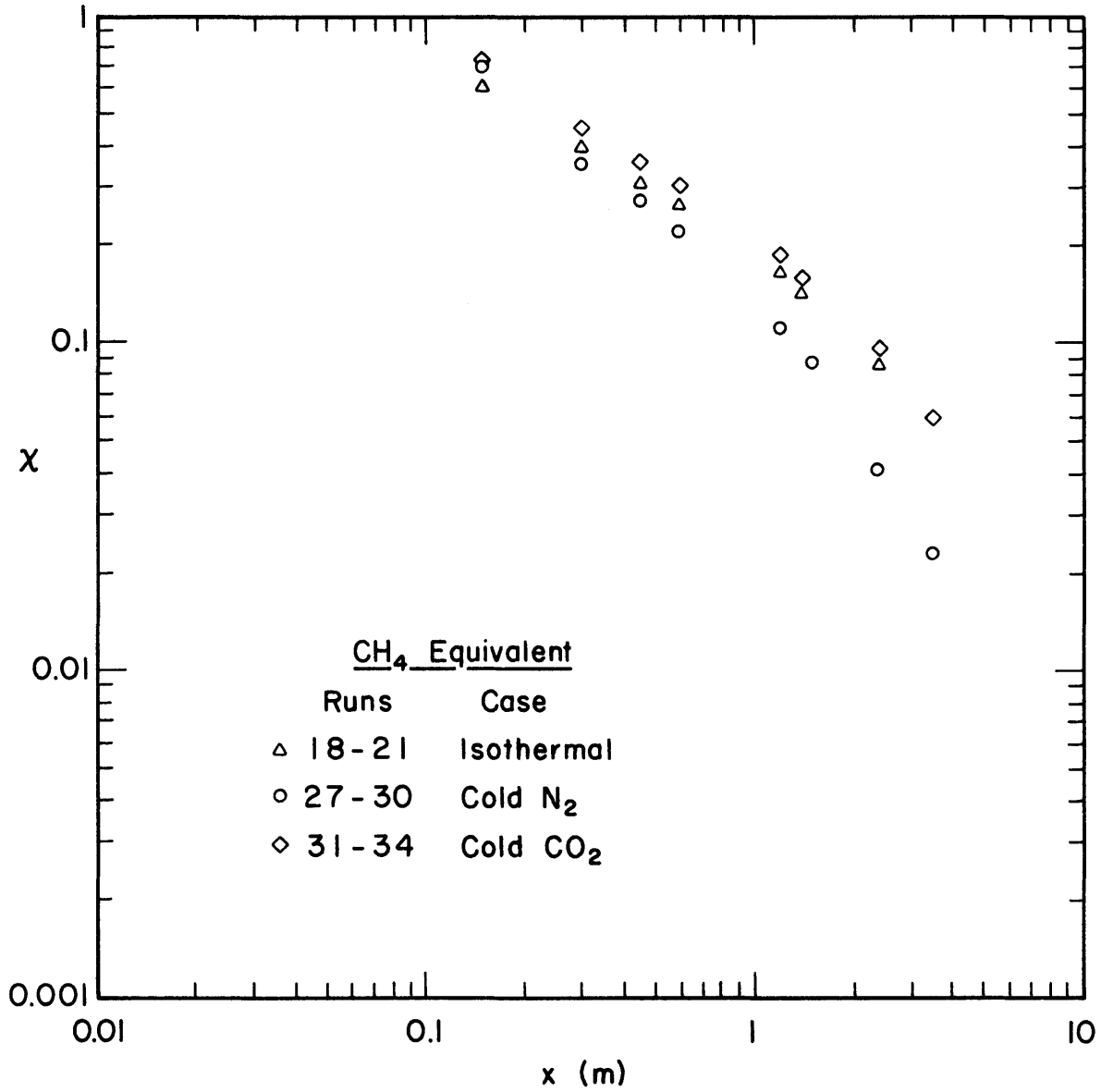

Figure 4-8. Surface Centerline Concentration Variation with Distance, $\ell_b \sim 4.0$, Q = 223 ccs, $u_* = 3.20$ cm/s

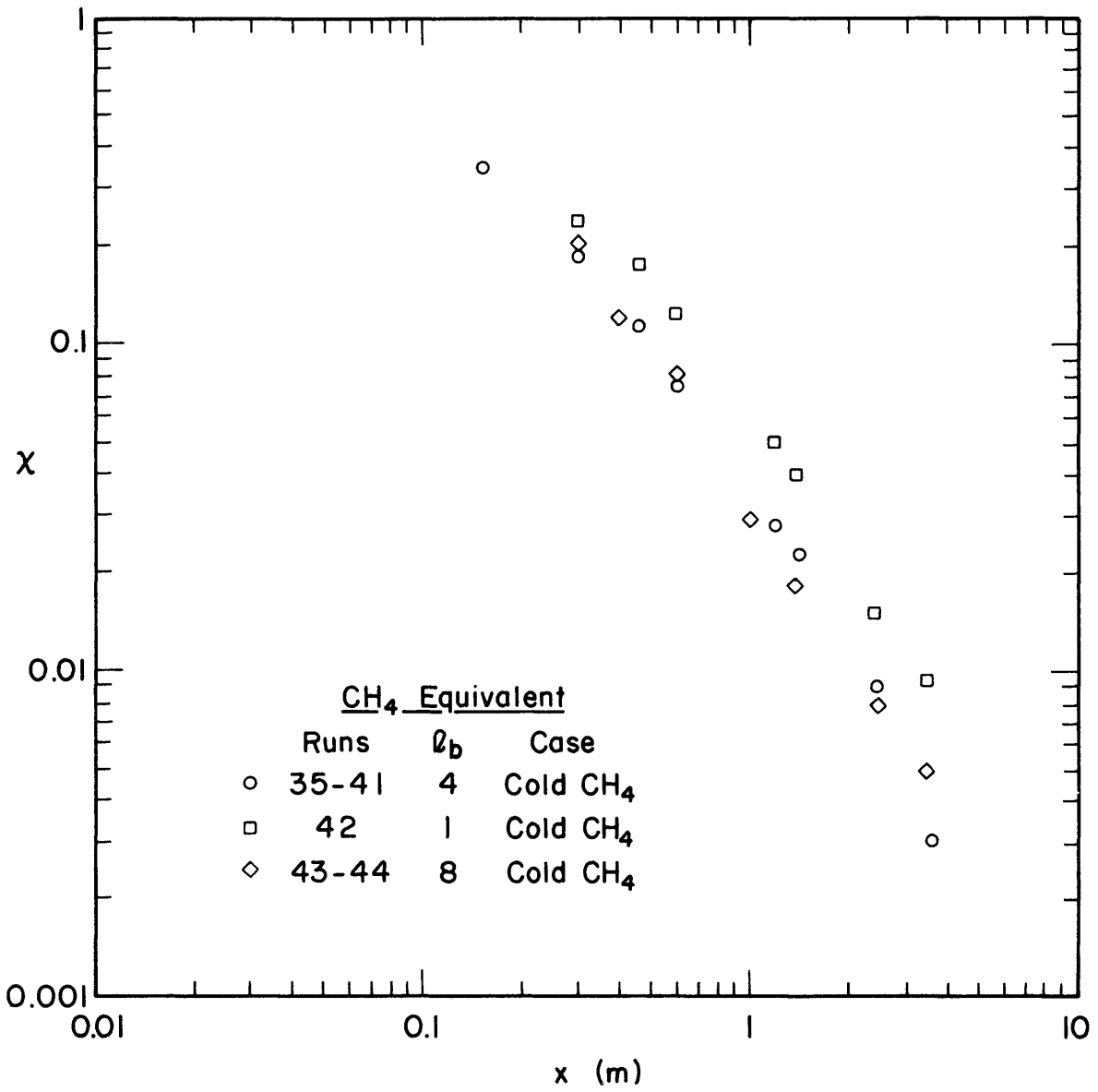

Figure 4-9. Surface Centerline Concentration Variation with Distance, Methane Runs, ℓ_b = 1, 4 and 8

gravities near 1.5 to assure similarity. Figures 4-4 and 4-6 where ℓ_b ~ 1 also produce similar isothermal plume results.

Cold plumes at ℓ_b ~ 1, or 5 do not indicate similar curves. They generally arrange themselves in order of initial temperature, where a lower source temperature results in faster dilution rates. An interesting exception is cold carbon dioxide where the relatively smaller initial temperature drop below ambient temperatures and the large specific heat capacity ratio $C^*_{p_o}/C^*_{p_a}$ results in centerline concentrations slightly above any isothermal counterpart. The high specific heat capacity of carbon dioxide means that during adiabatic mixing the local specific gravity remains larger than that of an isothermal counterpart plume of equivalent dilution. This higher density slightly inhibits vertical mixing (See Figure 4-5, 4-6, and 4-8).

Surface isopleths are plotted in Figures 4-10 to 4-17 for Runs 14 to 44. Plume assymmetry is associated with the small crossflow velocities mentioned earlier. On each curve the visual extent of the cloud associated with smoke or water droplets is indicated by a dashed line. Visual definition seems to fall off near molar concentrations of one percent.

Upwind plume motion is evident for ℓ_b ~ 4 and 9, but the plume release mapped for ℓ_b ~ 1 (Figure 4-16) displayed little upwind motion. Methane plumes (Figures 4-12, 4-16, and 4-17) are comparatively quite narrow. ℓ_b ~ 4 and 9 conditions (Figures 4-12 and 4-17) reflect the effects of a buoyant plume rapidly lofting into the air.

Limited lateral measurements are available for Runs 1 through 12 and wakes from sampling tubes artificially reduced plume concentrations. Nonetheless the observations made about plume lateral characteristics in

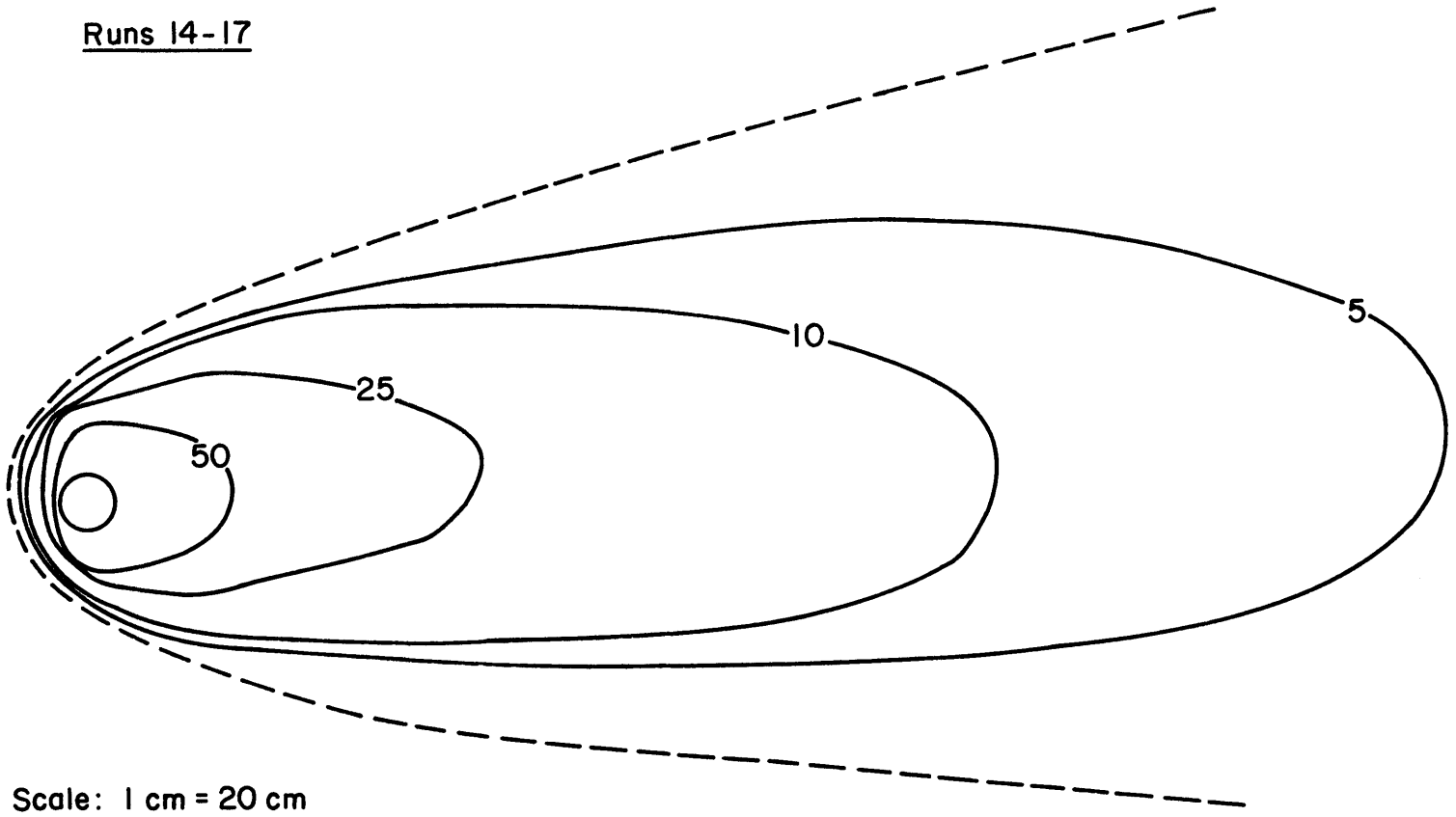

Figure 4-10. Surface Concentration Isopleths, Runs 14-17, Isothermal Gas, ℓ_b = 4.0, Q = 130 ccs, u_* = 1.85 cm/s

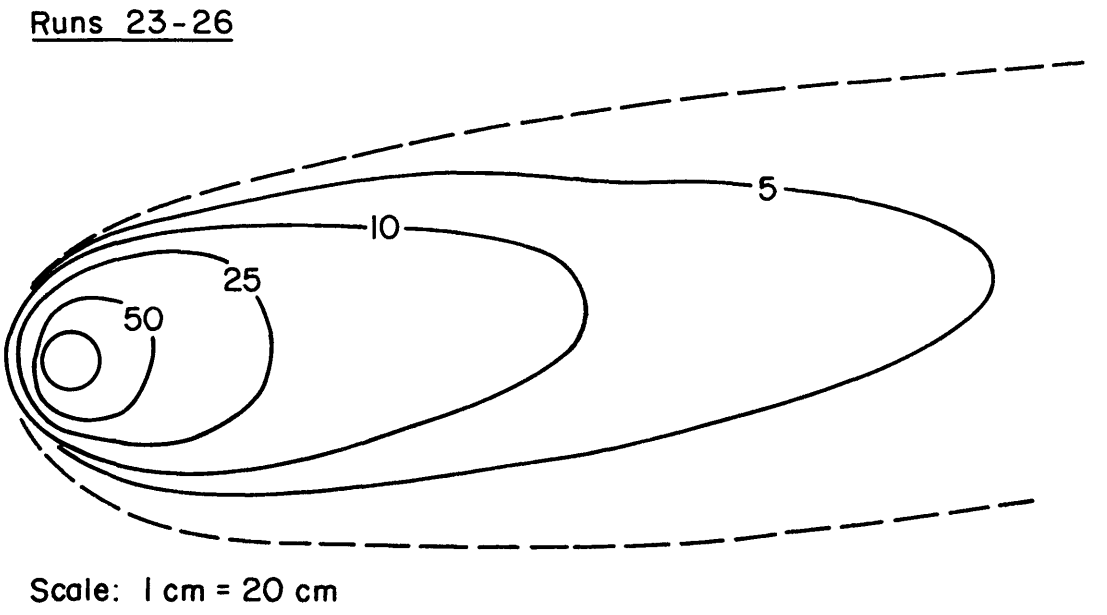

Figure 4-11. Surface Concentration Isopleths, Runs 23-26, Cold Nitrogen, ℓ_b = 4.0, Q = 130 ccs, u_* = 1.85 cm/s

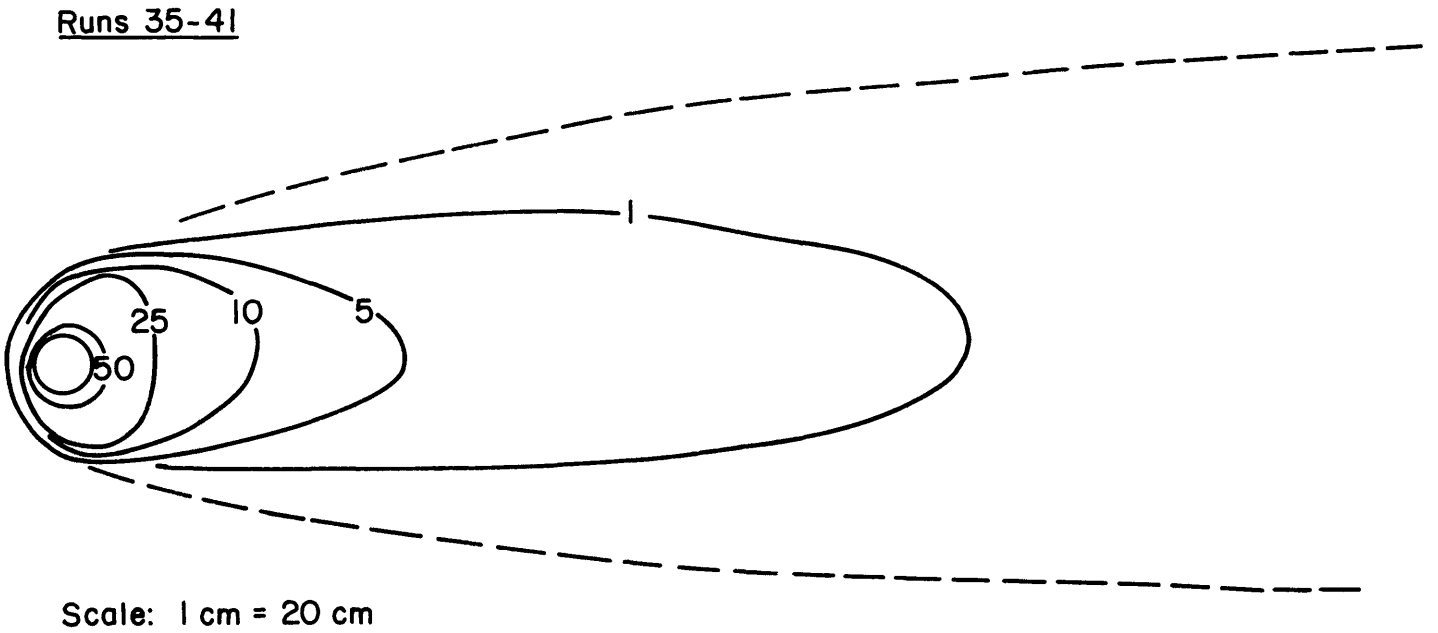

Figure 4-12. Surface Concentration Isopleths, Runs 35-41, Cold Methane, $\ell_b \simeq 2.9$, Q = 130 ccs, $u_* = 1.85$ cm/s

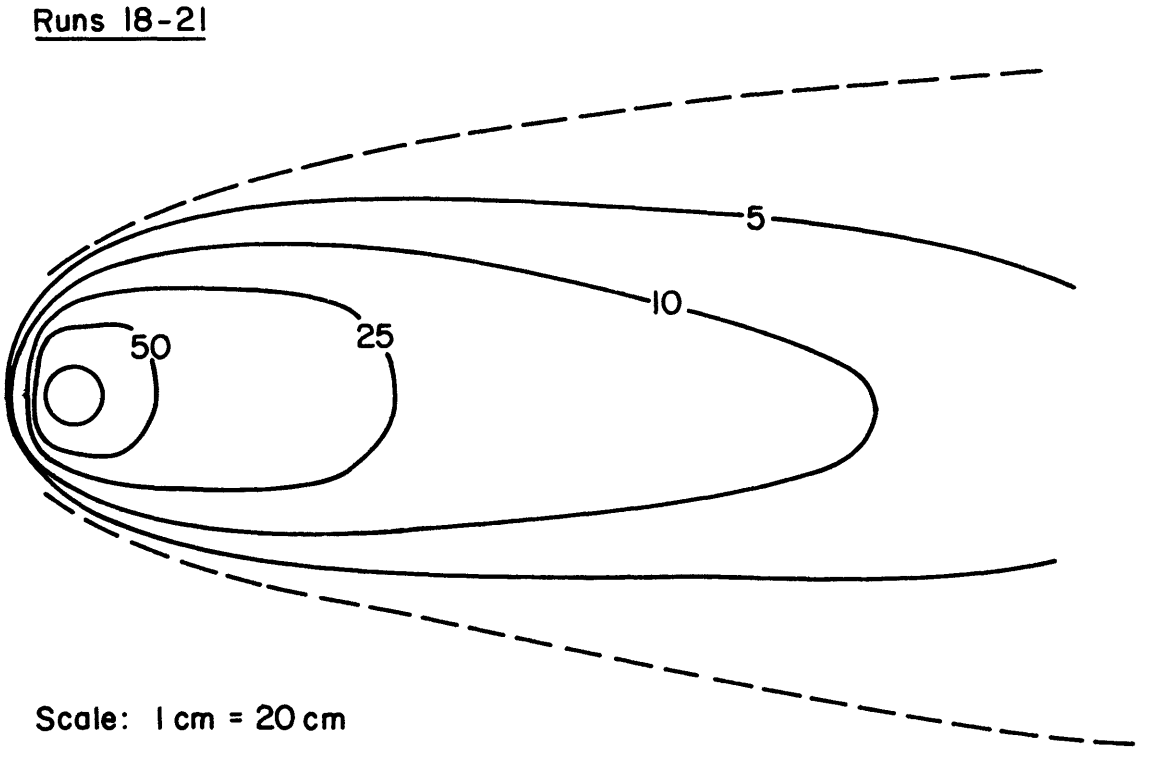

Figure 4-13. Surface Concentration Isopleths, Runs 18-21, Isothermal Gas, ℓ_b = 4.0, Q = 223 ccs, u_* = 3.20 cm/s

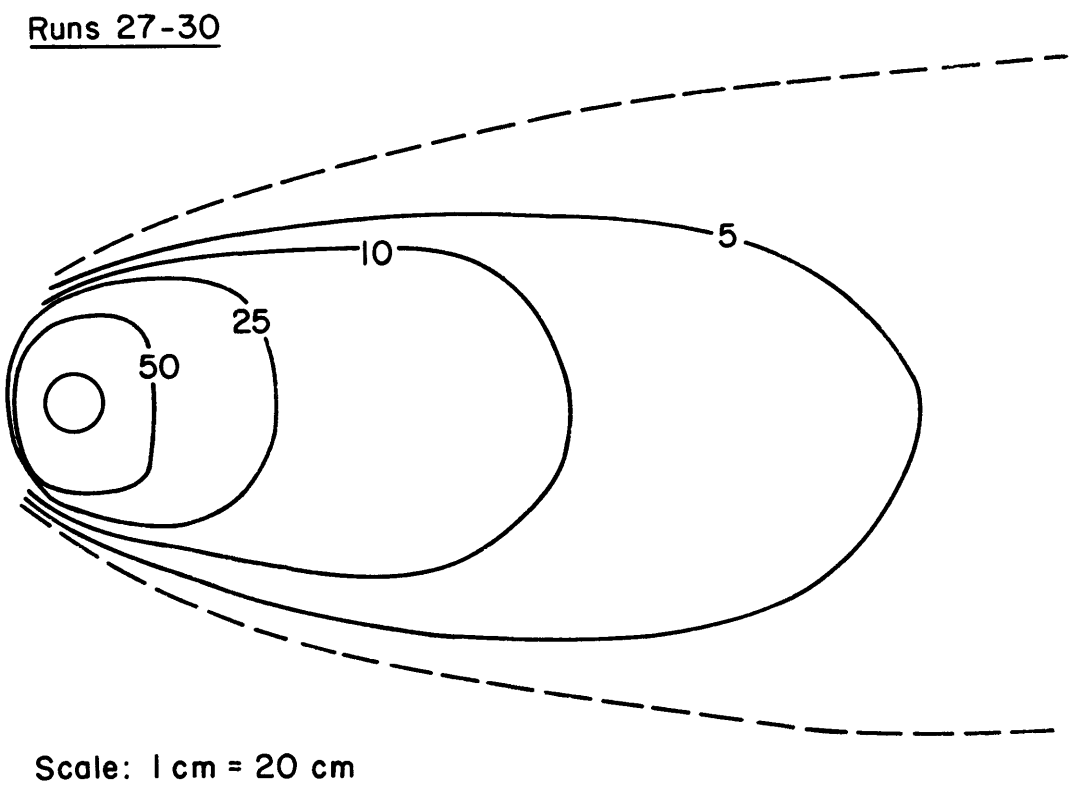

Figure 4-14. Surface Concentration Isopleths, Runs 27-30, Cold Nitrogen, ℓ_b = 4.0, Q = 223 ccs, u_* = 3.20 cm/s

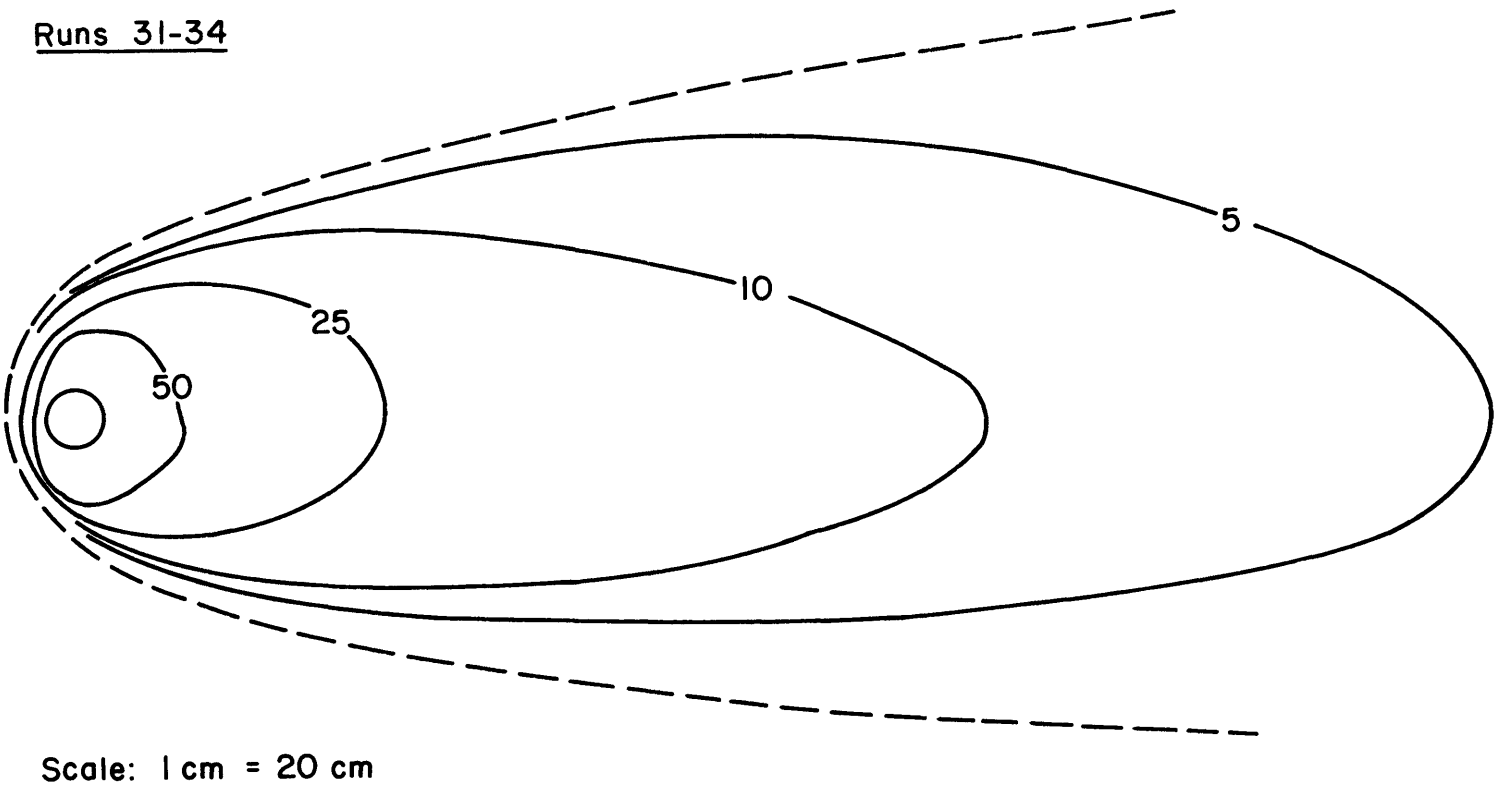

Figure 4-15. Surface Concentration Isopleths, Runs 31-34, Cold Carbon Dioxide, ℓ_b = 3.9, Q = 223 ccs, u_* = 3.20 cm/s

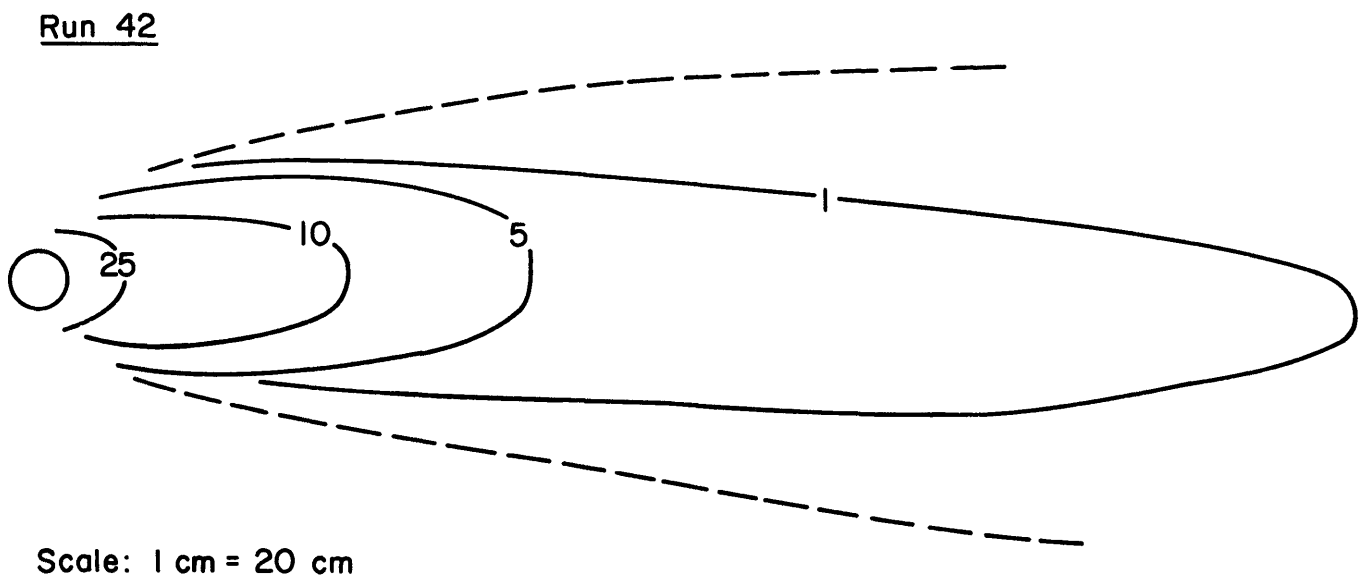

Figure 4-16. Surface Concentration Isopleths, Run 42, Cold Methane, ℓ_b = 0.8, Q = 130 ccs, u_* = 2.87 cm/s

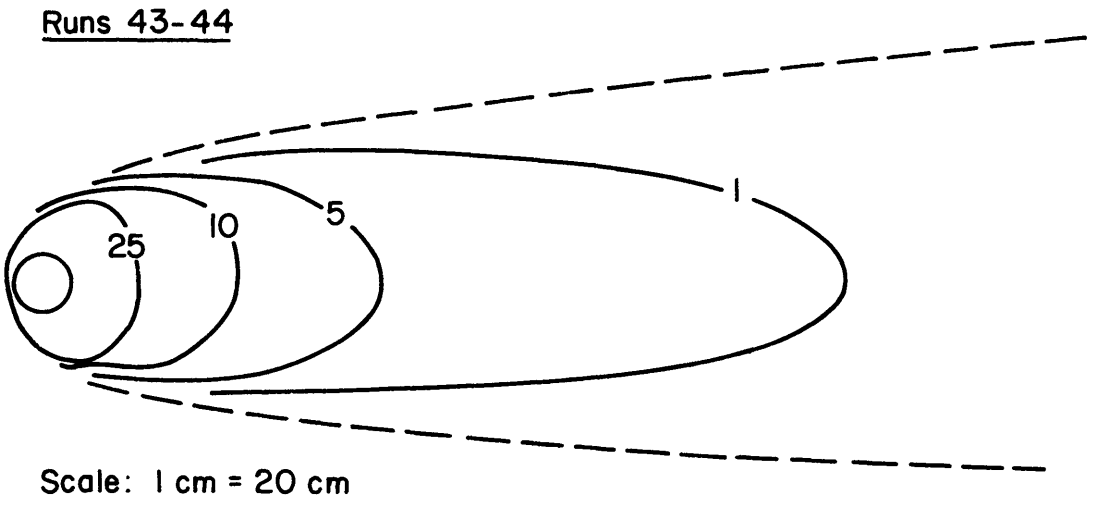

Figure 4-17. Surface Concentration Isopleths, Runs 43-44, Cold Methane, ℓ_b = 9.2, Q = 195 ccs, u_* = 1.45 cm/s

the paragraphs above seem to be consistent with data from the first twelve runs. At the lower bouyancy scale, $\ell_b \sim 1$, all plumes appeared to grow laterally at similar rates, indeed for Runs 10, 11, and 12 the isopleths were essentially coincident.

The plumes continue to grow laterally even after $\sqrt{g'H}$ is nearly zero. The growth rate for $x \geq 2$ m approaches values associated with mixing due to background ambient turbulence. It is likely that beyond the initial gravity spread region near the source, lateral growth is dependent on how rapidly surface heat transfer destroys the potential energy available to drive cloud fronts outward. Of course there is some trade off in the rate of buoyancy destruction between temperature difference and surface area since $\dot{Q} = h_s A(T_w - T)$.

4.3.1 Elevated Behavior

Vertical concentration profiles are available at $x = 0.3$, 0.6, 1.2, and 2.4 m downwind of the plume centerline for Runs 14 through 44 as Figures 4-18 through 4-23. In no case do we see the flat well mixed regions within the plumes proposed by several authors to result from thermal convection. Instead the vertical profiles decay in either a gaussian or exponential manner. The profiles reported for LNG spills at China Lake showed similar decay (Ermak et al., 1982).

Plume height evaluated from the vertical concentration profiles is plotted versus downwind distance in Figure 4-24. It is apparent that the isothermal, cold nitrogen, and cold carbon dioxide plumes all grow vertically at rates near Pasquill-Gifford category F or G conditions. The cold methane plume's vertical growth is initially retarded by its negative stratification, but after it becomes bouyant its height

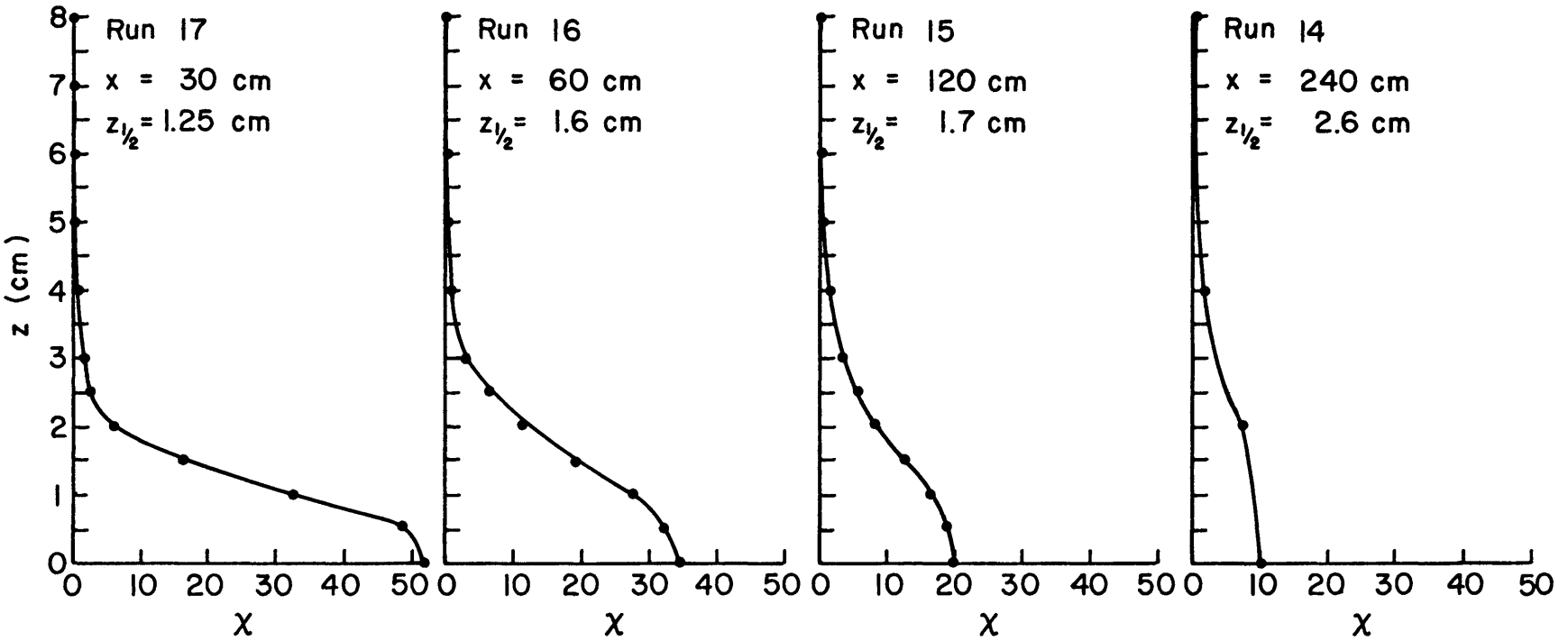

Figure 4-18. Vertical Concentration Profiles, Runs 14-17, Isothermal Gas, ℓ_b = 4.0, Q = 130 ccs, u_* = 1.85 cm/s

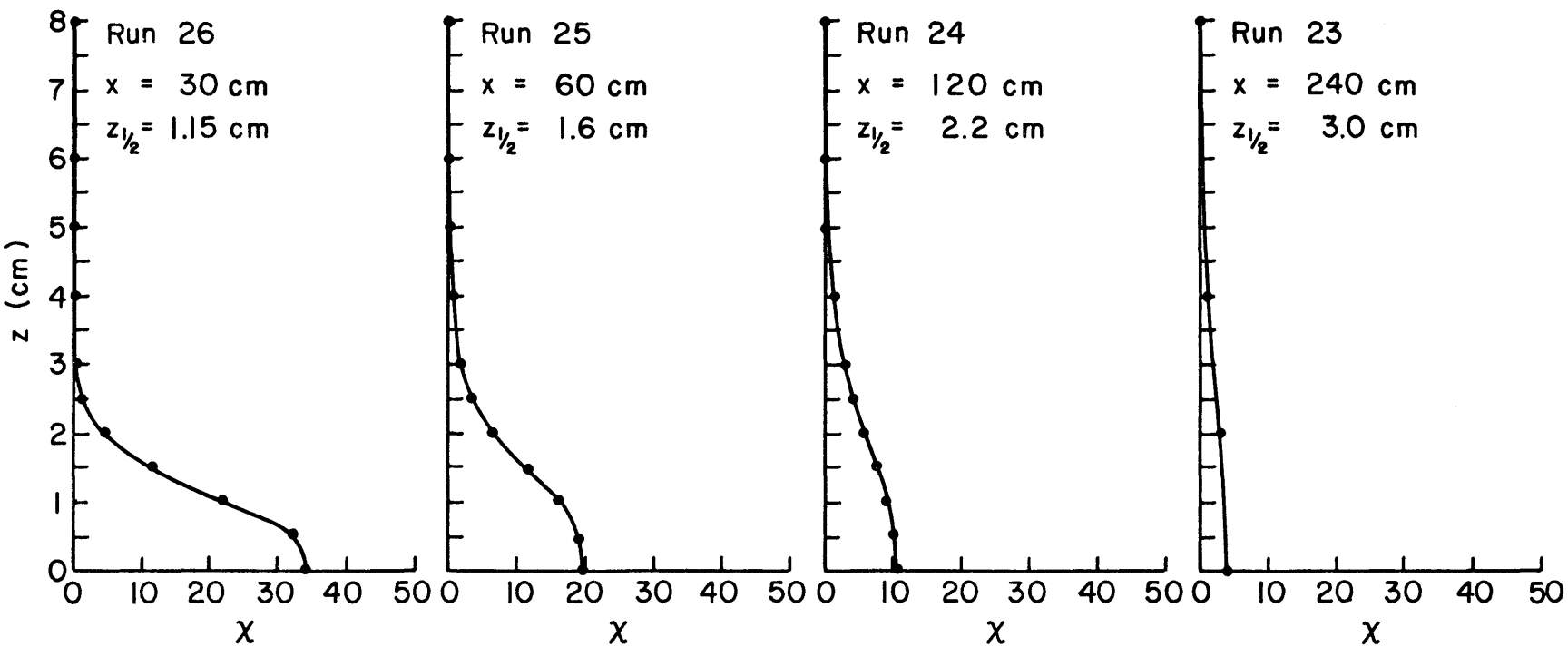

Figure 4-19. Vertical Concentration Profiles, Runs 23-26, Cold Nitrogen, ℓ_b = 4.0, Q = 130 ccs, u_* = 1.85 cm/s

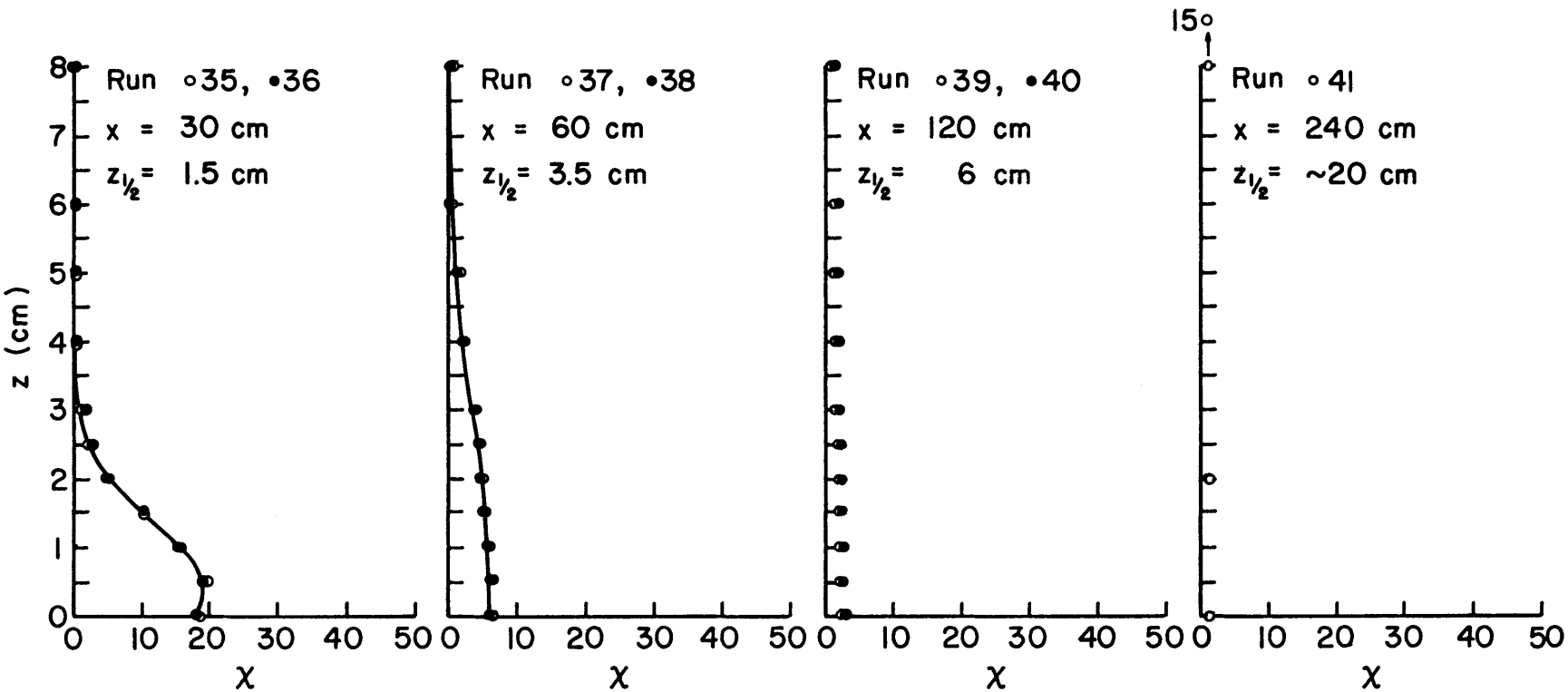

Figure 4-20. Vertical Concentration Profiles, Runs 35-41, Cold Methane, ℓ_b = 2.9, Q = 130 ccs, u_* = 1.85 cm/s

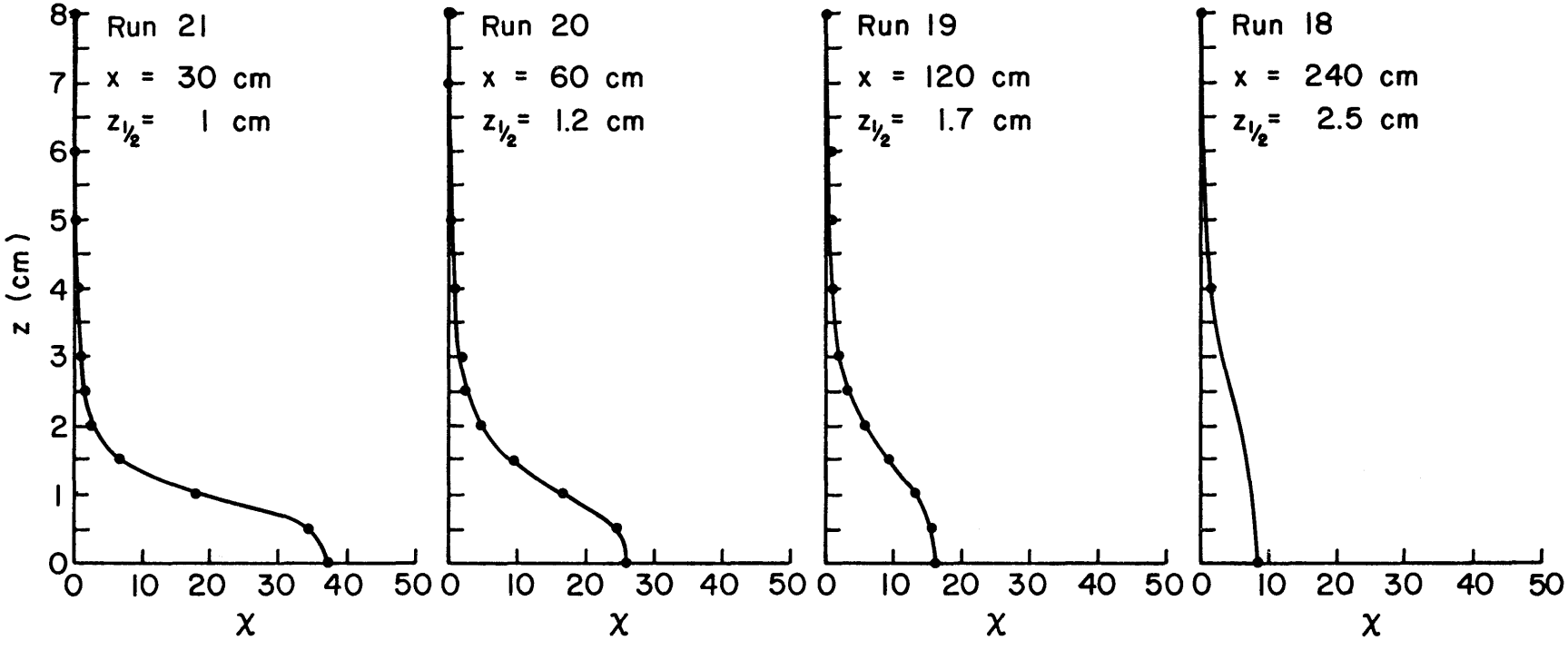

Figure 4-21. Vertical Concentration Profiles, Runs 18-21, Isothermal Gas, ℓ_b = 4.0, Q = 223 ccs, u_* = 3.20 cm/s

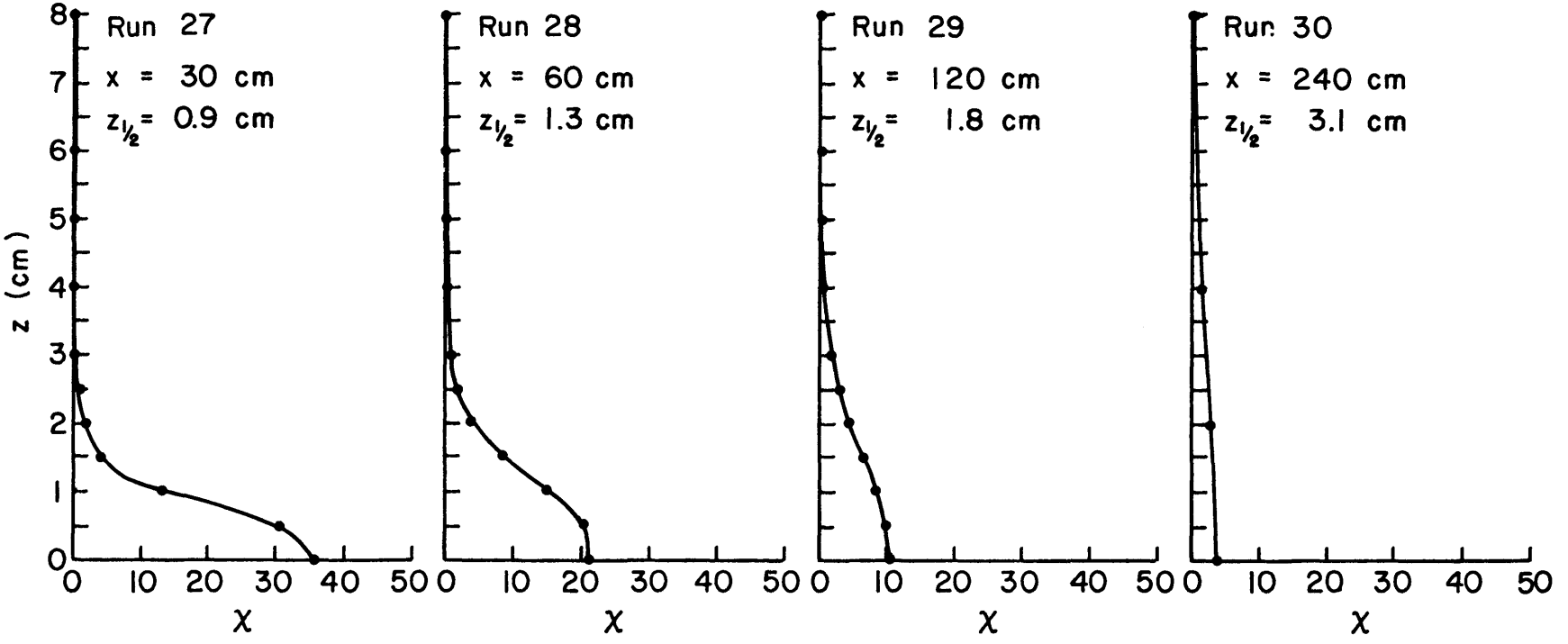

Figure 4-22. Vertical Concentration Profiles, Runs 27-30, Cold Nitrogen, ℓ_b = 4.0, Q = 223 ccs, u_* = 3.20 cm/s

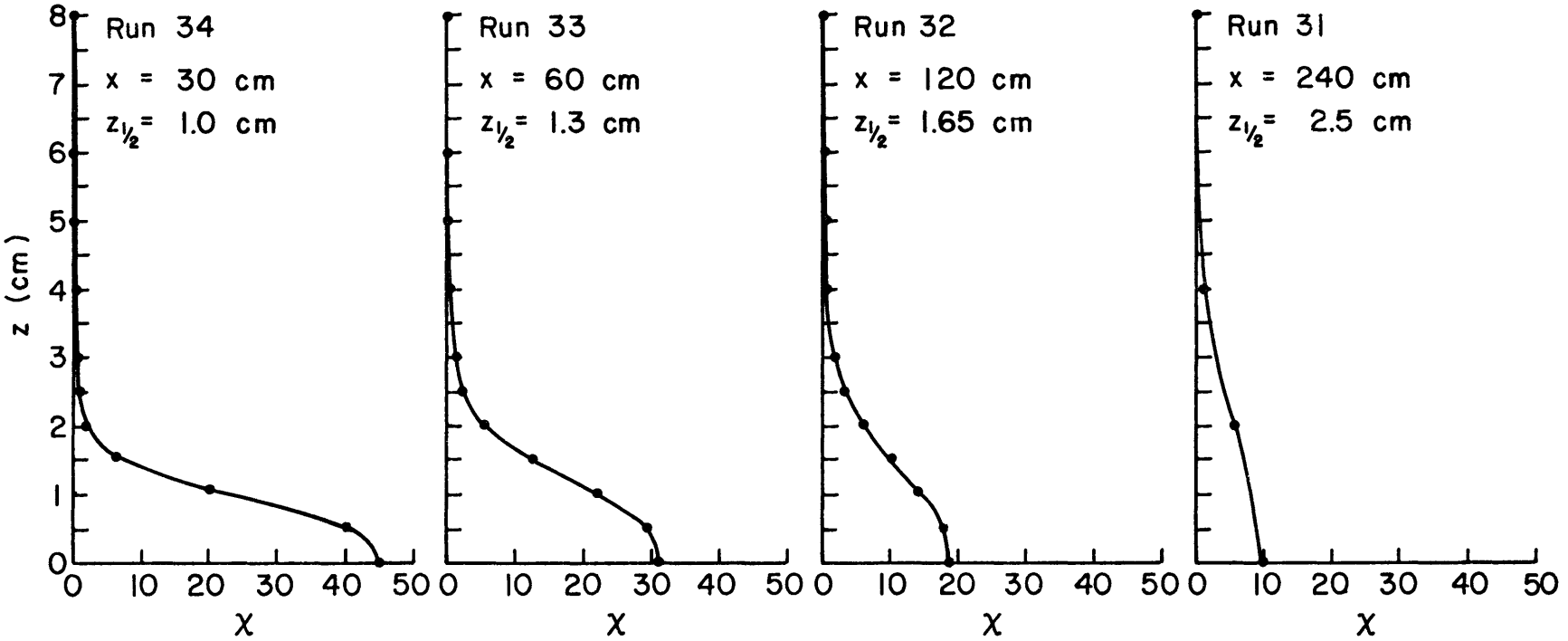

Figure 4-23. Vertical Concentration Profiles, Runs 31-34, Cold Carbon Dioxide, ℓ_b = 3.9, Q = 223 ccs, u_* = 3.20 cm/s

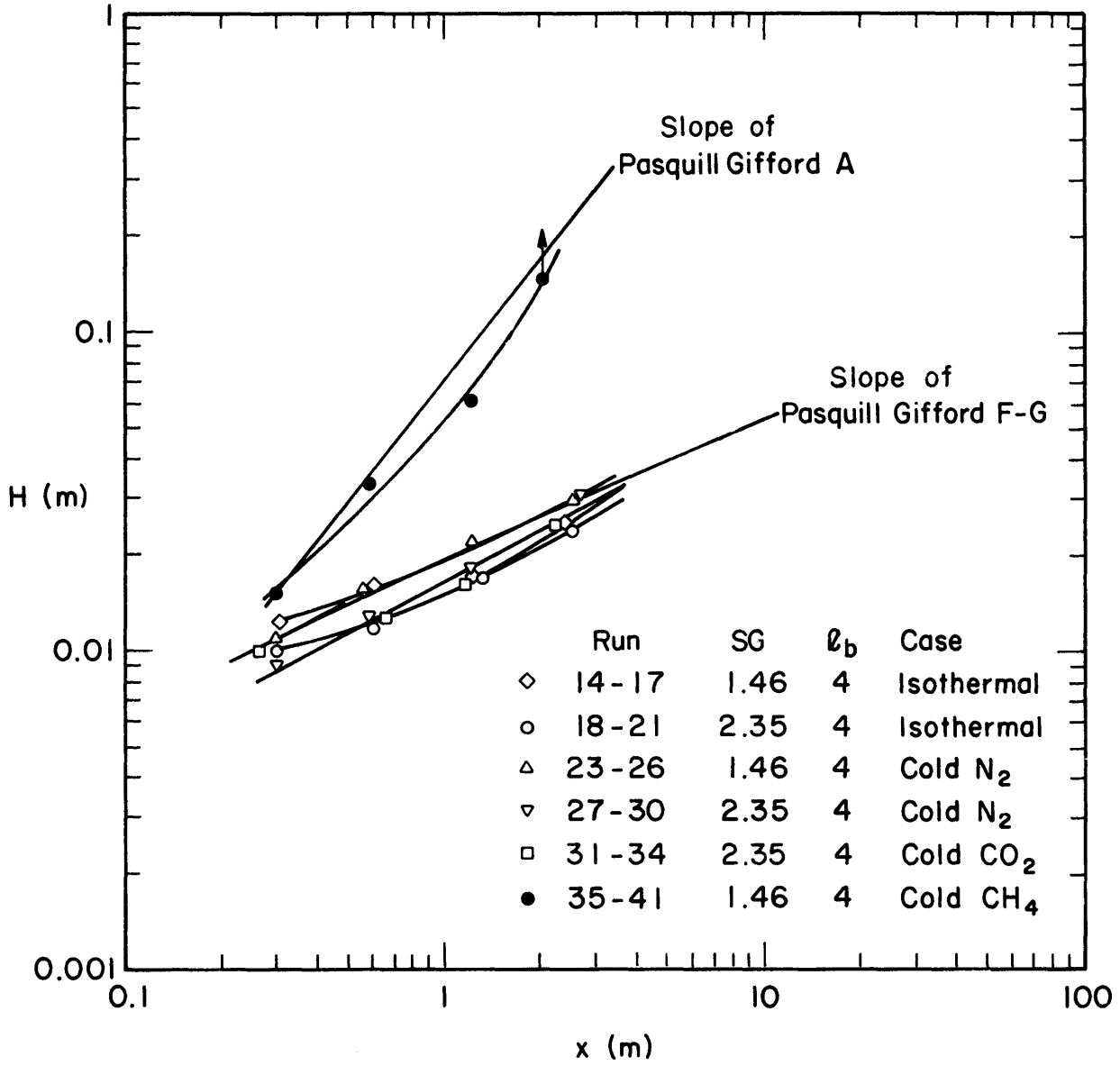

Figure 4-24. Plume Height versus Downwind Distance

increases as a passive plume in a Pasquill-Gifford A category atmosphere.

4.3.2 Methane Plumes at Various Wind Conditions

Methane plumes were released under a range of shear flow conditions (i.e. $\ell_b \sim 1$ to 8). Figure 4-9 displays the alongwind surface dilution of these plumes; unfortunately, these are not directly comparable conditions since the set includes a range of source strength rates; hence any conclusions drawn from this figure may be inappropriate. An alternative presentation is provided in Figure 4-25, where a dimensionless concentration, $K = \frac{T_o}{T_a}(\frac{\chi}{1-\chi})\frac{u_R L_R^2}{Q}$, suggested by Neff and Meroney (1982), is plotted versus downwind distance, x. This plot automatically normalizes for source variations in volume flow rate or temperature. A band of data associated with isothermal experiments falls above the methane data. Model methane plumes would produce these values if heat transfer effects were completely absent. The cold methane plumes dilute faster as buoyancy length scale, ℓ_b, increases or wind shear decreases.

During experimental Runs 1 through 12 sampling tubes were suspended above the model channels. The turbulent wakes of these tubes added artificial turbulence which reduced concentrations from Runs 1 and 7 below their counterpart experiments 14-17 and 18-21. A specific gravity effect becomes apparent when Runs 14-17 and 4 are compared to Runs 18-21 and 10 respectively. In each case the higher specific gravity gas seems to produce lower concentrations when released at constant values of the buoyancy length scale.

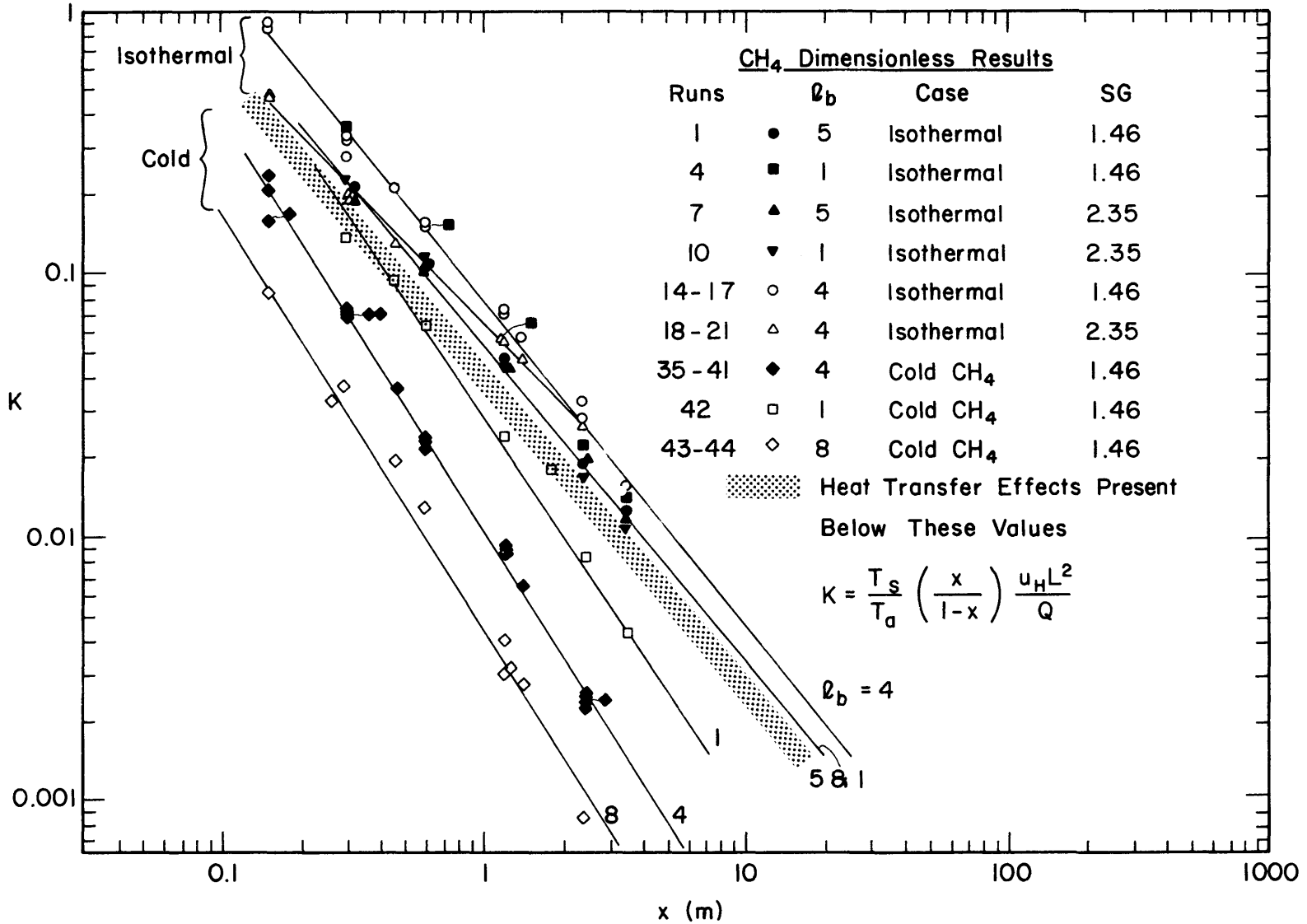

Figure 4-25. Dimensionless Concentration Coefficient Variation with Distance, Isothermal and Methane Runs

*During Runs 1-13 the wakes of sampling tube suspended over the cloud artificially reduced plume concentrations.

4.4 Temperature Test Results

During the cold gas runs, Runs 22-24, thermocouples monitored the gas temperatures at selected surface and elevated locations. Calibration differences between the various thermocouples plus the statistical variability of the cold plume and themal drift in the ground temperature made separation of gas temperatures from ambient temperatures difficult where $T_a - T < 1$ C. Thus one cannot expect accurate temperature measurements when concentrations fall below 1% even for nearly adiabatic plume mixing. This will only be limiting over the distances modeled for the methane runs.

Temperatures measured are summarized in tables found in Appendix E. Vertical temperature profiles are displayed in Figures 4-26 through 4-29. Thermal plume depths are similar to those of concentration. The vertical profiles will be used in Section 5.2 to define local stratification conditions during entrainment rate calculations.

It is also of interest to compare local plume temperatures to local concentrations. Figures 4-30 through 4-33 compare local temperatures and local concentrations for cold nitrogen, cold carbon dioxide and cold methane runs. Since a depth averaged numerical box model has been utilized to evaluate plume behavior in Sections 5.1 and 5.2 the depth averaged values of experimental concentrations and temperatures from the vertical traverses are also included on Figures 4-30 through 4-33. Re-evaporation of condensed water vapor results in the sudden change in slope or kinks observed on the respective figures. Predicted lines for dry adiabatic, and humid adiabatic mixing are noted. These curves are independent of any entrainment model and assume only adiabatic mixing of constant property ideal gases. (See Appendix B.)

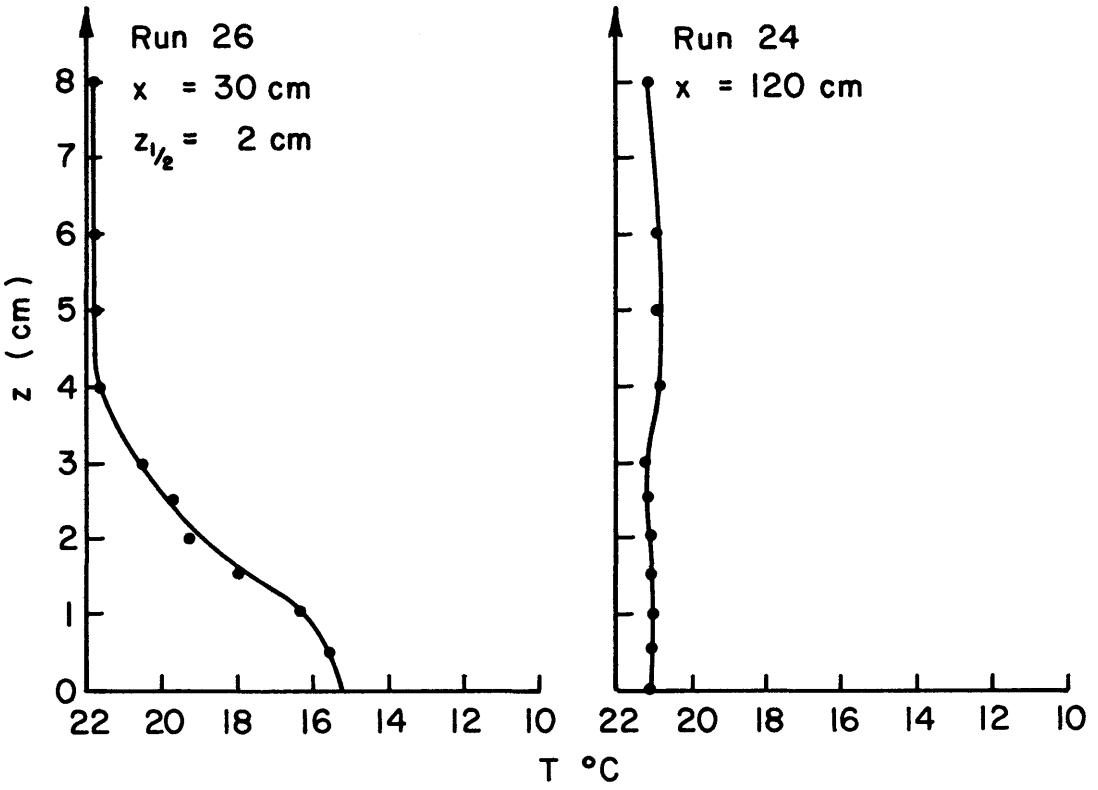

Figure 4-26. Vertical Temperature Profiles, Runs 24-26, Cold Nitrogen, ℓ_b = 4.0, Q = 130 ccs, u_* = 1.85 cm/s

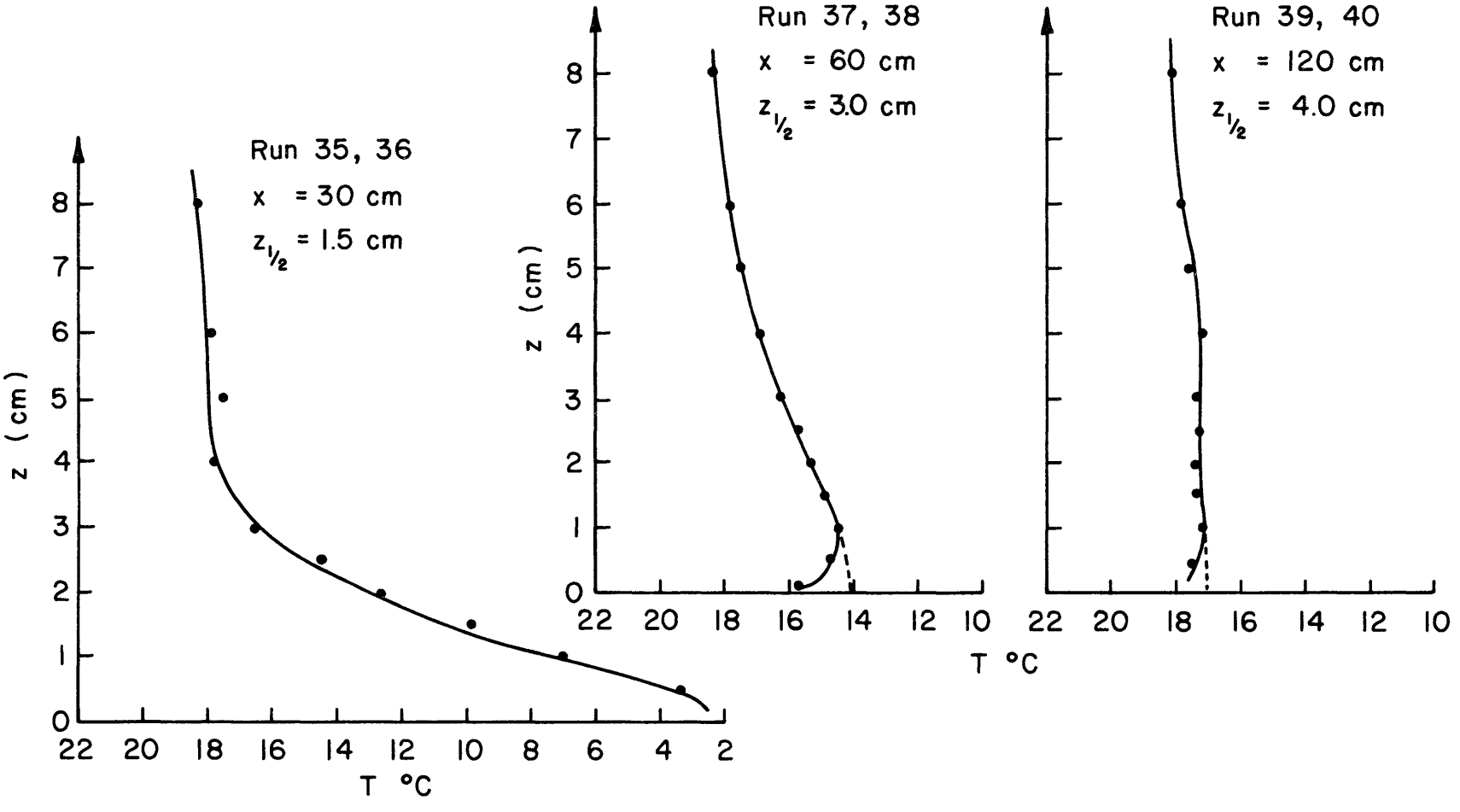

Figure 4-27. Vertical Temperature Profiles, Runs 35-40, Cold Methane, ℓ_b = 2.9, Q = 130 ccs, u_* = 1.85 cm/s

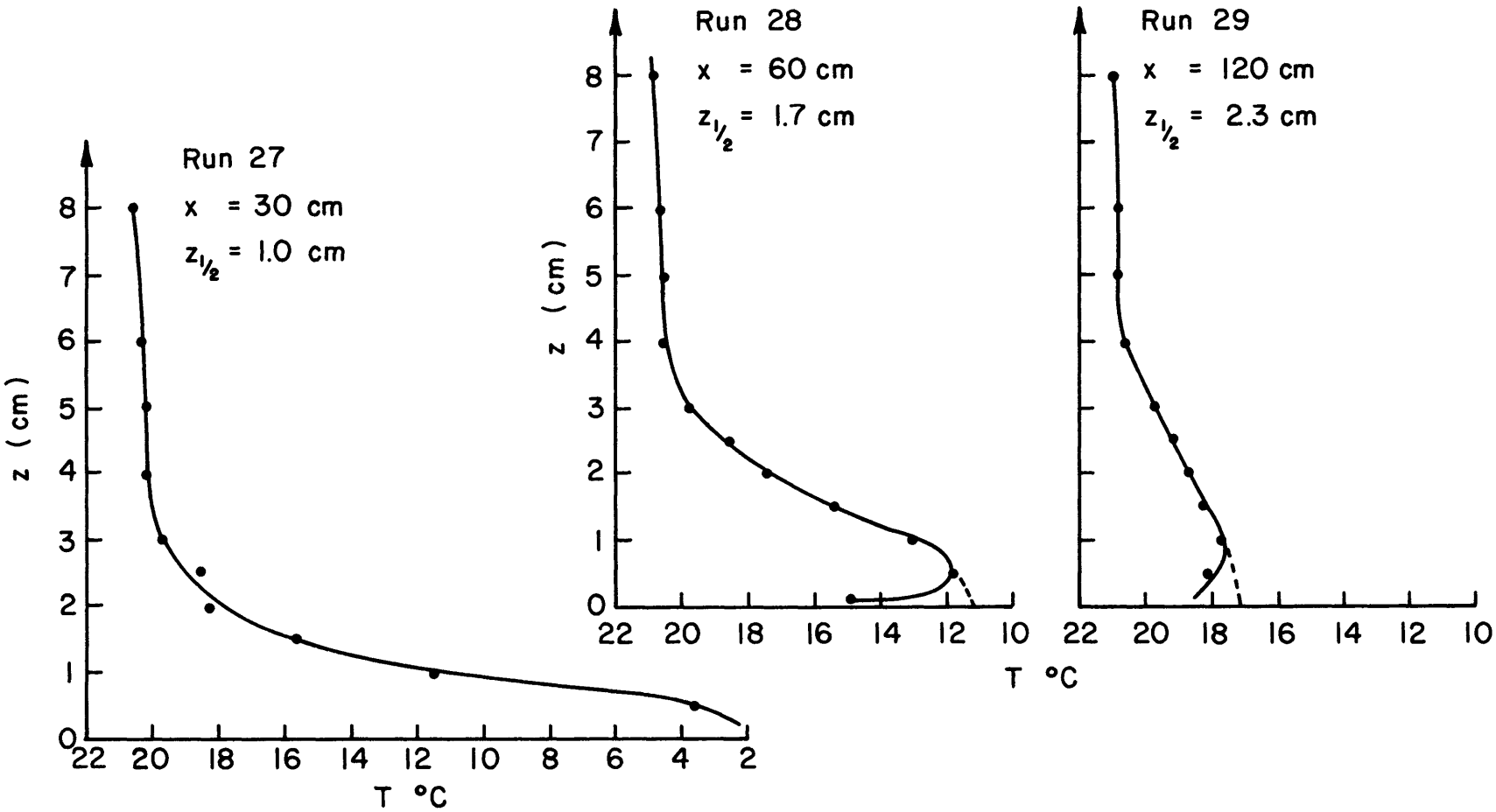

Figure 4-28. Vertical Temperature Profiles, Runs 27-29, Cold Nitrogen, ℓ_b = 4.0, Q = 223 ccs, u_* = 3.20 cm/s

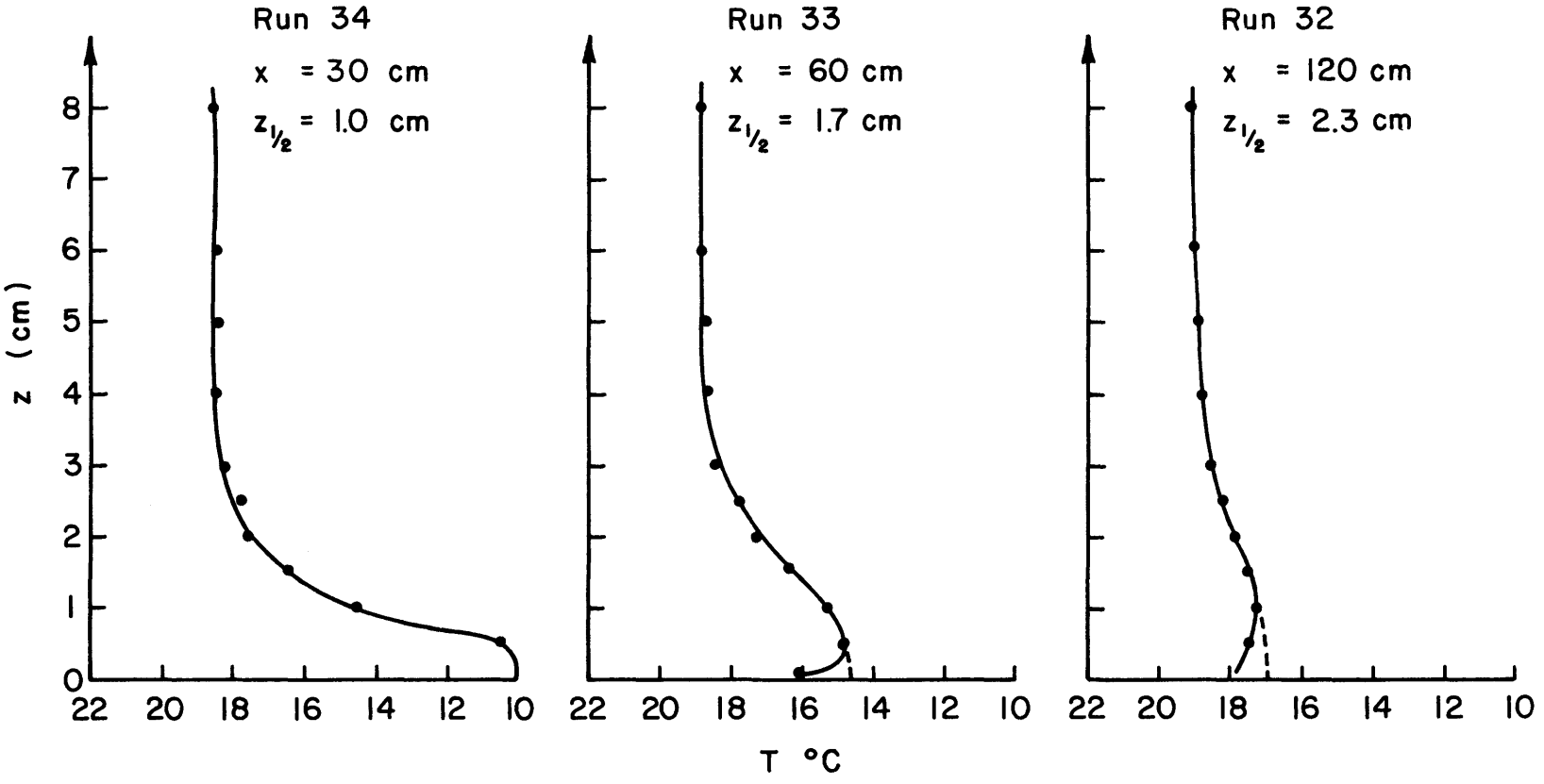

Figure 4-29. Vertical Temperature Profiles, Runs 32-34, Cold Carbon Dioxide, ℓ_b = 3.9, Q = 223 ccs, u_* = 3.20 cm/s

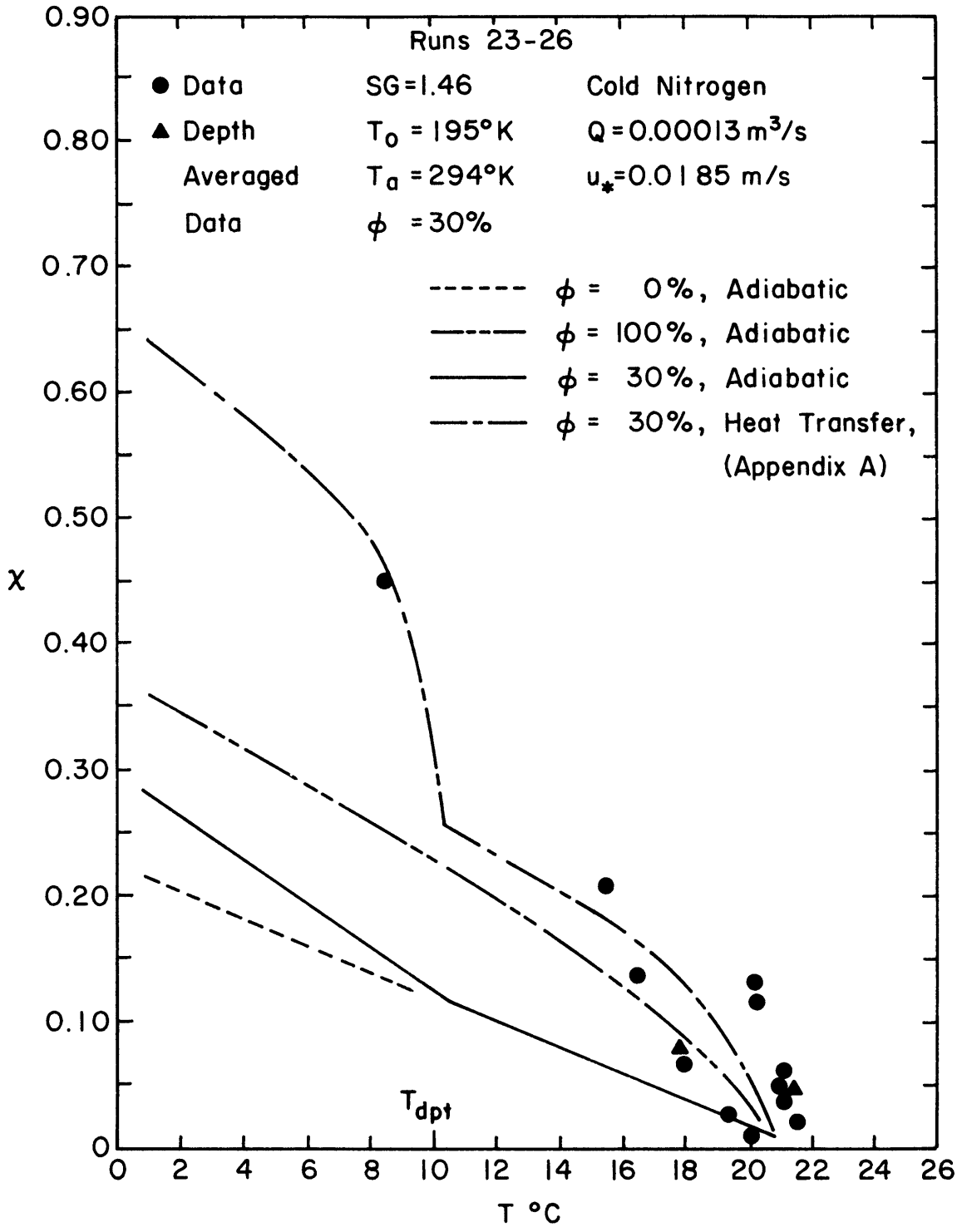

Figure 4-30. Concentration Against Temperature Measurements for Vertical Profile Stations, Runs 23-26, Cold Nitrogen, ℓ_b = 4.0, Q = 130 ccs, u_* = 1.85 cm/s

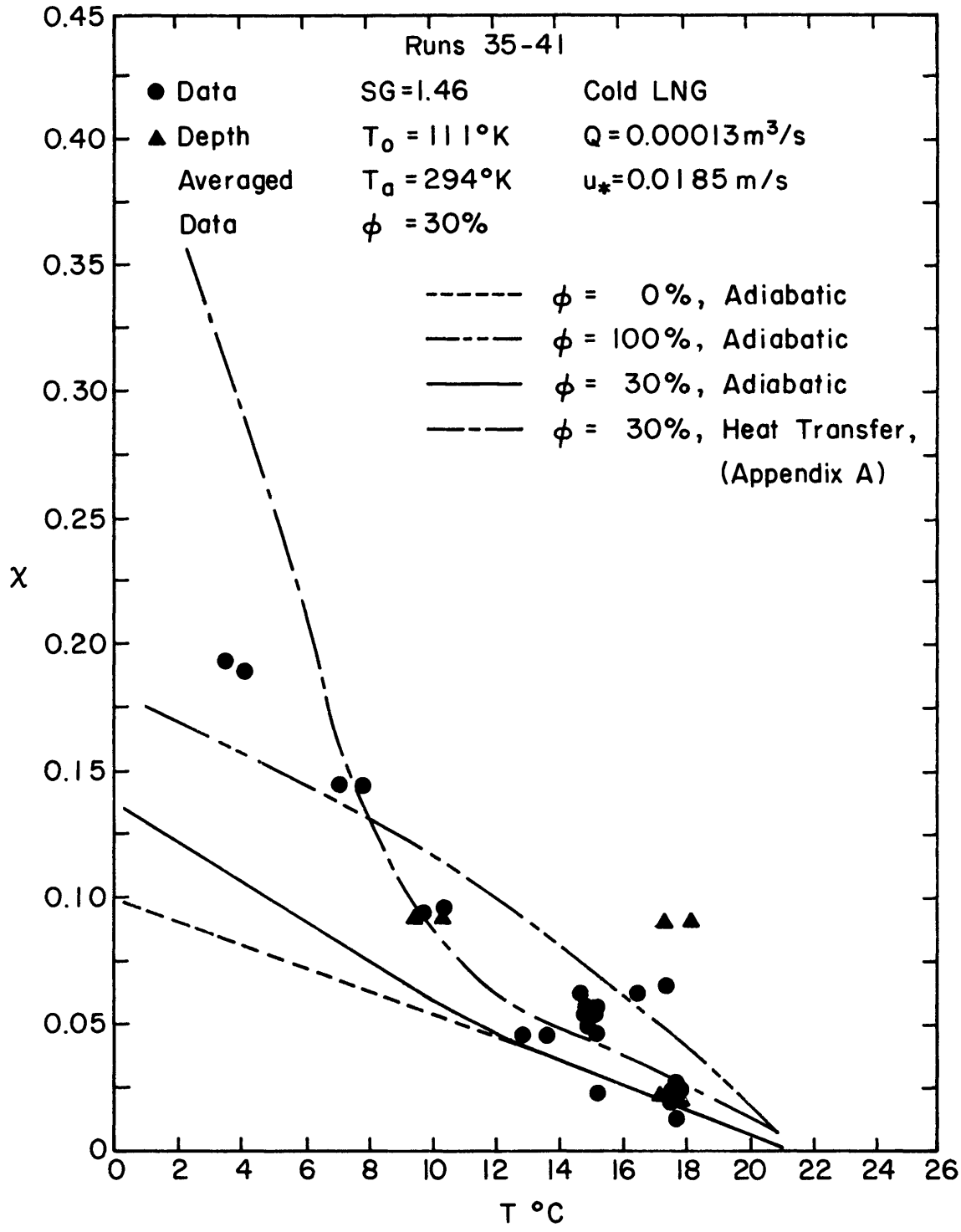

Figure 4-31. Concentration Against Temperature Measurements for Vertical Profile Stations, Runs 35-41, Cold Methane, ℓ_b = 2.9, Q = 130 ccs, u_* = 1.85 cm/s

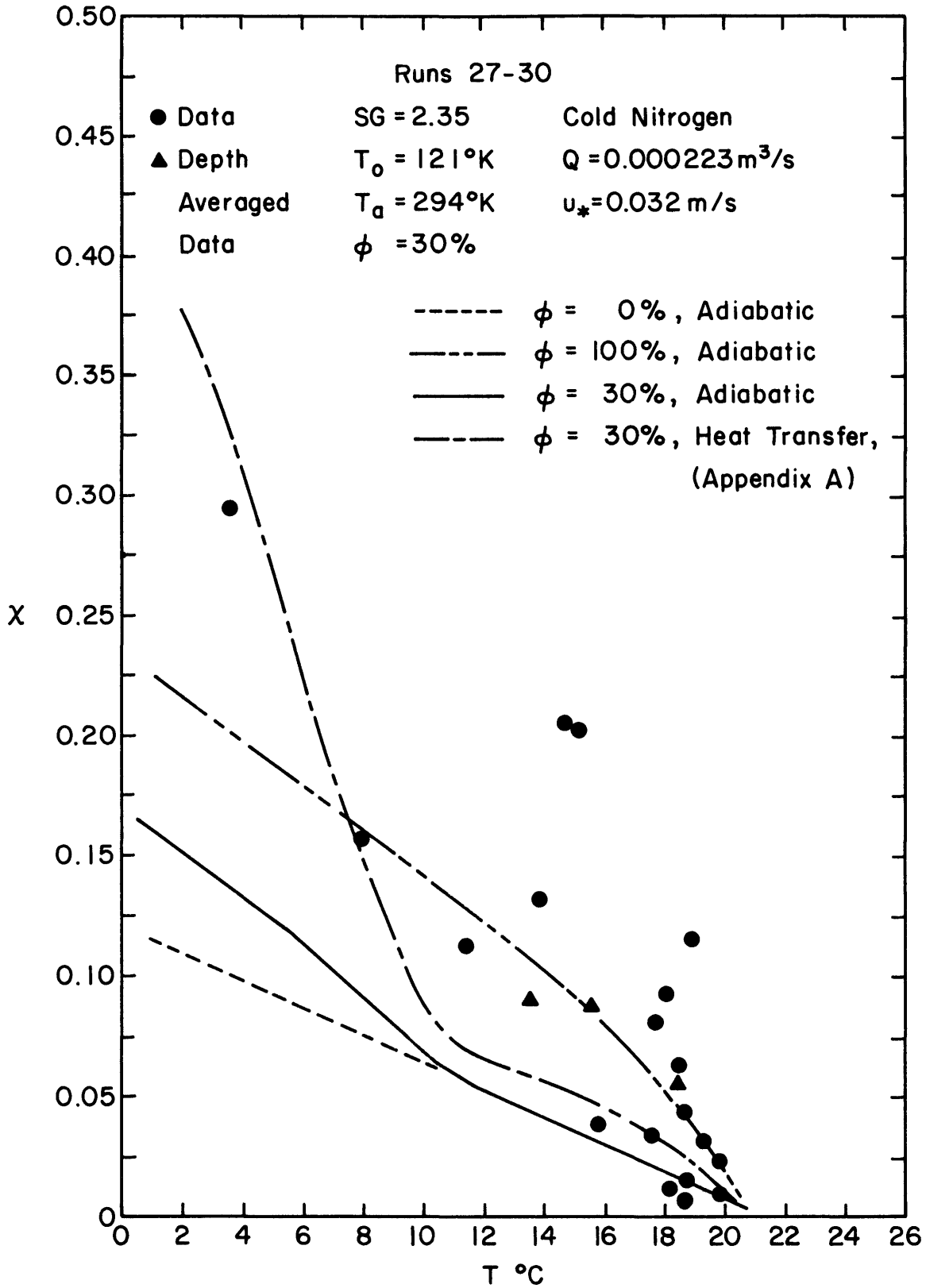

Figure 4-32. Concentration Against Temperature Measurements for Vertical Profile Stations, Runs 27-30, Cold Nitrogen, ℓ_b = 4.0, Q = 223 ccs, u_* = 3.20 cm/s

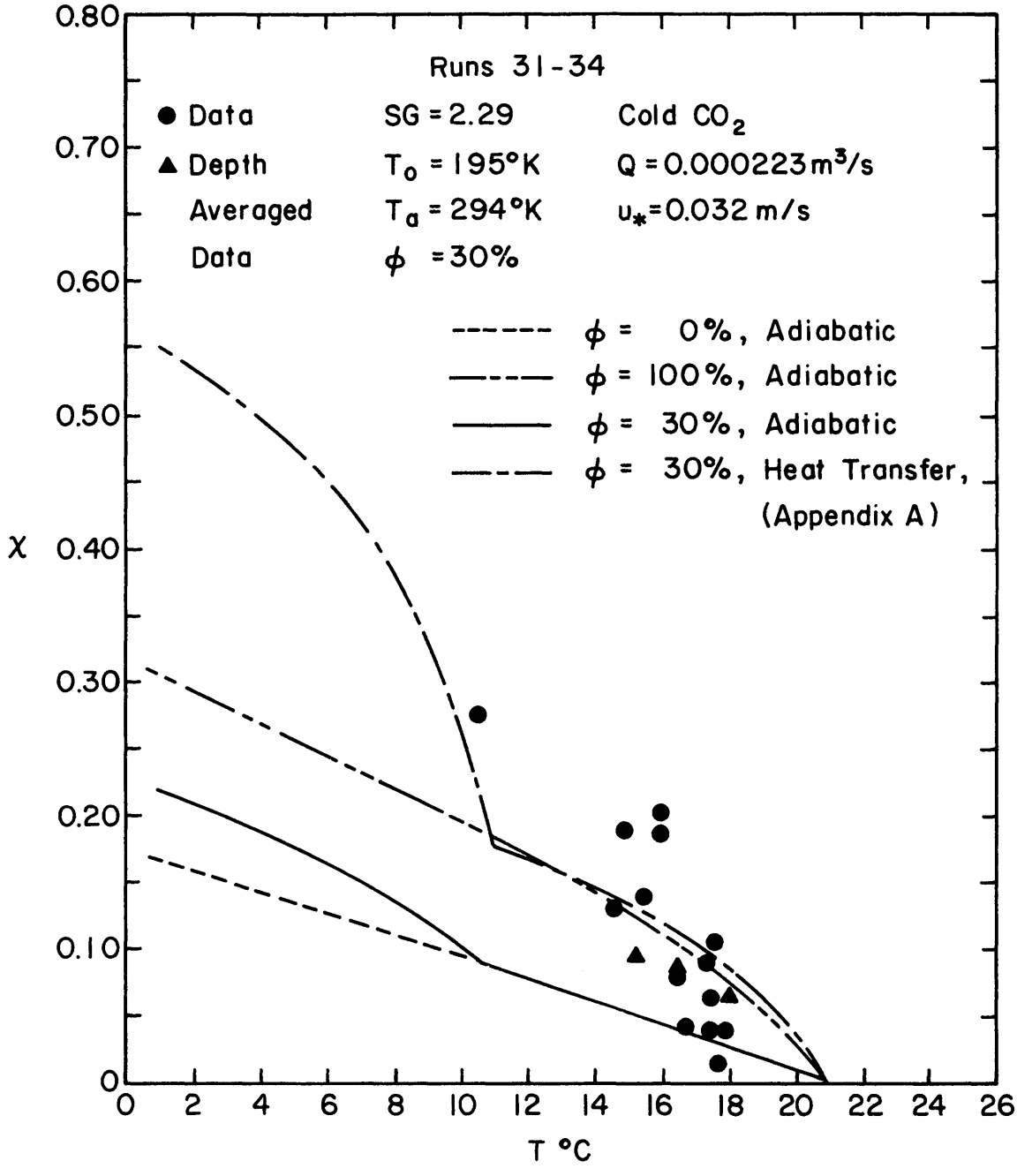

Figure 4-33. Concentration Against Temperature Measurements for Vertical Profile Stations, Runs 31-34, Cold Carbon Dioxide, ℓ_b = 3.9, Q = 223 ccs, u_* = 3.20 cm/s

5.0 DISCUSSION OF COLD GAS DISPERSION RESULTS

The number of analytic and numerical models seems to exceed the sets of data to evaluate them. Most of these models do contain a common physical foundation, but differ on the entrainment mechanisms or constants chosen. A generalized box model will be used in Section 5.1 to specify preferred entrainment mechanisms based on comparison with the new data. Conservation of gas species across downwind cloud sections permits estimation of entrainment rates across the cloud top to be discussed in Section 5.2.

5.1 Comparison of Cold Gas Data with Numerical Box Model

The box model described in Appendix A uses the assumption that local Froude numbers are evaluated at the cloud head to solve for cloud spread rate and an ad hoc entrainment hypothesis to solve for cloud dilution. Advection of the cloud by the wind field is considered by solving a momentum equation, whereas heat transfer effects are considered in an enthalpy transport equation. The model considers initial inertial effects by retaining the cloud density in advection terms. Model constants are tuned to fit the present data and that of Neff and Meroney (1982); however, examination of the following Table 5-1 suggests these values are consistent with other investigators.

5.1.1 Comparison Between Box Model and New Cold Cloud Results

Calculations with the box model were performed over the source area, wind speed, and roughness conditions examined experimentally. The equivalent ranges of dimensionless parameters are (See Table 5-2): SG = 1.4 and 2.35, Ri_* = 18.8 and 38.0, and z_o^* = 2.9 x 10^{-2} and 4.2 x 10^{-2}.

TABLE 5-1

CONSTANTS USED IN HEAT TRANSFER MODELS

MODEL	α_1	α_2	α_3	α_4	α_5	α_6	α_7	β_1	β_2	C_r	C_z	ξ_0	ξ_1	ξ_2	$\frac{C_f}{2}$
INSTANTANEOUS															
Eidsvik (1980)	1.3	0.5-1.5 0.7	1.3	3.5	0.5	0.3	-	-	(1)	$\frac{\alpha_5 U_F}{U_F(0)}$	-	-	0.045	-	2×10^{-3}
Cox and Carpenter (1980)	1.0	-	-	2 ? $\alpha\left(\frac{U_1}{U_*}\right)$	-	0.36 $\left(\frac{U_1}{\beta U_*}\right)$	-	-	(1)	0.6	-	~(0.07) McAdams	.1-.03	-	.01-.001
DENS 3A.HUM	1.0	0.54	1	2.5	-	0.3	3.5	0.9	0.1	0.1	0.1	0.07	0.045	0.32	-
DENS 4A.MOM	1.0	0.54	1	2.5	-	0.3	3.5	0.9	-	0.1	0.1	0.07	0.045	0.32	2×10^{-3}
CONTINUOUS															
Eidsvik (1980)	1.3	0.5-1.5	1.3	3.5	0.5	0.3	-	-	(1)	$\frac{\alpha_5 U_F}{U_F(0)}$	-	-	0.045	-	2×10^{-3}
Cox and Carpenter (1980)	1	-	-	2	-	0.36	-	-	(1)	0.6	-	(0.07)	1-0.03	-	.01-.001
Zeman (1982)	-	0.25	1	12.5	-	0.64	-	-	-	-	-	0.21	0.08	-	6.4×10^{-3}
Ermak et al. (1983)	1	0.50	1	1.6	-	0.4	-	-	-	-	-	0.21	0.038	-	1.4×10^{-3}
DENS 5A.CON	1	0.50	1	2.5	-	0.3	2.5	-	1	0.1	0.1	0.07	0.045	0.32	-
DENS 6AC.MOM	1	0.50	1	2	-	0.3	3	-	-	0.01	0.01	0.07	0.045	0.32	2×10^{-3}

$k = 0.4$, NOTE: $\xi_1 = \sqrt{\frac{C_f}{2}}$, $\alpha_1 = 1$ implied by $\beta_1 = 0.9$

Cloud dilution, χ, is plotted versus downwind distance, x, in Figures 5-1 through 5-7. These curves may be compared with experimental data discussed in Section 4.3. All figures are presented in terms of equivalent methane spill to emphasize heat transfer aspects.

When the gas parcels remain negatively buoyant throughout their dispersion history the box model faithfully predicts concentration decay and plume growth. For situations where parcel densities fall below ambient densities the model cannot predict the tendency for the cloud to lift off and narrow. If heat transfer effects were negligible one would expect isothermal and cold nitrogen runs to be coincident and methane or carbon dioxide runs would deviate only due to specific heat capacity effects. If only latent heat release occurred in the absence of surface heat transfer or source specific gravity effects similar comparative curve characteristics would appear. Instead one notes the strong heat transfer effects for $\ell_b \sim 5$ in Figures 5-1, 5-3, 5-5, and 5-6, whereas heat transfer effects are less apparent for $\ell_b \sim 1$ in Figures 5-2 and 5-4.

As noted earlier in Section 4.3 the large specific heat capcity ratio for CO_2 results in centerline concentrations above the cold nitrogen counterpart experiment. As seen in Figures 5-3, 5-4, and 5-6 the cold CO_2 plume inhibit mixing more than the quickly warmed nitrogen plume.

Cold cloud temperatures approach ambient values very rapidly due to adiabatic mixing with the surrounding air as well as surface heat transfer. Indeed to a first approximation an adiabatic analysis predicts $T^* \simeq \chi$. During adiabatic entrainment perturbations from the linear relation are caused by humidity and specific heat capacity

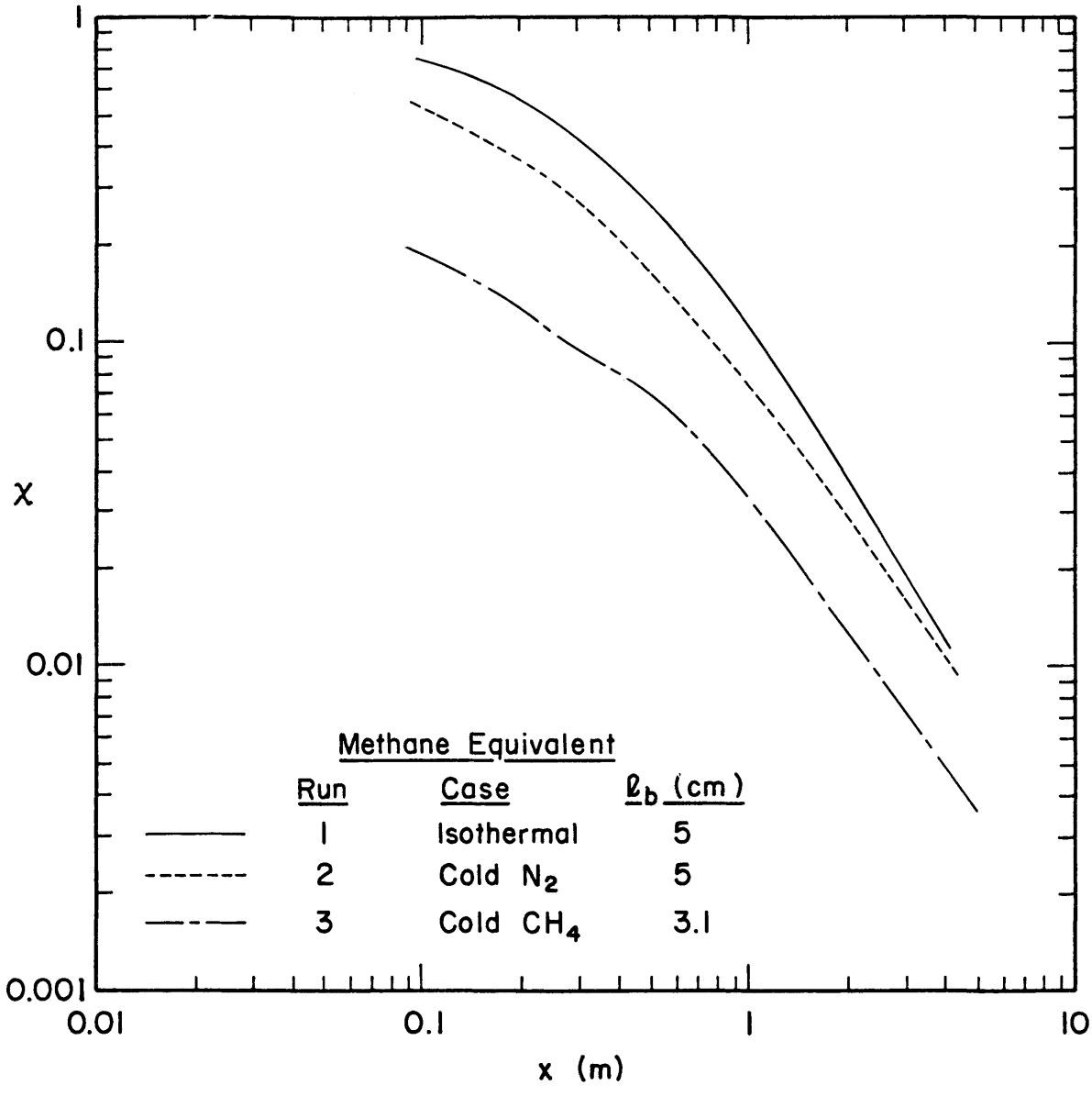

Figure 5-1. Box Model Predictions of Concentration versus Distance, Runs 1, 2, and 3, $\ell_b \simeq 5$, (see Data, Figure 4-3)

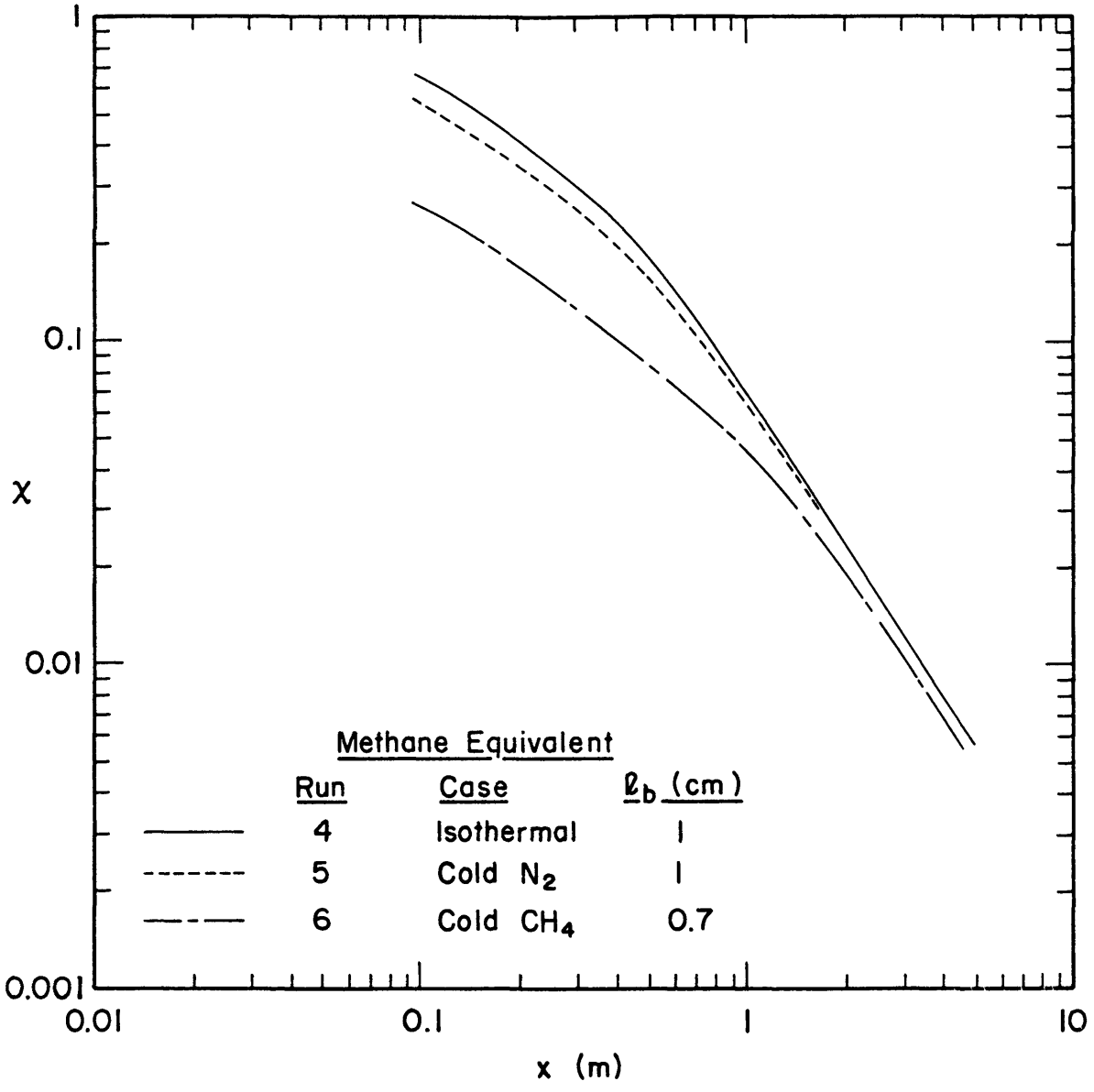

Figure 5-2. Box Model Predictions of Concentration versus Distance, Runs 4, 5, and 6, $\ell_b \simeq 1$ (see Data, Figure 4-4)

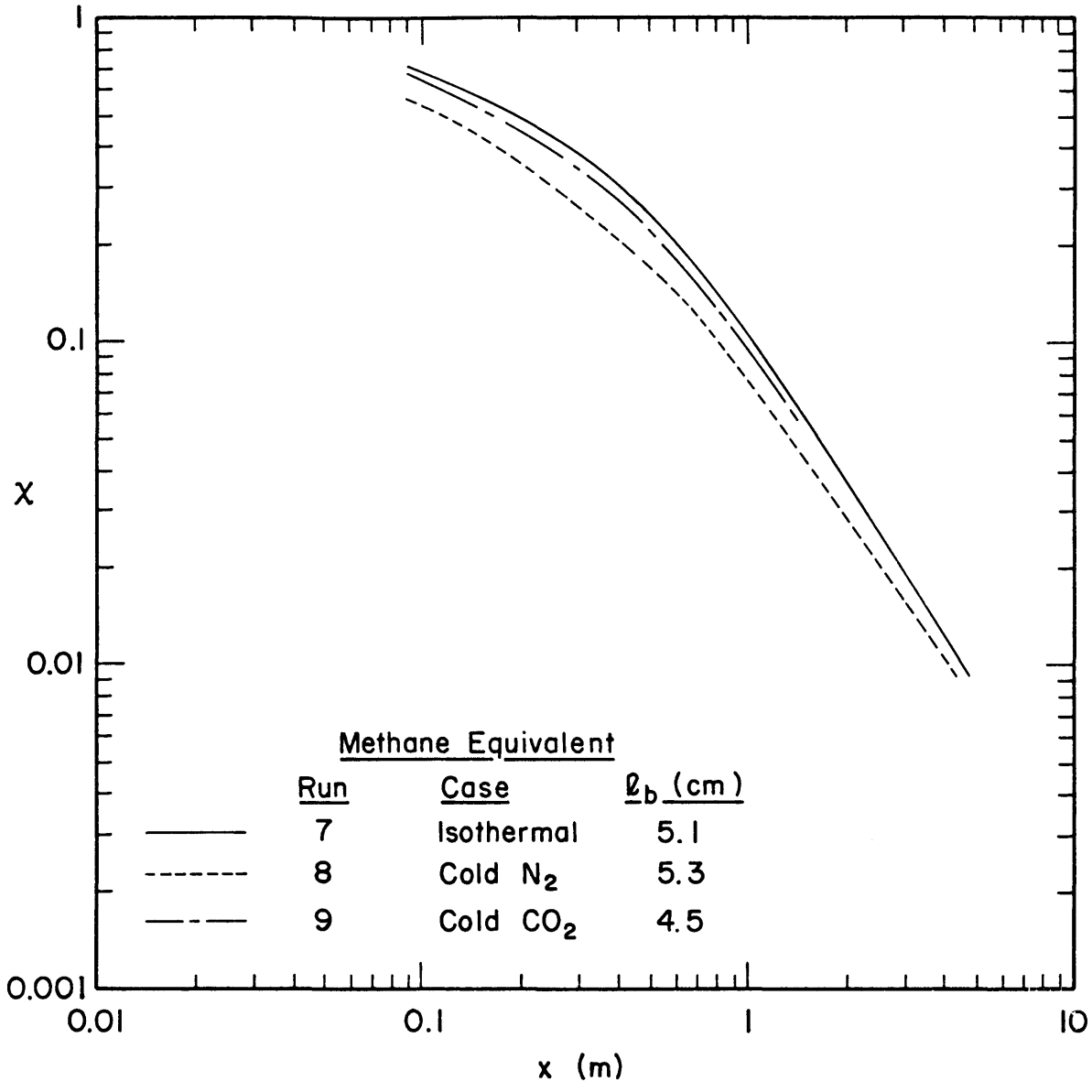

Figure 5-3. Box Model Predictions of Concentration versus Distance, Runs 7, 8, and 9, $\ell_b \simeq 5$ (see Data, Figure 4-5)

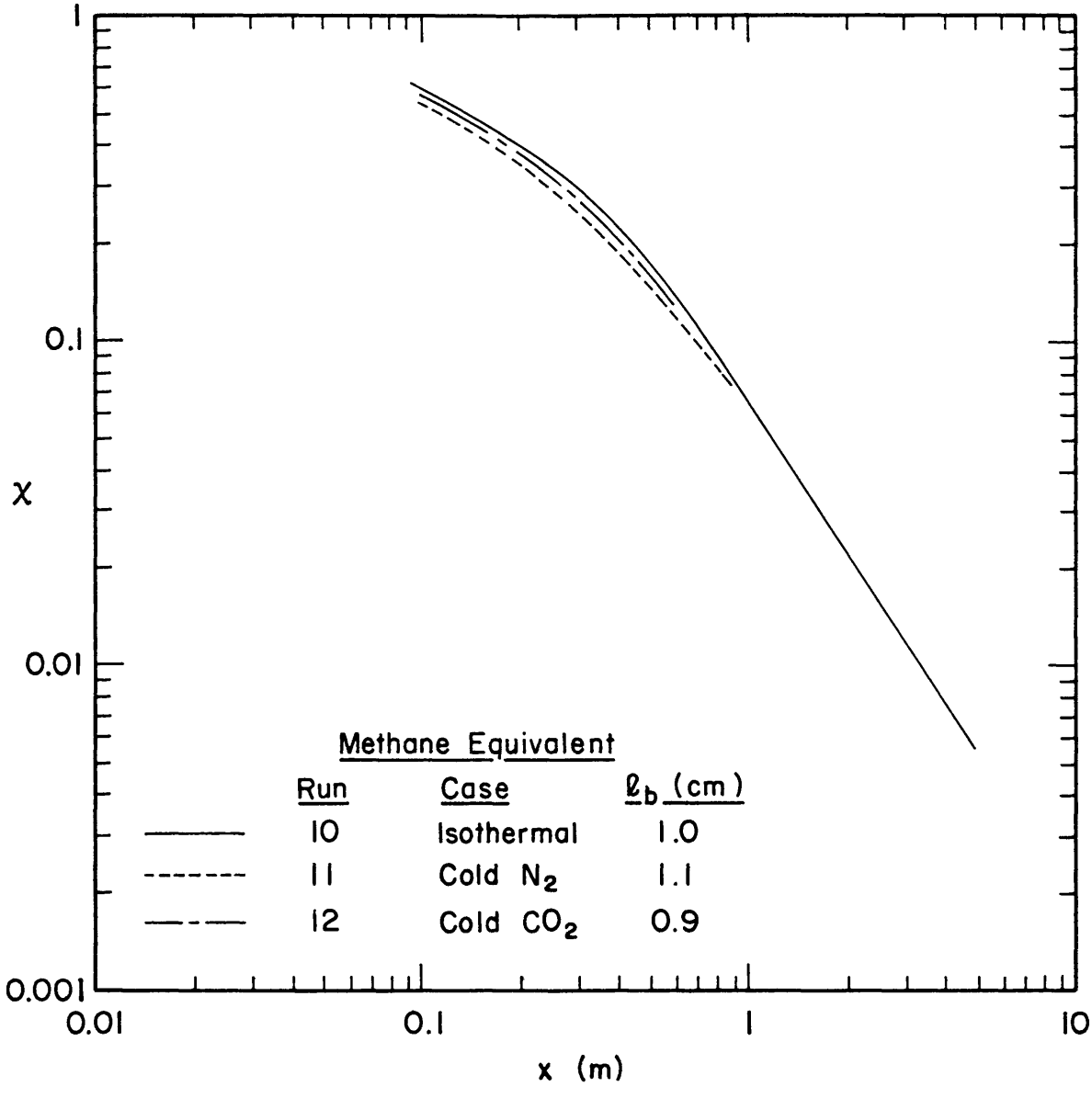

Figure 5-4. Box Model Predictions of Concentration versus Distance, Runs 10, 11, and 12, $\ell_b \simeq 1$
(See Data, Figure 4-6)

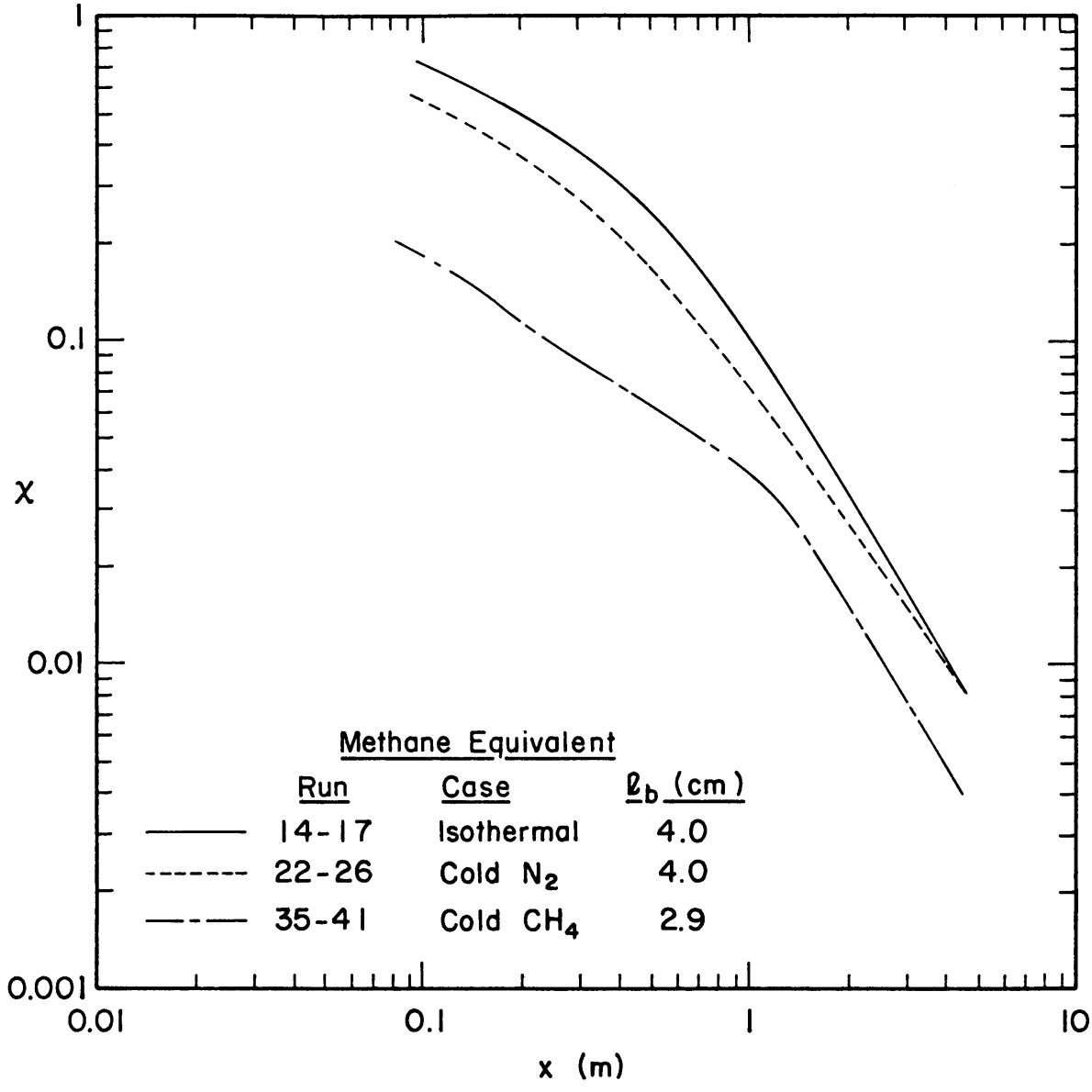

Figure 5-5. Box Model Predictions of Concentration versus Distance, Runs 14-17, 22-26, and 35-41, $\ell_b \simeq 4$
(See Data, Figure 4-7)

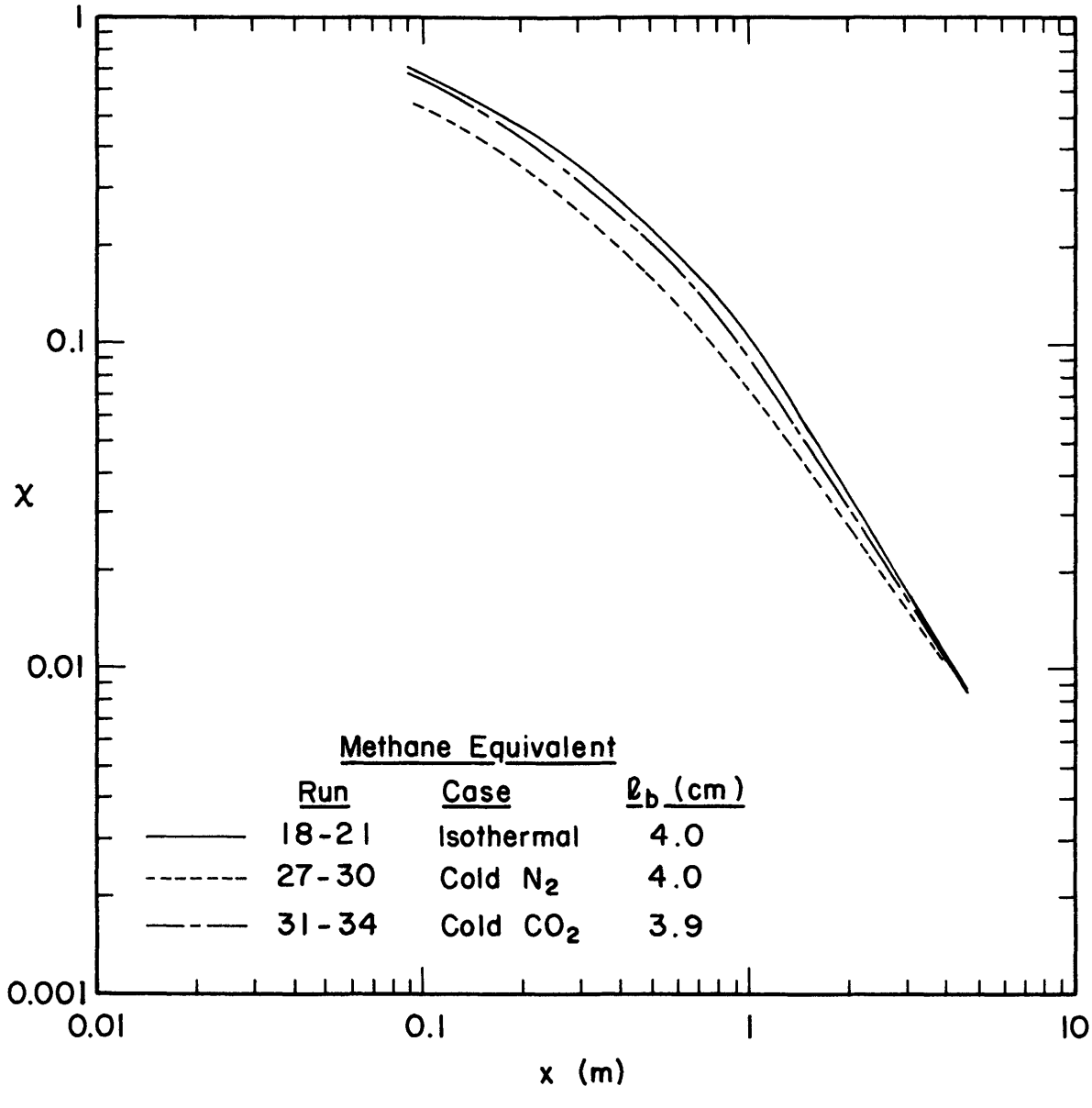

Figure 5-6. Box Model Predictions of Concentration versus Distance, Runs 18-21, 27-30, and 31-34, $\ell_b \simeq 4$
(See Data, Figure 4-8)

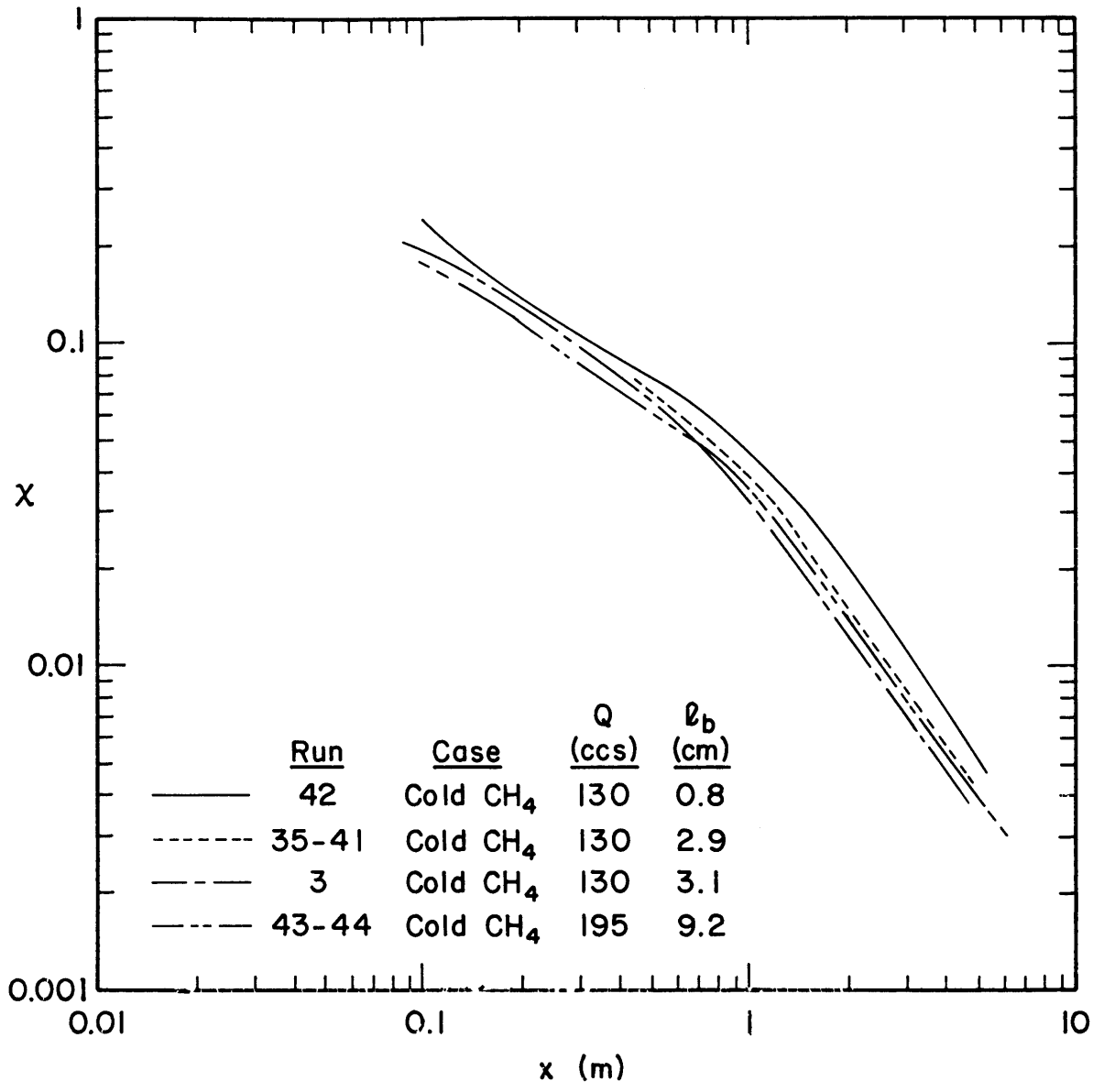

Figure 5-7. Box Model Predictions of Concentration versus Distance, Cold Methane Runs 42, 35-41, 3, and 43-44 ℓ_b **= 0.8-9.2** (See Data, Figures 4-9 and 4-3)

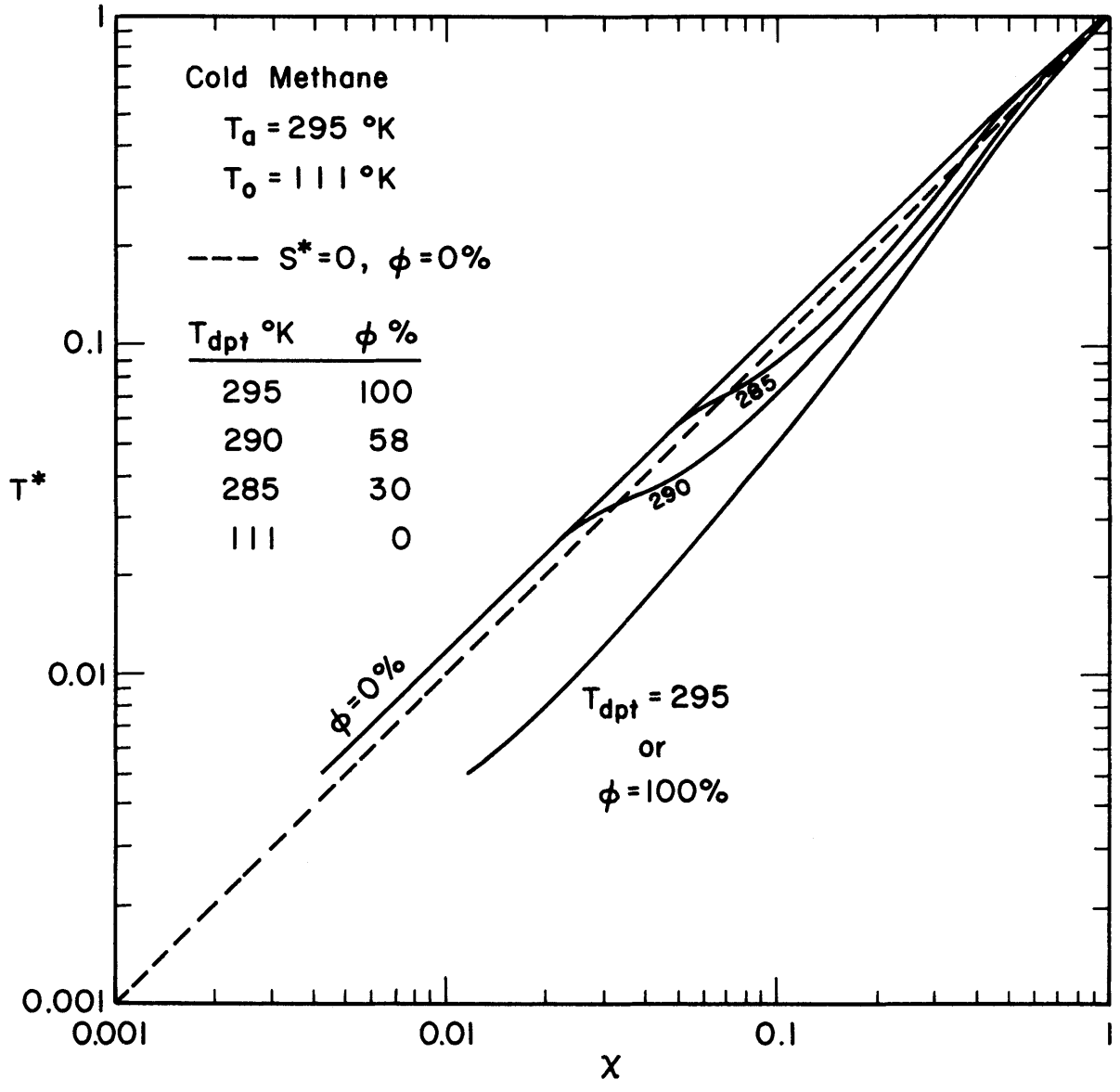

Figure 5-8. Dimensionless Temperature versus Concentration, Adiabatic Entrainment of Humid Air into a Cold Methane Plume, No Surface Heat Transfer

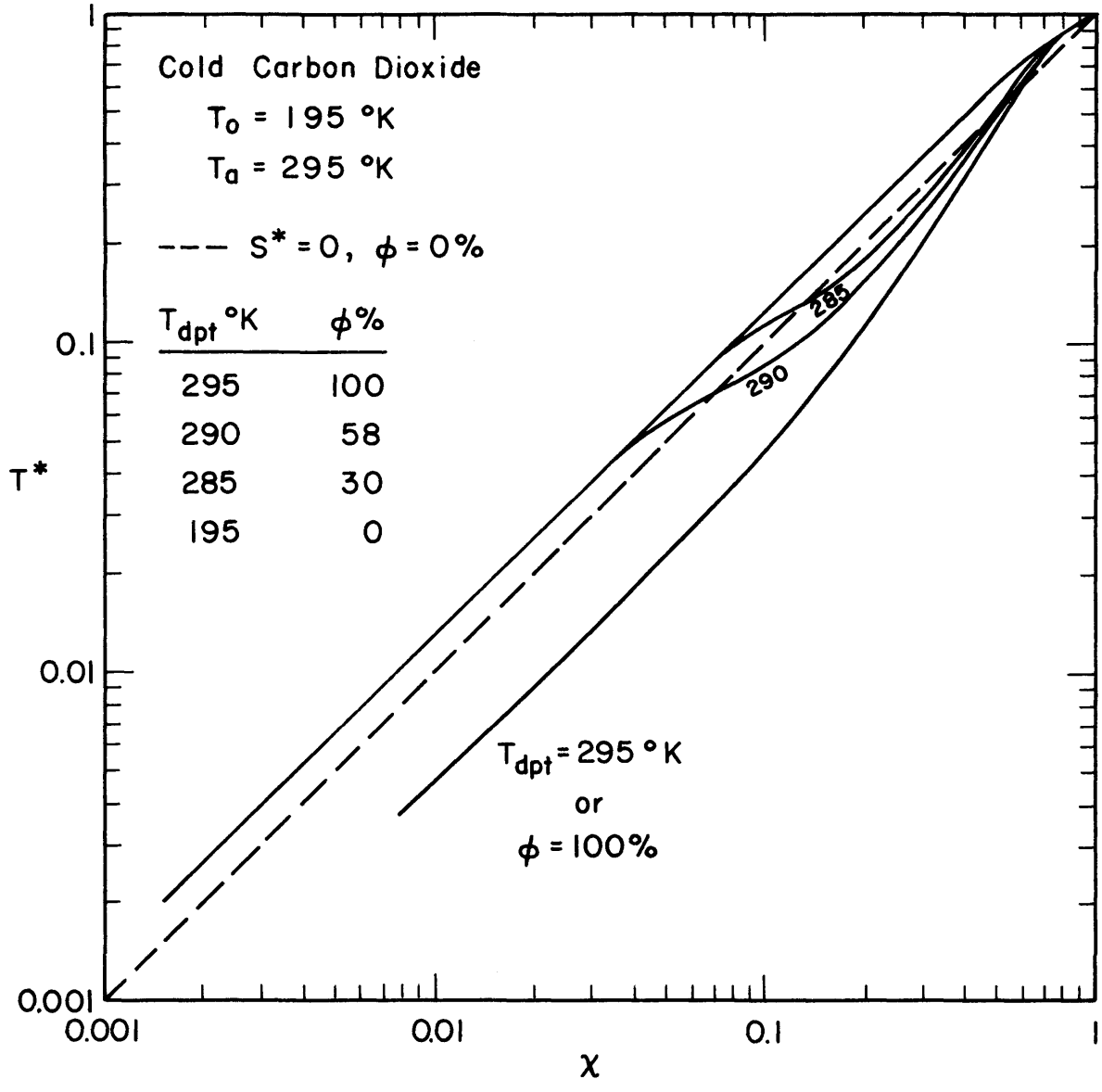

Figure 5-9. Dimensionless Temperature versus Concentration, Adiabatic Entrainment of Humid Air into a Cold Carbon Dioxide Plume, No Surface Heat Transfer

effects (see Appendix B). Figures 5-8 and 5-9 indicate that early plume heating caused by latent heat release is subsequently lost as water re-evaporates once the temperature raises above the dewpoint, T_{dpt}. Since the molar specific heat capacity for both propane and methane are larger than that of air the dimensionless temperature T^* asymtotically approaches lower real temperatures than would result from mixing a cold air plume with ambient air.

One advantage of a numerical model is that various assumptions and submodels can be switched on and off to test their influence. Figures 5-10 and 5-11 reflect the effects of different surface heat transfer assumptions on a cold methane plume released under conditions equivalent to Run 3 ($\ell_b \sim 5$). Under model conditions the perturbation effects of heat transfer and humidity are significant. Thermal effects result in 50% lower concentrations and a 40% narrower plume at a distance of one meter. Latent heat release only slightly perturbs the adiabatic dry plume results; thus surface heat transfer effects are dominant.

Figures 5-12 and 5-13 demonstrate the effects of different surface heat transfer assumptions on a cold carbon dioxide plume released under conditions equivalent to Run 9 ($\ell_b \sim 5$). In this case heat transfer caused deviations are essentially insignificant. Of course the thermal driving parameter, $\theta = 1 - T_o/T_a$, has reduced from 0.62 to 0.34 for the carbon dioxide plume case.

The box model reproduces the importance characteristics of thermal effect experiments discussed in Section 4.3. Of course the empirical constants (See Table 5-1) were selected to give the best overall agreement with model results. It is now appropriate to compare this model with independent field-scale cold-gas behavior.

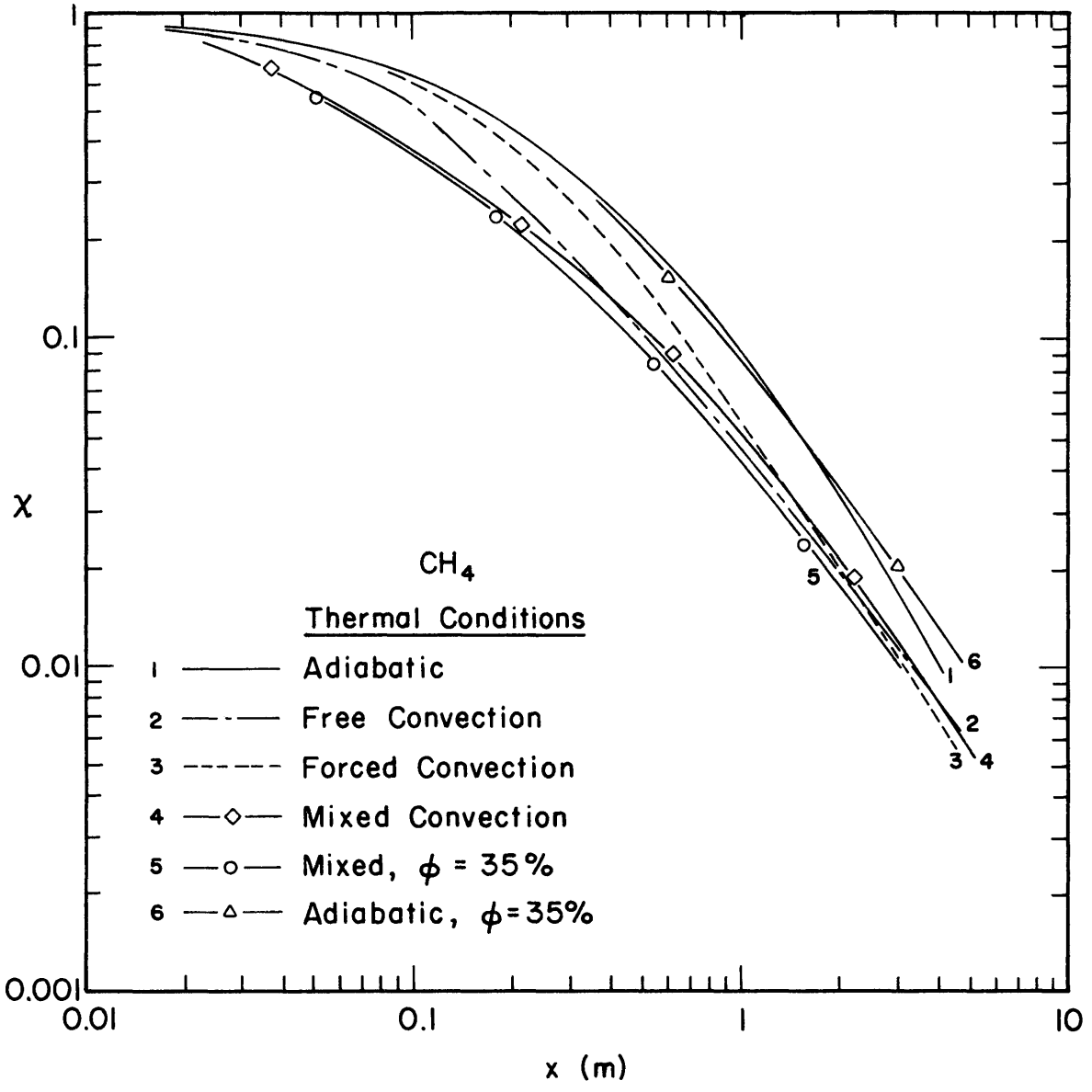

Figure 5-10. Centerline Surface Concentration Variation with Distance, Cold Methane Release, Calculated by Box Model for Various Thermal Conditions, ℓ_b = 5, Q = 130 ccs, u_* = 1.70 cm/s

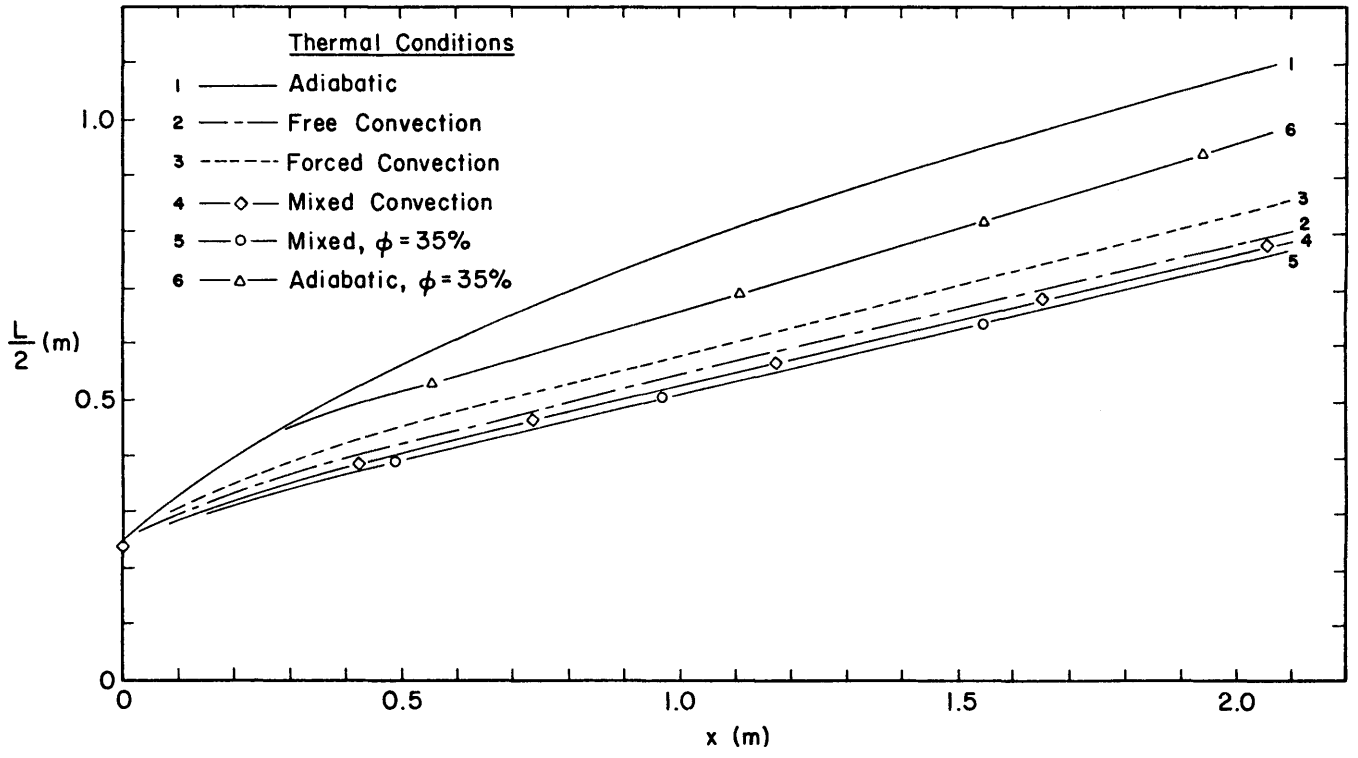

Figure 5-11. Lateral Plume Variation with Distance, Cold Methane Release, Calculated with Box Model for Various Thermal Conditions, ℓ_b = 5.0, Q = 130 ccs, u_* = 1.70 cm/s

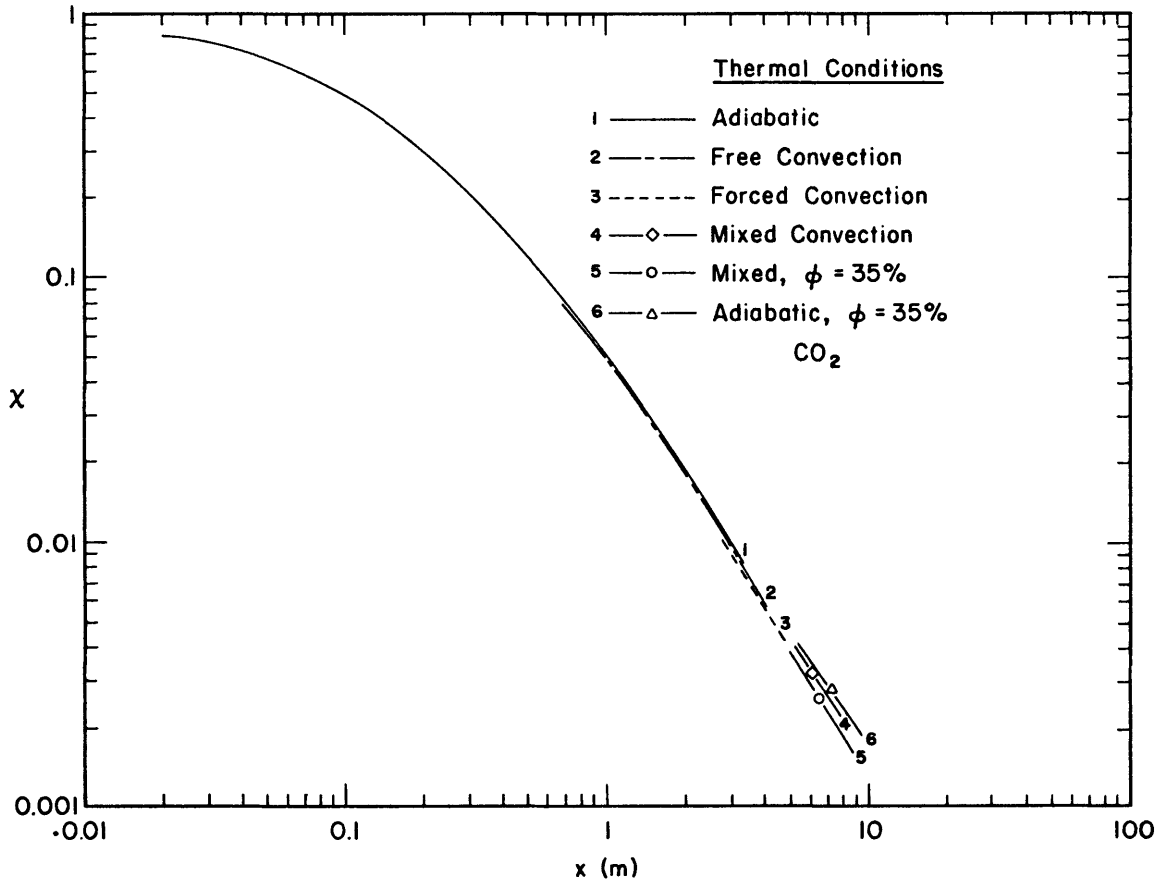

Figure 5-12. Centerline Surface Concentration Variation with Distance, Cold Carbon Dioxide Release, Calculated with Box Model for Various Thermal Conditions, ℓ_b = 5.0, Q = 223 ccs, u_* = 2.91 cm/s

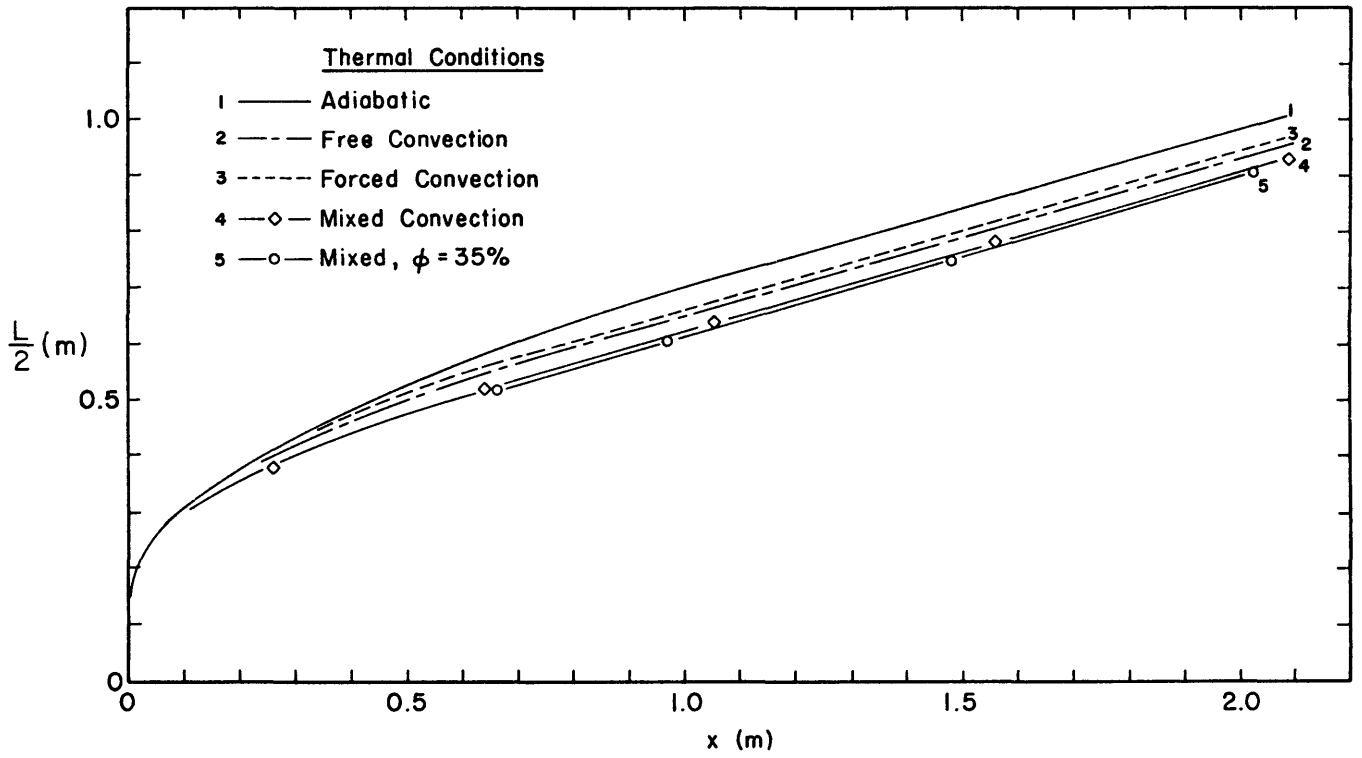

Figure 5-13. Lateral Plume Variation with Distance, Cold Carbon Dioxide Release, Calculated with Box Model for Various Thermal Conditions, ℓ_b = 5.0, Q = 223 ccs, u_* = 2.91 cm/s

5.1.2 Comparison Between Box Model and Maplin Sands Results

In 1980 a series of spills of up to 20 m^3 of LNG and refrigerated liquid propane onto the sea were performed by Shell Research Ltd. at Maplin Sands in the south of England. Both instantaneous and continuous releases of cryogenic liquids were made. Gas concentrations and temperatures were monitored from an extensive array of floating pontoons up to 650 m downwind. (See Puttock, Colenbrander, and Blackmore, 1982a, 1982b, and 1982c). As yet only a limited amount of data from these experiments have been published; however, this data provides an opportunity to critique the thermal assumptions and validity of the box model. Data from Puttock, et al. (1982a, 1982b) are compared below for the conditions summarized in Table 5-2.

Maximum concentrations versus downwind distance for LNG spills 29 and 15 are shown in Figures 5-14a and 5-15. Box model width predictions envelope the pontoon measurements. Figure 5-14b compares the predicted plume width to the plan view of the visible plume seen during the spill. Surface heat transfer is not involved in the HEGADAS numerical model simulation curves. Figure 5-16 compares concentration and temperature measurements during LNG spill 56. The predicted box model curve including heat transfer effects is shown together with the curve resulting from adiabatic entrainment of dry air.

Similarly maximum concentrations versus downwind distance for propane spills 46 and 54 are shown in Figures 5-17a and 5-19a. Figures 5-17b and 5-19b compare the predicted plume widths to the plan views of the visible plume seen during the spills. Again the box model width predictions envelope the pontoon measurements.

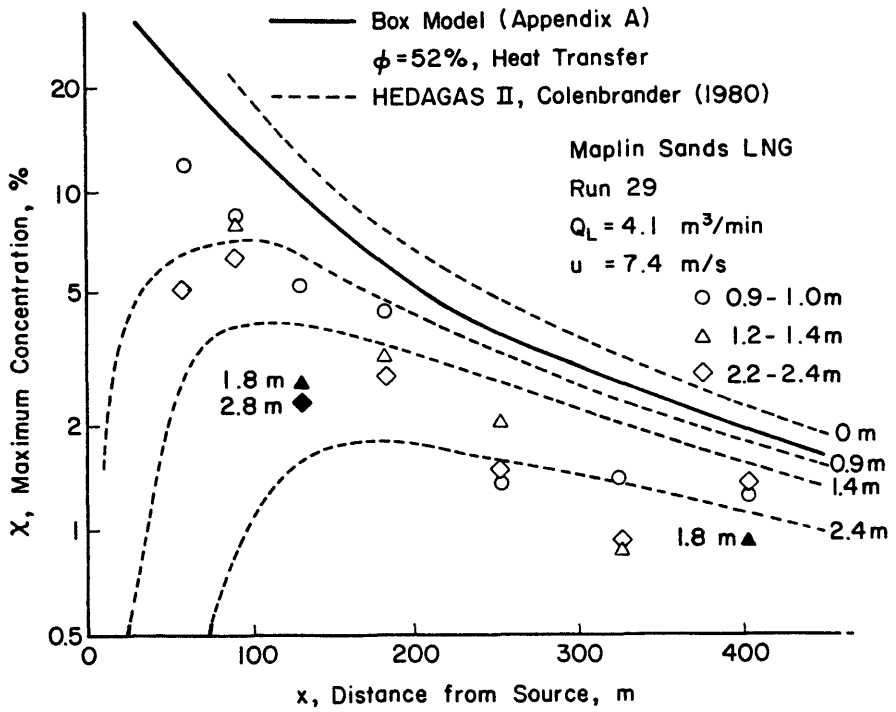

Figure 5-14a. Maximum Surface Concentrations for LNG Spill, Run 29 at Maplin Sands

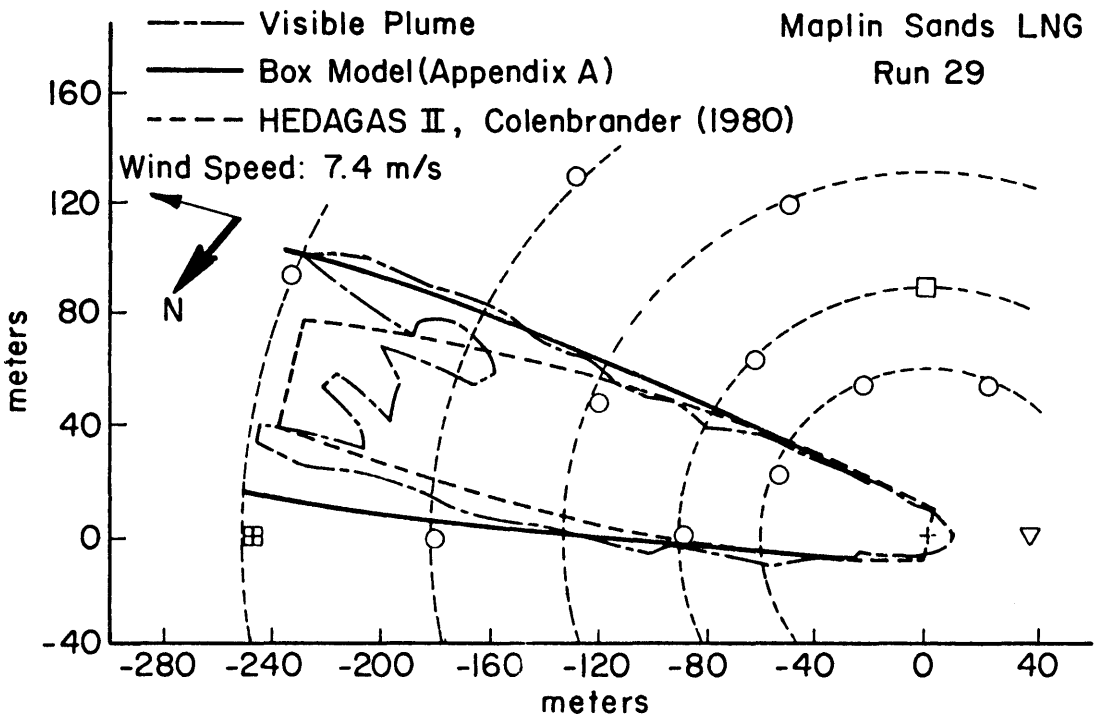

Figure 5-14b. Plan View for LNG Spill, Run 29 at Maplin Sands

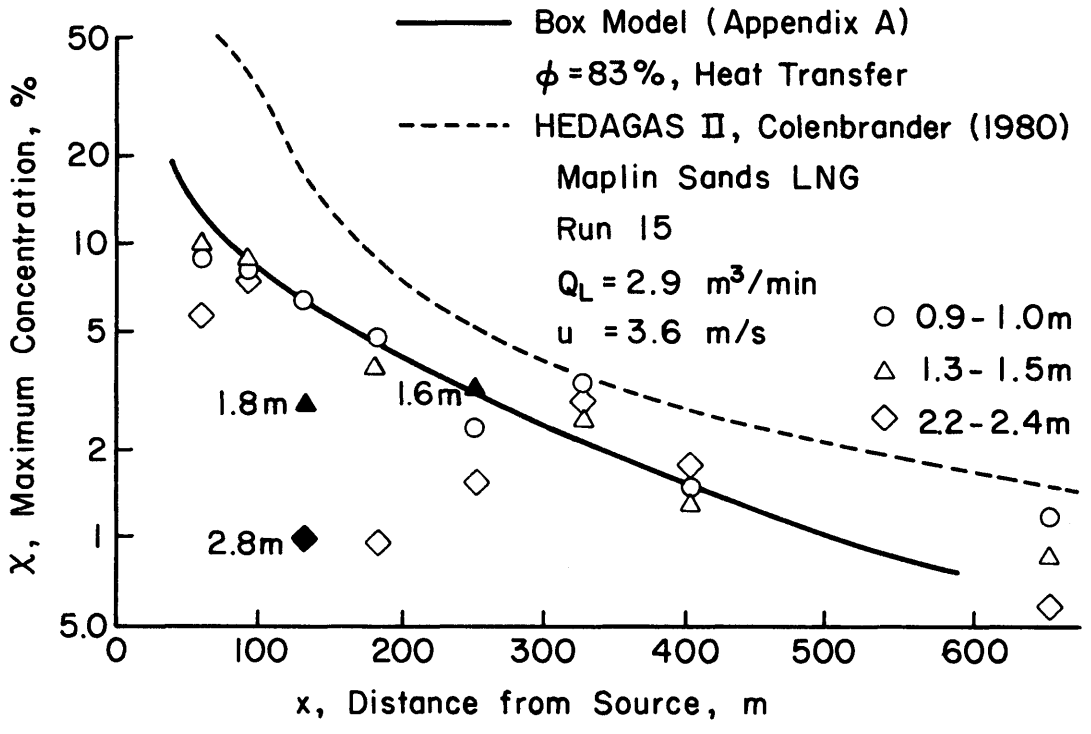

Figure 5-15. Maximum Surface Concentrations versus Downwind Distance for LNG Spill, Run 15 at Maplin Sands

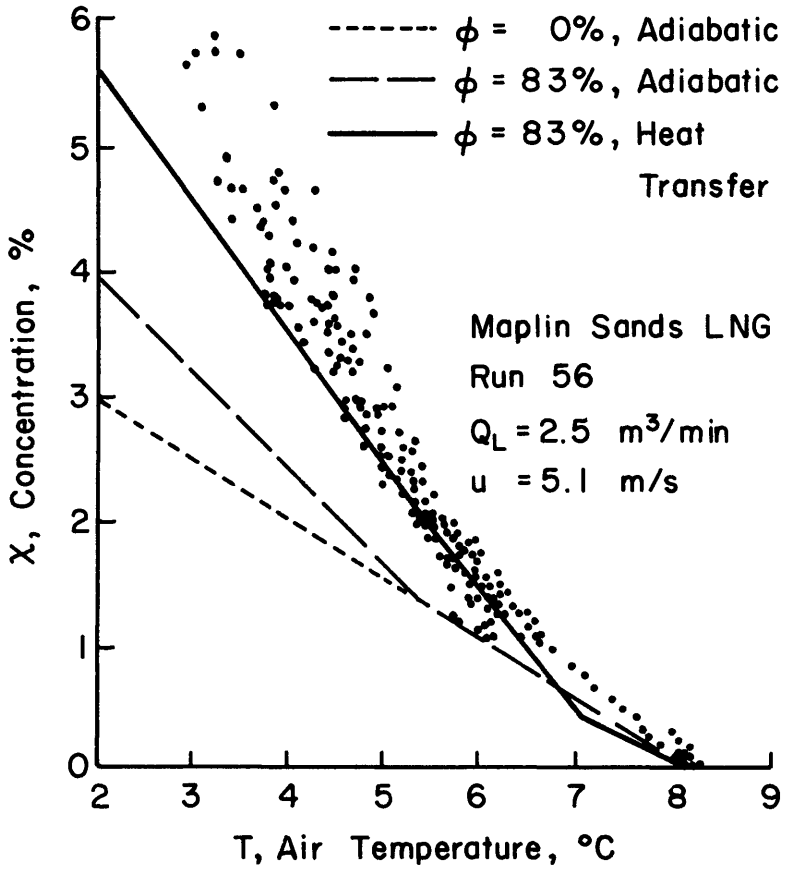

Figure 5-16. Concentration versus Temperature at 130 m from the Source, Maplin Sands LNG Spill, Run 56

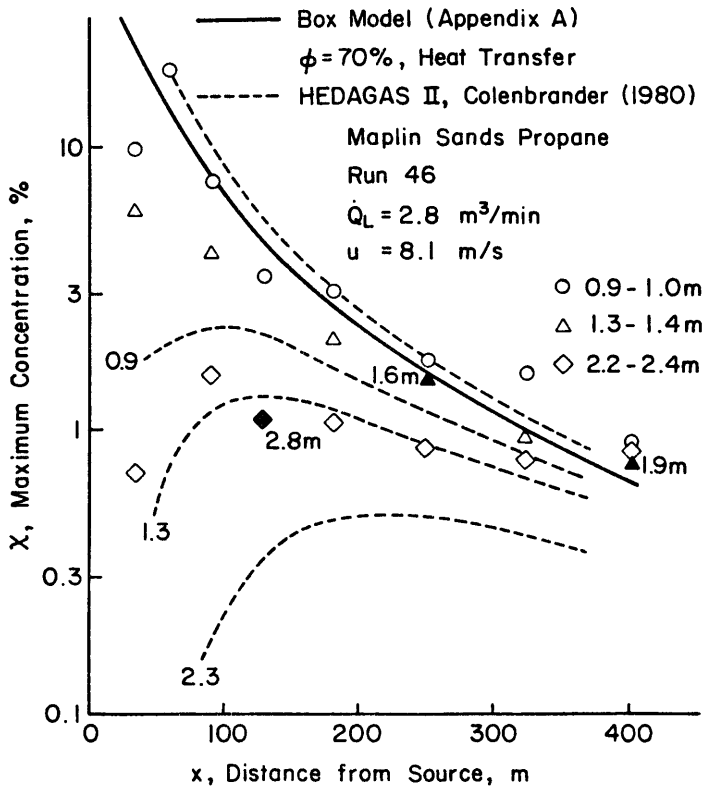

Figure 5-17a. Maximum Surface Concentrations for Propane Spill, Run 46 at Maplin Sands

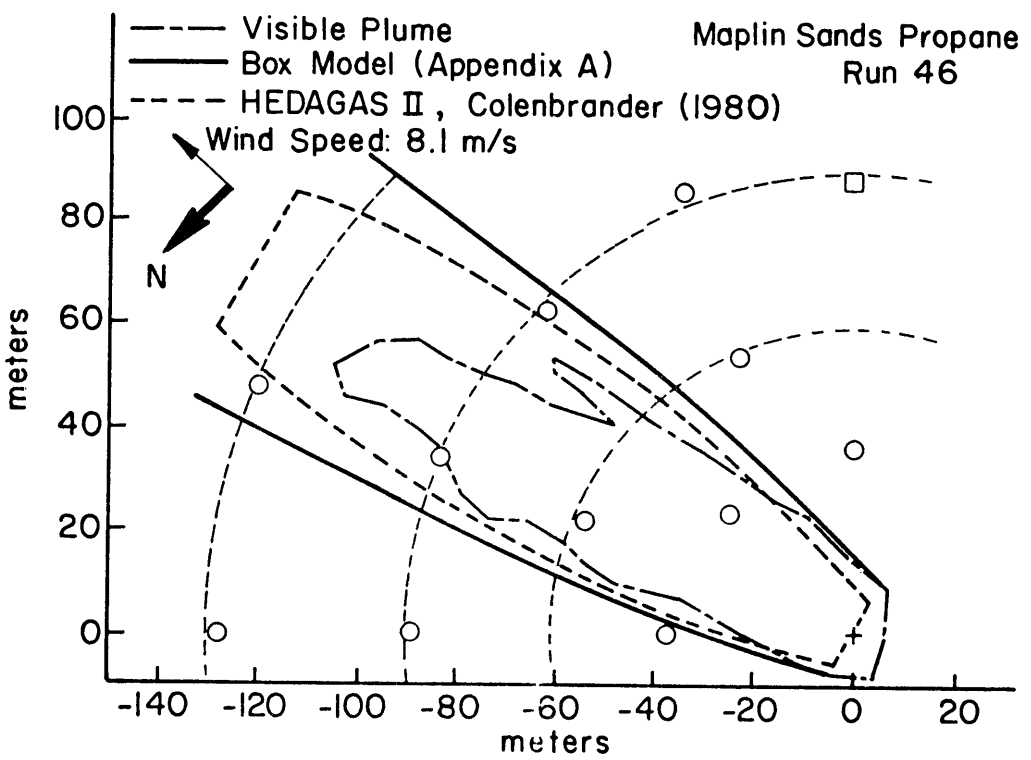

Figure 5-17b. Plan View for Propane Spill, Run 46 at Maplin Sands

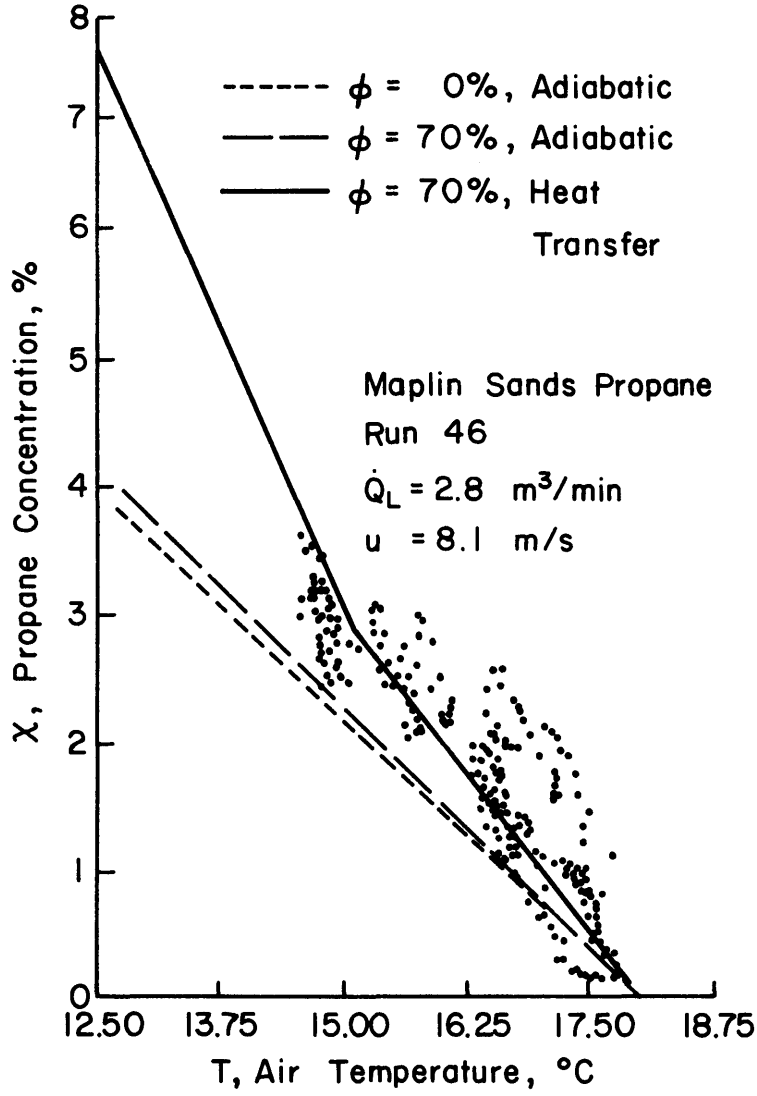

Figure 5-18. Concentration versus Temperature at 129 m from the Source, Maplin Sands LNG Spill, Run 46

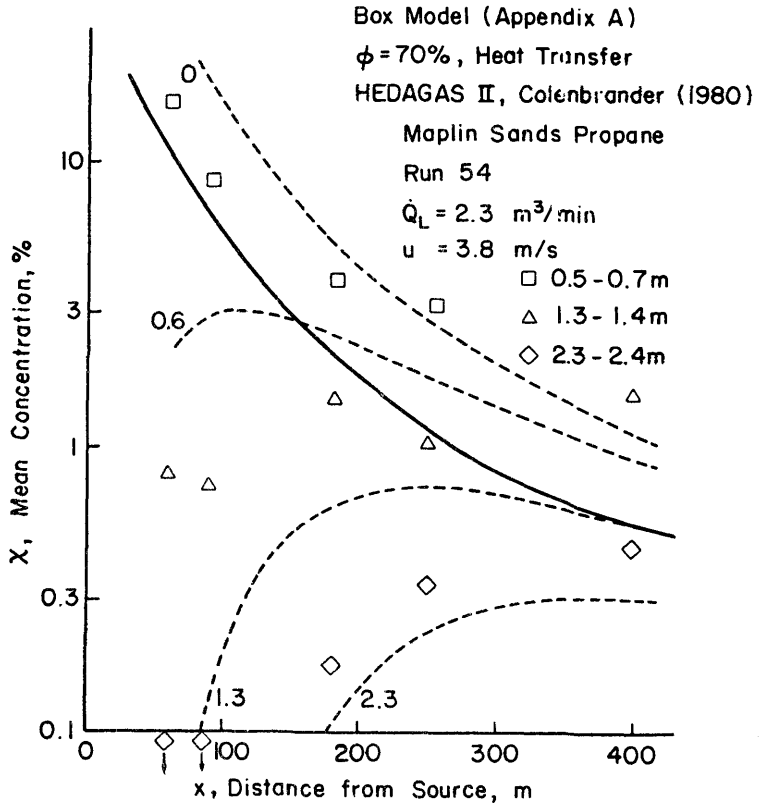

Figure 5-19a. Maximum Surface Concentrations for Propane Spill, Run 54 at Maplin Sands

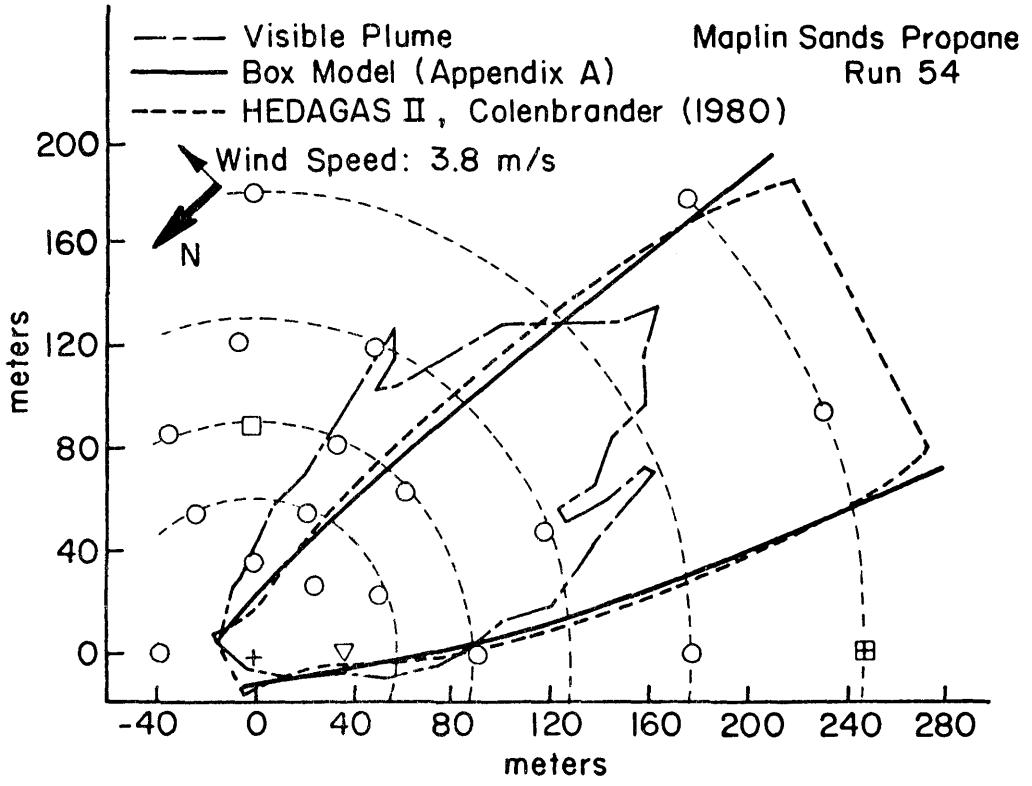

Figure 5-19b. Plan View for Propane Spill, Run 54 at Maplin Sands

Table 5-2

MAPLIN SAND CONTINUOUS SPILLS

Run No.	Q_L (m^3/min)	t_R (s)	u_R (m/s)	q_{10m} %	SG	Q_G (m^3/s)	H_o [Δ] (m)	u_* (m/s)	z_o (m)	T_o (K)	T_a (K)	T_{dpt} (K)	L_o [Δ] (m)	Ri_*	Re	Gr
Continuous LNG Spills																
15	2.9	285	3.5	88	1.45	88	0.12	0.122	5.9×10^{-5}	111	283	282	32.6	31.6	5380	4.3×10^{7}
29	4.1	225	7.4	52	1.46	21.6	0.16	0.252	2.8×10^{-5}	111	295	289.4	27.7	11.6	9201	1.1×10^{8}
56	~2.5	80	5.1	83	1.40	7.6	0.12	0.173	4.0×10^{-5}	111	281	280	20.9	15.2	5232	4.2×10^{7}
Continuous Propane Spills																
46	2.8	360	8.1	70	1.91	11.2	0.11	0.275	3.0×10^{-5}	231	291	288	19.6	13.3	7550	1.3×10^{7}
54	2.3	180	3.8	70	1.91	2.9	0.13	0.129	5.5×10^{-5}	231	291	288	15.0	70.1	9360	2.0×10^{7}

[Δ] H_o and L_o determined from Neff and Meroney (1982) expressions as in Table 5.2

Figure 5-18 compares propane concentrations and temperature measurements during propane spill 46. Again the heat transfer and humidity effects cause significant deviations from the adiabatic entrainment line. Examination of Figures 5-8 and 5-9 show what the extended curves would look like if such data were available.

5.2 Mixing Rates Across Plume Boundaries

To model the dispersion characteristics of thermal plumes, an understanding of the rate of air entrainment as influenced by local Richardson number must be established (see Sections 1.2.1 and 1.2.2). The concentration data generated during the test sequences resulted in lateral ground level concentrations across the entire plume and vertical concentrations at or near the plume centerline. From the data, a functional for the local concentration at any point was generated of the form:

$$\chi(x,y,z) = \chi_{o,\ell}(\chi)\exp\left[-\frac{1}{2}\left(\frac{y}{\sigma_y(x)}\right)^2\right]\exp\left[-\frac{1}{2}\left(\frac{z}{\sigma_y(x)}\right)^2\right]$$

where $\chi_{o,\ell}$ is the ground level, centerline (hence maximum) concentration for a given downwind x location and σ_y and σ_z are plume standard deviations. Determined from fitting curves to the lateral ground and centerline vertical data, Table 5-3 gives the values of $\chi_{o,\ell}$, σ_y andσ_z for the different run conditions for x = 30 and 60 cm, along with the maximum difference in temperature between cubical air and plume. An analytic expression in χ for local entrainment rates can be formed by performing a molar balance across consecutive cross sections, or alternatively by performing mass balance across plume sections.

Table 5-3. Dense Gas Plume Parameters Runs 14-41

Run	Q (cc/s)	u_* (cm/s)	x = 30 cm				x = 60 cm			
			$\chi_{o,L}$	σ_z (m)	σ_y (m)	ΔT (K)		σ_z (m)	σ_y (m)	ΔT (K)
14-17	130	1.85	.326	.0080	.20	-	.167	.0130	.19	-
18-21	223	3.20	.212	.0068	.21	-	.121	.0094	.26	-
22-26	130	1.85	.246	.0092	.23	9.0	.142	.0135	.25	3.0
27-30	223	3.20	.368	.0068	.31	19.0	.207	.0110	.31	9.0
31-34	223	3.20	.345	.0072	.27	8.5	.204	.0110	.28	4.5
35-41	130	1.85	.185	.0130	.15	16.0	.065	.0300	.25	7.0

5.2.1 Molar Balance Analysis

The average concentration over an arbitrary lateral plume cross section can be expressed as

$$\bar{\chi} = \frac{\dot{n}_s}{\dot{n}_s + \dot{n}_a}$$

where $\dot{n}_s$ is the source molar flux and $\dot{n}_a$ is the moles per second of entrained air passing through the cross section. In general,

$$\dot{n}_i = \frac{P_i Q_i}{R T_i} ,$$

but since all processes occurred under isobanic conditions, the average concentration can be written

$$\bar{\chi} = \frac{\frac{Q_s}{T_s}}{\frac{Q_s}{T_s} + \frac{Q_a}{T_a}} ,$$

where Q_s is the source flow rate, $Q_a = \int_\sigma u_e \, d\sigma$ and the integral represents the air entrainment over the plume/air surface up to the cross section of interest. Hence

$$\int_\sigma u_e \, d\sigma = \frac{T_a}{T_s} Q \left(\frac{1}{\bar{\chi}} - 1 \right) .$$

To determine the average entrainment velocity between cross sections located at x_1 and x_2 downwind of the source (see Figure 5-20) one uses

$$\int_{\sigma_2} u_e d\sigma - \int_{\sigma_1} u_e d\sigma = \frac{T_a}{T_s} Q_s \left(\frac{1}{\bar{\chi}_2} - \frac{1}{\bar{\chi}_1} \right).$$

Since

$$\int_{\sigma_2} u_e d\sigma - \int_{\sigma_1} u_e d\sigma = \bar{u}_e \, \Delta x \bar{B},$$

then

$$\bar{u}_e = \frac{T_a}{T_s} \frac{Q_s}{\bar{B} \Delta x} \left(\frac{1}{\bar{\chi}_2} - \frac{1}{\bar{\chi}_1} \right) ,$$

where $\bar{B}$ is an average plume width. Furthermore, assuming plug flow within the plume the average concentration can be written in terms of the centerline ground level concentration at a give cross section as

$$\bar{\chi} \simeq 0.215\ \chi_{o,h}\ .$$

(See Appendix C.) The final expression for the average entrainment velocity becomes

$$(\bar{u}_e)_{\Delta x} = 4.65\ \frac{T_a}{T_s}\ \frac{Q}{\bar{B}\Delta x}\left(\frac{1}{(\chi_{o,h})_2} - \frac{1}{(\chi_{o,h})_1}\right)$$

Table 5-4 lists the values of $\bar{u}_e$ calculated for runs 14-34 between cross sections located at x = 30 cm and x = 60 cm.

Table 5-4. Entrainment Velocities Calculated from Molar Balances

Run	$\bar{u}_e$ (cm/s)	$\frac{\bar{u}_e}{u_*}$
14-17	0.54	0.29
18-21	0.91	0.28
22-26	0.66	0.36
27-30	0.91	0.28
31-34	0.55	0.17

The parameter given in the third column is the ratio of the entrainment velocity to the atmospheric friction velocity, u_*. Although the proper parameter to divide u_e by is $v_* = [u_*^2 + 0.25(w_*)^2]^{1/2}$ the contribution of the w_* term causes v_* to differ from u_* by less than one percent.

5.2.2 Mass Balance Analysis

An alternative approach to determine the average entrainment velocity considers a mass balance over lateral plume cross sections as shown in Figure 5-20. The mass flow rate through any cross section is given by

$$\dot{m}_i = \int_{s_i} \rho(z,y)u(z)dA \ .$$

The difference in consecutive mass flow rates yields the entrained mass flow rate, i.e.

$$\dot{m}_2 - \dot{m}_1 = \dot{m}_e = \rho_a \overline{u_e}\ \bar{B}\Delta x \ .$$

The density can be written as

$$\rho_i = \frac{PM}{RT_i} = \frac{P}{RT_i}[(M_o\chi + M_a(1 - \chi)] \ .$$

The final expression for the entrainment velocity becomes

$$\frac{\overline{u_e}}{\bar{B}\Delta x} = \iint_{s_2} (1 - \chi + \frac{M_o}{M_a}\chi)\ \frac{T_a}{T(y,z)}\ u(z)dzdy - \iint_{s_1} (1 - \chi + \frac{M_o}{M_a}\chi)\ \frac{T_a}{T(y,z)}\ u(z)dzdy \ .$$

The plume boundary for the above integrations was chosen as the edge where the plume was diluted to 1 percent of the centerline ground level concentration; thus,

$$\delta_y = \sigma_y\ [-2\ \ell n(0.01)]^{1/2} = 3.035\sigma_y$$

$$\delta_z = \sigma_z(0) \left\{ -2\ \ell n \left[\frac{0.01}{\exp\left[-\frac{1}{2}(y/\sigma_y)^2\right]} \right] \right\}^{1/2}$$

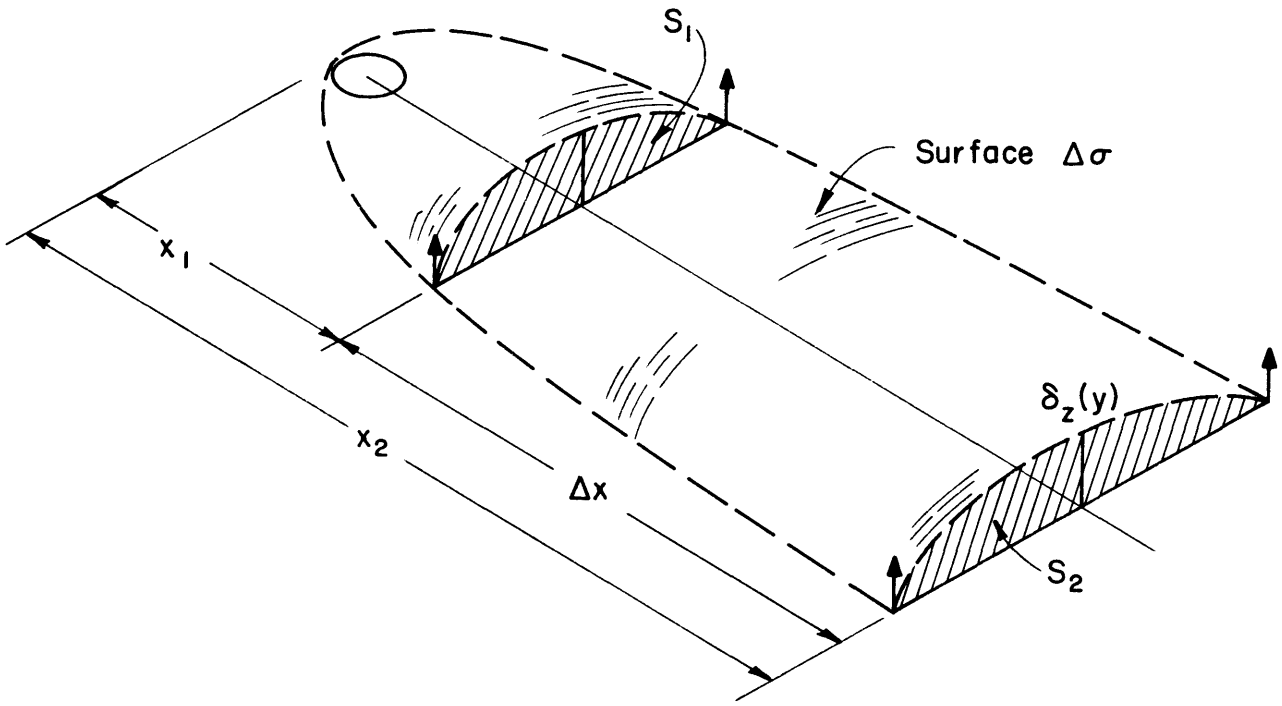

Figure 5-20. Plume Schematic for Mass Balance Calculations

The velocity within the plume was assumed to have the same profile as the approach wind and was given by

$$u(z) = \frac{u_*}{k} \ell n \left(\frac{z + z_o}{z_o} \right) ,$$

where z_o is the roughness length (0.0001 m) and k, the von Karman constant, is set to 0.4. The temperature was given the same form as the concentration distribution; i.e.

$$T(y,z) = T_a - (T_a - T_{o,lc}) \exp \left[- \frac{1}{2} \left(\frac{y}{\sigma_y} \right)^2 \right] \exp \left[- \frac{1}{2} \left(\frac{z}{\sigma_z} \right)^2 \right]$$

The appropriate expressions were numerically integrated and average entrainment velocities were calculated. Table 5-5 gives the results of entrainment velocities between x = 30 cm and x = 60 cm for the runs specified.

Table 5-5. Entrainment Velocities Calculated from Mass Balances

Run	u_e (cm/s)	$\frac{u_e}{u_*}$
14-17	0.81	0.44
18-21	1.52	0.48
23-26	1.46	0.79
27-30	2.01	0.63
31-34	1.74	0.54

5.2.3 Richardson Number Calculations

A comparison between entrainment velocity and Richardson number is desired. For entrainment rates that characterize the plume section between 30 and 60 cm, the local Richardson number at x = 30 cm was used,

$$Ri_* = \frac{g'H}{v_*} ,$$

where

$$g' = \left(\frac{\bar{\rho}_1 - \rho_a}{\rho_a}\right) g ,$$

$$H = \sigma_z \quad \text{at} \quad x = 30 \text{ cm}, \quad \text{and}$$

$$v_* = [u_*^2 + 0.25\, w_*^2]^{1/2} .$$

As previously noted, $u_* >> w_*$; therefore the Richardson numbers are based on u_*. Table 5-6 specified the final mixing parameters.

Table 5-6. Entrainment Velocities Summary Table

Run	Molar $\bar{u}_e$ (cm/s)	Mass Flux $\bar{u}_e$ (cm/s)	Ri_*
14-17	.54	.81	15.83
18-21	.91	1.52	7.19
23-26	.66	1.46	3.49
27-30	.91	2.01	1.98
31-34	.55	1.74	-6.42

5.2.4 Errors in the Molar and Mass Balance Analyses

Entrainment rates determined from the data are plotted versus local Richardson number in Figure 5-21. The data generally falls close to the expected values with the molar analysis results correlating better than the mass flux analysis. It should be noted, however that two main differences in the development of the two methodologies might explain the disparity.

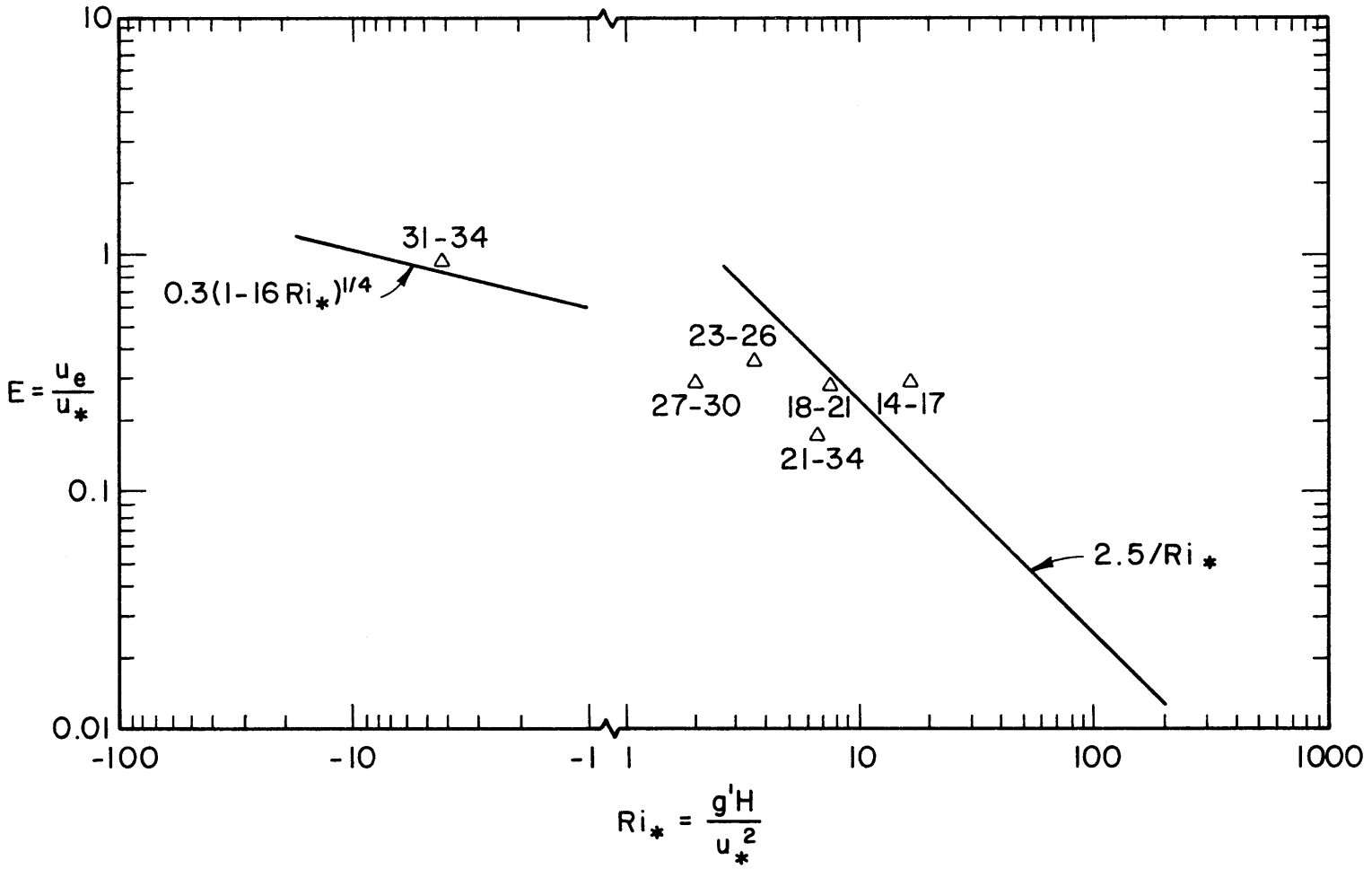

Figure 5-21. Entrainment Rate versus Richardson Number
(Molar Balance Analysis)

The molar analysis used an average plume concentration over the cross section, where the average concentration was defined as

$$\bar{\chi} = \frac{\int \chi \, dA}{\int dA} \quad .$$

On the other hand, the mass flux analysis evaluated the average velocity weighted concentration:

$$\bar{\chi} = \frac{\int \chi u \, dA}{\int u \, dA} \quad .$$

Table 5-7 compares the average concentration values obtained for the runs, both by area averaging and velocity weighted area averaging.

Table 5-7. Area and Velocity Weighted Area Mean Concentrations

Run	$\bar{\chi}_{30}$ Area	$\bar{\chi}_{30}$ Velocity Weighted Area	$\bar{\chi}_{60}$ Area	$\bar{\chi}_{60}$ Velocity Weighted Area
14-17	.065	.060	.034	.031
18-21	.047	.041	.026	.023
22-26	.054	.048	.030	.027
27-30	.072	.060	.045	.041
31-34	.069	.060	.044	.039
35-41	.034	.035	.014	.013

Since the values calculated are nearly equal to one another one concludes that concentration averaging is not very sensitive to velocity weighting.

The mass flux approach integrates a velocity weighted function in order to obtain mass flow rates. Errors in the velocity profile would in this case become crucial. One way to check the validity of the velocity profile used is to compare the mass flow rate of source gas through any cross section with the flow rate at the source, by evaluating

$$\int \chi \, udA = Q_s$$

Table 5-8 illustrates the comparison:

Table 5-8. Source Mass Balance Comparison

Run	Q_s (cc/s)	$\int \chi udA$ (cc/s) x = 30 cm	x = 60 cm
14-17	130	317	284
18-21	223	225	223
22-26	130	176	174
27-30	223	228	351
31-34	223	391	460

It would seem that the velocity profile used in the calculations was in all cases too high; hence the momentum lost to the plume at the source is significant, and the velocity profile must not be re-established to background levels even after 60 cm. Since the velocity errors were so great (as high as 100%), the molar analysis would seem to give more accurate results.

Figure 5-21 is a plot of the entrainment rate normalized by the friction velocity versus local Richardson number using results obtained from the molar balance analysis. It can be seen that over the range of Richardson numbers investigated, the entrainment effects are relatively constant, in contrast to theoretical expectations of a drop in entrainment rate with increasing Richardson number. Picknett (1981) and Meroney and Lohmeyer (1982) found that plume structure was influenced by the existence of gravity waves which tend to affect mixing. Perhaps in these cases gravity waves dominate mixing. Gravity waves (i.e. periodic undulations in cloud height) were found to exist where violent gravity spreading effects have subsided and caused increased dilution rates.

Meroney and Lohmeyer (1982) generated a numerical program which reproduced this phenomenon.

6.0 CONCLUSIONS

The primary goal of this laboratory program was to obtain an extensive set of reliable data on the behavior of cold dense gas clouds released into various simulated atmospheric boundary layers. Once the data were acquired they were examined for the relative importance of surface heat transfer and latent heat released during the condensation of water vapor. Finally the data were used to evaluate the behavior of a box model which included surface heat transfer and humidity conservation relations. Model predictions were compared to LNG and Propane spill data from the Maplin Sands test program.

6.1 Cold Dense Gas Cloud Data Base

Concentration, temperature, and visualization measurements were made for plumes emitted continuously from an area source at the bottom of a simulated atmospheric boundary layer. Isothermal dense gas mixtures, cold nitrogen, cold carbon dioxide, and cold methane were released at various combinations of source flow rate and reference wind speed such that the buoyancy length scale varied over an order of magnitude. The combination of experiments performed covered parameter ranges as follows:

$$0.7 \leq \ell_b \leq 9.2,$$

$$7.7 \leq (Ri_*)_o \leq 31.9,$$

$$9.9 \leq Re \leq 22.2,$$

$$0 \leq Gr \leq 209,$$

$$1.28 \leq SG \leq 2.41,$$

$$\phi \simeq 35\%,$$

$$u_*/u_R = 0.075,$$

$$z_o^* \simeq 0.05,$$

$$C_{p_o}^* / C_{p_a}^* = 1,\ 1.22,\ \text{and } 1.30,\ \text{and}$$

$$MW = 15,\ 28,\ 42.3,\ \text{and } 44.$$

Puttock et al. (1981) suggest that for density effects to be important $(Ri_*)_o > 10$. Thus the experimental range includes both passive and dense plume conditions by this criteria. The Reynolds number, $Re = (g_o' H_o^3)^{1/2}/\nu$ seems too low to avoid viscous effects upon spread rate; but recall that the length scale, H_o, reflects the height of a slumped plume. Nonetheless viscous effects of a laminar sublayer near the ground may be significant. Terms are defined in Table 4-2 and the list of references.

In several experiments some measurements under identical conditions were replicated up to five times. The mean concentrations measured displayed very little scatter (< 10%).

A total of 44 separate measurement runs were made over the conditions noted above and in Table 4-2. The sampling tubes installed above the floor in Runs 1-12 may have introduced wake turbulence which artificially enhanced mixing and systematically reduced concentrations measured by up to 20%. Nonetheless run intercomparisons are still informative. Concentration data are tabulated in Appendix C in terms of mole fraction measured in the laboratory, equivalent methane concentrations, and dimensionless concentration coefficient, $K = \frac{\chi}{1-\chi} \frac{u_R L_R^2}{Q_o} \left(\frac{T_o}{T_a}\right)$. Temperature data are tabulated in Appendix D.

6.2 Scaled Behavior of Cold Dense Clouds

All data were interpreted in terms of their equivalent molar methane concentration to permit comparison of runs with the same volume source strength but different molar source flow rates. Methane data at different source flow rates were compared in terms of dimensionless concentration, K. The results of the discussions found in Sections 4.1 through 4.4 are summarized as follows:

- The simulated atmospheric boundary layer strongly resembled the behavior of a neutrally stratified flow over a 10 cm surface roughness. Surface drag resulted in a shear coefficient $u_*/u_R = 0.075$. The velocity profiles near the ground displayed a logarithmic behavior and turbulence intensities produced by mechanical shear near the surface reached values of $u'/\bar{u} \simeq 0.25$ maximum.

- Dense gases released from the area source when $\ell_b \geq 3$ ($Ri_* \simeq 25$ or 30) exhibited strong gravity driven flow behavior. All gases moved upwind against the wind field until they were turned back and around the main body of the plume. These gases produced a horse-shoe shaped vortex, which bent downwind about the source. For the $\ell_b \sim 1$ condition upwind motion was minimal.

- Downwind the clouds spread in a flat mattress-like cross section whose edges produced a parabolic shape with open end downwind.

- Isothermal, cold nitrogen, and cold carbon dioxide plumes always remained negatively buoyant. The stable stratification supressed vertical mixing; thus the vertical growth rates followed the character of Pasquill-Gifford Category G plume behavior (stable atmosphere).

• The cold methane plumes become positively buoyant after sufficient contact with the warm ground surface. Vertical growth rates appeared to approach Pasquill-Gifford Category A plume behavior (unstable atmosphere). The plumes appeared to lift above the floor although plume mixing was so intense an elevated concentration maximum did not occur.

• Isothermal plumes when plotted in terms of dimensionless concentration, K, gave similar concentration behavior for a range of bouyancy length scales, ℓ_b = 1 to 5, and a range of volume source rates; thus for situations where source vertical momentum is small either buoyancy scale, ℓ_b, or Richardson number, Ri_*, is sufficient to scale plume behavior.

• Cold nitrogen plumes at $\ell_b \sim 4$ or 5 displayed the effects of heat transfer without the complication of specific heat capacity variation between source gas and ambient air. The carbon dioxide plumes, however, required proportionally larger heat transfer to reduce the local buoyancy flux; hence the cold carbon dioxide plumes resisted mixing even longer than the isothermal plume mixtures.

• The cold plumes at $\ell_b \sim 1$ to 5 did not display similar patterns of concentration decay. The concentration profiles generally arrange themselves in order of initial temperature, where lower source temperatures result in faster dilution rates. (Note exception of carbon dioxide Runs 9 and 31-34 where the large specific heat capacity ratio results in concentrations above their isothermal counterpart, Runs 7 and 18-21.

• Vertical concentration profiles decay in a Gaussian like manner in the vertical for both isothermal and cold plumes. The cold plumes mixed vertically more rapidly since heat transfer destroyed the negative bouyancy.

• The empirical formulas for source plume width recommended by Neff and Meroney (1982) predicted the plume widths measured for both isothermal and cold plumes.

6.3 Characteristics of Data Comparison to Box Model

The simple box model performed suprisingly well. Indeed within the expected variability of the phenomenon, it is hard to justify using a much more complex model to predict hazards of toxic or flammable gases, even when heat transfer and humidity effects may be significant. The results from the discussion in Section 5.1 are summarized here as follows:

• The box model reproduced the general behavior of concentration, χ, and plume width, L, versus downwind distance for the range of conditions studied. The absolute values predicted were not always exact, but the relative behavior of isothermal and cold plumes was reproduced.

• For situations where parcel densities fall below ambient densities the box model reviewed did not predict the tendency for the cloud to lift off and narrow.

• The box model reproduced the essence of temperature and concentration combinations measured. The model clearly indicated the influence of heat transfer and water vapor condensation and re-evaporation.

- The box model confirms that model experiments with isothermal dense gases will conservatively predict mean concentration distributions for cold dense gas spills. A cold gas model experiment will actually overpredict plume dilution due to exaggerated destruction of negative buoyancy caused by distortion of the thermal phenomenon at small model scales.

- The box model suggests that thermal effects are less significant at field spill scales. Hence a model experiment with an isothermal simulant may actually reproduce field dispersion very closely.

- Numerical calculations suggest the initial conditions imposed (i.e. H_o, L_o, u_o) strongly influence the accuracy of subsequent numerical predictions of concentration field. Close attention should be given to initial conditions when comparing different box or slab models.

- The box model (Apendix A) calibrated against the model experiments (Runs 1-44) predicted the behavior of the independent field scale measurements of LNG and Propane behavior at Maplin sands. Predictions of centerline concentration decay and plume width were very good. Plume widths were almost coincident with visually observed cloud edges. Concentrations were close to field concentrations measured at 0.5 m above the sea surface. Temperatures and concentration correlations were predicted within experimental scatter.

6.4 Mixing Rate Results

- Average local entrainment rates were calculated for a wide range of thermal plumes. Mixing was not systematically affected by local Richardson numbers perhaps due to the dominance of gravity waves.

- The wind velocity profile within the plume may differ significantly from the ambient wind profile even where gravity spreading

effects have subsided. Hence, a molar balance analysis will give more accurate entrainment rate values that a mass balance analysis since it is insensitive to velocity profile measurements as assumptions concerning the re-establishment of a background profile.

REFERENCES

Cermak, J. E. (1975), Applications of Fluid Mechanics to Wind Engineering - A Freeman Scholar Lecture, J. of Fluids Engineering, Vol. 97, pp. 9-38.

Chan, S. T. (1983), FEM3 - A Finite Element Model for the Simulation of Heavy Gas Dispersion and Incompressible Flow User's Manual, Lawrence Livermore National Laboratory Report UCRL-53397, 83 pp.

Colenbrander, G. W. (1980), A Mathematical Model for the Transient Behavior of Dense Vapor Clouds, Kininblyike/Shell Laboratories, Amsterdam, Netherlands, 29 pp.

Cox, R. A. and Carpenter, R. J., (1980), Further Development of a Dense Vapor Cloud Dispersion Model for Hazard Analysis, Heavy Gas and Risk Assessment, D. Reidel Publishing Company, pp. 55-87.

Csanady, G. T. (1973), Turbulent Diffusion in the Enviroment, Geophysics and Astrophysics Monograph, D. Reidel Publishing Co., 248 pp.

Deardorff, J. W., Willis, G. E., and Lilly, D. K., (1969), Laboratory Investigation of Non-Steady Penetrative Convection, J. Fluid Mechanics, Vol. 35, pp. 7-31.

Eidsvik, K. J. (1980), A Model for Heavy Gas Dispersion in the Atmosphere, Atmospheric Environment, Vol. 14, pp. 764-777.

England, W. G., Teuscher, L. N., Hansen, L. E., and Freeman, B. E. (1978), Atmospheric Dispersion of Liquefied Natural Gas Vapor Clouds Using SIGMET, a Three-dimensional Time-dependent Hydrodynamic Computer Model, Proc. 1978 Heat Transfer and Fluid Mechanics Institute (Ed. C. T. Crave and W. L. Grasshondler), Stanford University Press, pp. 4-20.

Ermak, D. L., Chan, S. T., Morgan, D. L., and Mavis, L. K. (1982), A Comparison of Dense Gas Dispersion Model Simulations with Burro Series LNG Spill Test Results, J. of Hazardous Materials, Vol. 6, Nos. 1 and 2, pp. 129-160.

Fay, J. A. (1980), Gravitational Spread and Dilution of Heavy Vapor Clouds, 2nd Intl. Symposium on Stratified Flow, Proceedings of, Trondheim, Norway, 24-27 June, pp. 471-494.

Fay, J. A. and Ranck, D. (1981), Scale Effects in Liquified Fuel Gas Vapor Dispersion, Report for DOE Contract No. DE-AC02-77EV04204, Fluid Dynamics Laboratory, Mass. Inst. of Technology, Cambridge, Mass., 95 pp.

Germeles, A. E., and Drake, E. M., (1975), Gravity Spreading and Atmospheric Dispersion of LNG Vapor Clouds, Proceedings 4th Intl. Symposium on Transport of Hazardous Cargoes by Sea and Inland Waterway, Jacksonville, Florida, pp. 519-539.

Halitsky, J. (1969), Gas Diffusion Near Buildings, Section 5.5 of Meteorology and Atomic Energy - 1968, U. S. Atomic Energy Commission, pp. 221-255.

Hall, D. J. (1979), Further Experiments on a Model of an Escape of Heavy Gas, Report LR(312)AP, Warren Springs Laboratory, UK, 47 pp.

Jakob, M. (1949), Heat Transfer, John Wiley and Sons, Inc., New York, Vol. 1, pp. 758.

Janssen, L. A. M (1981), Wind Tunnel Modelling of the Dispersion of LNG Vapor Clouds in the Atmospheric Boundary Layers, TNO Ref. nr.:81-07020, File nr.:8710-13770, Apeldoorn, Netherlands, June.

Jensen, N. O. (1981), Entrainment Through the Top of a Heavy Gas Cloud, Air Pollution Modeling and Its Applications, C. De Wispelaere, ed., Plenum Press, New York, 11 pp.

Kantha, L. H., Phillips, O. M., and Azad, R. S. (1977), On Turbulent Entrainment at a Stable Density Interface, J. Fluid Mechanics, Vol. 79, pp. 753-768.

Kato, H. and Phillips, O. M. (1969), On the Penetration of a Turbulent Layer into a Stratified Fluid, J. Fluid Mechanics, Vol. 37, pp. 643-655.

Kline, S. J. (1965), Similitude and Approximation Theory, McGraw-Hill Book Co., New York, 229 pp.

Lofquist, K. (1960), Flow and Stress Near on Interface Between Stratified Liquids, The Physics of Fluids, Vol. 3, No. 2, pp. 158-175.

Lohmeyer A., Meroney, R. N., and Plate, E (1980), Model Investigations of the Spreading of Heavy Gases Released from an Instantaneous Volume Source at the Ground, Air Pollution Modeling and Its Application I, C. de Wispelaere, ed., Plenum Publishing Corp., pp. 433-448.

McNider, R. T. and Pielke, R. A. (1981), Diurnal Boundary-layer Development over Sloping Terrain, J. of Atmospheric Sciences, Vol. 38, No. 10, pp. 2198-2212.

McQuaid, J. (1976), Some Experiments on the Structure of Stably Stratified Shear Flows, Technical Paper P21, Safety in Mines Research Establishment, Sheffield, U.K., pp. 485-490.

Meroney, R. N. (1979), Lift Off of Buoyant Gas Initially on the Ground, J. of Industrial Aerodynamics, pp. 1-11.

Meroney, R. N. and Lohmeyer, A. (1982), Gravity Spreading and Dispersion of Dense Gas Clouds Released Suddenly into a Turbulent Boundary Layer, Gas Research Institute Report No. GRI-81/0025, 220 pp

Meroney, R. N. and Lohmeyer, A (1983), Prediction of Propane Cloud Dispersion by a Wind-Tunnel-Data Calibrated Box Model, Accepted by J. of Hazardous Materials, 33 pp.

Meroney, R. N, Neff, D. E., Cermak, J. E., and Megahed, M. (1977), Dispersion of Vapor From LNG Spills-Simulation in a Meteorological Wind Tunnel, Fluid Dynamics and Diffusion Laboratory Report CER76-77RNM-JEC-DEN-MM57, Colorado State University, Fort Collins, 152 p.

Neff, D. E., and Meroney, R. N. (1982), The Behavior of LNG Vapor Clouds: Laboratory Tests on the Similarity of Heavy Plume Dynamics, Gas Research Institute Report GRI-80/0145, 135 pp.

Neff, D. E. and Meroney, R. N. (1981), The Behavior of LNG Vapor Clouds: Wind Tunnel Simulations of 40 m^3 LNG Spill Tests at China Lake Naval Weapons Center, California, Gas Research Institute Report GRI-80/0094, 164 pp.

Neff, D. E., Meroney, R. N., and Cermak, J. E. (1976), Wind Tunnel Study of Negatively Buoyant Plume Due to an LNG Spill, Fluid Dynamics and Diffusion Laboratory Report CER76-77DEN-RNM-JEC22, Colorado State University, Fort Collins, 241 pp.

Picknett, R. G. (1981), Dispersion of Dense Gas Puffs Released in the Atmosphere at Ground Level, Atmospheric Environment, Vol. 15, pp. 509-525.

Puttock, J. S., Blackmore, D. R., and Colenbrander, G. W. (1982c), Field Experiments on Dense Gas Dispersion, J. of Hazardous Materials, Vol. 6, Nos. 1 and 2, pp. 13-42.

Puttock, J. S., Colenbrander, G. W., and Blackmore, D. R. (1982a), Maplin Sands Experiments of 1980: Dispersion Results from Continuous Releases of Refrigerated Liquid Propane, Symposium on Heavy Gases and Risk Analysis, Frankfort, BRD, 15 pp.

Puttock, J. S., Colenbrander, G. W., and Blackmore, D. R. (1982b), Maplin Sands Experiments of 1980: Dispersion Results from Continuous Releases of Refrigerated Liquid Propane and LNG, NATO/CCMS 13th Int. Tech. Meeting on Air Pollution Modeling and its Application, France, 19 pp.

Reynolds, W. C. (1968), Amorphology of the Prediction Methods, Proceedings Computation of Turbulent Boundary Layers - 1968, AFOSR - IFP - Stanford Conference, Vol. 1, pp. 1-15.

Sandborn, V. A. (1972), Resistance Temperature Transducers, Metrology Press, Fort Collins, Colorado, USA, 545 pp.

Skinner, G. T. and Ludwig, G. R. (1978), Physical Modeling of Dispersion in the Atmospheric Boundary Layer, Calspan Advanced Technology Center, Calspan Report No. 201, May.

Tennekes, H. and Lumley, J. L. (1972), A First Course in Turbulence, The MIT Press, Boston, 300 pp.

van Ulden, A. P. (1974), On the Spreading of a Heavy Gas Released Near the Ground, Proceedings of First Intl. Loss Prevention Symposium, the Hague, Delft, Elsevier, Amsterdam, Netherlands, pp. 431-439.

Zeman, O. (1982), The Dynamics and Modeling of Heavier-than-air Cold Gas Releases, Atmospheric Environment, Vol. 16, No. 4, pp. 741-751.

APPENDIX A

Numerical Box Model Program

APPENDIX A: Numerical Box Model Program:

Consider a dense cloud which is continuously released through a vertical rectangular area of width, L_o, and height, H_o, that undergoes a slumping motion in which L increases with time. As the cloud moves downwind the cloud section mixes with ambient air, but maintains uniform properties internally at each downwind section. The lateral velocity is assumed to vary linearly from zero at the center to a maximum at the outer edge of the cloud. Such a dispersion scenario will proceed as sketched in Figure A-1 and A-2. Sketches of how the experimental cloud was perceived to disperse are shown to the right of each box model sketch. Although the simplistic model may reproduce lateral cloud dimensions and maximum concentrations measured, it cannot correctly reproduce the actual lateral variation of height and concentration in space. Indeed, if the box model is calibrated to reproduce maximum concentrations measured at various downwind centerline locations, then the laterally averaged bulk concentrations predicted will always be too high, and the entrainment rates used will actually be too low for the reality of local entrainment physics. Nonetheless, such a model has engineering value.

Conventional wisdom assumes that lateral speed of the cloud front is proportional to the excess hydrostatic head within the cloud:

$$\frac{dL}{dt} = u_x(H)\frac{dL}{dx} = 2\alpha_1(g'H)^{1/2} \qquad (A-1)$$

in which α_1 is a constant of order unity and $g' = g(\rho - \rho_a)/\rho_o$, ($\rho_o$ is sometimes chosen as local cloud density and sometimes chosen as ambient air density, ρ_a). This expression is used in the models developed by

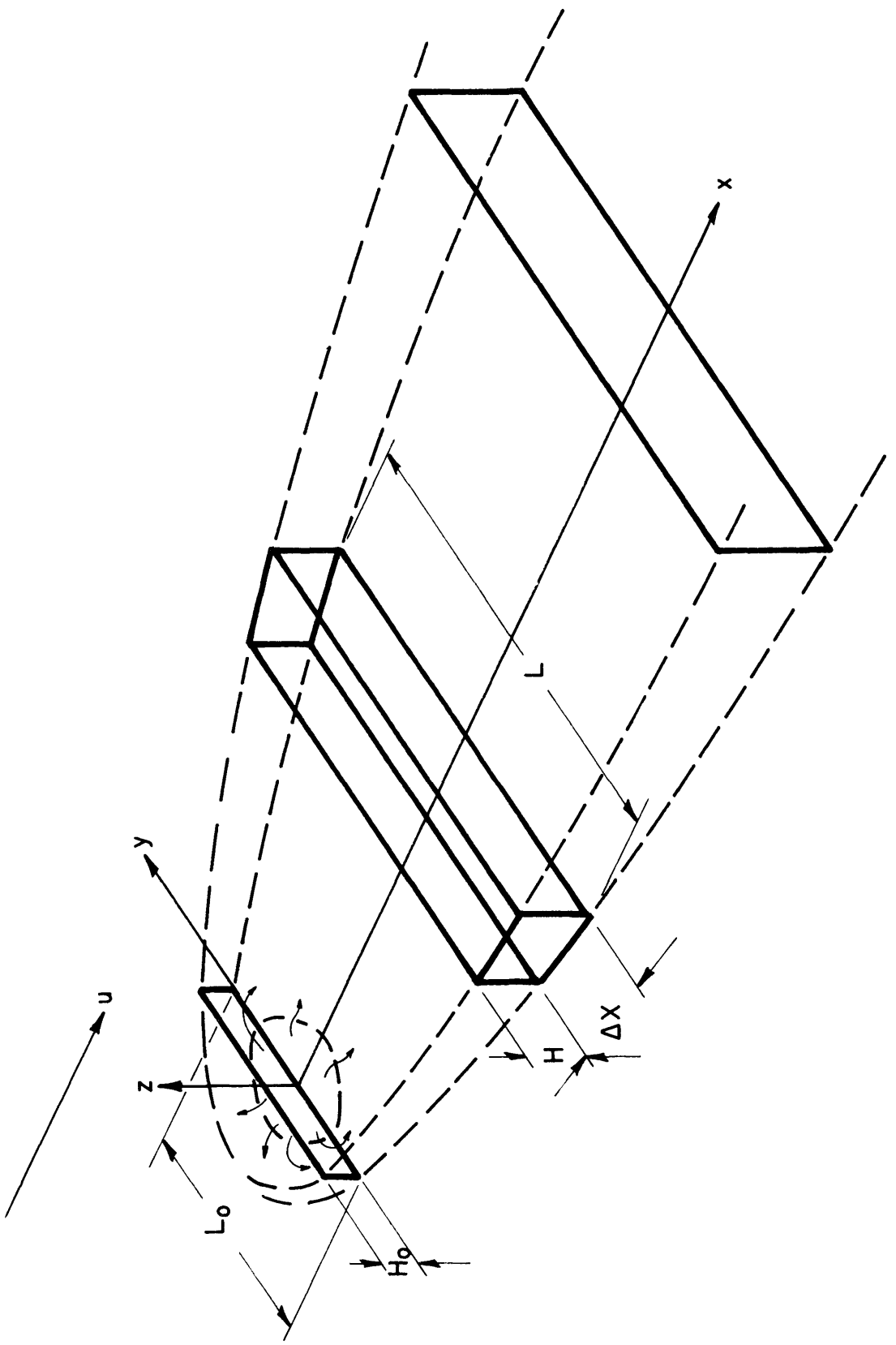

Figure A-1. Dense Plume Plan View for Box Model

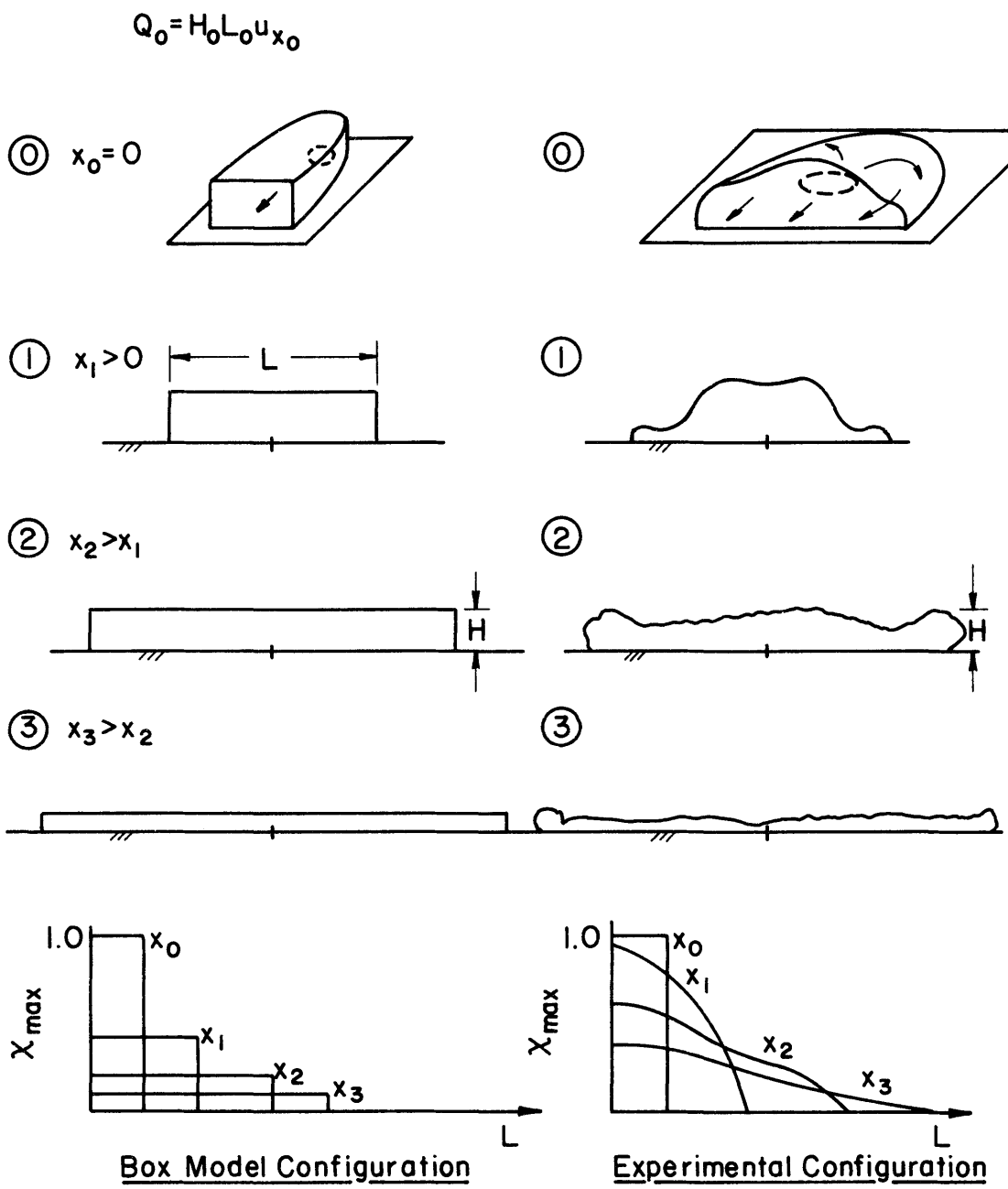

Figure A-2. Dense Plume Cross-section Sequence, Box Model versus Actual

van Ulden (1974), Germeles and Drake (1975), Cox and Carpenter (1980), Fay (1980), and Fay and Ranck (1981). This expression works well for stationary one-dimensional spread; however, it cannot account for upwind motions of a cloud near the source.

In terms of starred quantities which are dimensionless with length and velocity scales equal to $L = H_o$ and $U = (g'_o H_o)^{1/2}$ the lateral growth equation is

$$u_x^* \frac{dL^*}{dx^*} = 2\alpha_1 \left(\frac{\Delta\rho}{\Delta\rho_o} \frac{\rho_a}{\rho} H^*\right)^{1/2}, \qquad \text{(A-2)}$$

where u_x^* is the local longitudinal wind velocity evaluated at local cloud depth, H^*. This velocity is determined initially from Equation (A-1) and subsequently from a momentum equation.

Eventually cloud buoyancy $\Delta\rho$ may become zero or even negative, but the lateral dimensions of a cloud continue to grow due to background turbulence. This growth rate is normally proportional to u_*, the boundary layer friction velocity. Hence the right hand side of Equation (A-2) is never permitted to fall below $\alpha_7/Ri_*^{1/2}$, where α_7 is a constant of the order one and $Ri_* = g'_o H_o/u_*^2$.

Dilution of the gas cloud is assumed to occur by entrainment across the upper surface at a speed w_e and by entrainment at the lateral edges at a speed v_e, (see Figure A-3). The cloud volume will then increase at a rate:

$$\frac{u_o^* L_o^*}{(1-\theta)} \frac{d\chi^{-1}}{dx^*} = \frac{d(u_x^* H^* L^*/(1-T^*\theta))}{dx^*} = w_e^* L^* + 2v_e^* H^* \qquad \text{(A-3)}$$

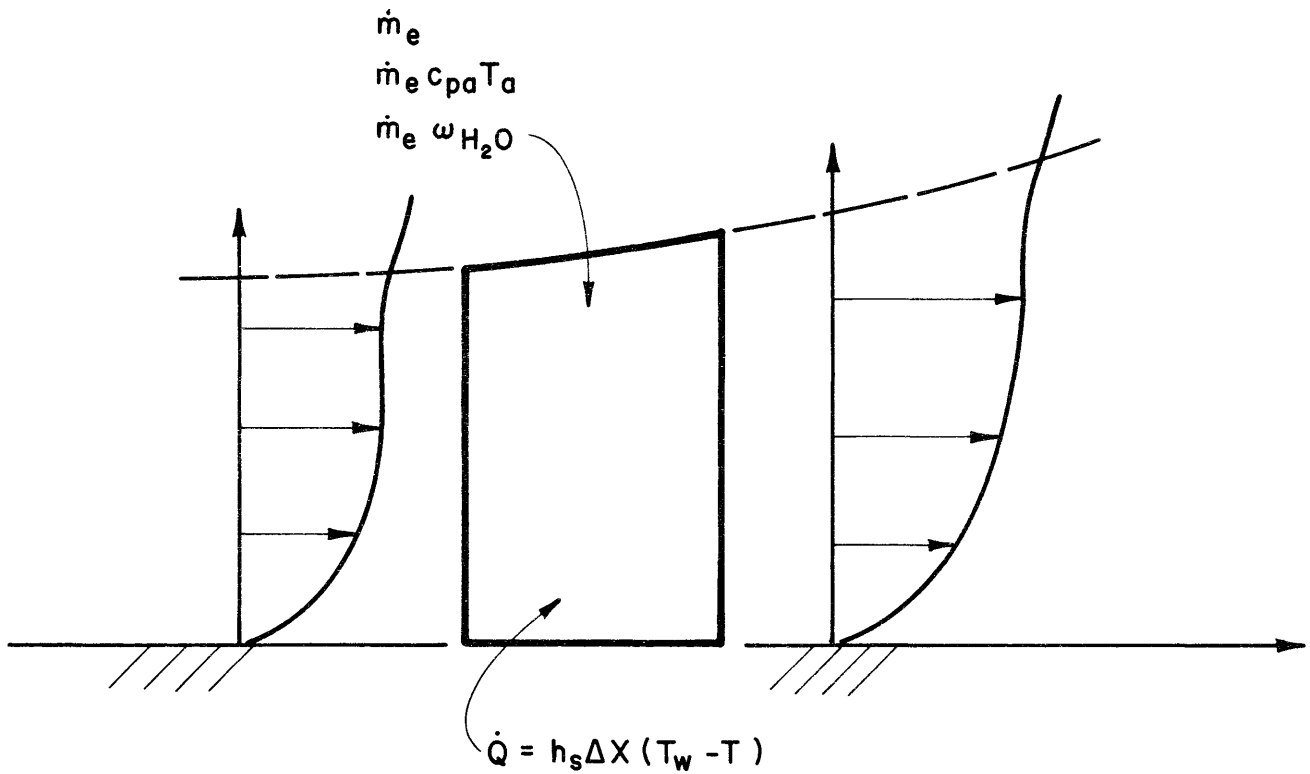

Figure A-3. Control Volume for Heat, Mass and Momentum Transport in Box Model

where χ = is mole fraction, $\theta = 1 - T_o/T_a$, T^* is dimensionless temperature equal to $(T_a - T)/(T_a - T_o)$, and

$$\chi = \left(\frac{1 - T^*\theta}{1 - \theta}\right)\left(\frac{u_o^* L_o^*}{u_x^* H^* L^*}\right) \tag{A-4}$$

At early times, when $Ri_*^{1/2} >> 1$ and gravitational spreading dominates, the concensus is that u_ℓ and u_z should be proportional to $(g'H)^{1/2}$; thus

$$v_e^* = c_\ell \, u_g^* \tag{A-5}$$

$$w_e^* = c_z \, u_g^* \tag{A-6}$$

where the constants c_ℓ and c_z range from 0.0 to 1.0 depending upon the modeler's bias. (See Lohmeyer, Meroney, and Plate (1980).)

The behavior of the box model algorithms is critically dependent on entrainment constants selected. Since the entrainment rate velocities are strongly influenced by self generated mixing associated with heating as well as background mechanical turbulence a modified entrainment expression similar to that proposed by Eidsvik (1980) is used.

$$w_e^* = c_z \, u_g^* + \frac{\alpha_4 v^*}{\frac{\alpha_4}{\alpha_6} + Ri} \tag{A-7}$$

where $u_g^* = \alpha_1 \sqrt{\frac{\Delta\rho}{\Delta\rho_o} H^*}$,

$$\frac{\Delta\rho}{\Delta\rho_o} = \left(\frac{\chi\beta + T^*\theta - T^*\beta\theta}{\beta + \theta - \beta\theta}\right)\left(\frac{1 - \theta}{1 - T^*\theta}\right) ,$$

$$Ri = Ri_* H^* \frac{\rho_a}{\rho} \frac{\Delta\rho}{\Delta\rho_o} ,$$

$$\frac{\rho}{\rho_a} = \frac{\chi + (1 - \chi)(1 - \beta)}{(1 - \beta)(1 - T^*\theta)} , \text{ and}$$

$$v^{*2} = \frac{\alpha_3^2}{Ri_*} + \alpha_2^2 \left[\frac{Gr}{Re^2} \frac{(1 + s^*)}{(1 + \chi s^*)} \frac{(1 - T^*\theta)}{(1 - \theta)} h_s^* H^* T^*\right]^{2/3} ,$$

but $$s^* = \frac{C_{p_o}^*}{C_{p_a}^*} - 1 ,$$

$$\beta = 1 - \frac{M_a}{M_o} ,$$

$$Gr = \frac{g\beta(T_a - T_o)H_o^3}{\nu^2} ,$$

$$Re = (g'_o H_o^3)^{1/2}/\nu ,$$

and h_s^* is a dimensionless surface heat transfer coefficient. Note that v^* is a weighted sum of turbulence velocity scales due to mechanical shear, u_*, and buoyancy, w_*. Ri acts to inhibit or accelerate entrainment depending on the buoyancy state of the cloud.

The effects of surface heat transfer to the cloud or entrainment of moist air on the thermal state of the cloud may be determined from conservation of enthalpy. An appropriate conservation expression for the box model is

$$\frac{d(\chi^{-1}e^{*})}{dx^{*}} = \frac{(1-\theta)}{u_o^{*}L_o^{*}}(h_s^{*}L^{*}T^{*}) + (HS)(LHTS)(1-\beta) \quad . \qquad \text{(A-8)}$$

$$\frac{d\chi^{-1}}{dx^{*}}[\omega_{\phi,T_a} - \omega_{100,T} - F(T)(1-\chi)\chi]$$

where

$$e^{*} = h^{*}/(C_{p_o}^{*}(T_a - T_o)$$

$$= -\frac{(1+\chi s^{*})T^{*}}{(1+s^{*})}$$

} and h^{*} is molar specific enthalpy referenced to ambient temperature, i.e. $e_o^{*} = -1$,

HS = Heavyside Operator { i.e. HS = 1 if $T < T_{dewpoint}$; HS = 0 if $T \geq T_{dewpoint}$ },

$$LHTS = \frac{M_o \ell_{H_2O}}{C_{p_o}^{*}(T_a - T_o)}$$ = Dimensionless latent heat of evaporation of water where ℓ_{H_2O} [Energy/mass H_2O], is latent heat of water,

$$\omega_{\phi,T} = 3.76 \times 10^{-6} \exp[4886(\frac{1}{273} - \frac{1}{T})]$$

= mass fraction of water vapor present from Clausius Clapyeron Equation, and

$$F(T) = \omega_{100,T}\left(\frac{4886}{T^2}\right)(T_a - T_o).$$

A momentum expression accounts for the longitudinal acceleration of the cloud section as it entrains ambient air. The expression below accounts for entrainment effects as well as surface drag.

$$\frac{dN^*}{dx^*} = u_x^*(H^*)\frac{d(\chi^{-1})}{dx^*} - \alpha_5\,(1 - \theta)\,\frac{\rho u_x^{*2} L^*}{\rho_a u_o^* L_o^*} \qquad \text{(A-9)}$$

where $N^* = (1 - T^*\theta)\,\frac{\rho}{\rho_a}\,\frac{u_x^*}{\chi}$, and

α_5 = Surface drag coefficient.

When a cold plume is released over a ground surface then heat transfer will occur at a rate depending upon the mode of convection. One may expect surface heat transfer to occur as forced, free, or mixed mode convection depending upon cloud velocity and temperature. If heat transfer is governed by forced convection then as a close approximation the Stanton number, St, will be proportional to the surface friction coefficient, $\frac{C_f}{2}$; thus

$$h_s = \rho u_x C_p \sqrt{\frac{C_f}{2}}$$

or $$h_s^* = \xi_1 \frac{(1 + \chi s^*)}{(1 + s^*)} \quad \frac{1}{(1 - T^*\theta)} \quad \frac{1}{Ri_*^{1/2}} \qquad \text{(A-10a)}$$

Under free convection conditions the Nusselt number, Nu, is found to be a fraction of the Grashof number, Gr; i.e.

$$Nu = \xi_o\, Gr^{1/3}.$$

In terms of the dimensionless parameters defined earlier this suggests

$$h_s = \xi_o \lambda\, (g\beta(T_w - T)/\nu^2)^{1/3}$$

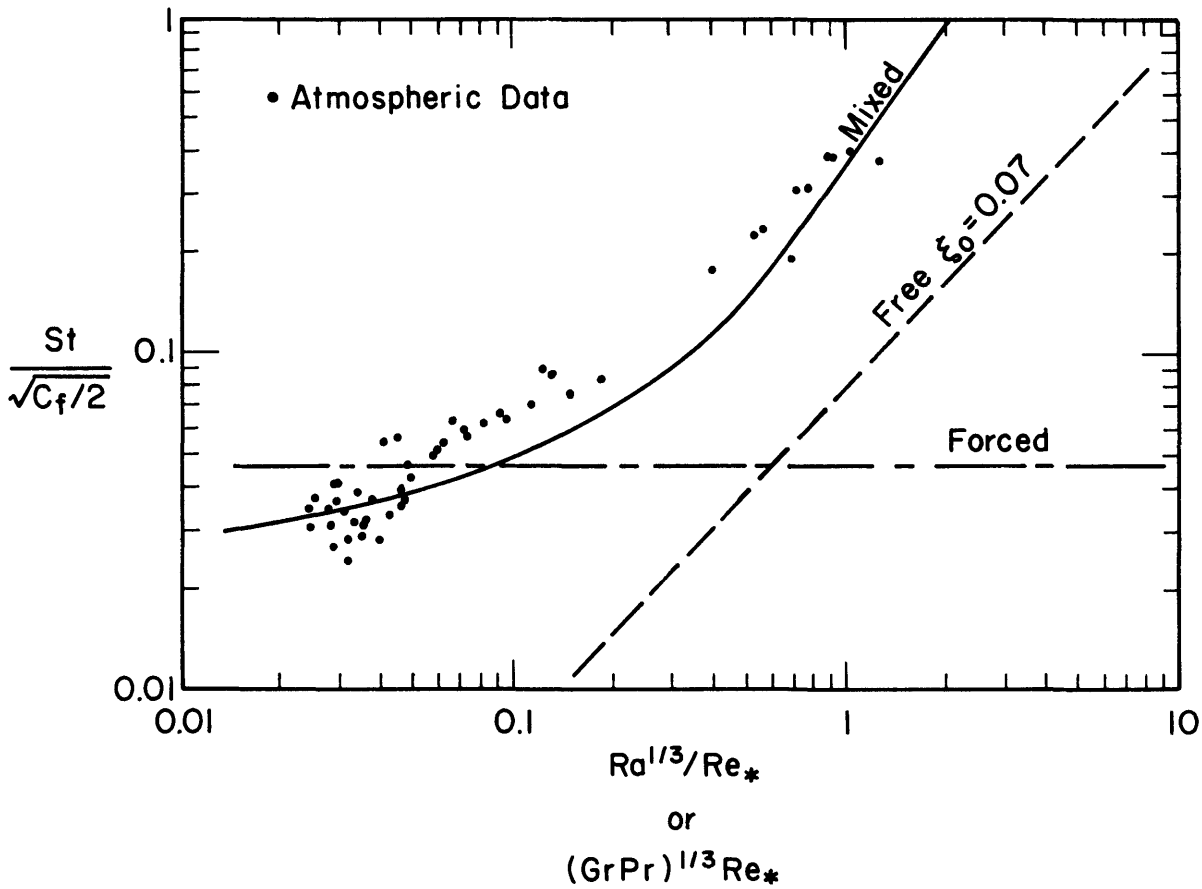

Figure A-4. Alternative Surface Heat Transport Expressions

or $$h_s^* = \xi_o \frac{Gr^{1/3}}{Re\ Pr} \frac{(1 + \lambda^*)}{(1 + s^*)} T^{*1/3} \qquad \text{(A-10b)}$$

where $$Gr = \frac{g\beta(T_w - T_o)}{2} H_o^3,$$

$$Re = \frac{(g'_o H_o)^{1/2} H_o}{a},$$

$$Pr = \frac{\mu_a C_{p_a}}{\lambda_a}, \text{ and}$$

$$\lambda^* = \frac{\lambda_o}{\lambda_a} - 1 .$$

Leovy (1969) correlated mixed-convection data from atmospheric data. He found that an empirical expression proportional to the square root of the temperature difference between the air and the boundary temperature correlated surface heat transfer coefficients over a wide range in Rayleigh and Reynolds numbers. The appropriate expression is then

$$h_s^* = \xi_2 \left(\frac{Gr}{Re_*^3 Ri_* Pr} \right)^{1/2} \frac{(1 + \chi_s^*)}{(1 + s^*)(1 - T^*\theta)} T^{*1/2} \qquad \text{(A-10c)}$$

where $$Re_* = \frac{u_* H_o}{a}.$$

Figure (A-4) shows the manner in which the three relations (10a, 10b, and 10c) are related. The program is written in such a manner that any one expression can be specified or the maximum value of h_s^* used.

Equations (A-2), (A-3), (A-8), and (A-9) were integrated by a fourth-order Runga-Kutta scheme. Entrainment rates were specified by

Equations (A-5), (A-6), and (A-7). Initial conditions were chosen as $x_o^* = 0$, $e_o^* = -1$, $H_o^* = 1$, $\chi_o = 1$. Additional data required are T_a, T_o, T_{dpt}, u_*, z_o, $C_{p_o}^*$, M_o, and H_o, and L_o. Constants found to fit the data most satisfactorily were

$c_\ell = 0.01$ $c_z = 0.01$	From Fay (1980)
$\alpha_1 = 1.00$ $\alpha_2 = 0.50$ $\alpha_3 = 1.00$ $\alpha_4 = 2.00$ $\alpha_6 = 0.30$	Modified slightly from Eidsvik (1980)
$k = 0.40$ $\alpha_5 = 0.002$ $\alpha_7 = 3.00$	From neutrally buoyant wind shear data
$\xi_0 = 0.07$	From Jakob (1949) - Free Convection
$\xi_1 = 0.045$	From $(\alpha_5)^{1/2}$ - Free Convection
$\xi_2 = 0.32$	From Leovy (1969) - Mixed Convection

When L_o and H_o cannot be determined experiementally then emperical expressions can be used to specify their values. Neff et.al. (1982) correlated initial plume width data for continuous source release of dense gas in turbulent shear flows. They suggest an empirical expression for plume width at source center, i.e.

$$L_o = 18.2(\ell_b/f^{0.8}) \tag{A-11}$$

where $\ell_b = g'_o Q/u_{H_o}^3$,

$f = Q^{1/2} g'_o / u_{H_o}^{5/2}$,

Q = Source strength,

u_{H_o} = Source plume velocity evaluated at initial plume height H_o, and

$$H_o = \left(\frac{Q}{L_o \chi_o}\right)\left[\frac{1}{\frac{u_*}{k} \ln \beta_2 \frac{H_o}{z_o} + \alpha_1 \sqrt{g'_o H_o}}\right].$$

Note that L_o and H_o must be evaluated iteratively since relations are non-homogeneous.

APPENDIX B

Temperature Varation During Adiabatic Mixing of Moist or Dry Gases

Appendix B: Temperature Variation During Adiabatic Mixing of Moist or Dry Gases

Assumption of adiabatic mixing of ideal constant-property gases permits the construction of a formula for mole fraction, χ, in terms of a function of temperature. Conservation of total enthalpy, E, requires

$$E = n\, C_p^*(T - T_a) = n_o C_{p_o}^* (T - T_a) + n_a\, C_{p_a}^* (T - T_a), \tag{B-1}$$

but when there is moisture in the air and no surface heat transfer it is also true that

$$E = n_o C_{p_o}^* (T_o - T_a) + n_a M_a \ell_{H_2O}(\omega\phi, T_a - \omega_{100,T})HS. \tag{B-2}$$

The second term adjusts for the fraction of moisture condensed into water droplets.

In terms of starred or dimensionless variables the expressions become

$$E^* = -\frac{1}{\chi}\,\frac{1 + \chi s^*}{1 + s^*}\,T^* \tag{B-3}$$

$$E^* = -1 + (HS)\frac{(1 - \chi)}{\chi}\,\frac{M_{air}\,\ell_{H_2O}}{C_{p_o}^*(T_a - T_o)}\,(\omega\phi, T_a - \omega_{100,T}) \tag{B-4}$$

or solving for mole fraction,

$$\chi = \frac{T^* + P^*}{1 + P^* + s^*(1 - T^* + P^*)} \tag{B-5}$$

where

$$P^* = HS \left(\frac{M_{air}\, \ell_{H_2O}}{C^*_{p_o} (T_a - T_o)} \right) \left(\omega_{\phi, T_a} - \omega_{100, T} \right)$$

$$\omega_{\phi, T} = 3.7 \times 10^{-3} \exp \left(4886 \left(\frac{1}{273} - \frac{1}{T} \right) \right) .$$

Variation of T, T_a, T_o, T_{dpt}, and gas properties results in curves on Figures 4-30 to 4-32 and 5-8 to 5-9.

APPENDIX C

Analytic Mixing Rate Expressions

APPENDIX C - Plume Average Concentration Calculations

It would be convenient to establish a relationship between average plume concentration and maximum cross section concentration. Letting

$$\bar{\chi} = \frac{\int \chi(y,z)\,dA}{\int dA} \quad ,$$

and using a suitable expression for $\chi(y,z)$, yields

$$\bar{\chi} = \frac{2\int_0^{\delta_y}\int_0^{\delta_z} \chi_{o,lc} \exp\left[-\frac{1}{2}\left(\frac{z}{\sigma_z}\right)^2\right] \exp\left[-\frac{1}{2}\left(\frac{y}{\sigma_y}\right)^2\right] dydz}{2\int_0^{\delta_y}\int_0^{\delta_z} dydz}$$

$$= \frac{\chi_{o,lc}\int_0^{3.035} \exp(-\frac{1}{2}\zeta^2)\int_0^{\delta_z/\sigma_y} \exp(-\frac{1}{2}\xi^2)\,d\xi\,d\zeta}{\int_0^{3.035}\left\{-2\,\ell n\left[\frac{.01}{\exp(-\frac{1}{2}\zeta^2)}\right]\right\} d\zeta}$$

$$= \frac{\chi_{o,lc}\sqrt{\pi}}{7.233}\int_0^{2.14} \exp(-\phi^2)\,\mathrm{erf}\left\{-\frac{1}{2}\,\ell n\left[\frac{.01}{\exp(-\phi^2)}\right]\right\} d\phi$$

$$\bar{\chi} = 0.215\,\chi_{o,lc}$$

Similarly, $\overline{\Delta T} = 0.215(T_a - T_{o,lc})$

APPENDIX D

Data Tables: Concentration

RUN NUMBER 1

OPERATOR --ANDREI-- DAY 356 YEAR 1982

LENGTH SCALE	1.0
REFERENCE WIND HEIGHT (CM)	2.0
TRACER CONCENTRATION (%)	2.4892
WIND SPEED (CM/S)	22.70
FLOW RATE (CCS)	130.0
AIR TEMP. (C)	21.0
SOURCE GAS TEMP. (C)	21.0
ATM. PRESSURE (IN. HG)	25.00

TUBE NO.	X (CM)	Y (CM)	Z (CM)	MODEL CONCENTRATION (%)	FIELD CONCENTRATION (%)	DIMENSIONLESS CONCENTRATION
4	30.00	50.00	0.00	.31	.81	.217E-02
5	30.00	40.00	0.00	5.05	12.35	.372E-01
6	30.00	30.00	0.00	9.62	21.99	.744E-01
7	30.00	20.00	0.00	18.11	36.95	.155E+00
8	30.00	10.00	0.00	22.98	44.14	.208E+00
9	30.00	0.00	0.00	25.29	47.27	.236E+00
10	30.00	-10.00	0.00	22.53	43.52	.203E+00
11	30.00	-20.00	0.00	13.37	29.37	.110E+00
12	30.00	-30.00	0.00	6.15	14.80	.458E-01
13	30.00	-40.00	0.00	.66	1.73	.465E-02
14	30.00	-50.00	0.00	0.00	0.00	.000E+00
15	60.00	10.00	0.00	13.83	29.83	.112E+00
16	60.00	0.00	0.00	13.05	28.45	.105E+00
17	60.00	0.00	1.00	10.96	24.58	.860E-01
18	60.00	0.00	2.00	5.22	12.73	.385E-01
19	60.00	0.00	4.00	.59	1.54	.413E-02
20	60.00	-10.00	0.00	11.09	24.83	.871E-01
21	60.00	-20.00	0.00	9.11	20.98	.700E-01
22	60.00	-30.00	0.00	5.02	12.28	.369E-01
23	60.00	-40.00	0.00	1.74	4.48	.124E-01
24	60.00	-50.00	0.00	.11	.28	.749E-03
25	60.00	-60.00	0.00	.00	.00	.600E-05
26	60.00	-70.00	0.00	.00	.00	.149E-05
28	120.00	90.00	0.00	.00	.00	.126E-04
29	120.00	75.00	0.00	.06	.15	.397E-03
30	120.00	60.00	0.00	1.34	3.47	.949E-02
31	120.00	45.00	0.00	3.46	8.66	.250E-01
32	120.00	30.00	0.00	5.41	13.16	.399E-01
33	120.00	15.00	0.00	6.32	15.17	.472E-01
35	120.00	-15.00	0.00	5.43	13.19	.401E-01
36	240.00	120.00	0.00	.02	.04	.108E-03
37	240.00	90.00	0.00	.10	.25	.673E-03
38	240.00	60.00	0.00	1.61	4.14	.114E-01
39	240.00	30.00	0.00	2.51	6.37	.180E-01
40	240.00	0.00	0.00	2.68	6.80	.192E-01
41	240.00	0.00	1.00	2.58	6.55	.185E-01
42	240.00	0.00	3.00	1.41	3.66	.100E-01
43	240.00	0.00	8.00	.16	.41	.110E-02
44	240.00	-30.00	0.00	2.50	6.37	.179E-01
45	240.00	-60.00	0.00	.89	2.32	.627E-02
46	240.00	-90.00	0.00	.00	.01	.305E-04
47	240.00	-120.00	0.00	.01	.02	.587E-04
48	350.00	30.00	0.00	1.52	3.92	.108E-01
49	350.00	0.00	0.00	1.73	4.46	.123E-01
50	350.00	-30.00	0.00	1.82	4.67	.129E-01

RUN NUMBER 2

OPERATOR --NEFF -- DAY 38 YEAR 1983
LENGTH SCALE 1.0
REFERENCE WIND HEIGHT (CM) 2.0
TRACER CONCENTRATION (%) .4335
WIND SPEED (CM/S) 22.70
FLOW RATE (CCS) 130.0
AIR TEMP. (C) 21.0
SOURCE GAS TEMP. (C) -78.
ATM. PRESSURE (IN. HG) 25.00

TUBE NO.	X (CM)	Y (CM)	Z (CM)	MODEL CONCENTRATION (%)	FIELD CONCENTRATION (%)	DIMENSIONLESS CONCENTRATION
4	30.00	50.00	0.00	.01	.02	.463E-04
5	30.00	40.00	0.00	5.06	8.56	.247E-01
6	30.00	30.00	0.00	11.21	18.15	.585E-01
7	30.00	20.00	0.00	16.48	25.74	.914E-01
8	30.00	10.00	0.00	19.62	30.01	.113E+00
9	30.00	0.00	0.00	23.00	34.42	.138E+00
10	30.00	-10.00	0.00	20.60	31.31	.120E+00
11	30.00	-20.00	0.00	13.17	21.04	.703E-01
12	30.00	-30.00	0.00	5.51	9.29	.270E-01
13	30.00	-40.00	0.00	.39	.68	.181E-02
14	30.00	-50.00	0.00	0.00	0.00	.000E+00
15	60.00	10.00	0.00	9.89	16.16	.508E-01
16	60.00	0.00	0.00	9.59	15.71	.491E-01
17	60.00	0.00	1.00	7.72	12.81	.388E-01
18	60.00	0.00	2.00	4.46	7.58	.216E-01
19	60.00	0.00	4.00	.53	.93	.247E-02
20	60.00	-10.00	0.00	7.87	13.05	.396E-01
21	60.00	-20.00	0.00	7.55	12.55	.378E-01
22	60.00	-30.00	0.00	3.40	5.82	.163E-01
23	60.00	-40.00	0.00	1.06	1.85	.496E-02
24	60.00	-50.00	0.00	.03	.05	.139E-03
30	120.00	60.00	0.00	.16	.28	.742E-03
31	120.00	45.00	0.00	1.56	2.71	.734E-02
32	120.00	30.00	0.00	3.10	5.32	.148E-01
33	120.00	15.00	0.00	3.33	5.71	.160E-01
34	120.00	0.00	0.00	3.16	5.42	.151E-01
35	120.00	-15.00	0.00	2.52	4.34	.120E-01
37	240.00	90.00	0.00	0.00	0.00	.000E+00
38	240.00	60.00	0.00	.20	.35	.928E-03
39	240.00	30.00	0.00	.79	1.38	.369E-02
40	240.00	0.00	0.00	.77	1.34	.359E-02
41	240.00	0.00	1.00	.75	1.31	.350E-02
42	240.00	0.00	3.00	.63	1.10	.294E-02
43	240.00	0.00	8.00	.39	.68	.181E-02
44	240.00	-30.00	0.00	.55	.96	.256E-02
45	240.00	-60.00	0.00	.12	.21	.557E-03
46	240.00	-90.00	0.00	.12	.21	.557E-03
48	350.00	30.00	0.00	.31	.54	.144E-02
49	350.00	0.00	0.00	.33	.58	.153E-02
50	350.00	-30.00	0.00	.31	.54	.144E-02

RUN NUMBER 3

OPERATOR --NEFF -- DAY 38 YEAR 1983

LENGTH SCALE	1.0
REFERENCE WIND HEIGHT (CM)	2.0
TRACER CONCENTRATION (%)	100.0000
WIND SPEED (CM/S)	22.70
FLOW RATE (CCS)	130.0
AIR TEMP. (C)	21.0
SOURCE GAS TEMP. (C)	-145
ATM. PRESSURE (IN. HG)	25.00

TUBE NO.	X (CM)	Y (CM)	Z (CM)	MODEL CONCENTRATION (%)	FIELD CONCENTRATION (%)	DIMENSIONLESS CONCENTRATION
4	30.00	50.00	0.00	.14	.16	.426E-03
5	30.00	40.00	0.00	.34	.39	.104E-02
6	30.00	30.00	0.00	3.30	3.79	.104E-01
7	30.00	20.00	0.00	15.00	16.91	.537E-01
8	30.00	10.00	0.00	19.74	22.10	.748E-01
9	30.00	0.00	0.00	20.24	22.64	.772E-01
10	30.00	-10.00	0.00	17.58	19.74	.649E-01
11	30.00	-20.00	0.00	6.94	7.92	.227E-01
12	30.00	-30.00	0.00	.58	.67	.177E-02
13	30.00	-40.00	0.00	.06	.07	.183E-03
14	30.00	-50.00	0.00	.08	.09	.243E-03
15	60.00	10.00	0.00	8.30	9.45	.275E-01
16	60.00	0.00	0.00	6.52	7.44	.212E-01
17	60.00	0.00	1.00	6.28	7.17	.204E-01
18	60.00	0.00	2.00	5.34	6.11	.172E-01
19	60.00	0.00	4.00	2.80	3.22	.876E-02
20	60.00	-10.00	0.00	4.86	5.56	.155E-01
21	60.00	-20.00	0.00	2.68	3.08	.837E-02
22	60.00	-30.00	0.00	.44	.51	.134E-02
23	60.00	-40.00	0.00	.10	.12	.304E-03
24	60.00	-50.00	0.00	.04	.05	.122E-03
25	60.00	-60.00	0.00	.04	.05	.122E-03
28	120.00	90.00	0.00	0.00	0.00	.000E+00
29	120.00	75.00	0.00	.08	.09	.243E-03
30	120.00	60.00	0.00	.08	.09	.243E-03
31	120.00	45.00	0.00	.26	.30	.793E-03
32	120.00	30.00	0.00	1.40	1.61	.432E-02
33	120.00	15.00	0.00	2.02	2.32	.627E-02
34	120.00	0.00	0.00	1.82	2.09	.564E-02
35	120.00	-15.00	0.00	1.04	1.20	.320E-02
36	240.00	120.00	0.00	.06	.07	.183E-03
37	240.00	90.00	0.00	.08	.09	.243E-03
38	240.00	60.00	0.00	.10	.12	.304E-03
39	240.00	30.00	0.00	.50	.58	.153E-02
40	240.00	0.00	0.00	.56	.65	.171E-02
41	240.00	0.00	1.00	.56	.65	.171E-02
42	240.00	0.00	3.00	.52	.60	.159E-02
43	240.00	0.00	8.00	.48	.55	.147E-02
44	240.00	-30.00	0.00	.18	.21	.548E-03
45	240.00	-60.00	0.00	.04	.05	.122E-03
46	240.00	-90.00	0.00	.04	.05	.122E-03
47	240.00	-120.00	0.00	.06	.07	.183E-03
48	350.00	30.00	0.00	.28	.32	.854E-03
49	350.00	0.00	0.00	.30	.35	.915E-03
50	350.00	-30.00	0.00	.14	.16	.426E-03

RUN NUMBER 4

OPERATOR --NEFF -- DAY 95 YEAR 1983
LENGTH SCALE 1.0
REFERENCE WIND HEIGHT (CM) 2.0
TRACER CONCENTRATION (%) 2.5051
WIND SPEED (CM/S) 38.80
FLOW RATE (CCS) 130.0
AIR TEMP. (C) 21.0
SOURCE GAS TEMP. (C) 20.0
ATM. PRESSURE (IN. HG) 25.00

TUBE NO.	X (CM)	Y (CM)	Z (CM)	MODEL CONCENTRATION (%)	FIELD CONCENTRATION (%)	DIMENSIONLESS CONCENTRATION
5	30.00	40.00	0.00	.01	.03	.119E-03
6	30.00	30.00	0.00	.27	.71	.322E-02
7	30.00	20.00	0.00	13.39	28.98	.184E+00
8	30.00	10.00	0.00	22.00	42.68	.336E+00
9	30.00	0.00	0.00	23.30	44.50	.361E+00
10	30.00	-10.00	0.00	20.27	40.16	.302E+00
11	30.00	-20.00	0.00	5.58	13.49	.703E-01
12	30.00	-30.00	0.00	.01	.03	.119E-03
15	60.00	10.00	0.00	12.09	26.63	.164E+00
16	60.00	0.00	0.00	11.48	25.50	.154E+00
17	60.00	0.00	1.00	7.29	17.19	.936E-01
18	60.00	0.00	2.00	2.06	5.26	.250E-01
19	60.00	0.00	4.00	.41	1.08	.490E-02
20	60.00	-10.00	0.00	8.09	18.85	.105E+00
21	60.00	-20.00	0.00	4.51	11.09	.562E-01
22	60.00	-30.00	0.00	.10	.26	.119E-02
23	60.00	-40.00	0.00	0.00	0.00	.000E+00
30	120.00	60.00	0.00	0.00	0.00	.000E+00
31	120.00	45.00	0.00	.16	.42	.191E-02
32	120.00	30.00	0.00	3.48	8.69	.429E-01
33	120.00	15.00	0.00	5.77	13.91	.729E-01
34	120.00	0.00	0.00	4.88	11.93	.610E-01
35	120.00	-15.00	0.00	2.75	6.95	.336E-01
36	240.00	120.00	0.00	0.00	0.00	.000E+00
38	240.00	60.00	0.00	.10	.26	.119E-02
39	240.00	30.00	0.00	1.38	3.56	.166E-01
40	240.00	0.00	0.00	2.23	5.68	.271E-01
41	240.00	0.00	1.00	2.14	5.46	.260E-01
42	240.00	0.00	3.00	1.14	2.95	.137E-01
43	240.00	0.00	8.00	.20	.53	.238E-02
44	240.00	-30.00	0.00	0.00	0.00	.000E+00
48	350.00	30.00	0.00	.62	1.62	.742E-02
49	350.00	0.00	0.00	1.04	2.70	.125E-01
50	350.00	-30.00	0.00	.60	1.57	.718E-02

RUN NUMBER 5

OPERATOR --ANDREI-- DAY 356 YEAR 1982
LENGTH SCALE 1.0
REFERENCE WIND HEIGHT (CM) 2.0
TRACER CONCENTRATION (%) .4335
WIND SPEED (CM/S) 38.80
FLOW RATE (CCS) 130.0
AIR TEMP. (C) 21.0
SOURCE GAS TEMP. (C) -78.
ATM. PRESSURE (IN. HG) 25.00

TUBE NO.	X (CM)	Y (CM)	Z (CM)	MODEL CONCENTRATION (%)	FIELD CONCENTRATION (%)	DIMENSIONLESS CONCENTRATION
4	30.00	50.00	0.00	.01	.02	.803E-04
5	30.00	40.00	0.00	.02	.04	.161E-03
6	30.00	30.00	0.00	4.09	6.97	.338E-01
7	30.00	20.00	0.00	15.81	24.80	.149E+00
8	30.00	10.00	0.00	20.95	31.76	.210E+00
9	30.00	0.00	0.00	22.40	33.65	.229E+00
10	30.00	-10.00	0.00	18.50	28.51	.180E+00
11	30.00	-20.00	0.00	6.11	10.25	.515E-01
12	30.00	-30.00	0.00	.02	.04	.188E-03
13	30.00	-40.00	0.00	.01	.02	.689E-04
15	60.00	10.00	0.00	11.67	18.84	.105E+00
16	60.00	0.00	0.00	11.03	17.88	.981E-01
17	60.00	0.00	1.00	6.82	11.40	.580E-01
18	60.00	0.00	2.00	2.08	3.59	.168E-01
19	60.00	0.00	4.00	.41	.72	.326E-02
20	60.00	-10.00	0.00	6.70	11.20	.569E-01
21	60.00	-20.00	0.00	3.68	6.29	.302E-01
22	60.00	-30.00	0.00	.12	.20	.917E-03
23	60.00	-40.00	0.00	.01	.02	.866E-04
30	120.00	60.00	0.00	.01	.02	.917E-04
31	120.00	45.00	0.00	.77	1.35	.617E-02
32	120.00	30.00	0.00	3.56	6.09	.292E-01
33	120.00	15.00	0.00	4.40	7.48	.365E-01
34	120.00	0.00	0.00	3.46	5.92	.283E-01
35	120.00	-15.00	0.00	1.71	2.97	.138E-01
37	240.00	90.00	0.00	.01	.01	.556E-04
38	240.00	60.00	0.00	.32	.56	.253E-02
39	240.00	30.00	0.00	1.51	2.62	.121E-01
40	240.00	0.00	0.00	1.40	2.43	.112E-01
41	240.00	0.00	1.00	1.30	2.26	.104E-01
42	240.00	0.00	3.00	.95	1.65	.756E-02
43	240.00	0.00	8.00	.35	.62	.282E-02
44	240.00	-30.00	0.00	.20	.36	.161E-02
45	240.00	-60.00	0.00	.01	.02	.904E-04
48	350.00	30.00	0.00	.81	1.41	.643E-02
49	350.00	0.00	0.00	.73	1.28	.583E-02
50	350.00	-30.00	0.00	.26	.46	.209E-02

RUN NUMBER 6

OPERATOR --NEFF -- DAY 38 YEAR 1983
LENGTH SCALE 1.0
REFERENCE WIND HEIGHT (CM) 2.0
TRACER CONCENTRATION (%) 100.0000
WIND SPEED (CM/S) 38.80
FLOW RATE (CCS) 130.0
AIR TEMP. (C) 21.0
SOURCE GAS TEMP. (C) -150
ATM. PRESSURE (IN. HG) 25.00

TUBE NO.	X (CM)	Y (CM)	Z (CM)	MODEL CONCENTRATION (%)	FIELD CONCENTRATION (%)	DIMENSIONLESS CONCENTRATION
4	30.00	50.00	0.00	.02	.02	.999E-04
5	30.00	40.00	0.00	0.00	0.00	.000E+00
6	30.00	30.00	0.00	.86	.95	.433E-02
7	30.00	20.00	0.00	16.46	17.92	.984E-01
9	30.00	0.00	0.00	25.96	27.98	.175E+00
10	30.00	-10.00	0.00	22.94	24.80	.149E+00
11	30.00	-20.00	0.00	12.90	14.10	.740E-01
12	30.00	-30.00	0.00	.48	.53	.241E-02
13	30.00	-40.00	0.00	.02	.02	.999E-04
14	30.00	-50.00	0.00	.02	.02	.999E-04
15	60.00	10.00	0.00	10.56	11.57	.590E-01
16	60.00	0.00	0.00	10.54	11.55	.588E-01
17	60.00	0.00	1.00	7.00	7.70	.376E-01
18	60.00	0.00	2.00	3.40	3.75	.176E-01
19	60.00	0.00	4.00	.60	.66	.301E-02
20	60.00	-10.00	0.00	8.74	9.59	.478E-01
21	60.00	-20.00	0.00	7.10	7.81	.382E-01
22	60.00	-30.00	0.00	1.74	1.92	.884E-02
23	60.00	-40.00	0.00	.02	.02	.999E-04
24	60.00	-50.00	0.00	0.00	0.00	.000E+00
25	60.00	-60.00	0.00	0.00	0.00	.000E+00
29	120.00	75.00	0.00	.02	.02	.999E-04
30	120.00	60.00	0.00	.02	.02	.999E-04
31	120.00	45.00	0.00	.06	.07	.300E-03
32	120.00	30.00	0.00	2.98	3.29	.153E-01
33	120.00	15.00	0.00	4.08	4.50	.212E-01
34	120.00	0.00	0.00	3.88	4.28	.202E-01
35	120.00	-15.00	0.00	3.14	3.47	.162E-01
36	240.00	120.00	0.00	0.00	0.00	.000E+00
37	240.00	90.00	0.00	.02	.02	.999E-04
38	240.00	60.00	0.00	.02	.02	.999E-04
39	240.00	30.00	0.00	1.24	1.37	.627E-02
40	240.00	0.00	0.00	1.62	1.79	.822E-02
41	240.00	0.00	1.00	1.52	1.68	.771E-02
42	240.00	0.00	3.00	.66	.73	.332E-02
43	240.00	0.00	8.00	.06	.07	.300E-03
44	240.00	-30.00	0.00	.92	1.02	.464E-02
45	240.00	-60.00	0.00	0.00	0.00	.000E+00
46	240.00	-90.00	0.00	0.00	0.00	.000E+00
47	240.00	-120.00	0.00	.02	.02	.999E-04
48	350.00	30.00	0.00	.80	.89	.403E-02
49	350.00	0.00	0.00	.94	1.04	.474E-02
50	350.00	-30.00	0.00	.68	.75	.342E-02

RUN NUMBER 7

OPERATOR --NEFF -- DAY 95 YEAR 1983

LENGTH SCALE	1.0
REFERENCE WIND HEIGHT (CM)	2.0
TRACER CONCENTRATION (%)	.6162
WIND SPEED (CM/S)	38.80
FLOW RATE (CCS)	223.0
AIR TEMP. (C)	21.0
SOURCE GAS TEMP. (C)	29.0
ATM. PRESSURE (IN. HG)	25.00

TUBE NO.	X (CM)	Y (CM)	Z (CM)	MODEL CONCENTRATION (%)	FIELD CONCENTRATION (%)	DIMENSIONLESS CONCENTRATION
4	30.00	50.00	0.00	.68	1.78	.475E-02
5	30.00	40.00	0.00	4.49	11.04	.326E-01
6	30.00	30.00	0.00	8.95	20.60	.682E-01
7	30.00	20.00	0.00	16.63	34.49	.138E+00
8	30.00	10.00	0.00	19.71	39.32	.170E+00
9	30.00	0.00	0.00	19.98	39.73	.173E+00
10	30.00	-10.00	0.00	19.79	39.44	.171E+00
11	30.00	-20.00	0.00	12.99	28.27	.104E+00
12	30.00	-30.00	0.00	5.63	13.61	.414E-01
14	30.00	-50.00	0.00	0.00	0.00	.000E+00
17	60.00	0.00	1.00	7.26	17.13	.543E-01
18	60.00	0.00	2.00	1.81	4.64	.128E-01
19	60.00	0.00	4.00	.21	.55	.146E-02
20	60.00	-10.00	0.00	9.94	22.56	.766E-01
21	60.00	-20.00	0.00	8.79	20.28	.668E-01
22	60.00	-30.00	0.00	4.71	11.54	.343E-01
23	60.00	-40.00	0.00	1.71	4.39	.121E-01
24	60.00	-50.00	0.00	.32	.84	.223E-02
25	60.00	-60.00	0.00	0.00	0.00	.000E+00
29	120.00	75.00	0.00	.01	.03	.694E-04
30	120.00	60.00	0.00	.73	1.90	.510E-02
31	120.00	45.00	0.00	2.39	6.07	.170E-01
32	120.00	30.00	0.00	4.42	10.88	.321E-01
33	120.00	15.00	0.00	5.52	13.36	.405E-01
34	120.00	0.00	0.00	4.83	11.81	.352E-01
35	120.00	-15.00	0.00	4.91	11.99	.358E-01
36	240.00	120.00	0.00	.01	.03	.694E-04
37	240.00	90.00	0.00	0.00	0.00	.000E+00
38	240.00	60.00	0.00	.86	2.24	.602E-02
39	240.00	30.00	0.00	2.04	5.21	.144E-01
40	240.00	0.00	0.00	2.43	6.17	.173E-01
41	240.00	0.00	1.00	2.29	5.83	.163E-01
42	240.00	0.00	3.00	.79	2.06	.552E-02
43	240.00	0.00	8.00	.09	.24	.625E-03
44	240.00	-30.00	0.00	2.69	6.80	.192E-01
45	240.00	-60.00	0.00	.94	2.44	.658E-02
46	240.00	-90.00	0.00	.01	.03	.694E-04
47	240.00	-120.00	0.00	.01	.03	.694E-04
48	350.00	30.00	0.00	1.33	3.44	.935E-02
49	350.00	0.00	0.00	1.64	4.22	.116E-01
50	350.00	-30.00	0.00	1.52	3.91	.107E-01

RUN NUMBER 8

OPERATOR --NEFF -- DAY 38 YEAR 1983
LENGTH SCALE 1.0
REFERENCE WIND HEIGHT (CM) 2.0
TRACER CONCENTRATION (%) .4107
WIND SPEED (CM/S) 38.80
FLOW RATE (CCS) 223.0
AIR TEMP. (C) 21.0
SOURCE GAS TEMP. (C) -155
ATM. PRESSURE (IN. HG) 25.00

TUBE NO.	X (CM)	Y (CM)	Z (CM)	MODEL CONCENTRATION (%)	FIELD CONCENTRATION (%)	DIMENSIONLESS CONCENTRATION
5	30.00	40.00	0.00	10.38	10.96	.324E-01
6	30.00	30.00	0.00	19.08	20.04	.659E-01
7	30.00	20.00	0.00	29.44	30.73	.117E+00
8	30.00	10.00	0.00	32.19	33.54	.133E+00
9	30.00	0.00	0.00	36.11	37.53	.158E+00
10	30.00	-10.00	0.00	32.20	33.55	.133E+00
11	30.00	-20.00	0.00	26.13	27.33	.988E-01
12	30.00	-30.00	0.00	12.49	13.17	.399E-01
13	30.00	-40.00	0.00	.81	.86	.228E-02
14	30.00	-50.00	0.00	0.00	0.00	.000E+00
15	60.00	10.00	0.00	18.56	19.50	.637E-01
16	60.00	0.00	0.00	17.90	18.82	.609E-01
17	60.00	0.00	1.00	11.83	12.48	.375E-01
18	60.00	0.00	2.00	3.07	3.26	.885E-02
19	60.00	0.00	4.00	.32	.34	.897E-03
20	60.00	-10.00	0.00	15.38	16.19	.508E-01
21	60.00	-20.00	0.00	15.85	16.68	.526E-01
22	60.00	-30.00	0.00	8.68	9.18	.266E-01
23	60.00	-40.00	0.00	2.73	2.90	.784E-02
24	60.00	-50.00	0.00	.10	.11	.280E-03
25	60.00	-60.00	0.00	0.00	0.00	.000E+00
28	120.00	90.00	0.00	0.00	0.00	.000E+00
29	120.00	75.00	0.00	0.00	0.00	.000E+00
30	120.00	60.00	0.00	.10	.11	.280E-03
31	120.00	45.00	0.00	3.91	4.15	.114E-01
32	120.00	30.00	0.00	7.36	7.79	.222E-01
33	120.00	15.00	0.00	8.51	9.00	.260E-01
34	120.00	0.00	0.00	7.25	7.67	.218E-01
35	120.00	-15.00	0.00	6.82	7.22	.204E-01
36	240.00	120.00	0.00	.03	.03	.838E-04
37	240.00	90.00	0.00	0.00	0.00	.000E+00
38	240.00	60.00	0.00	.32	.34	.897E-03
39	240.00	30.00	0.00	2.87	3.05	.825E-02
40	240.00	0.00	0.00	2.88	3.06	.828E-02
41	240.00	0.00	1.00	2.73	2.90	.784E-02
42	240.00	0.00	3.00	1.73	1.84	.492E-02
43	240.00	0.00	8.00	.21	.22	.588E-03
44	240.00	-30.00	0.00	2.74	2.91	.787E-02
45	240.00	-60.00	0.00	.60	.64	.169E-02
46	240.00	-90.00	0.00	.01	.01	.279E-04
47	240.00	-120.00	0.00	0.00	0.00	.000E+00
48	350.00	30.00	0.00	1.65	1.75	.469E-02
49	350.00	0.00	0.00	1.74	1.85	.495E-02
50	350.00	-30.00	0.00	1.66	1.76	.472E-02

RUN NUMBER 9

OPERATOR --ANDREI-- DAY 356 YEAR 1982
LENGTH SCALE 1.0
REFERENCE WIND HEIGHT (CM) 2.0
TRACER CONCENTRATION (%) .6879
WIND SPEED (CM/S) 38.80
FLOW RATE (CCS) 223.0
AIR TEMP. (C) 21.0
SOURCE GAS TEMP. (C) -70.
ATM PRESSURE (IN. HG) 25.00

TUBE NO.	X (CM)	Y (CM)	Z (CM)	MODEL CONCENTRATION (%)	FIELD CONCENTRATION (%)	DIMENSIONLESS CONCENTRATION
4	30.00	50.00	0.00	0.00	0.00	.000E+00
5	30.00	40.00	0.00	1.88	3.39	.921E-02
6	30.00	30.00	0.00	23.39	35.83	.147E+00
7	30.00	20.00	0.00	40.39	55.34	.326E+00
8	30.00	10.00	0.00	37.98	52.83	.294E+00
9	30.00	0.00	0.00	33.11	47.51	.238E+00
10	30.00	-10.00	0.00	28.39	42.03	.191E+00
11	30.00	-20.00	0.00	17.98	28.61	.105E+00
12	30.00	-30.00	0.00	8.50	14.52	.446E-01
13	30.00	-40.00	0.00	5.12	8.98	.259E-01
14	30.00	-50.00	0.00	0.00	0.00	.000E+00
15	60.00	10.00	0.00	19.95	31.30	.120E+00
16	60.00	0.00	0.00	16.80	26.97	.970E-01
17	60.00	0.00	1.00	11.22	18.77	.607E-01
18	60.00	0.00	2.00	2.53	4.54	.125E-01
21	60.00	-20.00	0.00	11.83	19.71	.645E-01
22	60.00	-30.00	0.00	6.23	10.83	.319E-01
23	60.00	-40.00	0.00	1.91	3.44	.936E-02
24	60.00	-50.00	0.00	.00	.01	.179E-04
25	60.00	-60.00	0.00	0.00	0.00	.000E+00
28	120.00	90.00	0.00	.00	.01	.233E-04
29	120.00	75.00	0.00	0.00	0.00	.000E+00
30	120.00	60.00	0.00	.04	.07	.178E-03
31	120.00	45.00	0.00	4.82	8.48	.243E-01
32	120.00	30.00	0.00	10.49	17.66	.563E-01
33	120.00	15.00	0.00	9.74	16.48	.518E-01
35	120.00	-15.00	0.00	6.24	10.85	.520E-01
36	240.00	120.00	0.00	0.00	0.00	.000E+00
37	240.00	90.00	0.00	0.00	0.00	.000E+00
38	240.00	60.00	0.00	1.06	1.92	.514E-02
40	240.00	0.00	0.00	3.52	6.26	.176E-01
41	240.00	0.00	1.00	3.30	5.88	.164E-01
42	240.00	0.00	3.00	1.29	2.33	.627E-02
43	240.00	0.00	8.00	.11	.21	.544E-03
44	240.00	-30.00	0.00	3.24	5.78	.161E-01
45	240.00	-60.00	0.00	.91	1.65	.441E-02
46	240.00	-90.00	0.00	.00	.00	.194E-05
48	350.00	30.00	0.00	2.76	4.94	.137E-01
49	350.00	0.00	0.00	2.87	5.13	.142E-01

RUN NUMBER 10

OPERATOR --ANDREI-- DAY 356 YEAR 1982

LENGTH SCALE	1.0
REFERENCE WIND HEIGHT (CM)	2.0
TRACER CONCENTRATION (%)	.6154
WIND SPEED (CM/S)	66.60
FLOW RATE (CCS)	223.0
AIR TEMP. (C)	21.0
SOURCE GAS TEMP. (C)	21.0
ATM. PRESSURE (IN. HG)	25.00

TUBE NO.	X (CM)	Y (CM)	Z (CM)	MODEL CONCENTRATION (%)	FIELD CONCENTRATION (%)	DIMENSIONLESS CONCENTRATION
4	30.00	50.00	0.00	.00	.00	.127E-04
5	30.00	40.00	0.00	.34	.89	.406E-02
6	30.00	30.00	0.00	.39	1.02	.467E-02
8	30.00	10.00	0.00	.60	1.57	.719E-02
9	30.00	0.00	0.00	16.19	33.85	.231E+00
10	30.00	-10.00	0.00	13.58	29.40	.188E+00
11	30.00	-40.00	0.00	.01	.03	.132E-03
14	30.00	-50.00	0.00	0.00	0.00	.000E+00
15	60.00	10.00	0.00	8.70	20.16	.114E+00
17	60.00	0.00	1.00	3.64	9.11	.452E-01
18	60.00	0.00	2.00	.87	2.27	.105E-01
22	60.00	-30.00	0.00	4.14	10.27	.516E-01
23	60.00	-40.00	0.00	.01	.02	.111E-03
30	120.00	60.00	0.00	.01	.04	.161E-03
31	120.00	45.00	0.00	.08	.22	.984E-03
32	120.00	30.00	0.00	2.40	6.12	.294E-01
33	120.00	15.00	0.00	3.73	9.32	.463E-01
34	120.00	0.00	0.00	2.88	7.28	.354E-01
35	120.00	-15.00	0.00	2.74	6.94	.336E-01
37	240.00	90.00	0.00	0.00	0.00	.000E+00
38	240.00	60.00	0.00	.03	.07	.303E-03
39	240.00	30.00	0.00	.89	2.32	.107E-01
40	240.00	0.00	0.00	1.41	3.66	.171E-01
41	240.00	0.00	1.00	1.28	3.32	.155E-01
42	240.00	0.00	3.00	.63	1.64	.752E-02
43	240.00	0.00	8.00	.09	.23	.106E-02
44	240.00	-30.00	0.00	.90	2.36	.109E-01
45	240.00	-60.00	0.00	.01	.02	.871E-04
48	350.00	30.00	0.00	.56	1.46	.667E-02
49	350.00	0.00	0.00	.72	1.88	.862E-02
50	350.00	-30.00	0.00	.86	2.26	.104E-01

RUN NUMBER 11

OPERATOR --NEFF -- DAY 38 YEAR 1983

LENGTH SCALE	1.0
REFERENCE WIND HEIGHT (CM)	2.0
TRACER CONCENTRATION (%)	.4107
WIND SPEED (CM/S)	66.60
FLOW RATE (CCS)	223.0
AIR TEMP. (C)	21.0
SOURCE GAS TEMP. (C)	-155
ATM. PRESSURE (IN. HG)	25.00

TUBE NO.	X (CM)	Y (CM)	Z (CM)	MODEL CONCENTRATION (%)	FIELD CONCENTRATION (%)	DIMENSIONLESS CONCENTRATION
4	30.00	50.00	0.00	0.00	0.00	.000E+00
5	30.00	40.00	0.00	0.00	0.00	.000E+00
6	30.00	30.00	0.00	.02	.02	.959E-04
7	30.00	20.00	0.00	19.01	19.97	.113E+00
8	30.00	10.00	0.00	32.09	33.44	.227E+00
9	30.00	0.00	0.00	36.17	37.59	.272E+00
10	30.00	-10.00	0.00	31.94	33.28	.225E+00
11	30.00	-20.00	0.00	13.85	14.60	.771E-01
12	30.00	-30.00	0.00	.02	.02	.959E-04
13	30.00	-40.00	0.00	0.00	0.00	.000E+00
14	30.00	-50.00	0.00	0.00	0.00	.000E+00
15	60.00	10.00	0.00	17.85	18.76	.104E+00
16	60.00	0.00	0.00	15.66	16.48	.890E-01
17	60.00	0.00	1.00	7.40	7.83	.383E-01
18	60.00	0.00	2.00	1.79	1.90	.874E-02
20	60.00	-10.00	0.00	12.08	12.74	.659E-01
21	60.00	-20.00	0.00	12.64	13.33	.694E-01
22	60.00	-30.00	0.00	.73	.78	.353E-02
23	60.00	-40.00	0.00	0.00	0.00	.000E+00
24	60.00	-50.00	0.00	0.00	0.00	.000E+00
25	60.00	-60.00	0.00	0.00	0.00	.000E+00
28	120.00	90.00	0.00	0.00	0.00	.000E+00
31	120.00	45.00	0.00	.07	.07	.336E-03
32	120.00	30.00	0.00	2.55	2.71	.125E-01
33	120.00	15.00	0.00	6.23	6.60	.319E-01
34	120.00	0.00	0.00	5.56	5.89	.282E-01
35	120.00	-15.00	0.00	5.46	5.78	.277E-01
40	240.00	0.00	0.00	2.63	2.79	.130E-01
41	240.00	0.00	1.00	2.27	2.41	.111E-01
42	240.00	0.00	3.00	1.51	1.60	.735E-02
43	240.00	0.00	8.00	.22	.23	.106E-02
44	240.00	-30.00	0.00	1.63	1.73	.794E-02
45	240.00	-60.00	0.00	0.00	0.00	.000E+00
48	350.00	30.00	0.00	.64	.68	.309E-02
49	350.00	0.00	0.00	1.33	1.41	.646E-02
50	350.00	-30.00	0.00	1.79	1.90	.874E-02

RUN NUMBER 12

OPERATOR --ANDREI-- DAY 361 YEAR 1982

LENGTH SCALE	1.0
REFERENCE WIND HEIGHT (CM)	2.0
TRACER CONCENTRATION (%)	.6879
WIND SPEED (CM/S)	66.60
FLOW RATE (CCS)	223.0
AIR TEMP. (C)	21.0
SOURCE GAS TEMP. (C)	-68.
ATM. PRESSURE (IN. HG)	25.00

TUBE NO.	X (CM)	Y (CM)	Z (CM)	MODEL CONCENTRATION (%)	FIELD CONCENTRATION (%)	DIMENSIONLESS CONCENTRATION
4	30.00	50.00	0.00	.00	.00	.126E-04
5	30.00	40.00	0.00	.00	.00	.630E-05
6	30.00	30.00	0.00	.07	.13	.575E-03
7	30.00	20.00	0.00	13.47	22.34	.130E+00
8	30.00	10.00	0.00	25.53	38.77	.286E+00
9	30.00	0.00	0.00	30.45	44.71	.365E+00
10	30.00	-10.00	0.00	23.65	36.39	.258E+00
11	30.00	-20.00	0.00	10.10	17.19	.936E-01
12	30.00	-30.00	0.00	.01	.03	.115E-03
13	30.00	-40.00	0.00	0.00	0.00	.000E+00
14	30.00	-50.00	0.00	0.00	0.00	.000E+00
15	60.00	10.00	0.00	14.66	24.08	.143E+00
17	60.00	0.00	1.00	6.54	11.45	.583E-01
18	60.00	0.00	2.00	1.63	2.98	.138E-01
19	60.00	0.00	4.00	.21	.38	.172E-02
20	60.00	-10.00	0.00	9.68	16.52	.893E-01
21	60.00	-20.00	0.00	9.39	16.07	.863E-01
22	60.00	-30.00	0.00	.46	.85	.387E-02
28	120.00	90.00	0.00	.00	.01	.298E-04
32	120.00	30.00	0.00	2.08	3.78	.177E-01
33	120.00	15.00	0.00	5.67	9.98	.500E-01
34	120.00	0.00	0.00	4.94	8.75	.433E-01
35	120.00	-15.00	0.00	4.48	7.98	.391E-01
37	240.00	90.00	0.00	.01	.02	.936E-04
39	240.00	30.00	0.00	.91	1.66	.762E-02
40	240.00	0.00	0.00	2.24	4.06	.191E-01
41	240.00	0.00	1.00	2.06	3.74	.175E-01
42	240.00	0.00	3.00	1.15	2.10	.966E-02
43	240.00	0.00	8.00	.13	.24	.107E-02
44	240.00	-30.00	0.00	1.37	2.49	.115E-01
45	240.00	-60.00	0.00	.02	.03	.139E-03
48	350.00	30.00	0.00	.47	.86	.390E-02
49	350.00	0.00	0.00	1.15	2.10	.966E-02
50	350.00	-30.00	0.00	1.59	2.90	.135E-01

RUN NUMBER 13
OPERATOR --HEFF -- DAY 67 YEAR 1983
FILE NAME GRI13
FLOW RATE (CCS) 130.0
WIND SPEED (CM/S) 22.70
REF. WIND HEIGHT (CM) 2.0
AIR TEMP. (C) 23.0
SOURCE GAS TEMP. (C) 23.0
TRACER CONC. (PPM) 30000.0
BACKGROUND CONC. (PPM) 4.99

TUBE NO.	X (CM)	Y (CM)	Z (CM)	MODEL CONCENTRATION (%)	FIELD CONCENTRATION (%)	DIMENSIONLESS CONCENTRATION
30	30.00	50.00	0.00	.97	2.54	.683E-02
31	30.00	40.00	0.00	6.24	15.08	.465E-01
32	30.00	30.00	0.00	12.64	27.85	.101E+00
33	30.00	20.00	0.00	22.91	44.21	.208E+00
34	30.00	10.00	0.00	30.28	53.67	.303E+00
41	30.00	-30.00	0.00	.60	1.58	.419E-02
42	30.00	-40.00	0.00	1.82	4.72	.130E-01
43	30.00	-50.00	0.00	.00	.01	.347E-04
44	60.00	-70.00	0.00	0.00	0.00	.000E+00
45	60.00	-60.00	0.00	.00	.01	.139E-04
46	60.00	-50.00	0.00	.86	2.25	.603E-02
47	60.00	-40.00	0.00	3.99	9.98	.291E-01
48	60.00	-30.00	0.00	7.56	17.90	.571E-01
49	60.00	-20.00	0.00	12.77	28.08	.102E+00
50	60.00	-10.00	0.00	15.97	33.63	.133E+00
51	60.00	0.00	0.00	11.53	25.80	.911E-01
55	60.00	10.00	0.00	15.80	33.36	.131E+00
56	120.00	-15.00	0.00	7.89	18.59	.598E-01
57	120.00	0.00	0.00	5.97	14.47	.443E-01
61	120.00	15.00	0.00	8.02	18.87	.609E-01
62	120.00	30.00	0.00	7.65	18.10	.579E-01
63	120.00	45.00	0.00	5.25	12.87	.387E-01
64	120.00	60.00	0.00	2.94	7.49	.212E-01
65	120.00	75.00	0.00	1.04	2.72	.732E-02
66	120.00	90.00	0.00	.00	.01	.134E-04
67	120.00	105.00	0.00	0.00	0.00	.000E+00
68	240.00	120.00	0.00	0.00	0.00	.000E+00
69	240.00	90.00	0.00	.94	2.48	.665E-02
70	240.00	60.00	0.00	2.57	6.58	.185E-01
71	240.00	30.00	0.00	3.66	9.19	.265E-01
72	240.00	0.00	0.00	2.62	6.68	.188E-01
73	240.00	0.00	2.00	2.05	5.30	.147E-01
74	240.00	0.00	4.00	1.07	2.89	.754E-02
75	240.00	0.00	8.00	.18	.47	.125E-02
76	240.00	-30.00	0.00	3.35	8.47	.242E-01
77	240.00	-60.00	0.00	1.69	4.39	.120E-01
78	240.00	-90.00	0.00	0.00	0.00	.000E+00
79	240.00	-120.00	0.00	0.00	0.00	.000E+00
80	350.00	-30.00	0.00	2.16	5.55	.154E-01
81	350.00	0.00	0.00	1.36	3.55	.964E-02
82	350.00	30.00	0.00	4.75	11.74	.348E-01

RUN NUMBER 14
OPERATOR --NEFF -- DAY 70 YEAR 1983
FILE NAME GRI14
FLOW RATE (CCS) 130.0
WIND SPEED (CM/S) 22.70
REF. WIND HEIGHT (CM) 2.0
AIR TEMP. (C) 25.0
SOURCE GAS TEMP. (C) 25.0
TRACER CONC. (PPM) 36059.1
BACKGROUND CONC. (PPM) 6.94

TUBE NO.	X (CM)	Y (CM)	Z (CM)	MODEL CONCENTRATION (%)	FIELD CONCENTRATION (%)	DIMENSIONLESS CONCENTRATION
30	30.00	50.00	0.00	.10	.28	.725E-03
31	30.00	40.00	0.00	5.71	13.99	.423E-01
32	30.00	30.00	0.00	12.78	28.23	.102E+00
33	30.00	20.00	0.00	24.25	46.22	.224E+00
34	30.00	10.00	0.00	30.03	53.54	.300E+00
35	30.00	0.00	0.00	32.09	55.91	.330E+00
38	45.00	0.00	0.00	23.37	45.01	.213E+00
39	30.00	-10.00	0.00	25.56	47.97	.240E+00
40	30.00	-20.00	0.00	14.22	30.80	.116E+00
41	30.00	-30.00	0.00	4.50	11.23	.329E-01
42	30.00	-40.00	0.00	.01	.03	.749E-04
43	30.00	-50.00	0.00	0.00	0.00	.000E+00
44	60.00	-70.00	0.00	.00	.01	.243E-04
45	60.00	-60.00	0.00	.00	.00	.403E-05
46	60.00	-50.00	0.00	.00	.00	.118E-04
47	60.00	-40.00	0.00	.52	1.40	.368E-02
48	60.00	-30.00	0.00	4.38	10.95	.320E-01
49	60.00	-20.00	0.00	8.61	20.19	.658E-01
50	60.00	-10.00	0.00	13.94	30.31	.113E+00
51	60.00	0.00	0.00	18.14	37.31	.155E+00
55	60.00	10.00	0.00	18.58	37.99	.159E+00
56	120.00	-15.00	0.00	6.32	15.35	.472E-01
57	120.00	0.00	0.00	9.14	21.27	.703E-01
60	140.00	0.00	0.00	7.66	18.21	.579E-01
61	120.00	15.00	0.00	9.82	22.62	.760E-01
62	120.00	30.00	0.00	8.48	19.92	.647E-01
63	120.00	45.00	0.00	5.69	13.95	.422E-01
64	120.00	60.00	0.00	2.83	7.26	.204E-01
65	120.00	75.00	0.00	.72	1.90	.504E-02
66	120.00	90.00	0.00	0.00	0.00	.000E+00
67	120.00	105.00	0.00	0.00	0.00	.000E+00
68	240.00	120.00	0.00	.01	.02	.466E-04
69	240.00	90.00	0.00	1.10	2.90	.777E-02
70	240.00	60.00	0.00	3.20	8.14	.231E-01
71	240.00	30.00	0.00	4.54	11.32	.332E-01
72	240.00	0.00	0.00	4.23	10.59	.308E-01
73	240.00	0.00	2.00	2.86	7.33	.206E-01
74	240.00	0.00	4.00	.75	1.98	.525E-02
75	240.00	0.00	8.00	.11	.30	.771E-03
76	240.00	-30.00	0.00	2.04	5.29	.145E-01
77	240.00	-60.00	0.00	.02	.07	.172E-03
78	240.00	-90.00	0.00	0.00	0.00	.000E+00
79	240.00	-120.00	0.00	.01	.02	.409E-04
80	350.00	-30.00	0.00	1.39	3.65	.986E-02
81	350.00	0.00	0.00	2.20	5.69	.157E-01
82	350.00	30.00	0.00	4.04	10.14	.294E-01

RUN NUMBER 15
OPERATOR --SPARKS-- DAY 70 YEAR 1983
FILE NAME GRI15
FLOW RATE (CCS) 130.0
WIND SPEED (CM/S) 22.70
REF. WIND HEIGHT (CM) 2.0
AIR TEMP. (C) 25.0
SOURCE GAS TEMP. (C) 25.0
TRACER CONC. (PPM) 36059.1
BACKGROUND CONC. (PPM) 4.95

TUBE NO.	X (CM)	Y (CM)	Z (CM)	MODEL CONCENTRATION (%)	FIELD CONCENTRATION (%)	DIMENSIONLESS CONCENTRATION
2	-35.00	0.00	0.00	.00	.01	.150E-04
3	-30.00	0.00	0.00	.01	.02	.406E-04
4	-25.00	0.00	0.00	.02	.04	.109E-03
5	-20.00	0.00	0.00	.03	.09	.230E-03
6	-15.00	0.00	0.00	8.17	19.28	.621E-01
17	0.00	-35.00	0.00	.01	.03	.883E-04
18	0.00	-40.00	0.00	0.00	0.00	.000E+00
19	15.00	-5.00	0.00	54.83	76.52	.848E+00
20	15.00	0.00	0.00	56.66	77.83	.913E+00
21	15.00	5.00	0.00	56.46	77.69	.906E+00
22	15.00	10.00	0.00	51.69	74.18	.747E+00
23	15.00	15.00	0.00	41.78	65.83	.501E+00
24	15.00	20.00	0.00	28.79	52.04	.282E+00
25	15.00	25.00	0.00	18.95	38.56	.163E+00
26	15.00	30.00	0.00	12.30	27.36	.980E-01
27	15.00	35.00	0.00	6.47	15.67	.483E-01
28	15.00	40.00	0.00	1.37	3.60	.971E-02
29	15.00	45.00	0.00	.06	.16	.426E-03
35	30.00	0.00	0.00	31.48	55.22	.321E+00
39	30.00	-10.00	0.00	25.63	48.05	.241E+00
40	30.00	-20.00	0.00	14.79	31.78	.121E+00
41	30.00	-30.00	0.00	6.30	15.30	.470E-01
42	30.00	-40.00	0.00	.03	.09	.235E-03
43	30.00	-50.00	0.00	.00	.00	.250E-05
56	120.00	-15.00	0.00	6.92	16.64	.519E-01
57	120.00	0.00	0.00	8.52	20.00	.650E-01
61	120.00	15.00	0.00	9.30	21.58	.716E-01
62	120.00	30.00	0.00	8.30	19.56	.633E-01
63	120.00	45.00	0.00	5.91	14.42	.438E-01
64	120.00	60.00	0.00	3.26	8.29	.235E-01
65	120.00	75.00	0.00	1.32	3.48	.937E-02
66	120.00	90.00	0.00	.04	.10	.249E-03
67	120.00	105.00	0.00	.00	.01	.267E-04
68	240.00	120.00	0.00	.01	.02	.603E-04
69	240.00	90.00	0.00	1.43	3.75	.101E-01
70	240.00	60.00	0.00	3.10	7.91	.224E-01
71	240.00	30.00	0.00	3.92	9.87	.285E-01
91	120.00	0.00	.50	8.06	19.05	.612E-01
92	120.00	0.00	1.00	6.69	16.14	.501E-01
93	120.00	0.00	1.50	5.01	12.40	.368E-01
94	120.00	0.00	2.00	3.21	8.18	.232E-01
95	120.00	0.00	2.50	2.09	5.43	.149E-01
96	120.00	0.00	3.00	1.25	3.29	.885E-02
97	120.00	0.00	4.00	.45	1.19	.312E-02
98	120.00	0.00	5.00	.21	.57	.150E-02
99	120.00	0.00	6.00	.11	.29	.758E-03
100	120.00	0.00	8.00	.06	.16	.425E-03

RUN NUMBER 16
OPERATOR --SPARKS-- DAY 70 YEAR 1983
FILE NAME GRI16
FLOW RATE (CCS) 130.0
WIND SPEED (CM/S) 22.70
REF. WIND HEIGHT (CM) 2.0
AIR TEMP. (C) 25.0
SOURCE GAS TEMP. (C) 25.0
TRACER CONC. (PPM) 36059.1
BACKGROUND CONC. (PPM) 6.61

TUBE NO.	X (CM)	Y (CM)	Z (CM)	MODEL CONCENTRATION (%)	FIELD CONCENTRATION (%)	DIMENSIONLESS CONCENTRATION
2	-35.00	0.00	0.00	.00	.00	.104E-04
3	-30.00	0.00	0.00	.00	.01	.155E-04
4	-25.00	0.00	0.00	.01	.02	.507E-04
5	-20.00	0.00	0.00	.06	.17	.431E-03
6	-15.00	0.00	0.00	8.73	20.44	.668E-01
7	0.00	15.00	0.00	47.03	70.45	.620E+00
8	0.00	20.00	0.00	25.84	48.33	.243E+00
9	0.00	25.00	0.00	12.74	28.16	.102E+00
10	0.00	30.00	0.00	1.72	4.48	.122E-01
11	0.00	35.00	0.00	.18	.49	.129E-02
12	0.00	40.00	0.00	.27	.71	.187E-02
13	0.00	-15.00	0.00	38.55	62.75	.438E+00
14	0.00	-20.00	0.00	10.76	24.46	.843E-01
15	0.00	-25.00	0.00	.29	.77	.203E-02
16	0.00	-30.00	0.00	.04	.11	.274E-03
27	15.00	35.00	0.00	6.89	16.58	.517E-01
28	15.00	40.00	0.00	1.62	4.23	.115E-01
29	15.00	45.00	0.00	.06	.17	.444E-03
35	30.00	0.00	0.00	31.35	55.07	.319E+00
39	30.00	-10.00	0.00	25.57	47.98	.240E+00
40	30.00	-20.00	0.00	14.88	31.94	.122E+00
41	30.00	-30.00	0.00	6.50	15.73	.486E-01
42	30.00	-40.00	0.00	.07	.19	.485E-03
43	30.00	-50.00	0.00	0.00	0.00	.000E+00
44	60.00	-70.00	0.00	.02	.05	.136E-03
45	60.00	-60.00	0.00	.02	.06	.149E-03
46	60.00	-50.00	0.00	.03	.09	.233E-03
47	60.00	-40.00	0.00	1.97	5.12	.140E-01
48	60.00	-30.00	0.00	5.36	13.19	.395E-01
49	60.00	-20.00	0.00	9.76	22.50	.756E-01
50	60.00	-10.00	0.00	14.55	31.37	.119E+00
51	60.00	0.00	0.00	16.69	34.98	.140E+00
55	60.00	10.00	0.00	17.74	36.66	.151E+00
68	240.00	120.00	0.00	.00	.01	.243E-04
69	240.00	90.00	0.00	1.37	3.59	.969E-02
70	240.00	60.00	0.00	2.90	7.43	.209E-01
71	240.00	30.00	0.00	3.65	9.24	.265E-01
91	60.00	0.00	.50	15.93	33.72	.132E+00
92	60.00	0.00	1.00	12.70	28.08	.102E+00
93	60.00	0.00	1.50	8.49	19.94	.648E-01
94	60.00	0.00	2.00	4.50	11.22	.329E-01
95	60.00	0.00	2.50	2.43	6.27	.174E-01
96	60.00	0.00	3.00	1.14	3.01	.806E-02
97	60.00	0.00	4.00	.32	.86	.226E-02
98	60.00	0.00	5.00	.16	.42	.111E-02
99	60.00	0.00	6.00	.07	.18	.471E-03
100	60.00	0.00	8.00	.03	.09	.239E-03

RUN NUMBER 18
OPERATOR --SPARKS-- DAY 72 YEAR 1983
FILE NAME GRI18
FLOW RATE (CCS) 223.0
WIND SPEED (CM/S) 42.30
REF. WIND HEIGHT (CM) 2.0
AIR TEMP. (C) 25.0
SOURCE GAS TEMP. (C) 25.0
TRACER CONC. (PPM) 13000.0
BACKGROUND CONC. (PPM) 5.23

TUBE NO.	X (CM)	Y (CM)	Z (CM)	MODEL CONCENTRATION (%)	FIELD CONCENTRATION (%)	DIMENSIONLESS CONCENTRATION
30	30.00	50.00	0.00	.01	.02	.469E-04
31	30.00	40.00	0.00	.33	.87	.249E-02
32	30.00	30.00	0.00	6.48	15.68	.526E-01
33	30.00	20.00	0.00	15.62	33.20	.140E+00
34	30.00	10.00	0.00	21.22	41.96	.204E+00
35	30.00	0.00	0.00	0.00	0.00	.000E+00
38	45.00	0.00	0.00	14.86	31.91	.132E+00
40	30.00	-20.00	0.00	16.31	34.34	.148E+00
41	30.00	-30.00	0.00	7.50	17.88	.615E-01
42	30.00	-40.00	0.00	1.98	5.15	.153E-01
43	30.00	-50.00	0.00	0.00	0.00	.000E+00
44	60.00	-70.00	0.00	0.00	0.00	.000E+00
45	60.00	-60.00	0.00	0.00	0.00	.000E+00
46	60.00	-50.00	0.00	0.00	0.00	.000E+00
47	60.00	-40.00	0.00	2.87	7.34	.224E-01
48	60.00	-30.00	0.00	6.48	15.69	.526E-01
49	60.00	-20.00	0.00	10.39	23.74	.880E-01
50	60.00	-10.00	0.00	11.49	25.84	.985E-01
51	60.00	0.00	0.00	12.11	27.01	.105E+00
55	60.00	10.00	0.00	12.02	26.83	.104E+00
56	120.00	-15.00	0.00	6.66	16.07	.541E-01
57	120.00	0.00	0.00	6.96	16.73	.568E-01
60	140.00	0.00	0.00	6.00	14.62	.484E-01
61	120.00	15.00	0.00	5.46	13.42	.438E-01
62	120.00	30.00	0.00	2.56	6.59	.199E-01
63	120.00	45.00	0.00	0.00	0.00	.000E+00
64	120.00	60.00	0.00	.01	.02	.482E-04
65	120.00	75.00	0.00	.01	.03	.931E-04
66	120.00	90.00	0.00	.02	.06	.167E-03
67	120.00	105.00	0.00	0.00	0.00	.000E+00
68	240.00	120.00	0.00	0.00	0.00	.000E+00
69	240.00	90.00	0.00	0.00	0.00	.000E+00
70	240.00	60.00	0.00	.02	.04	.115E-03
71	240.00	30.00	0.00	0.00	0.00	.000E+00
72	240.00	0.00	0.00	3.34	8.49	.262E-01
73	240.00	0.00	2.00	0.00	0.00	.000E+00
74	240.00	0.00	4.00	.38	1.03	.293E-02
75	240.00	0.00	8.00	.09	.24	.693E-03
76	240.00	-30.00	0.00	3.51	8.90	.276E-01
77	240.00	-60.00	0.00	1.68	4.38	.129E-01
78	240.00	-90.00	0.00	.01	.04	.114E-03
79	240.00	-120.00	0.00	.00	.01	.218E-04
80	350.00	-30.00	0.00	0.00	0.00	.000E+00
81	350.00	0.00	0.00	0.00	0.00	.000E+00

RUN NUMBER 19
OPERATOR --SPARKS-- DAY 72 YEAR 1983
FILE NAME GRI19
FLOW RATE (CCS) 223.0
WIND SPEED (CM/S) 42.30
REF. WIND HEIGHT (CM) 2.0
AIR TEMP (C) 25.0
SOURCE GAS TEMP. (C) 25.0
TRACER CONC. (PPM) 130000.0
BACKGROUND CONC. (PPM) 4.50

TUBE NO.	X (CM)	Y (CM)	Z (CM)	MODEL CONCENTRATION (%)	FIELD CONCENTRATION (%)	DIMENSIONLESS CONCENTRATION
2	-35.00	0.00	0.00	0.00	0.00	.000E+00
3	-30.00	0.00	0.00	.00	.00	.194E-06
4	-25.00	0.00	0.00	.01	.04	.110E-03
5	-20.00	0.00	0.00	0.00	0.00	.000E+00
6	-15.00	0.00	0.00	9.77	22.53	.822E-01
17	0.00	-35.00	0.00	.04	.11	.314E-03
18	0.00	-40.00	0.00	.00	.01	.323E-04
19	15.00	-5.00	0.00	34.80	58.90	.405E+00
20	15.00	0.00	0.00	36.50	60.68	.436E+00
21	15.00	5.00	0.00	38.40	62.60	.473E+00
22	15.00	10.00	0.00	38.60	62.79	.477E+00
23	15.00	15.00	0.00	33.64	57.64	.385E+00
24	15.00	20.00	0.00	23.73	45.51	.236E+00
25	15.00	25.00	0.00	14.95	32.06	.133E+00
26	15.00	30.00	0.00	8.52	19.99	.706E-01
27	15.00	35.00	0.00	3.38	8.59	.265E-01
28	15.00	40.00	0.00	.25	.66	.189E-02
29	15.00	45.00	0.00	.01	.04	.103E-03
35	30.00	0.00	0.00	19.45	39.33	.183E+00
39	30.00	-10.00	0.00	20.01	40.18	.190E+00
40	30.00	-20.00	0.00	14.99	32.13	.134E+00
41	30.00	-30.00	0.00	6.65	16.07	.541E-01
42	30.00	-40.00	0.00	1.80	4.68	.139E-01
43	30.00	-50.00	0.00	.00	.01	.243E-04
56	120.00	-15.00	0.00	6.82	16.41	.555E-01
57	120.00	0.00	0.00	6.68	16.11	.543E-01
61	120.00	15.00	0.00	6.57	15.87	.533E-01
62	120.00	30.00	0.00	4.16	10.43	.329E-01
63	120.00	45.00	0.00	1.63	4.25	.126E-01
64	120.00	60.00	0.00	.25	.66	.188E-02
65	120.00	75.00	0.00	.25	.66	.188E-02
66	120.00	90.00	0.00	.02	.04	.126E-03
67	120.00	105.00	0.00	.02	.04	.115E-03
68	240.00	120.00	0.00	0.00	0.00	.000E+00
69	240.00	90.00	0.00	.00	.00	.194E-06
70	240.00	60.00	0.00	.40	1.06	.304E-02
71	240.00	30.00	0.00	2.22	5.74	.172E-01
91	120.00	0.00	.50	6.49	15.70	.527E-01
92	120.00	0.00	1.00	5.34	13.14	.428E-01
93	120.00	0.00	1.50	3.76	9.50	.297E-01
94	120.00	0.00	2.00	2.21	5.71	.171E-01
95	120.00	0.00	2.50	1.37	3.60	.106E-01
96	120.00	0.00	3.00	.78	2.07	.597E-02
97	120.00	0.00	4.00	.42	1.13	.323E-02
98	120.00	0.00	5.00	.23	.62	.177E-02
99	120.00	0.00	6.00	.13	.34	.951E-03
100	120.00	0.00	8.00	.07	.19	.528E-03

RUN NUMBER 17
OPERATOR --NEFF -- DAY 70 YEAR 1983
FILE NAME GRI17
FLOW RATE (CCS) 130.0
WIND SPEED (CM/S) 22.70
REF. WIND HEIGHT (CM) 2.0
AIR TEMP. (C) 25.0
SOURCE GAS TEMP. (C) 25.0
TRACER CONC. (PPM) 36059.1
BACKGROUND CONC. (PPM) 6.94

TUBE NO.	X (CM)	Y (CM)	Z (CM)	MODEL CONCENTRATION (%)	FIELD CONCENTRATION (%)	DIMENSIONLESS CONCENTRATION
7	0.00	15.00	0.00	47.39	70.75	.629E+00
8	0.00	20.00	0.00	26.65	49.37	.254E+00
9	0.00	25.00	0.00	11.68	26.20	.923E-01
10	0.00	30.00	0.00	1.19	3.13	.839E-02
11	0.00	35.00	0.00	.03	.09	.235E-03
12	0.00	40.00	0.00	.06	.16	.420E-03
13	0.00	-15.00	0.00	38.54	62.73	.438E+00
14	0.00	-20.00	0.00	6.42	15.55	.479E-01
15	0.00	-25.00	0.00	.03	.09	.226E-03
16	0.00	-30.00	0.00	.01	.02	.637E-04
17	0.00	-35.00	0.00	.00	.01	.338E-04
18	0.00	-40.00	0.00	.01	.01	.387E-04
20	15.00	0.00	0.00	55.73	77.17	.879E+00
21	15.00	5.00	0.00	55.45	76.97	.869E+00
22	15.00	10.00	0.00	51.44	73.98	.740E+00
23	15.00	15.00	0.00	42.50	66.50	.516E+00
24	15.00	20.00	0.00	30.48	54.07	.306E+00
25	15.00	25.00	0.00	20.07	40.26	.175E+00
26	15.00	30.00	0.00	12.95	28.54	.104E+00
27	15.00	35.00	0.00	6.18	15.03	.460E-01
28	15.00	40.00	0.00	.91	2.40	.640E-02
29	15.00	45.00	0.00	.04	.11	.284E-03
30	30.00	50.00	0.00	.31	.82	.215E-02
31	30.00	40.00	0.00	6.22	15.12	.464E-01
32	30.00	30.00	0.00	13.67	29.83	.111E+00
33	30.00	20.00	0.00	24.71	46.84	.229E+00
34	30.00	10.00	0.00	29.33	52.71	.290E+00
35	30.00	0.00	0.00	28.42	51.60	.277E+00
39	30.00	-10.00	0.00	24.48	46.53	.226E+00
40	30.00	-20.00	0.00	14.44	31.19	.118E+00
41	30.00	-30.00	0.00	5.54	13.60	.409E-01
42	30.00	-40.00	0.00	.01	.02	.416E-04
43	30.00	-50.00	0.00	0.00	0.00	.000E+00
68	240.00	120.00	0.00	.00	.01	.182E-04
69	240.00	90.00	0.00	.02	.06	.161E-03
70	240.00	60.00	0.00	2.79	7.16	.201E-01
71	240.00	30.00	0.00	3.50	8.88	.254E-01
91	30.00	0.00	.50	25.68	48.12	.241E+00
92	30.00	0.00	1.00	15.17	32.44	.125E+00
93	30.00	0.00	1.50	6.75	16.28	.506E-01
94	30.00	0.00	2.00	2.23	5.76	.159E-01
95	30.00	0.00	2.50	.94	2.49	.665E-02
96	30.00	0.00	3.00	.39	1.05	.276E-02
97	30.00	0.00	4.00	.15	.41	.108E-02
98	30.00	0.00	5.00	.09	.23	.604E-03
100	30.00	0.00	8.00	.01	.04	.952E-04

RUN NUMBER 20
OPERATOR --NEFF -- DAY 72 YEAR 1983
FILE NAME GRI20
FLOW RATE (CCS) 223.0
WIND SPEED (CM/S) 42.30
REF. WIND HEIGHT (CM) 2.0
AIR TEMP. (C) 25.0
SOURCE GAS TEMP. (C) 25.0
TRACER CONC. (PPM) 13000.0
BACKGROUND CONC. (PPM) 5.99

TUBE NO.	X (CM)	Y (CM)	Z (CM)	MODEL CONCENTRATION (%)	FIELD CONCENTRATION (%)	DIMENSIONLESS CONCENTRATION
2	-35.00	0.00	0.00	0.00	0.00	.000E+00
3	-30.00	0.00	0.00	0.00	0.00	.000E+00
4	-25.00	0.00	0.00	0.00	0.00	.000E+00
5	-20.00	0.00	0.00	.02	.04	.123E-03
6	-15.00	0.00	0.00	7.25	17.35	.593E-01
7	0.00	15.00	0.00	40.73	64.85	.521E+00
8	0.00	20.00	0.00	21.71	42.68	.210E+00
9	0.00	25.00	0.00	9.87	22.72	.831E-01
10	0.00	30.00	0.00	.81	2.15	.622E-02
11	0.00	35.00	0.00	.11	.30	.859E-03
12	0.00	40.00	0.00	.31	.83	.235E-02
13	0.00	-15.00	0.00	32.24	56.09	.361E+00
14	0.00	-20.00	0.00	15.58	33.13	.140E+00
15	0.00	-25.00	0.00	4.65	11.58	.370E-01
16	0.00	-30.00	0.00	8.97	20.91	.747E-01
27	15.00	35.00	0.00	3.36	8.53	.264E-01
28	15.00	40.00	0.00	.19	.50	.143E-02
29	15.00	45.00	0.00	.00	.01	.181E-04
35	30.00	0.00	0.00	19.43	39.30	.183E+00
39	30.00	-10.00	0.00	19.89	40.00	.188E+00
40	30.00	-20.00	0.00	14.71	31.65	.131E+00
41	30.00	-30.00	0.00	6.30	15.30	.511E-01
42	30.00	-40.00	0.00	1.16	3.06	.893E-02
43	30.00	-50.00	0.00	0.00	0.00	.000E+00
44	60.00	-70.00	0.00	.01	.03	.970E-04
45	60.00	-60.00	0.00	.01	.02	.636E-04
46	60.00	-50.00	0.00	.23	.62	.178E-02
47	60.00	-40.00	0.00	1.99	5.18	.154E-01
48	60.00	-30.00	0.00	5.20	12.85	.417E-01
49	60.00	-20.00	0.00	9.42	21.82	.789E-01
50	60.00	-10.00	0.00	11.90	26.61	.102E+00
51	60.00	0.00	0.00	11.47	25.81	.983E-01
55	60.00	10.00	0.00	12.40	27.55	.107E+00
68	240.00	120.00	0.00	0.00	0.00	.000E+00
69	240.00	90.00	0.00	0.00	0.00	.000E+00
70	240.00	60.00	0.00	.53	1.42	.408E-02
71	240.00	30.00	0.00	2.55	6.57	.199E-01
91	60.00	0.00	.50	10.55	24.95	.895E-01
92	60.00	0.00	1.00	6.88	16.56	.561E-01
93	60.00	0.00	1.50	3.64	9.22	.287E-01
94	60.00	0.00	2.00	1.59	4.16	.123E-01
95	60.00	0.00	2.50	.88	2.32	.671E-02
96	60.00	0.00	3.00	.65	1.72	.495E-02
97	60.00	0.00	4.00	.26	.70	.198E-02
98	60.00	0.00	5.00	.12	.32	.919E-03
99	60.00	0.00	6.00	.06	.15	.430E-03
100	60.00	0.00	8.00	.02	.06	.184E-03

RUN NUMBER 21
OPERATOR --SPARKS-- DAY 72 YEAR 1983
FILE NAME GRI21
FLOW RATE (CCS) 223.0
WIND SPEED (CM/S) 42.30
REF. WIND HEIGHT (CM) 2.0
AIR TEMP. (C) 25.0
SOURCE GAS TEMP. (C) 25.0
TRACER CONC (PPM) 13000.0
BACKGROUND CONC (PPM) 4.93

TUBE NO.	X (CM)	Y (CM)	Z (CM)	MODEL CONCENTRATION (%)	FIELD CONCENTRATION (%)	DIMENSIONLESS CONCENTRATION
7	0.00	15.00	0.00	41.25	65.34	.533E+00
8	0.00	20.00	0.00	22.14	43.29	.216E+00
9	0.00	25.00	0.00	11.47	25.81	.983E-01
10	0.00	30.00	0.00	1.49	3.91	.115E-01
11	0.00	35.00	0.00	.02	.05	.151E-03
12	0.00	40.00	0.00	.30	.79	.225E-02
13	0.00	-15.00	0.00	32.88	56.80	.372E+00
14	0.00	-20.00	0.00	16.22	34.20	.147E+00
15	0.00	-25.00	0.00	5.89	14.39	.475E-01
16	0.00	-30.00	0.00	.17	.45	.127E-02
17	0.00	-35.00	0.00	.00	.01	.340E-04
18	0.00	-40.00	0.00	.01	.02	.535E-04
20	15.00	0.00	0.00	36.80	60.99	.442E+00
21	15.00	5.00	0.00	38.30	62.50	.471E+00
22	15.00	10.00	0.00	38.85	63.04	.482E+00
23	15.00	15.00	0.00	34.49	58.57	.400E+00
24	15.00	20.00	0.00	25.19	47.48	.255E+00
25	15.00	25.00	0.00	16.10	34.01	.146E+00
26	15.00	30.00	0.00	9.39	21.77	.787E-01
27	15.00	35.00	0.00	4.38	10.95	.347E-01
28	15.00	40.00	0.00	.31	.83	.236E-02
29	15.00	45.00	0.00	.00	.01	.224E-04
30	30.00	50.00	0.00	0.00	0.00	.000E+00
31	30.00	40.00	0.00	3.01	7.69	.235E-01
32	30.00	30.00	0.00	9.14	21.26	.763E-01
33	30.00	20.00	0.00	17.98	37.05	.166E+00
34	30.00	10.00	0.00	20.30	40.61	.193E+00
35	30.00	0.00	0.00	18.02	37.11	.167E+00
39	30.00	-10.00	0.00	19.57	39.51	.185E+00
40	30.00	-20.00	0.00	14.92	32.01	.133E+00
41	30.00	-30.00	0.00	6.70	16.15	.544E-01
42	30.00	-40.00	0.00	1.57	4.12	.121E-01
43	30.00	-50.00	0.00	0.00	0.00	.000E+00
68	240.00	120.00	0.00	0.00	0.00	.000E+00
69	240.00	90.00	0.00	0.00	0.00	.000E+00
70	240.00	60.00	0.00	.47	1.24	.355E-02
71	240.00	30.00	0.00	2.47	6.37	.192E-01
91	30.00	0.00	.50	16.13	34.05	.146E+00
92	30.00	0.00	1.00	7.51	17.90	.616E-01
93	30.00	0.00	1.50	2.53	6.52	.197E-01
94	30.00	0.00	2.00	.84	2.22	.642E-02
95	30.00	0.00	2.50	.42	1.12	.319E-02
96	30.00	0.00	3.00	.28	.74	.212E-02
97	30.00	0.00	4.00	.10	.27	.754E-03
98	30.00	0.00	5.00	.05	.13	.365E-03
99	30.00	0.00	6.00	.01	.03	.832E-04
100	30.00	0.00	8.00	.01	.01	.391E-04

RUN NUMBER 22
OPERATOR --SPARKS-- DAY 74 YEAR 1983
FILE NAME CR122
FLOW RATE (CCS) 130.0
WIND SPEED (CM/S) 24.70
REF. WIND HEIGHT (CM) 2.0
AIR TEMP. (C) 21.0
SOURCE GAS TEMP. (C) -78.
TRACER CONC (PPM) 9500.0
BACKGROUND CONC. (PPM) 3.15

TUBE NO.	X (CM)	Y (CM)	Z (CM)	MODEL CONCENTRATION (%)	FIELD CONCENTRATION (%)	DIMENSIONLESS CONCENTRATION
30	30.00	50.00	0.00	0.00	0.00	.000E+00
31	30.00	40.00	0.00	0.00	0.00	.000E+00
32	30.00	30.00	0.00	7.45	12.40	.406E-01
33	30.00	20.00	0.00	14.89	23.51	.882E-01
34	30.00	10.00	0.00	19.73	30.15	.124E+00
35	30.00	0.00	0.00	19.67	30.08	.123E+00
38	45.00	0.00	0.00	13.66	21.75	.797E-01
39	30.00	-10.00	0.00	13.48	21.49	.786E-01
40	30.00	-20.00	0.00	5.22	8.83	.278E-01
41	30.00	-30.00	0.00	.01	.02	.618E-04
42	30.00	-40.00	0.00	.00	.00	.276E-05
43	30.00	-50.00	0.00	0.00	0.00	.000E+00
44	60.00	-70.00	0.00	.01	.01	.271E-04
45	60.00	-60.00	0.00	0.00	0.00	.000E+00
46	60.00	-50.00	0.00	0.00	0.00	.000E+00
47	60.00	-40.00	0.00	0.00	0.00	.000E+00
48	60.00	-30.00	0.00	.29	.50	.145E-02
49	60.00	-20.00	0.00	3.17	5.44	.165E-01
50	60.00	-10.00	0.00	6.83	11.40	.369E-01
51	60.00	0.00	0.00	10.25	16.71	.576E-01
55	60.00	10.00	0.00	11.22	18.17	.637E-01
56	120.00	-15.00	0.00	2.14	3.70	.110E-01
57	120.00	0.00	0.00	4.38	7.45	.231E-01
60	140.00	0.00	0.00	3.38	5.79	.176E-01
61	120.00	15.00	0.00	5.09	8.61	.270E-01
62	120.00	30.00	0.00	4.44	7.55	.234E-01
64	120.00	60.00	0.00	1.84	3.19	.945E-02
65	120.00	75.00	0.00	.00	.00	.117E-04
66	120.00	90.00	0.00	.00	.00	.133E-04
67	120.00	105.00	0.00	0.00	0.00	.000E+00
68	240.00	120.00	0.00	0.00	0.00	.000E+00
69	240.00	90.00	0.00	0.00	0.00	.000E+00
70	240.00	60.00	0.00	.60	1.05	.304E-02
71	240.00	30.00	0.00	1.66	2.89	.853E-02
72	240.00	0.00	0.00	1.12	1.95	.572E-02
73	240.00	0.00	2.00	.86	1.49	.435E-02
74	240.00	0.00	4.00	.52	.92	.265E-02
75	240.00	0.00	8.00	.14	.25	.718E-03
76	240.00	-30.00	0.00	.12	.20	.583E-03
77	240.00	-60.00	0.00	0.00	0.00	.000E+00
78	240.00	-90.00	0.00	0.00	0.00	.000E+00
79	240.00	-120.00	0.00	0.00	0.00	.000E+00
80	350.00	-30.00	0.00	.01	.02	.639E-04
81	350.00	0.00	0.00	.34	.59	.170E-02
82	350.00	30.00	0.00	.77	1.34	.391E-02

RUN NUMBER 23
OPERATOR --SPARKS-- DAY 74 YEAR 1983
FILE NAME GRI23
FLOW RATE (CCS) 130.0
WIND SPEED (CM/S) 24.70
REF. WIND HEIGHT (CM) 2.0
AIR TEMP. (C) 21.0
SOURCE GAS TEMP. (C) -78.
TRACER CONC (PPM) 9500.0
BACKGROUND CONC. (PPM) 3.53

TUBE NO.	X (CM)	Y (CM)	Z (CM)	MODEL CONCENTRATION (%)	FIELD CONCENTRATION (%)	DIMENSIONLESS CONCENTRATION
30	30.00	50.00	0.00	0.00	0.00	.000E+00
31	30.00	40.00	0.00	.08	.15	.423E-03
32	30.00	30.00	0.00	15.30	24.09	.911E-01
33	30.00	20.00	0.00	20.93	31.74	.133E+00
34	30.00	10.00	0.00	24.44	36.23	.163E+00
35	30.00	0.00	0.00	24.17	35.89	.161E+00
38	45.00	0.00	0.00	17.24	26.79	.105E+00
39	30.00	-10.00	0.00	19.61	29.99	.123E+00
40	30.00	-20.00	0.00	11.91	19.20	.682E-01
41	30.00	-30.00	0.00	2.11	3.64	.109E-01
42	30.00	-40.00	0.00	0.00	0.00	.000E+00
43	30.00	-50.00	0.00	0.00	0.00	.000E+00
44	60.00	-70.00	0.00	.00	.01	.147E-04
45	60.00	-60.00	0.00	.00	.00	.725E-05
46	60.00	-50.00	0.00	0.00	0.00	.000E+00
47	60.00	-40.00	0.00	.04	.07	.189E-03
48	60.00	-30.00	0.00	3.53	6.05	.185E-01
49	60.00	-20.00	0.00	6.93	11.57	.375E-01
50	60.00	-10.00	0.00	10.53	17.13	.593E-01
51	60.00	0.00	0.00	13.16	21.03	.764E-01
55	60.00	10.00	0.00	14.18	22.50	.833E-01
56	120.00	-15.00	0.00	4.47	7.59	.236E-01
57	120.00	0.00	0.00	6.19	10.39	.333E-01
60	140.00	0.00	0.00	5.00	8.47	.265E-01
61	120.00	15.00	0.00	6.80	11.36	.368E-01
62	120.00	30.00	0.00	6.18	10.38	.332E-01
63	120.00	45.00	0.00	3.38	5.78	.176E-01
64	120.00	60.00	0.00	.08	.13	.381E-03
65	120.00	75.00	0.00	0.00	0.00	.000E+00
66	120.00	90.00	0.00	.01	.01	.320E-04
67	120.00	105.00	0.00	0.00	0.00	.000E+00
68	240.00	120.00	0.00	0.00	0.00	.000E+00
69	240.00	90.00	0.00	0.00	0.00	.000E+00
70	240.00	60.00	0.00	.87	1.53	.445E-02
71	240.00	30.00	0.00	2.69	4.63	.139E-01
72	240.00	0.00	0.00	2.23	3.84	.115E-01
73	240.00	0.00	2.00	1.74	3.01	.892E-02
74	240.00	0.00	4.00	.17	.29	.841E-03
75	240.00	0.00	8.00	.24	.43	.124E-02
76	240.00	-30.00	0.00	.59	1.03	.299E-02
77	240.00	-60.00	0.00	0.00	0.00	.000E+00
78	240.00	-90.00	0.00	0.00	0.00	.000E+00
79	240.00	-120.00	0.00	.00	.00	.777E-05
80	350.00	-30.00	0.00	.08	.15	.425E-03
81	350.00	0.00	0.00	.93	1.62	.473E-02
82	350.00	30.00	0.00	1.42	2.47	.726E-02

RUN NUMBER 24
OPERATOR --SPARKS-- DAY 74 YEAR 1983
FILE NAME GRI24
FLOW RATE (CCS) 130.0
WIND SPEED (CM/S) 24.70
REF. WIND HEIGHT (CM) 2.0
AIR TEMP. (C) 21.0
SOURCE GAS TEMP. (C) -78.
TRACER CONC. (PPM) 9500.0
BACKGROUND CONC. (PPM) 3.74

TUBE NO.	X (CM)	Y (CM)	Z (CM)	MODEL CONCENTRATION (%)	FIELD CONCENTRATION (%)	DIMENSIONLESS CONCENTRATION
2	-35.00	0.00	0.00	0.00	0.00	.000E+00
3	-30.00	0.00	0.00	0.00	0.00	.000E+00
4	-25.00	0.00	0.00	.01	.01	.413E-04
5	-20.00	0.00	0.00	.01	.03	.755E-04
6	-15.00	0.00	0.00	9.07	14.92	.503E-01
17	0.00	-35.00	0.00	.01	.02	.636E-04
18	0.00	-40.00	0.00	0.00	0.00	.000E+00
19	15.00	-5.00	0.00	43.71	57.70	.391E+00
20	15.00	0.00	0.00	46.58	60.51	.440E+00
21	15.00	5.00	0.00	47.79	61.66	.461E+00
22	15.00	10.00	0.00	43.17	57.16	.383E+00
23	15.00	15.00	0.00	36.81	50.58	.294E+00
24	15.00	20.00	0.00	27.40	39.87	.190E+00
25	15.00	25.00	0.00	21.84	32.92	.141E+00
26	15.00	30.00	0.00	12.13	19.52	.696E-01
27	15.00	35.00	0.00	.18	.32	.918E-03
28	15.00	40.00	0.00	.00	.00	.397E-05
29	15.00	45.00	0.00	0.00	0.00	.000E+00
35	30.00	0.00	0.00	24.39	36.17	.163E+00
39	30.00	-10.00	0.00	20.44	31.10	.130E+00
40	30.00	-20.00	0.00	12.98	20.77	.752E-01
41	30.00	-30.00	0.00	1.75	3.03	.897E-02
42	30.00	-40.00	0.00	0.00	0.00	.000E+00
43	30.00	-50.00	0.00	0.00	0.00	.000E+00
56	120.00	-15.00	0.00	4.68	7.94	.248E-01
57	120.00	0.00	0.00	6.29	10.56	.339E-01
61	120.00	15.00	0.00	6.86	11.46	.371E-01
62	120.00	30.00	0.00	6.27	10.52	.337E-01
63	120.00	45.00	0.00	3.49	5.98	.182E-01
64	120.00	60.00	0.00	.08	.13	.379E-03
65	120.00	75.00	0.00	0.00	0.00	.000E+00
66	120.00	90.00	0.00	0.00	0.00	.000E+00
67	120.00	105.00	0.00	0.00	0.00	.000E+00
68	240.00	120.00	0.00	0.00	0.00	.000E+00
69	240.00	90.00	0.00	0.00	0.00	.000E+00
70	240.00	60.00	0.00	.94	1.64	.478E-02
71	240.00	30.00	0.00	2.84	4.88	.147E-01
91	120.00	0.00	.50	6.11	10.26	.328E-01
92	120.00	0.00	1.00	5.47	9.23	.292E-01
93	120.00	0.00	1.50	4.55	7.72	.240E-01
94	120.00	0.00	2.00	3.38	5.79	.176E-01
95	120.00	0.00	2.50	2.50	4.30	.129E-01
96	120.00	0.00	3.00	1.82	3.15	.932E-02
97	120.00	0.00	4.00	.64	1.12	.324E-02
98	120.00	0.00	5.00	.24	.42	.122E-02
99	120.00	0.00	6.00	.10	.18	.509E-03
100	120.00	0.00	8.00	.04	.07	.190E-03

RUN NUMBER 25
OPERATOR --SPARKS-- DAY 75 YEAR 1983
FILE NAME GRI25
FLOW RATE (CCS) 130.0
WIND SPEED (CM/S) 24.70
REF. WIND HEIGHT (CM) 2.0
AIR TEMP. (C) 22.4
SOURCE GAS TEMP. (C) -78.
TRACER CONC. (PPM) 9550.0
BACKGROUND CONC. (PPM) 3.57

TUBE NO.	X (CM)	Y (CM)	Z (CM)	MODEL CONCENTRATION (%)	FIELD CONCENTRATION (%)	DIMENSIONLESS CONCENTRATION
2	-35.00	0.00	0.00	0.00	0.00	.000E+00
3	-30.00	0.00	0.00	0.00	0.00	.000E+00
4	-25.00	0.00	0.00	0.00	0.00	.000E+00
5	-20.00	0.00	0.00	.00	.00	.581E-05
6	-15.00	0.00	0.00	18.62	28.67	.115E+00
7	0.00	15.00	0.00	44.11	58.09	.396E+00
8	0.00	20.00	0.00	27.74	40.27	.193E+00
9	0.00	25.00	0.00	11.56	18.68	.656E-01
10	0.00	30.00	0.00	.25	.43	.124E-02
11	0.00	35.00	0.00	.03	.05	.156E-03
12	0.00	40.00	0.00	.06	.10	.281E-03
13	0.00	-15.00	0.00	31.20	44.35	.228E+00
14	0.00	-20.00	0.00	14.75	23.31	.868E-01
15	0.00	-25.00	0.00	.80	1.40	.405E-02
16	0.00	-30.00	0.00	.01	.01	.290E-04
27	15.00	35.00	0.00	1.72	2.98	.877E-02
28	15.00	40.00	0.00	.03	.06	.165E-03
29	15.00	45.00	0.00	0.00	0.00	.000E+00
35	30.00	0.00	0.00	23.86	35.50	.157E+00
39	30.00	-10.00	0.00	21.53	32.53	.138E+00
40	30.00	-20.00	0.00	14.67	23.19	.862E-01
41	30.00	-30.00	0.00	8.52	14.06	.467E-01
42	30.00	-40.00	0.00	.06	.11	.319E-03
43	30.00	-50.00	0.00	0.00	0.00	.000E+00
44	60.00	-70.00	0.00	.00	.01	.188E-04
45	60.00	-60.00	0.00	.00	.00	.126E-04
46	60.00	-50.00	0.00	.02	.03	.833E-04
47	60.00	-40.00	0.00	2.37	4.09	.122E-01
48	60.00	-30.00	0.00	6.27	10.51	.335E-01
49	60.00	-20.00	0.00	9.24	15.18	.511E-01
50	60.00	-10.00	0.00	11.82	19.07	.673E-01
51	60.00	0.00	0.00	12.24	19.68	.700E-01
55	60.00	10.00	0.00	12.68	20.33	.729E-01
68	240.00	120.00	0.00	0.00	0.00	.000E+00
69	240.00	90.00	0.00	0.00	0.00	.000E+00
70	240.00	60.00	0.00	1.09	1.91	.555E-02
71	240.00	30.00	0.00	1.77	3.07	.903E-02
91	60.00	0.00	.50	11.99	19.32	.684E-01
92	60.00	0.00	1.00	9.98	16.29	.556E-01
93	60.00	0.00	1.50	7.20	11.99	.389E-01
94	60.00	0.00	2.00	3.97	6.77	.207E-01
95	60.00	0.00	2.50	2.13	3.69	.109E-01
96	60.00	0.00	3.00	1.24	2.15	.628E-02
97	60.00	0.00	4.00	.22	.39	.112E-02
98	60.00	0.00	5.00	.06	.10	.289E-03
99	60.00	0.00	6.00	.02	.04	.116E-03
100	60.00	0.00	8.00	.00	.01	.249E-04

RUN NUMBER 26
OPERATOR --SPARKS-- DAY 75 YEAR 1983
FILE NAME GR126
FLOW RATE (CCS) 130.0
WIND SPEED (CM/S) 24.70
REF. WIND HEIGHT (CM) 2.0
AIR TEMP. (C) 22.4
SOURCE GAS TEMP. (C) -78.
TRACER CONC. (PPM) 9550.0
BACKGROUND CONC. (PPM) 3.57

TUBE NO.	X (CM)	Y (CM)	Z (CM)	MODEL CONCENTRATION (%)	FIELD CONCENTRATION (%)	DIMENSIONLESS CONCENTRATION
7	0.00	15.00	0.00	48.11	61.96	.465E+00
8	0.00	20.00	0.00	33.19	46.60	.249E+00
9	0.00	25.00	0.00	11.08	17.96	.625E-01
10	0.00	30.00	0.00	.05	.09	.258E-03
11	0.00	35.00	0.00	.01	.02	.567E-04
12	0.00	40.00	0.00	.06	.10	.278E-03
13	0.00	-15.00	0.00	29.52	42.39	.210E+00
14	0.00	-20.00	0.00	14.92	23.55	.879E-01
15	0.00	-25.00	0.00	.38	.67	.193E-02
16	0.00	-30.00	0.00	.00	.00	.121E-04
17	0.00	-35.00	0.00	.00	.00	.111E-04
18	0.00	-40.00	0.00	0.00	0.00	.000E+00
20	15.00	0.00	0.00	45.60	59.56	.421E+00
21	15.00	5.00	0.00	47.08	60.99	.446E+00
22	15.00	10.00	0.00	43.77	57.76	.390E+00
23	15.00	15.00	0.00	37.86	51.70	.306E+00
24	15.00	20.00	0.00	29.55	42.43	.210E+00
25	15.00	25.00	0.00	23.53	35.09	.154E+00
26	15.00	30.00	0.00	13.73	21.86	.799E-01
27	15.00	35.00	0.00	.41	.71	.205E-02
28	15.00	40.00	0.00	.01	.01	.301E-04
29	15.00	45.00	0.00	0.00	0.00	.000E+00
30	30.00	50.00	0.00	0.00	0.00	.000E+00
31	30.00	40.00	0.00	.44	.77	.220E-02
32	30.00	30.00	0.00	15.22	23.98	.901E-01
33	30.00	20.00	0.00	20.59	31.29	.130E+00
34	30.00	10.00	0.00	23.92	35.58	.158E+00
35	30.00	0.00	0.00	22.33	33.56	.144E+00
39	30.00	-10.00	0.00	20.31	30.93	.128E+00
40	30.00	-20.00	0.00	13.69	21.79	.796E-01
41	30.00	-30.00	0.00	6.18	10.37	.330E-01
42	30.00	-40.00	0.00	.00	.00	.359E-05
43	30.00	-50.00	0.00	0.00	0.00	.000E+00
68	240.00	120.00	0.00	0.00	0.00	.000E+00
69	240.00	90.00	0.00	0.00	0.00	.000E+00
70	240.00	60.00	0.00	.43	.76	.218E-02
71	240.00	30.00	0.00	1.87	3.24	.955E-02
91	30.00	0.00	.50	20.95	31.77	.133E+00
92	30.00	0.00	1.00	13.68	21.78	.795E-01
93	30.00	0.00	1.50	6.75	11.28	.363E-01
94	30.00	0.00	2.00	2.46	4.24	.126E-01
95	30.00	0.00	2.50	1.04	1.81	.527E-02
96	30.00	0.00	3.00	.57	1.00	.289E-02
97	30.00	0.00	4.00	.13	.22	.632E-03
98	30.00	0.00	5.00	.04	.08	.222E-03
99	30.00	0.00	6.00	.02	.03	.905E-04
100	30.00	0.00	8.00	.01	.01	.403E-04

RUN NUMBER 27
OPERATOR --SPARKS-- DAY 75 YEAR 1983
FILE NAME GRI27
FLOW RATE (CCS) 223.0
WIND SPEED (CM/S) 42.30
REF. WIND HEIGHT (CM) 2.0
AIR TEMP. (C) 22.4
SOURCE GAS TEMP. (C) -152
TRACER CONC. (PPM) 9550.0
BACKGROUND CONC. (PPM) 3.90

TUBE NO.	X (CM)	Y (CM)	Z (CM)	MODEL CONCENTRATION (%)	FIELD CONCENTRATION (%)	DIMENSIONLESS CONCENTRATION
7	0.00	15.00	0.00	67.97	69.82	.660E+00
8	0.00	20.00	0.00	50.59	52.74	.318E+00
9	0.00	25.00	0.00	43.64	45.77	.241E+00
10	0.00	30.00	0.00	20.42	21.86	.798E-01
11	0.00	35.00	0.00	.37	.41	.117E-02
12	0.00	40.00	0.00	.11	.12	.329E-03
13	0.00	-15.00	0.00	67.79	69.65	.654E+00
14	0.00	-20.00	0.00	48.04	50.19	.287E+00
15	0.00	-25.00	0.00	.77	.84	.241E-02
16	0.00	-30.00	0.00	.20	.21	.610E-03
17	0.00	-35.00	0.00	.01	.01	.170E-04
18	0.00	-40.00	0.00	.00	.00	.212E-05
20	15.00	0.00	0.00	69.54	71.34	.710E+00
21	15.00	5.00	0.00	61.92	63.93	.505E+00
22	15.00	10.00	0.00	64.22	66.18	.558E+00
23	15.00	15.00	0.00	62.25	64.26	.513E+00
24	15.00	20.00	0.00	52.54	54.68	.344E+00
25	15.00	25.00	0.00	40.58	42.67	.212E+00
26	15.00	30.00	0.00	31.82	33.72	.145E+00
27	15.00	35.00	0.00	24.34	25.96	.100E+00
28	15.00	40.00	0.00	2.33	2.54	.742E-02
29	15.00	45.00	0.00	.01	.01	.383E-04
30	30.00	50.00	0.00	.02	.02	.547E-04
31	30.00	40.00	0.00	15.95	17.14	.590E-01
32	30.00	30.00	0.00	25.84	27.52	.108E+00
33	30.00	20.00	0.00	36.51	38.53	.179E+00
34	30.00	10.00	0.00	35.63	37.63	.172E+00
35	30.00	0.00	0.00	33.70	35.65	.158E+00
39	30.00	-10.00	0.00	36.13	38.14	.176E+00
40	30.00	-20.00	0.00	31.00	32.87	.140E+00
41	30.00	-30.00	0.00	20.20	21.62	.787E-01
42	30.00	-40.00	0.00	.91	.99	.285E-02
43	30.00	-50.00	0.00	0.00	0.00	.000E+00
68	240.00	120.00	0.00	0.00	0.00	.000E+00
69	240.00	90.00	0.00	.02	.02	.587E-04
70	240.00	60.00	0.00	1.97	2.15	.626E-02
71	240.00	30.00	0.00	3.69	4.01	.119E-01
91	30.00	0.00	.50	28.58	30.38	.124E+00
92	30.00	0.00	1.00	11.99	12.93	.424E-01
93	30.00	0.00	1.50	3.66	3.98	.118E-01
94	30.00	0.00	2.00	1.12	1.22	.352E-02
95	30.00	0.00	2.50	.55	.60	.172E-02
96	30.00	0.00	3.00	.36	.40	.113E-02
97	30.00	0.00	4.00	.14	.16	.447E-03
98	30.00	0.00	5.00	.07	.08	.218E-03
99	30.00	0.00	6.00	.03	.03	.893E-04
100	30.00	0.00	8.00	.01	.01	.277E-04

RUN NUMBER 28
OPERATOR --SPARKS-- DAY 75 YEAR 1983
FILE NAME GRI28
FLOW RATE (CCS) 223.0
WIND SPEED (CM/S) 42.30
REF. WIND HEIGHT (CM) 2.0
AIR TEMP. (C) 22.4
SOURCE GAS TEMP. (C) -152
TRACER CONC. (PPM) 9550.0
BACKGROUND CONC. (PPM) 4.26

TUBE NO.	X (CM)	Y (CM)	Z (CM)	MODEL CONCENTRATION (%)	FIELD CONCENTRATION (%)	DIMENSIONLESS CONCENTRATION
2	-35.00	0.00	0.00	0.00	0.00	.000E+00
3	-30.00	0.00	0.00	.02	.03	.731E-04
4	-25.00	0.00	0.00	.04	.05	.137E-03
5	-20.00	0.00	0.00	.52	.57	.162E-02
6	-15.00	0.00	0.00	51.00	53.15	.323E+00
7	0.00	15.00	0.00	69.54	71.34	.710E+00
8	0.00	20.00	0.00	53.26	55.40	.354E+00
9	0.00	25.00	0.00	40.24	42.33	.209E+00
10	0.00	30.00	0.00	3.76	4.09	.122E-01
11	0.00	35.00	0.00	.01	.02	.451E-04
12	0.00	40.00	0.00	.09	.10	.280E-03
13	0.00	-15.00	0.00	74.62	76.21	.914E+00
14	0.00	-20.00	0.00	55.48	57.60	.387E+00
15	0.00	-25.00	0.00	36.21	38.22	.176E+00
16	0.00	-30.00	0.00	1.11	1.20	.347E-02
27	15.00	35.00	0.00	16.75	17.99	.625E-01
28	15.00	40.00	0.00	.16	.18	.510E-03
29	15.00	45.00	0.00	.00	.00	.747E-06
35	30.00	0.00	0.00	34.59	36.56	.164E+00
39	30.00	-10.00	0.00	35.15	37.14	.168E+00
40	30.00	-20.00	0.00	31.21	33.10	.141E+00
41	30.00	-30.00	0.00	20.26	21.69	.790E-01
42	30.00	-40.00	0.00	4.71	5.11	.153E-01
43	30.00	-50.00	0.00	0.00	0.00	.000E+00
44	60.00	-70.00	0.00	.01	.01	.204E-04
45	60.00	-60.00	0.00	0.00	0.00	.000E+00
46	60.00	-50.00	0.00	.35	.38	.110E-02
47	60.00	-40.00	0.00	7.91	8.56	.267E-01
48	60.00	-30.00	0.00	14.18	15.26	.513E-01
49	60.00	-20.00	0.00	18.93	20.29	.726E-01
50	60.00	-10.00	0.00	20.10	21.53	.782E-01
51	60.00	0.00	0.00	20.34	21.77	.794E-01
55	60.00	10.00	0.00	20.74	22.19	.813E-01
68	240.00	120.00	0.00	.01	.01	.225E-04
69	240.00	90.00	0.00	0.00	0.00	.000E+00
70	240.00	60.00	0.00	1.46	1.59	.461E-02
71	240.00	30.00	0.00	3.77	4.10	.122E-01
91	60.00	0.00	.50	18.99	20.36	.729E-01
92	60.00	0.00	1.00	13.94	15.01	.503E-01
93	60.00	0.00	1.50	7.91	8.57	.267E-01
94	60.00	0.00	2.00	3.26	3.55	.105E-01
95	60.00	0.00	2.50	1.52	1.66	.481E-02
96	60.00	0.00	3.00	.86	.93	.268E-02
97	60.00	0.00	4.00	.24	.26	.745E-03
98	60.00	0.00	5.00	.09	.10	.292E-03
99	60.00	0.00	6.00	.04	.04	.120E-03
100	60.00	0.00	8.00	.01	.01	.390E-04

RUN NUMBER 29
OPERATOR --NEFF -- DAY 75 YEAR 1983
FILE NAME GR129
FLOW RATE (CCS) 223.0
WIND SPEED (CM/S) 42.30
REF. WIND HEIGHT (CM) 2.0
AIR TEMP. (C) 22.4
SOURCE GAS TEMP. (C) -152
TRACER CONC. (PPM) 9550.0
BACKGROUND CONC. (PPM) 4.32

TUBE NO.	X (CM)	Y (CM)	Z (CM)	MODEL CONCENTRATION (%)	FIELD CONCENTRATION (%)	DIMENSIONLESS CONCENTRATION
2	-35.00	0.00	0.00	0.00	0.00	.000E+00
3	-30.00	0.00	0.00	0.00	0.00	.000E+00
4	-25.00	0.00	0.00	.01	.01	.183E-04
5	-20.00	0.00	0.00	1.66	1.81	.525E-02
6	-15.00	0.00	0.00	33.36	35.31	.156E+00
17	0.00	-35.00	0.00	.09	.10	.290E-03
18	0.00	-40.00	0.00	.06	.06	.181E-03
19	15.00	-5.00	0.00	55.94	58.06	.395E+00
20	15.00	0.00	0.00	64.49	66.44	.564E+00
21	15.00	5.00	0.00	61.56	63.58	.498E+00
22	15.00	10.00	0.00	55.46	57.58	.387E+00
23	15.00	15.00	0.00	57.27	59.37	.417E+00
24	15.00	20.00	0.00	49.57	51.73	.306E+00
25	15.00	25.00	0.00	39.78	41.86	.205E+00
26	15.00	30.00	0.00	32.94	34.88	.153E+00
27	15.00	35.00	0.00	24.81	26.45	.103E+00
28	15.00	40.00	0.00	1.34	1.46	.422E-02
29	15.00	45.00	0.00	.00	.00	.149E-05
35	30.00	0.00	0.00	33.84	35.80	.159E+00
39	30.00	-10.00	0.00	33.11	35.04	.154E+00
40	30.00	-20.00	0.00	29.92	31.76	.133E+00
41	30.00	-30.00	0.00	20.32	21.76	.793E-01
42	30.00	-40.00	0.00	7.30	7.90	.245E-01
43	30.00	-50.00	0.00	0.00	0.00	.000E+00
56	120.00	-15.00	0.00	9.73	10.51	.335E-01
57	120.00	0.00	0.00	9.82	10.61	.338E-01
61	120.00	15.00	0.00	10.26	11.08	.355E-01
62	120.00	30.00	0.00	9.51	10.28	.327E-01
63	120.00	45.00	0.00	5.02	5.45	.164E-01
64	120.00	60.00	0.00	.54	.59	.168E-02
65	120.00	75.00	0.00	.05	.06	.169E-03
66	120.00	90.00	0.00	.07	.08	.223E-03
67	120.00	105.00	0.00	.04	.04	.127E-03
68	240.00	120.00	0.00	0.00	0.00	.000E+00
69	240.00	90.00	0.00	0.00	0.00	.000E+00
70	240.00	60.00	0.00	1.26	1.38	.398E-02
71	240.00	30.00	0.00	3.96	4.30	.128E-01
91	120.00	0.00	.50	9.39	10.15	.322E-01
92	120.00	0.00	1.00	8.06	8.72	.272E-01
93	120.00	0.00	1.50	6.42	6.96	.213E-01
94	120.00	0.00	2.00	4.51	4.90	.147E-01
95	120.00	0.00	2.50	3.19	3.47	.102E-01
96	120.00	0.00	3.00	2.27	2.47	.721E-02
97	120.00	0.00	4.00	.65	.71	.203E-02
98	120.00	0.00	5.00	.21	.23	.651E-03
99	120.00	0.00	6.00	.09	.10	.289E-03
100	120.00	0.00	8.00	.05	.06	.170E-03

RUN NUMBER 30
OPERATOR --SPARKS-- DAY 77 YEAR 1983
FILE NAME GRI30
FLOW RATE (CCS) 223.0
WIND SPEED (CM/S) 42.30
REF. WIND HEIGHT (CM) 2.0
AIR TEMP. (C) 21.0
SOURCE GAS TEMP. (C) -152
TRACER CONC. (PPM) 9550.0
BACKGROUND CONC. (PPM) 3.77

TUBE NO.	X (CM)	Y (CM)	Z (CM)	MODEL CONCENTRATION (%)	FIELD CONCENTRATION (%)	DIMENSIONLESS CONCENTRATION
30	30.00	50.00	0.00	0.00	0.00	.000E+00
31	30.00	40.00	0.00	5.74	6.23	.190E-01
32	30.00	30.00	0.00	21.29	22.77	.845E-01
33	30.00	20.00	0.00	32.79	34.72	.152E+00
34	30.00	10.00	0.00	31.83	33.73	.146E+00
35	30.00	0.00	0.00	34.37	36.34	.164E+00
38	45.00	0.00	0.00	26.26	27.97	.111E+00
39	30.00	-10.00	0.00	37.99	40.05	.191E+00
40	30.00	-20.00	0.00	33.82	35.77	.160E+00
41	30.00	-30.00	0.00	21.51	23.01	.856E-01
42	30.00	-40.00	0.00	1.16	1.26	.366E-02
43	30.00	-50.00	0.00	0.00	0.00	.000E+00
44	60.00	-70.00	0.00	.00	.01	.151E-04
45	60.00	-60.00	0.00	.00	.00	.247E-05
46	60.00	-50.00	0.00	.02	.03	.735E-04
47	60.00	-40.00	0.00	6.28	6.81	.209E-01
48	60.00	-30.00	0.00	14.62	15.73	.535E-01
49	60.00	-20.00	0.00	20.12	21.54	.786E-01
50	60.00	-10.00	0.00	20.84	22.30	.822E-01
51	60.00	0.00	0.00	21.26	22.73	.843E-01
55	60.00	10.00	0.00	19.13	20.50	.739E-01
56	120.00	-15.00	0.00	9.82	10.61	.340E-01
57	120.00	0.00	0.00	10.12	10.94	.352E-01
60	140.00	0.00	0.00	8.07	8.73	.274E-01
61	120.00	15.00	0.00	9.43	10.19	.325E-01
62	120.00	30.00	0.00	8.48	9.18	.290E-01
63	120.00	45.00	0.00	4.54	4.93	.148E-01
64	120.00	60.00	0.00	.21	.23	.651E-03
65	120.00	75.00	0.00	0.00	0.00	.000E+00
66	120.00	90.00	0.00	.00	.00	.343E-05
67	120.00	105.00	0.00	.00	.00	.150E-05
68	240.00	120.00	0.00	0.00	0.00	.000E+00
69	240.00	90.00	0.00	0.00	0.00	.000E+00
70	240.00	60.00	0.00	1.30	1.42	.412E-02
71	240.00	30.00	0.00	3.43	3.73	.111E-01
72	240.00	0.00	0.00	3.77	4.09	.122E-01
73	240.00	0.00	2.00	2.83	3.07	.909E-02
74	240.00	0.00	4.00	1.51	1.64	.477E-02
75	240.00	0.00	8.00	.19	.21	.593E-03
76	240.00	-30.00	0.00	.19	.21	.593E-03
77	240.00	-60.00	0.00	.35	.38	.111E-02
78	240.00	-90.00	0.00	0.00	0.00	.000E+00
79	240.00	-120.00	0.00	0.00	0.00	.000E+00
80	350.00	-30.00	0.00	2.12	2.30	.676E-02
81	350.00	0.00	0.00	2.03	2.21	.646E-02
82	350.00	30.00	0.00	1.90	2.07	.606E-02

RUN NUMBER 31
OPERATOR --SPARKS-- DAY 77 YEAR 1983
FILE NAME GRI31
FLOW RATE (CCS) 223.0
WIND SPEED (CM/S) 42.30
REF. WIND HEIGHT (CM) 2.0
AIR TEMP. (C) 21.0
SOURCE GAS TEMP. (C) -78.
TRACER CONC. (PPM) 5920.0
BACKGROUND CONC. (PPM) 4.01

TUBE NO.	X (CM)	Y (CM)	Z (CM)	MODEL CONCENTRATION (%)	FIELD CONCENTRATION (%)	DIMENSIONLESS CONCENTRATION
30	30.00	50.00	0.00	.34	.60	.172E-02
31	30.00	40.00	0.00	11.17	18.09	.633E-01
32	30.00	30.00	0.00	18.82	28.95	.117E+00
33	30.00	20.00	0.00	28.83	41.57	.204E+00
34	30.00	10.00	0.00	30.11	43.08	.217E+00
35	30.00	0.00	0.00	32.08	45.35	.238E+00
38	45.00	0.00	0.00	24.95	36.87	.167E+00
39	30.00	-10.00	0.00	34.08	47.59	.260E+00
40	30.00	-20.00	0.00	26.50	38.78	.181E+00
41	30.00	-30.00	0.00	14.79	23.37	.874E-01
42	30.00	-40.00	0.00	4.13	7.04	.217E-01
43	30.00	-50.00	0.00	0.00	0.00	.000E+00
44	60.00	-70.00	0.00	.00	.01	.151E-04
45	60.00	-60.00	0.00	.00	.00	.279E-06
46	60.00	-50.00	0.00	.61	1.06	.308E-02
47	60.00	-40.00	0.00	5.50	9.28	.293E-01
48	60.00	-30.00	0.00	10.89	17.67	.615E-01
49	60.00	-20.00	0.00	16.56	25.85	.998E-01
50	60.00	-10.00	0.00	19.30	29.58	.120E+00
51	60.00	0.00	0.00	20.39	31.03	.129E+00
55	60.00	10.00	0.00	18.79	28.90	.116E+00
56	120.00	-15.00	0.00	10.49	17.08	.590E-01
57	120.00	0.00	0.00	11.37	18.40	.646E-01
60	140.00	0.00	0.00	9.73	15.92	.542E-01
61	120.00	15.00	0.00	10.46	17.02	.588E-01
62	120.00	30.00	0.00	8.62	14.22	.475E-01
63	120.00	45.00	0.00	5.36	9.05	.285E-01
64	120.00	60.00	0.00	1.96	3.39	.100E-01
65	120.00	75.00	0.00	.06	.11	.320E-03
66	120.00	90.00	0.00	0.00	0.00	.000E+00
67	120.00	105.00	0.00	0.00	0.00	.000E+00
68	240.00	120.00	0.00	0.00	0.00	.000E+00
69	240.00	90.00	0.00	.13	.24	.675E-03
70	240.00	60.00	0.00	2.62	4.51	.135E-01
71	240.00	30.00	0.00	4.99	8.44	.264E-01
72	240.00	0.00	0.00	5.76	9.69	.307E-01
73	240.00	0.00	2.00	3.20	5.49	.166E-01
74	240.00	0.00	4.00	.12	.22	.619E-03
75	240.00	0.00	8.00	.09	.15	.444E-03
76	240.00	-30.00	0.00	4.61	7.83	.243E-01
77	240.00	-60.00	0.00	.81	1.41	.411E-02
78	240.00	-90.00	0.00	0.00	0.00	.000E+00
79	240.00	-120.00	0.00	0.00	0.00	.000E+00
80	350.00	-30.00	0.00	3.13	5.37	.163E-01
81	350.00	0.00	0.00	3.37	5.77	.175E-01
82	350.00	30.00	0.00	3.53	6.04	.184E-01

RUN NUMBER 32
OPERATOR --SPARKS-- DAY 77 YEAR 1983
FILE NAME GRI32
FLOW RATE (CCS) 223.0
WIND SPEED (CM/S) 42.30
REF. WIND HEIGHT (CM) 2.0
AIR TEMP. (C) 21.0
SOURCE GAS TEMP. (C) -78.
TRACER CONC. (PPM) 5920.0
BACKGROUND CONC. (PPM) 4.59

TUBE NO.	X (CM)	Y (CM)	Z (CM)	MODEL CONCENTRATION (%)	FIELD CONCENTRATION (%)	DIMENSIONLESS CONCENTRATION
2	-35.00	0.00	0.00	0.00	0.00	.000E+00
3	-30.00	0.00	0.00	0.00	0.00	.000E+00
4	-25.00	0.00	0.00	.01	.01	.415E-04
5	-20.00	0.00	0.00	.44	.77	.222E-02
6	-15.00	0.00	0.00	19.30	29.59	.120E+00
17	0.00	-35.00	0.00	.07	.13	.359E-03
18	0.00	-40.00	0.00	0.00	0.00	.000E+00
19	15.00	-5.00	0.00	58.37	71.13	.706E+00
20	15.00	0.00	0.00	63.81	75.59	.887E+00
21	15.00	5.00	0.00	58.05	70.85	.696E+00
22	15.00	10.00	0.00	52.26	65.79	.551E+00
23	15.00	15.00	0.00	49.52	63.28	.494E+00
24	15.00	20.00	0.00	38.82	52.72	.319E+00
25	15.00	25.00	0.00	28.93	41.69	.205E+00
26	15.00	30.00	0.00	22.19	33.38	.144E+00
27	15.00	35.00	0.00	11.14	18.04	.631E-01
28	15.00	40.00	0.00	1.67	2.90	.857E-02
29	15.00	45.00	0.00	.14	.24	.684E-03
35	30.00	0.00	0.00	32.92	46.30	.247E+00
39	30.00	-10.00	0.00	37.57	51.39	.303E+00
40	30.00	-20.00	0.00	30.89	43.99	.225E+00
41	30.00	-30.00	0.00	18.38	28.34	.113E+00
42	30.00	-40.00	0.00	7.04	11.74	.381E-01
43	30.00	-50.00	0.00	0.00	0.00	.000E+00
56	120.00	-15.00	0.00	11.61	18.74	.661E-01
57	120.00	0.00	0.00	11.50	18.58	.654E-01
61	120.00	15.00	0.00	10.84	17.60	.612E-01
62	120.00	30.00	0.00	8.68	14.31	.478E-01
63	120.00	45.00	0.00	5.23	8.84	.278E-01
64	120.00	60.00	0.00	5.23	8.84	.278E-01
65	120.00	75.00	0.00	.06	.11	.308E-03
66	120.00	90.00	0.00	0.00	0.00	.000E+00
67	120.00	105.00	0.00	0.00	0.00	.000E+00
68	240.00	120.00	0.00	0.00	0.00	.000E+00
69	240.00	90.00	0.00	.11	.19	.546E-03
70	240.00	60.00	0.00	2.39	4.12	.123E-01
71	240.00	30.00	0.00	4.89	8.28	.259E-01
91	120.00	0.00	.50	11.10	17.99	.628E-01
92	120.00	0.00	1.00	8.99	14.79	.497E-01
93	120.00	0.00	1.50	6.38	10.69	.343E-01
94	120.00	0.00	2.00	3.69	6.31	.193E-01
95	120.00	0.00	2.50	2.27	3.92	.117E-01
96	120.00	0.00	3.00	1.53	2.65	.780E-02
97	120.00	0.00	4.00	.55	.97	.281E-02
98	120.00	0.00	5.00	.22	.39	.111E-02
99	120.00	0.00	6.00	.11	.19	.552E-03
100	120.00	0.00	8.00	.06	.10	.279E-03

RUN NUMBER 33
OPERATOR --SPARKS-- DAY 77 YEAR 1983
FILE NAME GRI33
FLOW RATE (CCS) 223.0
WIND SPEED (CM/S) 42.30
REF. WIND HEIGHT (CM) 2.0
AIR TEMP. (C) 21.0
SOURCE GAS TEMP. (C) -78.
TRACER CONC. (PPM) 5920.0
BACKGROUND CONC. (PPM) 3.87

TUBE NO.	X (CM)	Y (CM)	Z (CM)	MODEL CONCENTRATION (%)	FIELD CONCENTRATION (%)	DIMENSIONLESS CONCENTRATION
2	-35.00	0.00	0.00	0.00	0.00	.000E+00
3	-30.00	0.00	0.00	.00	.00	.279E-06
4	-25.00	0.00	0.00	0.00	0.00	.000E+00
5	-20.00	0.00	0.00	.10	.18	.510E-03
6	-15.00	0.00	0.00	7.99	13.23	.437E-01
7	0.00	15.00	0.00	65.17	76.67	.942E+00
8	0.00	20.00	0.00	44.97	58.94	.411E+00
9	0.00	25.00	0.00	30.85	43.94	.224E+00
10	0.00	30.00	0.00	12.44	19.97	.715E-01
11	0.00	35.00	0.00	.68	1.19	.345E-02
12	0.00	40.00	0.00	.16	.29	.823E-03
13	0.00	-15.00	0.00	69.91	80.32	.117E+01
14	0.00	-20.00	0.00	45.59	59.54	.422E+00
15	0.00	-25.00	0.00	24.54	36.35	.164E+00
16	0.00	-30.00	0.00	1.47	2.56	.751E-02
27	15.00	35.00	0.00	16.05	25.15	.962E-01
28	15.00	40.00	0.00	5.59	9.42	.298E-01
29	15.00	45.00	0.00	.53	.93	.269E-02
35	30.00	0.00	0.00	34.47	48.02	.265E+00
39	30.00	-10.00	0.00	34.67	48.25	.267E+00
40	30.00	-20.00	0.00	26.27	38.49	.179E+00
41	30.00	-30.00	0.00	14.63	23.14	.862E-01
42	30.00	-40.00	0.00	2.49	4.30	.129E-01
43	30.00	-50.00	0.00	0.00	0.00	.000E+00
44	60.00	-70.00	0.00	.02	.03	.884E-04
45	60.00	-60.00	0.00	.01	.03	.722E-04
46	60.00	-50.00	0.00	.14	.25	.725E-03
47	60.00	-40.00	0.00	4.63	7.85	.244E-01
48	60.00	-30.00	0.00	9.90	16.19	.553E-01
49	60.00	-20.00	0.00	13.99	22.23	.819E-01
50	60.00	-10.00	0.00	20.06	30.59	.126E+00
51	60.00	0.00	0.00	20.50	31.17	.130E+00
55	60.00	10.00	0.00	20.29	30.90	.128E+00
68	240.00	120.00	0.00	0.00	0.00	.000E+00
69	240.00	90.00	0.00	.39	.68	.196E-02
70	240.00	60.00	0.00	3.37	5.78	.176E-01
71	240.00	30.00	0.00	5.52	9.30	.294E-01
91	60.00	0.00	.50	19.42	29.75	.121E+00
92	60.00	0.00	1.00	13.86	22.04	.810E-01
93	60.00	0.00	1.50	7.67	12.73	.418E-01
94	60.00	0.00	2.00	3.26	5.59	.170E-01
95	60.00	0.00	2.50	1.62	2.81	.829E-02
96	60.00	0.00	3.00	.94	1.64	.478E-02
97	60.00	0.00	4.00	.33	.57	.165E-02
98	60.00	0.00	5.00	.12	.21	.613E-03
99	60.00	0.00	6.00	.05	.09	.265E-03
100	60.00	0.00	8.00	.02	.03	.803E-04

RUN NUMBER 34
OPERATOR --SPARKS-- DAY 77 YEAR 1983
FILE NAME GRI34
FLOW RATE (CCS) 223.0
WIND SPEED (CM/S) 42.30
REF. WIND HEIGHT (CM) 2.0
AIR TEMP. (C) 21.0
SOURCE GAS TEMP. (C) -78.
TRACER CONC. (PPM) 5920.0
BACKGROUND CONC. (PPM) 3.60

TUBE NO.	X (CM)	Y (CM)	Z (CM)	MODEL CONCENTRATION (%)	FIELD CONCENTRATION (%)	DIMENSIONLESS CONCENTRATION
7	0.00	15.00	0.00	67.01	78.11	.102E+01
8	0.00	20.00	0.00	45.63	59.58	.422E+00
9	0.00	25.00	0.00	33.04	46.43	.248E+00
10	0.00	30.00	0.00	17.26	26.81	.105E+00
11	0.00	35.00	0.00	1.10	1.91	.559E-02
12	0.00	40.00	0.00	.13	.23	.661E-03
13	0.00	-15.00	0.00	62.04	74.17	.823E+00
14	0.00	-20.00	0.00	39.29	53.20	.326E+00
15	0.00	-25.00	0.00	17.23	26.78	.105E+00
16	0.00	-30.00	0.00	.38	.67	.193E-02
17	0.00	-35.00	0.00	.00	.01	.220E-04
18	0.00	-40.00	0.00	.01	.01	.323E-04
20	15.00	0.00	0.00	62.69	74.69	.845E+00
21	15.00	5.00	0.00	60.76	73.12	.779E+00
22	15.00	10.00	0.00	58.56	71.28	.711E+00
23	15.00	15.00	0.00	43.88	57.87	.394E+00
24	15.00	20.00	0.00	42.42	56.41	.371E+00
25	15.00	25.00	0.00	30.96	44.07	.226E+00
26	15.00	30.00	0.00	22.47	33.74	.146E+00
27	15.00	35.00	0.00	17.04	26.52	.103E+00
28	15.00	40.00	0.00	6.70	11.20	.361E-01
29	15.00	45.00	0.00	.39	.69	.199E-02
30	30.00	50.00	0.00	.91	1.59	.462E-02
31	30.00	40.00	0.00	11.77	18.99	.672E-01
32	30.00	30.00	0.00	21.15	32.03	.135E+00
33	30.00	20.00	0.00	31.64	44.85	.233E+00
34	30.00	10.00	0.00	18.92	29.07	.117E+00
35	30.00	0.00	0.00	31.59	44.78	.232E+00
39	30.00	-10.00	0.00	31.77	44.99	.234E+00
40	30.00	-20.00	0.00	26.00	38.16	.177E+00
41	30.00	-30.00	0.00	15.38	24.20	.915E-01
42	30.00	-40.00	0.00	3.27	5.60	.170E-01
43	30.00	-50.00	0.00	0.00	0.00	.000E+00
68	240.00	120.00	0.00	0.00	0.00	.000E+00
69	240.00	90.00	0.00	.40	.70	.201E-02
70	240.00	60.00	0.00	3.39	5.81	.177E-01
71	240.00	30.00	0.00	3.39	5.81	.177E-01
91	30.00	0.00	.50	27.64	40.16	.192E+00
92	30.00	0.00	1.00	12.69	20.33	.731E-01
93	30.00	0.00	1.50	3.83	6.53	.209E-01
94	30.00	0.00	2.00	1.08	1.89	.552E-02
95	30.00	0.00	2.50	.50	.87	.252E-02
96	30.00	0.00	3.00	.31	.55	.158E-02
97	30.00	0.00	4.00	.10	.17	.485E-03
98	30.00	0.00	5.00	.04	.07	.213E-03
99	30.00	0.00	6.00	.01	.02	.440E-04
100	30.00	0.00	8.00	.00	.00	.530E-05

RUN NUMBER 35
OPERATOR --NEFF -- DAY 80 YEAR 1983
FILE NAME GRI35
FLOW RATE (CCS) 130.0
WIND SPEED (CM/S) 24.70
REF. WIND HEIGHT (CM) 2.0
AIR TEMP. (C) 19.0
SOURCE GAS TEMP. (C) -152
TRACER CONC. (PPM) 333300.0
BACKGROUND CONC. (PPM) 46.10

TUBE NO.	X (CM)	Y (CM)	Z (CM)	MODEL CONCENTRATION (%)	FIELD CONCENTRATION (%)	DIMENSIONLESS CONCENTRATION
7	0.00	15.00	0.00	45.97	48.12	.268E+00
8	0.00	20.00	0.00	26.13	27.82	.111E+00
9	0.00	25.00	0.00	.19	.20	.589E-03
10	0.00	30.00	0.00	.01	.01	.182E-04
11	0.00	35.00	0.00	.00	.00	.842E-05
12	0.00	40.00	0.00	.05	.06	.164E-03
13	0.00	-15.00	0.00	39.37	41.45	.204E+00
14	0.00	-20.00	0.00	.45	.49	.143E-02
15	0.00	-25.00	0.00	.01	.01	.259E-04
16	0.00	-30.00	0.00	.00	.00	.133E-05
17	0.00	-35.00	0.00	.00	.00	.139E-05
18	0.00	-40.00	0.00	0.00	0.00	.000E+00
20	15.00	0.00	0.00	43.22	45.35	.240E+00
21	15.00	5.00	0.00	41.65	43.76	.225E+00
22	15.00	10.00	0.00	39.95	42.03	.209E+00
23	15.00	15.00	0.00	37.72	39.77	.191E+00
24	15.00	20.00	0.00	29.82	31.66	.134E+00
25	15.00	25.00	0.00	3.93	4.27	.129E-01
26	15.00	30.00	0.00	.12	.13	.366E-03
27	15.00	35.00	0.00	.01	.01	.184E-04
28	15.00	40.00	0.00	.00	.00	.888E-05
29	15.00	45.00	0.00	0.00	0.00	.000E+00
30	30.00	50.00	0.00	0.00	0.00	.000E+00
31	30.00	40.00	0.00	.00	.00	.223E-05
32	30.00	30.00	0.00	.86	.94	.274E-02
33	30.00	20.00	0.00	16.84	18.09	.638E-01
34	30.00	10.00	0.00	18.90	20.26	.734E-01
35	30.00	0.00	0.00	7.47	8.09	.254E-01
39	30.00	-10.00	0.00	14.38	15.47	.529E-01
40	30.00	-20.00	0.00	1.81	1.97	.580E-02
41	30.00	-30.00	0.00	.01	.01	.427E-04
42	30.00	-40.00	0.00	0.00	0.00	.000E+00
43	30.00	-50.00	0.00	0.00	0.00	.000E+00
68	240.00	120.00	0.00	0.00	0.00	.000E+00
69	240.00	90.00	0.00	0.00	0.00	.000E+00
70	240.00	60.00	0.00	.20	.22	.630E-03
71	240.00	30.00	0.00	.73	.80	.233E-02
91	30.00	0.00	.50	18.16	19.48	.699E-01
92	30.00	0.00	1.00	14.41	15.50	.530E-01
93	30.00	0.00	1.50	9.57	10.34	.333E-01
94	30.00	0.00	2.00	4.31	4.68	.142E-01
95	30.00	0.00	2.50	1.86	2.03	.598E-02
96	30.00	0.00	3.00	.81	.88	.257E-02
97	30.00	0.00	4.00	.13	.14	.396E-03
98	30.00	0.00	5.00	.04	.04	.126E-03
99	30.00	0.00	6.00	.01	.01	.386E-04
100	30.00	0.00	8.00	.00	.00	.121E-04

RUN NUMBER 36
OPERATOR --SPARKS-- DAY 80 YEAR 1983
FILE NAME GRI36
FLOW RATE (CCS) 130.0
WIND SPEED (CM/S) 24.70
REF. WIND HEIGHT (CM) 2.0
AIR TEMP. (C) 19.0
SOURCE GAS TEMP. (C) -152
TRACER CONC. (PPM) 500000.0
BACKGROUND CONC. (PPM) 62.30

TUBE NO.	X (CM)	Y (CM)	Z (CM)	MODEL CONCENTRATION (%)	FIELD CONCENTRATION (%)	DIMENSIONLESS CONCENTRATION
7	0.00	15.00	0.00	34.23	36.20	.164E+00
8	0.00	20.00	0.00	9.14	9.88	.317E-01
9	0.00	25.00	0.00	.01	.01	.403E-04
10	0.00	30.00	0.00	0.00	0.00	.000E+00
11	0.00	35.00	0.00	.00	.00	.137E-05
12	0.00	40.00	0.00	.04	.04	.116E-03
13	0.00	-15.00	0.00	35.02	37.01	.170E+00
14	0.00	-20.00	0.00	.30	.32	.934E-03
15	0.00	-25.00	0.00	.01	.01	.212E-04
16	0.00	-30.00	0.00	.00	.00	.161E-06
17	0.00	-35.00	0.00	.00	.00	.286E-05
18	0.00	-40.00	0.00	0.00	0.00	.000E+00
20	15.00	0.00	0.00	34.25	36.22	.164E+00
21	15.00	5.00	0.00	32.53	34.45	.152E+00
22	15.00	10.00	0.00	33.02	34.95	.155E+00
23	15.00	15.00	0.00	31.22	33.10	.143E+00
24	15.00	20.00	0.00	23.63	25.22	.974E-01
25	15.00	25.00	0.00	1.03	1.12	.327E-02
26	15.00	30.00	0.00	.01	.01	.367E-04
27	15.00	35.00	0.00	.00	.00	.580E-05
28	15.00	40.00	0.00	.00	.00	.221E-06
29	15.00	45.00	0.00	.00	.00	.543E-06
30	30.00	50.00	0.00	0.00	0.00	.000E+00
31	30.00	40.00	0.00	.01	.01	.179E-04
32	30.00	30.00	0.00	.18	.20	.575E-03
33	30.00	20.00	0.00	14.38	15.47	.529E-01
34	30.00	10.00	0.00	17.29	18.56	.658E-01
35	30.00	0.00	0.00	16.81	18.05	.636E-01
39	30.00	-10.00	0.00	15.55	16.71	.580E-01
40	30.00	-20.00	0.00	2.94	3.20	.955E-02
41	30.00	-30.00	0.00	.00	.00	.676E-05
42	30.00	-40.00	0.00	0.00	0.00	.000E+00
43	30.00	-50.00	0.00	0.00	0.00	.000E+00
68	240.00	120.00	0.00	0.00	0.00	.000E+00
69	240.00	90.00	0.00	0.00	0.00	.000E+00
70	240.00	60.00	0.00	.06	.06	.185E-03
71	240.00	30.00	0.00	.73	.79	.230E-02
91	30.00	0.00	.50	17.46	18.74	.666E-01
92	30.00	0.00	1.00	14.60	15.71	.538E-01
93	30.00	0.00	1.50	9.93	10.73	.347E-01
94	30.00	0.00	2.00	4.62	5.01	.152E-01
95	30.00	0.00	2.50	2.22	2.42	.716E-02
96	30.00	0.00	3.00	1.20	1.30	.382E-02
97	30.00	0.00	4.00	.31	.34	.986E-03
98	30.00	0.00	5.00	.14	.15	.439E-03
99	30.00	0.00	6.00	.07	.08	.217E-03
100	30.00	0.00	8.00	.02	.03	.753E-04

RUN NUMBER 37
OPERATOR --NEFF -- DAY 81 YEAR 1983
FILE NAME GRI37
FLOW RATE (CCS) 130.0
WIND SPEED (CM/S) 24.70
REF. WIND HEIGHT (CM) 2.0
AIR TEMP. (C) 19.0
SOURCE GAS TEMP. (C) -152
TRACER CONC. (PPM) 500000.0
BACKGROUND CONC. (PPM) 13.72

TUBE NO.	X (CM)	Y (CM)	Z (CM)	MODEL CONCENTRATION (%)	FIELD CONCENTRATION (%)	DIMENSIONLESS CONCENTRATION
2	-35.00	0.00	0.00	.00	.00	.762E-05
3	-30.00	0.00	0.00	.01	.01	.188E-04
4	-25.00	0.00	0.00	.00	.00	.132E-04
5	-20.00	0.00	0.00	.06	.06	.175E-03
6	-15.00	0.00	0.00	5.95	6.45	.199E-01
7	0.00	15.00	0.00	36.08	38.10	.178E+00
8	0.00	20.00	0.00	9.40	10.16	.327E-01
9	0.00	25.00	0.00	.02	.02	.493E-04
10	0.00	30.00	0.00	.00	.00	.143E-04
11	0.00	35.00	0.00	.00	.00	.134E-04
12	0.00	40.00	0.00	.06	.06	.184E-03
13	0.00	-15.00	0.00	33.94	35.90	.162E+00
14	0.00	-20.00	0.00	.68	.74	.215E-02
15	0.00	-25.00	0.00	.01	.01	.324E-04
16	0.00	-30.00	0.00	.01	.01	.166E-04
27	15.00	35.00	0.00	.01	.01	.236E-04
28	15.00	40.00	0.00	.01	.01	.215E-04
29	15.00	45.00	0.00	.00	.00	.977E-05
35	30.00	0.00	0.00	18.35	19.68	.708E-01
39	30.00	-10.00	0.00	16.64	17.87	.629E-01
40	30.00	-20.00	0.00	5.31	5.76	.177E-01
41	30.00	-30.00	0.00	.03	.03	.893E-04
42	30.00	-40.00	0.00	.00	.00	.143E-04
43	30.00	-50.00	0.00	.00	.00	.143E-04
44	60.00	-70.00	0.00	.01	.01	.214E-04
45	60.00	-60.00	0.00	.00	.00	.112E-04
46	60.00	-50.00	0.00	.09	.10	.275E-03
47	60.00	-40.00	0.00	.08	.09	.265E-03
48	60.00	-30.00	0.00	.23	.25	.738E-03
49	60.00	-20.00	0.00	3.05	3.32	.992E-02
50	60.00	-10.00	0.00	5.93	6.43	.199E-01
51	60.00	0.00	0.00	6.25	6.77	.210E-01
55	60.00	10.00	0.00	6.34	6.87	.213E-01
68	240.00	120.00	0.00	.00	.00	.122E-04
69	240.00	90.00	0.00	.00	.00	.830E-05
70	240.00	60.00	0.00	.01	.01	.262E-04
71	240.00	30.00	0.00	.34	.37	.107E-02
91	60.00	0.00	.50	6.10	6.61	.205E-01
92	60.00	0.00	1.00	5.54	6.01	.185E-01
93	60.00	0.00	1.50	5.30	5.75	.176E-01
94	60.00	0.00	2.00	4.83	5.24	.160E-01
95	60.00	0.00	2.50	4.47	4.85	.147E-01
96	60.00	0.00	3.00	4.02	4.36	.132E-01
97	60.00	0.00	4.00	2.57	2.79	.830E-02
98	60.00	0.00	5.00	1.56	1.70	.499E-02
99	60.00	0.00	6.00	.74	.81	.235E-02
100	60.00	0.00	8.00	.23	.25	.711E-03

RUN NUMBER 38
OPERATOR --SPARKS-- DAY 81 YEAR 1983
FILE NAME GRI38
FLOW RATE (CCS) 130.0
WIND SPEED (CM/S) 24.70
REF. WIND HEIGHT (CM) 2.0
AIR TEMP. (C) 19.0
SOURCE GAS TEMP. (C) -152
TRACER CONC. (PPM) 333300.0
BACKGROUND CONC. (PPM) 20.67

TUBE NO.	X (CM)	Y (CM)	Z (CM)	MODEL CONCENTRATION (%)	FIELD CONCENTRATION (%)	DIMENSIONLESS CONCENTRATION
2	-35.00	0.00	0.00	.00	.00	.543E-06
3	-30.00	0.00	0.00	.00	.00	.500E-05
4	-25.00	0.00	0.00	.00	.00	.124E-04
5	-20.00	0.00	0.00	.02	.02	.625E-04
6	-15.00	0.00	0.00	.56	.61	.179E-02
7	0.00	15.00	0.00	43.32	45.45	.241E+00
8	0.00	20.00	0.00	11.22	12.11	.398E-01
9	0.00	25.00	0.00	.01	.02	.468E-04
10	0.00	30.00	0.00	.00	.00	.591E-05
11	0.00	35.00	0.00	.00	.00	.606E-05
12	0.00	40.00	0.00	.06	.07	.203E-03
13	0.00	-15.00	0.00	31.19	33.07	.143E+00
14	0.00	-20.00	0.00	.21	.23	.670E-03
15	0.00	-25.00	0.00	.01	.01	.160E-04
16	0.00	-30.00	0.00	.00	.00	.506E-05
27	15.00	35.00	0.00	.00	.00	.102E-04
28	15.00	40.00	0.00	.00	.00	.935E-05
29	15.00	45.00	0.00	.00	.00	.268E-05
35	30.00	0.00	0.00	17.45	18.73	.666E-01
39	30.00	-10.00	0.00	14.59	15.70	.538E-01
40	30.00	-20.00	0.00	2.01	2.18	.645E-02
41	30.00	-30.00	0.00	.00	.00	.922E-05
42	30.00	-40.00	0.00	.00	.00	.181E-05
43	30.00	-50.00	0.00	.00	.00	.181E-05
44	60.00	-70.00	0.00	.00	.00	.796E-05
45	60.00	-60.00	0.00	.00	.00	.280E-05
46	60.00	-50.00	0.00	.04	.04	.113E-03
47	60.00	-40.00	0.00	.03	.04	.110E-03
48	60.00	-30.00	0.00	.16	.17	.492E-03
49	60.00	-20.00	0.00	1.43	1.56	.457E-02
50	60.00	-10.00	0.00	5.44	5.90	.181E-01
51	60.00	0.00	0.00	6.38	6.92	.215E-01
55	60.00	10.00	0.00	6.93	7.51	.234E-01
68	240.00	120.00	0.00	.00	.00	.205E-05
69	240.00	90.00	0.00	.00	.00	.452E-06
70	240.00	60.00	0.00	.11	.12	.348E-03
71	240.00	30.00	0.00	.70	.76	.222E-02
91	60.00	0.00	.50	6.17	6.69	.207E-01
92	60.00	0.00	1.00	5.51	5.97	.184E-01
93	60.00	0.00	1.50	5.25	5.70	.175E-01
94	60.00	0.00	2.00	4.63	5.04	.153E-01
95	60.00	0.00	2.50	4.18	4.54	.137E-01
96	60.00	0.00	3.00	3.72	4.04	.122E-01
97	60.00	0.00	4.00	2.16	2.36	.697E-02
98	60.00	0.00	5.00	1.15	1.26	.367E-02
99	60.00	0.00	6.00	.46	.50	.147E-02
100	60.00	0.00	8.00	.11	.12	.338E-03

RUN NUMBER 39
OPERATOR --SPARKS-- DAY 81 YEAR 1983
FILE NAME GRI39
FLOW RATE (CCS) 130.0
WIND SPEED (CM/S) 24.70
REF. WIND HEIGHT (CM) 2.0
AIR TEMP. (C) 19.0
SOURCE GAS TEMP. (C) -152
TRACER CONC. (PPM) 333300.0
BACKGROUND CONC. (PPM) 53.91

TUBE NO.	X (CM)	Y (CM)	Z (CM)	MODEL CONCENTRATION (%)	FIELD CONCENTRATION (%)	DIMENSIONLESS CONCENTRATION
2	-35.00	0.00	0.00	0.00	0.00	.000E+00
3	-30.00	0.00	0.00	.01	.01	.361E-04
4	-25.00	0.00	0.00	0.00	0.00	.000E+00
5	-20.00	0.00	0.00	.01	.01	.384E-04
6	-15.00	0.00	0.00	6.28	6.81	.211E-01
17	0.00	-35.00	0.00	.10	.10	.302E-03
18	0.00	-40.00	0.00	.03	.04	.110E-03
19	15.00	-5.00	0.00	40.00	42.09	.210E+00
20	15.00	0.00	0.00	37.63	39.67	.190E+00
21	15.00	5.00	0.00	40.45	42.54	.214E+00
22	15.00	10.00	0.00	38.74	40.81	.199E+00
23	15.00	15.00	0.00	34.70	36.68	.167E+00
24	15.00	20.00	0.00	22.60	24.14	.920E-01
25	15.00	25.00	0.00	2.09	2.28	.673E-02
26	15.00	30.00	0.00	.08	.08	.239E-03
27	15.00	35.00	0.00	.00	.00	.271E-05
28	15.00	40.00	0.00	.00	.00	.193E-05
29	15.00	45.00	0.00	.00	.00	.127E-05
35	30.00	0.00	0.00	18.28	19.61	.705E-01
39	30.00	-10.00	0.00	14.88	16.00	.550E-01
40	30.00	-20.00	0.00	3.60	3.91	.118E-01
41	30.00	-30.00	0.00	.06	.07	.195E-03
42	30.00	-40.00	0.00	0.00	0.00	.000E+00
43	30.00	-50.00	0.00	0.00	0.00	.000E+00
56	120.00	-15.00	0.00	1.68	1.82	.537E-02
57	120.00	0.00	0.00	2.63	2.86	.849E-02
61	120.00	15.00	0.00	2.97	3.23	.965E-02
62	120.00	30.00	0.00	1.84	2.01	.592E-02
63	120.00	45.00	0.00	.42	.45	.131E-02
64	120.00	60.00	0.00	.04	.04	.119E-03
65	120.00	75.00	0.00	.04	.05	.138E-03
66	120.00	90.00	0.00	.03	.03	.874E-04
67	120.00	105.00	0.00	.02	.02	.655E-04
68	240.00	120.00	0.00	0.00	0.00	.000E+00
69	240.00	90.00	0.00	0.00	0.00	.000E+00
70	240.00	60.00	0.00	.10	.10	.301E-03
71	240.00	30.00	0.00	.76	.83	.241E-02
91	120.00	0.00	.50	2.54	2.76	.819E-02
92	120.00	0.00	1.00	2.29	2.49	.737E-02
93	120.00	0.00	1.50	2.24	2.44	.722E-02
94	120.00	0.00	2.00	2.11	2.30	.679E-02
95	120.00	0.00	2.50	2.05	2.23	.659E-02
96	120.00	0.00	3.00	1.98	2.16	.637E-02
97	120.00	0.00	4.00	1.71	1.87	.549E-02
98	120.00	0.00	5.00	1.47	1.60	.468E-02
99	120.00	0.00	6.00	1.01	1.10	.322E-02
100	120.00	0.00	8.00	.87	.95	.277E-02

RUN NUMBER 40
OPERATOR --SPARKS-- DAY 81 YEAR 1983
FILE NAME GRI40
FLOW RATE (CCS) 130.0
WIND SPEED (CM/S) 24.70
REF. WIND HEIGHT (CM) 2.0
AIR TEMP. (C) 19.0
SOURCE GAS TEMP. (C) -152
TRACER CONC. (PPM) 500000.0
BACKGROUND CONC. (PPM) 68.49

TUBE NO.	X (CM)	Y (CM)	Z (CM)	MODEL CONCENTRATION (%)	FIELD CONCENTRATION (%)	DIMENSIONLESS CONCENTRATION
2	-35.00	0.00	0.00	0.00	0.00	.000E+00
3	-30.00	0.00	0.00	.01	.01	.286E-04
4	-25.00	0.00	0.00	0.00	0.00	.000E+00
5	-20.00	0.00	0.00	.01	.01	.246E-04
6	-15.00	0.00	0.00	.07	.07	.216E-03
17	0.00	-35.00	0.00	.02	.03	.739E-04
18	0.00	-40.00	0.00	.01	.01	.291E-04
19	15.00	-5.00	0.00	32.58	34.50	.152E+00
20	15.00	0.00	0.00	32.84	34.77	.154E+00
21	15.00	5.00	0.00	32.56	34.48	.152E+00
22	15.00	10.00	0.00	32.17	34.09	.149E+00
23	15.00	15.00	0.00	30.92	32.80	.141E+00
24	15.00	20.00	0.00	18.14	19.45	.698E-01
25	15.00	25.00	0.00	.39	.42	.123E-02
26	15.00	30.00	0.00	.00	.01	.151E-04
27	15.00	35.00	0.00	.00	.00	.127E-05
28	15.00	40.00	0.00	.00	.00	.102E-05
29	15.00	45.00	0.00	0.00	0.00	.000E+00
35	30.00	0.00	0.00	17.77	19.07	.681E-01
39	30.00	-10.00	0.00	16.22	17.43	.610E-01
40	30.00	-20.00	0.00	4.01	4.35	.131E-01
41	30.00	-30.00	0.00	.01	.01	.234E-04
42	30.00	-40.00	0.00	0.00	0.00	.000E+00
43	30.00	-50.00	0.00	0.00	0.00	.000E+00
56	120.00	-15.00	0.00	1.69	1.84	.542E-02
57	120.00	0.00	0.00	2.58	2.80	.833E-02
61	120.00	15.00	0.00	2.50	2.72	.807E-02
62	120.00	30.00	0.00	.85	.93	.270E-02
63	120.00	45.00	0.00	.12	.14	.393E-03
64	120.00	60.00	0.00	.01	.02	.434E-04
65	120.00	75.00	0.00	.02	.02	.509E-04
66	120.00	90.00	0.00	.01	.01	.188E-04
67	120.00	105.00	0.00	.01	.01	.195E-04
68	240.00	120.00	0.00	0.00	0.00	.000E+00
69	240.00	90.00	0.00	0.00	0.00	.000E+00
70	240.00	60.00	0.00	.00	.00	.430E-05
71	240.00	30.00	0.00	.44	.48	.138E-02
91	120.00	0.00	.50	2.49	2.71	.804E-02
92	120.00	0.00	1.00	2.35	2.55	.757E-02
93	120.00	0.00	1.50	2.31	2.52	.746E-02
94	120.00	0.00	2.00	2.29	2.49	.738E-02
95	120.00	0.00	2.50	2.26	2.46	.728E-02
96	120.00	0.00	3.00	2.21	2.41	.712E-02
97	120.00	0.00	4.00	2.10	2.28	.674E-02
98	120.00	0.00	5.00	1.95	2.13	.627E-02
99	120.00	0.00	6.00	1.53	1.66	.488E-02
100	120.00	0.00	8.00	1.49	1.62	.477E-02

RUN NUMBER 41
OPERATOR --SPARKS-- DAY 81 YEAR 1983
FILE NAME GRI41
FLOW RATE (CCS) 130.0
WIND SPEED (CM/S) 24.70
REF. WIND HEIGHT (CM) 2.0
AIR TEMP. (C) 19.0
SOURCE GAS TEMP. (C) -152
TRACER CONC. (PPM) 500000.0
BACKGROUND CONC. (PPM) 72.99

TUBE NO.	X (CM)	Y (CM)	Z (CM)	MODEL CONCENTRATION (%)	FIELD CONCENTRATION (%)	DIMENSIONLESS CONCENTRATION
30	30.00	50.00	0.00	0.00	0.00	.000E+00
31	30.00	40.00	0.00	.00	.00	.756E-05
32	30.00	30.00	0.00	.05	.06	.170E-03
33	30.00	20.00	0.00	9.11	9.85	.316E-01
34	30.00	10.00	0.00	.03	.04	.106E-03
35	30.00	0.00	0.00	17.73	19.03	.679E-01
38	45.00	0.00	0.00	10.68	11.53	.377E-01
39	30.00	-10.00	0.00	16.56	17.78	.625E-01
40	30.00	-20.00	0.00	2.84	3.09	.922E-02
41	30.00	-30.00	0.00	.00	.00	.639E-05
42	30.00	-40.00	0.00	0.00	0.00	.000E+00
43	30.00	-50.00	0.00	0.00	0.00	.000E+00
44	60.00	-70.00	0.00	.01	.01	.243E-04
45	60.00	-60.00	0.00	.06	.06	.181E-03
46	60.00	-50.00	0.00	.05	.06	.166E-03
47	60.00	-40.00	0.00	.07	.08	.222E-03
48	60.00	-30.00	0.00	.17	.19	.552E-03
49	60.00	-20.00	0.00	1.91	2.08	.613E-02
50	60.00	-10.00	0.00	6.44	6.98	.217E-01
51	60.00	0.00	0.00	7.14	7.73	.242E-01
55	60.00	10.00	0.00	7.18	7.78	.244E-01
56	120.00	-15.00	0.00	1.52	1.66	.488E-02
57	120.00	0.00	0.00	2.72	2.96	.881E-02
60	140.00	0.00	0.00	2.09	2.28	.673E-02
61	120.00	15.00	0.00	2.53	2.75	.818E-02
62	120.00	30.00	0.00	.72	.79	.229E-02
63	120.00	45.00	0.00	.09	.10	.287E-03
64	120.00	60.00	0.00	.01	.01	.410E-04
65	120.00	75.00	0.00	.01	.02	.443E-04
66	120.00	90.00	0.00	.00	.00	.119E-04
67	120.00	105.00	0.00	.00	.00	.120E-04
68	240.00	120.00	0.00	0.00	0.00	.000E+00
69	240.00	90.00	0.00	0.00	0.00	.000E+00
70	240.00	60.00	0.00	.01	.02	.466E-04
71	240.00	30.00	0.00	.45	.49	.144E-02
72	240.00	0.00	0.00	.83	.90	.262E-02
73	240.00	0.00	2.00	.75	.82	.238E-02
74	240.00	0.00	8.00	.88	.96	.279E-02
75	240.00	0.00	15.00	.83	.91	.265E-02
76	240.00	-30.00	0.00	.16	.18	.520E-03
77	240.00	-60.00	0.00	.01	.01	.264E-04
78	240.00	-90.00	0.00	.01	.01	.206E-04
79	240.00	-120.00	0.00	.01	.01	.224E-04
80	350.00	-30.00	0.00	.10	.11	.314E-03
81	350.00	0.00	0.00	.00	.00	.140E-04
82	350.00	30.00	0.00	.28	.30	.876E-03

RUN NUMBER 42
OPERATOR --NEFF -- DAY 82 YEAR 1983
FILE NAME GRI42
FLOW RATE (CCS) 130.0
WIND SPEED (CM/S) 38.30
REF. WIND HEIGHT (CM) 2.0
AIR TEMP. (C) 20.0
SOURCE GAS TEMP. (C) -152
TRACER CONC. (PPM) 500000.0
BACKGROUND CONC. (PPM) 19.14

TUBE NO.	X (CM)	Y (CM)	Z (CM)	MODEL CONCENTRATION (%)	FIELD CONCENTRATION (%)	DIMENSIONLESS CONCENTRATION
30	30.00	50.00	0.00	0.00	0.00	.000E+00
31	30.00	40.00	0.00	.00	.00	.652E-05
32	30.00	30.00	0.00	.00	.00	.655E-05
33	30.00	20.00	0.00	6.81	7.37	.355E-01
34	30.00	10.00	0.00	20.70	22.16	.127E+00
35	30.00	0.00	0.00	22.39	23.93	.140E+00
38	45.00	0.00	0.00	16.28	17.49	.946E-01
39	30.00	-10.00	0.00	19.84	21.25	.120E+00
40	30.00	-20.00	0.00	7.34	7.95	.385E-01
41	30.00	-30.00	0.00	.00	.00	.214E-04
42	30.00	-40.00	0.00	0.00	0.00	.000E+00
43	30.00	-50.00	0.00	.00	.00	.460E-05
47	60.00	-40.00	0.00	.00	.00	.185E-04
48	60.00	-30.00	0.00	.44	.48	.217E-02
49	60.00	-20.00	0.00	6.91	7.49	.361E-01
50	60.00	-10.00	0.00	9.98	10.78	.539E-01
51	60.00	0.00	0.00	11.40	12.30	.626E-01
55	60.00	10.00	0.00	10.07	10.88	.545E-01
56	120.00	-15.00	0.00	4.17	4.52	.212E-01
57	120.00	0.00	0.00	4.71	5.11	.241E-01
60	140.00	0.00	0.00	3.73	4.05	.188E-01
61	120.00	15.00	0.00	3.36	3.65	.169E-01
62	120.00	30.00	0.00	.19	.20	.909E-03
63	120.00	45.00	0.00	.05	.05	.231E-03
64	120.00	60.00	0.00	.01	.01	.267E-04
68	240.00	120.00	0.00	.00	.00	.363E-05
69	240.00	90.00	0.00	.00	.00	.373E-06
70	240.00	60.00	0.00	.00	.00	.112E-05
71	240.00	30.00	0.00	.16	.18	.792E-03
72	240.00	0.00	0.00	1.68	1.82	.829E-02
73	240.00	0.00	2.00	1.42	1.55	.701E-02
74	240.00	0.00	8.00	1.00	1.09	.490E-02
75	240.00	0.00	15.00	.32	.35	.157E-02
76	240.00	-30.00	0.00	1.24	1.35	.610E-02
77	240.00	-60.00	0.00	.03	.04	.157E-03
78	240.00	-90.00	0.00	.00	.00	.106E-04
79	240.00	-120.00	0.00	.00	.00	.106E-04
80	350.00	-30.00	0.00	.77	.84	.378E-02
81	350.00	0.00	0.00	.88	.95	.430E-02
82	350.00	30.00	0.00	.11	.13	.560E-03

RUN NUMBER 43
OPERATOR --SPARKS-- DAY 82 YEAR 1983
FILE NAME GRI43
FLOW RATE (CCS) 195.0
WIND SPEED (CM/S) 19.30
REF. WIND HEIGHT (CM) 2.0
AIR TEMP. (C) 20.0
SOURCE GAS TEMP. (C) -152
TRACER CONC. (PPM) 500000.0
BACKGROUND CONC. (PPM) 49.45

TUBE NO.	X (CM)	Y (CM)	Z (CM)	MODEL CONCENTRATION (%)	FIELD CONCENTRATION (%)	DIMENSIONLESS CONCENTRATION
30	30.00	50.00	0.00	0.00	0.00	.000E+00
31	30.00	40.00	0.00	.01	.01	.191E-04
32	30.00	30.00	0.00	.11	.12	.185E-03
33	30.00	20.00	0.00	16.05	17.25	.313E-01
34	30.00	10.00	0.00	.31	.34	.512E-03
35	30.00	0.00	0.00	18.68	20.02	.376E-01
38	45.00	0.00	0.00	10.85	11.71	.199E-01
39	30.00	-10.00	0.00	18.42	19.76	.369E-01
40	30.00	-20.00	0.00	11.72	12.64	.217E-01
41	30.00	-30.00	0.00	.05	.05	.769E-04
42	30.00	-40.00	0.00	0.00	0.00	.000E+00
43	30.00	-50.00	0.00	0.00	0.00	.000E+00
44	60.00	-70.00	0.00	.00	.00	.633E-05
45	60.00	-60.00	0.00	0.00	0.00	.000E+00
46	60.00	-50.00	0.00	0.00	0.00	.000E+00
47	60.00	-40.00	0.00	0.00	0.00	.000E+00
48	60.00	-30.00	0.00	.20	.21	.321E-03
49	60.00	-20.00	0.00	4.11	4.46	.700E-02
50	60.00	-10.00	0.00	6.65	7.21	.116E-01
51	60.00	0.00	0.00	7.10	7.69	.125E-01
55	60.00	10.00	0.00	7.43	8.05	.131E-01
56	120.00	-15.00	0.00	1.83	1.99	.304E-02
57	120.00	0.00	0.00	2.29	2.49	.384E-02
60	140.00	0.00	0.00	1.71	1.86	.284E-02
61	120.00	15.00	0.00	2.50	2.72	.419E-02
62	120.00	30.00	0.00	.81	.89	.134E-02
63	120.00	45.00	0.00	.11	.12	.186E-03
64	120.00	60.00	0.00	.00	.00	.632E-05
65	120.00	75.00	0.00	.00	.00	.632E-05
66	120.00	90.00	0.00	.00	.00	.616E-06
67	120.00	105.00	0.00	.00	.00	.162E-05
68	240.00	120.00	0.00	0.00	0.00	.000E+00
69	240.00	90.00	0.00	0.00	0.00	.000E+00
70	240.00	60.00	0.00	.02	.02	.339E-04
71	240.00	30.00	0.00	.41	.44	.669E-03
72	240.00	0.00	0.00	.73	.80	.121E-02
73	240.00	0.00	4.00	.76	.83	.125E-02
74	240.00	0.00	11.00	.76	.83	.125E-02
75	240.00	0.00	20.00	.80	.87	.132E-02
76	240.00	-30.00	0.00	.17	.18	.277E-03
77	240.00	-60.00	0.00	0.00	0.00	.000E+00
78	240.00	-90.00	0.00	0.00	0.00	.000E+00
79	240.00	-120.00	0.00	.00	.00	.417E-07
80	350.00	-30.00	0.00	.09	.10	.152E-03
81	350.00	0.00	0.00	.46	.50	.756E-03
82	350.00	30.00	0.00	.19	.21	.309E-03

RUN NUMBER 44
OPERATOR --SPARKS-- DAY 82 YEAR 1983
FILE NAME GRI44
FLOW RATE (CCS) 195.0
WIND SPEED (CM/S) 19.30
REF. WIND HEIGHT (CM) 2.0
AIR TEMP. (C) 20.0
SOURCE GAS TEMP. (C) -152
TRACER CONC. (PPM) 500000.0
BACKGROUND CONC. (PPM) 71.46

TUBE NO.	X (CM)	Y (CM)	Z (CM)	MODEL CONCENTRATION (%)	FIELD CONCENTRATION (%)	DIMENSIONLESS CONCENTRATION
2	-35.00	0.00	0.00	0.00	0.00	.000E+00
3	-30.00	0.00	0.00	.04	.04	.618E-04
4	-25.00	0.00	0.00	0.00	0.00	.000E+00
5	-20.00	0.00	0.00	.05	.06	.830E-04
6	-15.00	0.00	0.00	1.76	1.91	.292E-02
13	0.00	-15.00	0.00	34.41	36.38	.858E-01
14	0.00	-20.00	0.00	6.49	7.03	.113E-01
15	0.00	-25.00	0.00	.01	.01	.158E-04
16	0.00	-30.00	0.00	0.00	0.00	.000E+00
17	0.00	-35.00	0.00	.02	.03	.380E-04
18	0.00	-40.00	0.00	.00	.00	.814E-06
19	15.00	-5.00	0.00	33.95	35.91	.840E-01
20	15.00	0.00	0.00	34.40	36.37	.857E-01
21	15.00	5.00	0.00	34.72	36.70	.870E-01
22	15.00	10.00	0.00	33.87	35.83	.837E-01
23	15.00	15.00	0.00	32.72	34.65	.795E-01
24	15.00	20.00	0.00	29.98	31.82	.700E-01
25	15.00	25.00	0.00	5.02	5.45	.865E-02
26	15.00	30.00	0.00	.13	.14	.211E-03
27	15.00	35.00	0.00	.00	.00	.663E-05
28	15.00	40.00	0.00	.00	.00	.313E-07
29	15.00	45.00	0.00	0.00	0.00	.000E+00
35	30.00	0.00	0.00	18.12	19.44	.362E-01
39	30.00	-10.00	0.00	17.60	18.88	.349E-01
40	30.00	-20.00	0.00	9.27	10.02	.167E-01
41	30.00	-30.00	0.00	.03	.03	.467E-04
42	30.00	-40.00	0.00	0.00	0.00	.000E+00
43	30.00	-50.00	0.00	0.00	0.00	.000E+00
56	120.00	-15.00	0.00	1.84	2.01	.307E-02
57	120.00	0.00	0.00	2.17	2.36	.363E-02
61	120.00	15.00	0.00	2.43	2.65	.408E-02
62	120.00	30.00	0.00	1.51	1.65	.251E-02
63	120.00	45.00	0.00	.32	.35	.528E-03
64	120.00	60.00	0.00	.00	.00	.636E-05
65	120.00	75.00	0.00	.00	.00	.355E-05
66	120.00	90.00	0.00	.00	.00	.202E-05
67	120.00	105.00	0.00	.00	.00	.474E-05
91	126.00	0.00	0.00	1.91	2.08	.319E-02
92	126.00	0.00	2.50	1.71	1.86	.285E-02
93	126.00	0.00	6.40	1.66	1.80	.275E-02
94	126.00	0.00	10.30	1.24	1.35	.205E-02
95	126.00	0.00	14.50	.72	.78	.118E-02
96	126.00	0.00	18.80	.35	.38	.566E-03
97	126.00	0.00	23.40	.12	.13	.202E-03
98	126.00	0.00	28.80	.03	.03	.501E-04
99	126.00	0.00	39.10	0.00	0.00	.000E+00
100	126.00	0.00	49.20	0.00	0.00	.000E+00

APPENDIX E

Data Tables: Temperature

Table E-1
Mean Temperature Measurements for Runs 23-26

Runs: 23-26
Source gas: 99.5% N_2, 0.5% CH_4
Specific gravity: 1.46
Flow rate: 130 ccs
Wind speed: 24.7 cm/s @ 2 cm

Thermocouple Number	x (cm)	y (cm)	z (cm)	$\bar{T}$ (k)
1	30	0	0.5	288.8
2	30	0	1.0	289.5
3	30	0	1.5	291.2
4	30	0	2.0	292.5
5	30	0	2.5	293.0
6	30	0	3.0	293.7
7	30	0	4.0	294.8
8	30	0	5.0	294.9
9	30	0	6.0	295.0
10	20	0	8.0	295.1
11	60	-10	0	293.5
12	60	0	0	293.3
13	60	0	6.5	-
14	60	0	1.0	-
15	60	0	1.5	-
16	60	0	2.0	-
17	60	0	2.5	-
18	60	0	3.0	-
19	60	0	4.0	-
20	60	0	5.0	-
21	60	0	6.0	-
22	60	0	8.0	-
23	120	0	0.5	294.4
24	120	0	1.0	294.2
25	120	0	1.5	294.2
26	120	0	2.0	294.3
27	120	0	2.5	294.4
28	120	0	3.0	294.6
29	120	0	4.0	294.0
30	120	0	5.0	294.0
31	120	0	6.0	294.2
32	120	0	8.0	294.3
33	15	0	0	

Table E-2
Mean Temperature Measurements for Runs 27-30

Runs: 27-30
Source gas: 99.5% N_2, 0.5% CH_4
Specific gravity: 2.35
Flow rate: 223 ccs
Wind speed: 42.3 cm/s @ 2 cm

Thermocouple Number	x (cm)	y (cm)	z (cm)	$\bar{T}$ (k)
1	30	0	0.5	276.8
2	30	0	1.0	284.6
3	30	0	1.5	288.9
4	30	0	2.0	291.3
5	30	0	2.5	291.8
6	30	0	3.0	292.9
7	30	0	4.0	293.5
8	30	0	5.0	293.3
9	30	0	6.0	293.5
10	20	0	8.0	293.8
11	60	-10	0	288.4
12	60	0	0	287.9
13	60	0	6.5	285.1
14	60	0	1.0	286.4
15	60	0	1.5	288.7
16	60	0	2.0	290.8
17	60	0	2.5	291.8
18	60	0	3.0	293.0
19	60	0	4.0	293.7
20	60	0	5.0	293.7
21	60	0	6.0	293.8
22	60	0	8.0	294.0
23	120	0	0.5	291.2
24	120	0	1.0	291.0
25	120	0	1.5	291.4
26	120	0	2.0	291.9
27	120	0	2.5	292.3
28	120	0	3.0	293.0
29	120	0	4.0	293.7
30	120	0	5.0	293.9
31	120	0	6.0	294.0
32	120	0	8.0	294.2
33	15	0	0	206.8

Table E-3
Mean Temperature Measurements for Runs 31-34

Runs: 31-34
Source gas: 99.5% N_2, 0.5% CH_4
Specific gravity: 2.35
Flow rate: 223 ccs
Wind speed: 42.3 cm/s @ 2 cm

Thermocouple Number	x (cm)	y (cm)	z (cm)	$\bar{T}$ (k)
1	30	0	0.5	283.7
2	30	0	1.0	287.7
3	30	0	1.5	289.7
4	30	0	2.0	290.7
5	30	0	2.5	290.9
6	30	0	3.0	291.3
7	30	0	4.0	291.6
8	30	0	5.0	291.5
9	30	0	6.0	291.7
10	20	0	8.0	291.8
11	60	-10	0	289.1
12	60	0	0	289.2
13	60	0	6.5	288.0
14	60	0	1.0	288.4
15	60	0	1.5	289.5
16	60	0	2.0	290.5
17	60	0	2.5	291.0
18	60	0	3.0	291.6
19	60	0	4.0	291.8
20	60	0	5.0	291.8
21	60	0	6.0	292.0
22	60	0	8.0	292.1
23	120	0	0.5	290.6
24	120	0	1.0	290.5
25	120	0	1.5	290.6
26	120	0	2.0	991.1
27	120	0	2.5	291.3
28	120	0	3.0	291.7
29	120	0	4.0	291.9
30	120	0	5.0	292.1
31	120	0	6.0	292.2
32	120	0	8.0	292.3
33	15	0	0	255.5

Table E-4
Mean Temperature Measurements for Runs 35, 38, and 39

Runs: 35, 38, 39
Source gas: 100% CH_4
Specific gravity: 1.46
Flow rate: 130 ccs
Wind speed: 24.7 cm/s @ 2 cm

Thermocouple Number	x (cm)	y (cm)	z (cm)	$\bar{T}$ (k)
1	30	0	0.5	276.5
2	30	0	1.0	280.2
3	30	0	1.5	283.0
4	30	0	2.0	285.9
5	30	0	2.5	287.6
6	30	0	3.0	290.0
7	30	0	4.0	291.0
8	30	0	5.0	290.8
9	30	0	6.0	291.1
10	20	0	8.0	291.4
11	60	-10	0	289.0
12	60	0	0	288.6
13	60	0	6.5	287.9
14	60	0	1.0	287.8
15	60	0	1.5	288.1
16	60	0	2.0	288.5
17	60	0	2.5	288.8
18	60	0	3.0	289.4
19	60	0	4.0	290.1
20	60	0	5.0	290.7
21	60	0	6.0	291.0
22	60	0	8.0	291.5
23	120	0	0.5	290.7
24	120	0	1.0	290.5
25	120	0	1.5	290.6
26	120	0	2.0	290.6
27	120	0	2.5	290.5
28	120	0	3.0	290.6
29	120	0	4.0	290.5
30	120	0	5.0	290.8
31	120	0	6.0	291.0
32	120	0	8.0	291.2
33	15	0	0	216.7

Table E-5
Mean Temperature Measurements for Runs 36, 37, 40, and 41

Runs: 36, 37, 40, 41
Source gas: 100% CH_4
Specific gravity: 1.46
Flow rate: 130 cc/s
Wind speed: 24.7 cm/s @ 2 cm

Thermocouple Number	x (cm)	y (cm)	z (cm)	$\bar{T}$ (k)
1	30	0	0.5	277.2
2	30	0	1.0	280.5
3	30	0	1.5	283.7
4	30	0	2.0	286.7
5	30	0	2.5	288.2
6	30	0	3.0	290.1
7	30	0	4.0	291.2
8	30	0	5.0	291.1
9	30	0	6.0	291.4
10	20	0	8.0	291.7
11	60	-10	0	289.5
12	60	0	0	289.2
13	60	0	6.5	288.2
14	60	0	1.0	288.1
15	60	0	1.5	288.3
16	60	0	2.0	288.3
17	60	0	2.5	288.5
18	60	0	3.0	288.7
19	60	0	4.0	289.3
20	60	0	5.0	290.0
21	60	0	6.0	290.4
22	60	0	8.0	291.2
23	120	0	0.5	290.7
24	120	0	1.0	290.6
25	120	0	1.5	290.6
26	120	0	2.0	290.5
27	120	0	2.5	290.6
28	120	0	3.0	290.6
29	120	0	4.0	290.5
30	120	0	5.0	290.5
31	120	0	6.0	290.6
32	120	0	8.0	290.9
33	15	0	0	213.8